
Measurement and Modelling of Three Dimensional Scapulohumeral Kinematics

NEWCASTLE UNIVERSITY LIBRARY

096 51050 7

Thesis L5780

Nicholas David Barnett, B. Eng. (Hons.)

This thesis is submitted in fulfilment of the requirements for the Degree of
Doctor of Philosophy

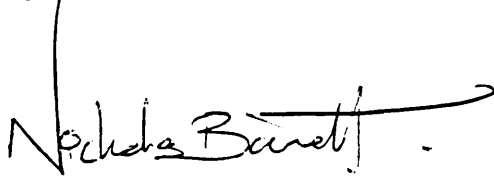
Centre for Rehabilitation and Engineering Studies
Department of Mechanical, Materials and Manufacturing Engineering
University of Newcastle upon Tyne

October 1996

Declaration

This Thesis describes work carried out by the author in the Department of Mechanical, Materials and Manufacturing Engineering of the University of Newcastle upon Tyne, United Kingdom, during the period October 1993 to October 1996, under the supervision of Professor G. R. Johnson.

This Thesis describes original work which has not been submitted for a higher degree at any other University and is the work solely of the undersigned author, except where acknowledged in the text.

A handwritten signature in black ink, reading "Nicholas Barnett". The signature is written in a cursive style with a long horizontal stroke extending to the right.

Nicholas David Barnett.

Copyright © 1996 by N. D. Barnett

The copyright of this thesis rests with the author. No quotation from it should be published without prior written consent and any information derived from it should be acknowledged.

Abstract

The term *scapulohumeral rhythm* is commonly used to describe the two dimensional rotation of the scapula accompanying motion of the arm. Despite the development of a variety of measurement techniques, including radiography, goniometry and three dimensional digitisation, the complete three dimensional kinematics of the scapula have never been presented. Nor have the effects of arm motions outside elevation in the coronal, sagittal or scapula planes been considered.

Employing the Isotrak®II electromagnetic measurement system, this study has developed and validated a new method to simultaneously measure the three dimensional kinematics of the scapula and humerus. Euler angle rotations of the scapula were defined in a sequence approximately analogous to clinical definitions. For the first time, the three dimensional displacements of the scapula have also been determined. 95% confidence intervals for lateral rotation of the scapula during humeral elevation in the coronal plane have been calculated at under 4°, significantly smaller than those presented by previous authors.

A mathematical model of three dimensional scapulohumeral kinematics has been developed, capable of predicting the position and orientation of the scapula for a given orientation of the humerus over a wide range of humeral motion. Using this model system, the effects of humeral azimuth, elevation and rotation on the kinematics of the scapula have been investigated.

Humeral elevation was seen to have the largest effect, causing the scapula to rotate laterally, retract and tip backwards. Humeral azimuth has no noticeable effect on the lateral rotation of the scapula, although it causes the scapula to retract, and to tip backwards slightly. Rotation of the humerus has little effect on the kinematics of the scapula. However, when approaching maximal internal rotation, the ligaments around the glenohumeral joint impose a kinematic constraint on the scapula, resulting in elevation of the scapula upon the thoracic cage.

Acknowledgements

In a piece of work of this size and duration, it is inevitable that there will be a number of people whom deserve my thanks.

Firstly, thanks must go to the Engineering and Physical Sciences Research Council for supporting me throughout the work, in a manner which I shortly hope to leave behind!

Equally, I would like to thank my supervisor, Professor Garth Johnson for his input to the work and many useful discussions, without which I may have finished a few months sooner, or perhaps not at all.

Within the department, a number of other people also deserve a mention including the technicians for helping me out with all of those “urgent” items, especially Mick Devine and his cherished CNC machines. Thanks also go to Dave Glennie for his invaluable programming skills, without which the data contained in this thesis may have never been collected. Furthermore, my statistical expertise would not be where it is today without the priceless advice of Dr. Andrew Metcalf of the Engineering Mathematics department.

I also wish to thank the other occupant of my office, Mike Buckley, for his very helpful discussions of three dimensional kinematics, and for volunteering his time as a highly photogenic model for the illustrations within the thesis.

Thanks also go to all of the other members, past and present, of CREST, especially Rod Duncan for his assistance in data collection, and to the secretaries within the department, especially Jeanne Elsom for her sense of humour.

Finally, thanks to Lou for maintaining my insanity throughout the writing-up period, and for the numerous games of footie on the roof...

Table of Contents

Declaration ii

Abstract iii

Acknowledgements..... iv

Table of Contents..... v

Chapter 1

Introduction..... 1

 1.1 Foreword 1

 1.2 Objectives..... 2

 1.3 Layout of the Thesis 3

Chapter 2

Introduction to the Shoulder Girdle Mechanism 4

 2.1 Clinical Terminology..... 4

 2.1.1 Anatomical Axes 4

 2.1.2 Anatomical Planes 5

 2.2 Skeletal Structure of the Shoulder Girdle Mechanism 6

 2.2.1 Introduction..... 6

 2.2.2 The Bones and Joints of the Shoulder Girdle Mechanism 7

 2.2.2.1 The Sternum 9

 2.2.2.2 The Clavicle..... 9

 2.2.2.3 The Scapula..... 9

 2.2.2.4 The Humerus 13

 2.3 Clinical Descriptions of Motion..... 13

 2.3.1 Abduction and Adduction 14

 2.3.2 Flexion and Extension 14

 2.3.3 Rotation..... 14

 2.3.4 Clinical Descriptions of the Motion of the Shoulder Girdle..... 15

2.3.5 Three Dimensional Finite Rotations and <i>Codman's Paradox</i>	17
2.4 Kinematic Descriptions of Anatomy.....	18
2.4.1 Passive and Active Soft Tissues	18
2.4.2 Function of Passive Tissues.....	18
2.4.3 Classification of Articulations	19
2.5 Kinematic Anatomy of the Shoulder Girdle Mechanism	21
2.5.1 Introduction.....	21
2.5.2 The Sternoclavicular Joint	22
2.5.3 The Acromioclavicular Joint.....	23
2.5.4 The Glenohumeral Joint	25
2.5.5 The Scapulothoracic Joint	26
2.6 Concluding Remarks	26
Chapter 3	
Three Dimensional Kinematics	28
3.1 Three Dimensional Rigid Body Motion	28
3.1.1 Displacements: The Position Vector	29
3.1.2 Orientations: The Rotation Matrix.....	29
3.1.3 Displacements and Orientations : The Frame	31
3.1.4 Co-ordinate Transformations.....	31
3.2 Representation of Orientation	32
3.2.1 Introduction.....	32
3.2.2 Euler Angles.....	33
3.2.2.1 Examples from the Literature	35
3.2.3 The Floating Axis System	36
3.2.4 Azimuth Elevation and Roll.....	37
3.2.5 Other Defined Systems	42
3.3 Complete Kinematic Descriptions.....	46
3.3.1 Introduction.....	46
3.3.2 The Finite Centre of Rotation	46
3.3.3 The Finite Helical Axis.....	47
Chapter 4	
Review of the Literature Regarding Measurement of Shoulder Motion	50
4.1 Introduction.....	50
4.1.1 History	50
4.1.2 Difficulties in Measurement of Scapulohumeral Rhythm.....	52
4.2 Measurement of Scapular Motion	53

4.2.1 Qualitative Observations of Scapular Motion.....	53
4.2.2 Two Dimensional Radiographic Techniques.....	56
4.2.3 Other Two Dimensional Measurement Techniques	66
4.2.4 Three Dimensional Measurement Techniques	70
4.2.4.1 Bi-Planar Radiography Techniques	71
4.2.4.2 Three Dimensional Digitisation Techniques.....	75
4.2.4.3 Other Three Dimensional Techniques	79
4.3 Summary of Relevant Findings	80

Chapter 5

Materials and Methods.....	83
5.1 Introduction.....	83
5.1.1 Criteria for a Suitable Measurement Technique	83
5.1.2 Progression of Research	84
5.2 Introduction to the Measurement Technique	86
5.2.1 Initial "Single Channel" Studies.....	86
5.2.2 "Two Channel" Studies	87
5.3 Polhemus Systems	89
5.3.1 Introduction.....	89
5.3.2 Specification of Systems Used.....	91
5.3.3 Host Computer.....	91
5.3.4 Important Warning Regarding Pacemakers.....	91
5.4 Development of the Locator	92
5.4.1 Assessment of Current Fixture	92
5.4.2 Anatomy of the Locator	93
5.4.3 Design of the Locator Feet.....	94
5.4.3.1 The Posterior Acromial Angle.....	94
5.4.3.2 The Root of the Scapula Spine	94
5.4.3.3 The Inferior Angle	95
5.4.4 Improving the Simplicity of Use	96
5.4.4.1 Adjustment of the Locator Leg Positions	96
5.4.4.2 Measurement of Scapula Dimensions	97
5.4.5 Other Design Considerations	98
5.4.6 Illustrations of the Prototype Locator.....	98
5.4.7 Modifications for Two Channel System.....	99
5.5 Other Materials and Hardware Development.....	100
5.5.1 Steral Receiver Mount	100

5.5.2 Fluid Filled Goniometer.....	101
5.5.3 Arm Splint.....	102
5.5.4 Data Collection Switch.....	103
5.5.5 Calibration Rig.....	103
5.6 Software	104
5.6.1 Data Collection Software	104
5.6.2 WinMat Data Analysis System	105
5.7 Data Analysis	107
5.7.1 Definition of Global Axes	107
5.7.2 Definition of Scapula Axes.....	110
5.8 Validation Techniques	111
5.8.1 Introduction.....	111
5.8.2 Confidence Interval and Prediction Interval Estimation	112
5.8.3 Factorial Experimental Design.....	115
5.9 Data Smoothing and Interpolation Techniques.....	118
5.9.1 Introduction.....	118
5.9.2 Repeated Measures and Superposition.....	120
5.9.3 Multiple Linear Regression	120
5.10 Concluding Remarks	121
 Chapter 6	
Validation of the Measurement Technique	122
6.1 Preliminary Results	122
6.2 Single Channel Validation Study.....	125
6.2.1 Design of the Experiment.....	125
6.2.2 Results	126
6.2.2.1 Rotations of the Scapula (x_γ , z_α' , y_β'' sequence)	127
6.2.2.2 Displacements of the Scapula.....	128
6.2.2.3 Regression Coefficients.....	129
6.2.2.4 Statistical Interpretation.....	129
6.2.3 Conclusions.....	129
6.3 Two Channel Validation Study	130
6.3.1 Design of the Experiment.....	130
6.3.2 Results	131
6.3.2.1 Measurements of Arm Position	131
6.3.2.2 Rotations of the Scapula (x_γ , z_α' , y_β'' sequence)	133
6.3.2.3 Displacements of the Scapula.....	134

6.3.2.4 Regression Coefficients.....	135
6.3.2.5 Statistical Interpretation.....	135
6.3.3 Conclusions.....	135
6.4 Concluding Remarks	136

Chapter 7

Modelling of Three Dimensional Scapulohumeral Kinematics	137
7.1 Objectives.....	137
7.2 Defining the Workspace	138
7.2.1 Workspace Representation.....	138
7.2.2 Issues Concerning Modelling of the Workspace	141
7.2.3 Functional Workspace Representation.....	142
7.2.4 Model Workspace Identification	144
7.3 Data Collection and Analysis.....	144
7.3.1 Task Identification	144
7.3.2 Subject details.....	150
7.3.3 Co-ordinate Frame Specification.....	150
7.4 Developing the Scapulohumeral Kinematic Model.....	151
7.4.1 Introduction.....	151
7.4.2 Summary of Regression Procedures	152
7.4.3 Issues Concerning the Modelling of Three Dimensional Kinematics	152
7.4.4 Input and Output Parameters for Regression Models	153
7.4.5 Validation of Subject Models	154
7.4.6 Development of a Generic Model.....	156
7.5 A Model of Three Dimensional Scapulohumeral Kinematics	157
7.5.1 Governing Constraint Equations	157
7.5.2 Model Validation.....	158
7.5.3 Subject Variation.....	162
7.6 Representation of Scapulohumeral Kinematics.....	163

Chapter 8

Discussion.....	172
8.1 Descriptions of Motion at the Shoulder	172
8.1.1 Total Shoulder Motion.....	172
8.1.2 Motion of the Scapula.....	174
8.1.3 Issues Concerning Comparisons of Results	175
8.2 Results During Validation	177
8.2.1 Evidence of a Learning Technique	177

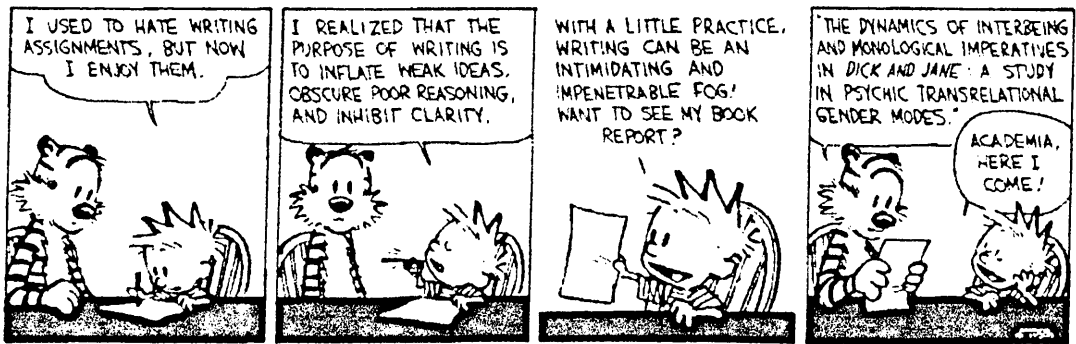
8.2.2 Validation Studies	179
8.3 Kinematic Model of the Scapula.....	186
8.3.1 Introduction.....	186
8.3.2 α - Lateral Rotation of the Scapula	187
8.3.3 β - Backward Tip of the Scapula	188
8.3.4 γ - Retraction of the Scapula.....	189
8.3.5 Displacements of the Scapula.....	190
8.3.6 Confidence Intervals of the Model.....	192
8.3.7 Choice of Co-ordinate System	194
8.4 Measuring Motions of the Scapula	196
8.4.1 Introduction.....	196
8.4.2 Inadequacies of Previous Measurement Techniques	196
8.4.3 Validation of Measurement Systems.....	198
8.4.4 Issues Concerning the Measurement Technique	200
8.5 An Application of the Model.....	202
Chapter 9	
Conclusions and Recommendations for Future Work.....	206
9.1 Conclusions.....	206
9.1.1 Design and Validation of the Measurement System.....	206
9.1.2 Results	207
9.1.3 General Issues.....	208
9.2 Recommendations for Further Work.....	208
9.2.1 Replicate Data Collection	209
9.2.2 Increased Humeral Workspace	209
9.2.3 Humeral Kinematics and Model Development.....	209
9.2.4 Other Recommendations.....	210
9.2.5 Concluding Statement	210
References	211
Appendix A1	
Winging of the Scapula: The Underlying Biomechanics and an Orthotic Solution.....	218
Appendix A2	
Helical Axis Parameters.....	229
Appendix A3	
Design Drawings.....	234

Appendix A4

Further Results.....248

Appendix A5

WinMat User Guide269



Chapter 1

Introduction

1.1 FOREWORD

In the evolution of man, the progression to the upright position; that of a biped as oppose to a quadruped, freed the upper limb and exposed a greater need for mobility at the expense of stability and load carrying capacity. The arm needed no longer to be a bearer of body weight, thus the pectoral girdle evolved as a mechanism, capable of providing a large range of motion while being less heavy than the pelvic girdle. The anatomy required to achieve this is complex, hence the shoulder cannot be described as an individual joint, as is true of the hip, but as a series of bones and joints which act together during motion in order to maintain stability of the arm.

Codman (1934) coined the term *scapulohumeral rhythm* to describe the rotation of the scapula accompanying motion of the arm. However, despite a long history of anatomical and biomechanical studies of the shoulder, measurement of this phenomenon has proven rather difficult as the motion of the scapula occurs beneath the skin, inhibiting the fixation of any externally applied measurement system. Many measurement techniques have been presented including radiography (most notably Inman *et al.* 1944, Freedman and Munro 1966, Poppen and Walker 1976) and goniometry (Doody *et al.*, 1970). It is only recently that three dimensional techniques have been employed in this measurement (Pronk, 1991, Johnson *et al.* 1993).

Nevertheless, there is a distinct lack of kinematic data relating to the three dimensional motions of the shoulder girdle mechanism, and the complete three dimensional kinematics of the scapula have never been presented. Nor have the

effects of arm motions outside elevation in the coronal, sagittal or scapula planes been considered.

Measurement and analysis of scapulohumeral motion is essential if a thorough understanding of shoulder kinematics is required. Without detailed knowledge of the orientation of bones within the shoulder girdle mechanism, it is not possible to predict contact forces occurring in joints needed for the design of prosthetic replacements. Similarly, the diagnosis of pathological shoulders is hindered if a full understanding of the "normal" shoulder girdle mechanism is not known.

1.2 OBJECTIVES

This study focuses on the kinematics of the scapula during active motions of the arm. The principal objective of this work was to produce a model of scapulohumeral kinematics capable of predicting the three dimensional position and orientation of the scapula for a given arm position. Using such a model, a database of normal scapulohumeral kinematics may be developed, or normal scapulohumeral kinematics during specific arm activities analysed. Beyond this, the scapulohumeral kinematics of pathological shoulders may be investigated, and the results used as a diagnostic aid.

However, due to the complex and hidden nature of scapular motion beneath the skin, a number of prerequisite objectives had to be fulfilled. These may be summarised as:

- To develop a non-invasive technique to measure the position and orientation of the scapula and the humerus in the living subject during active arm motion.
- To undertake a thorough validation of the measurement technique, quantifying inter-observer variations and the inherent measurement error.
- To investigate the kinematics of the scapula throughout a range of arm motions including azimuth, elevation and rotation of the humerus across a functional workspace, and not only in abduction and forward flexion of the arm.
- To investigate the inter-subject variability of scapulohumeral kinematics.
- To investigate the differences in scapulohumeral kinematics between dynamic and sequential static motions of the arm.

1.3 LAYOUT OF THE THESIS

Biomechanics is undoubtedly a multidisciplinary subject. Indeed, the work contained within this thesis covers a number of areas, including human anatomy, three dimensional kinematics and a variety of statistical techniques. This thesis is organised to introduce the reader to each of these issues, together with their relevance to the project. Beyond this, the development of the measurement technique, and its application and results in the modelling of three dimensional scapulohumeral kinematics are presented.

Chapter 2 introduces the anatomical structure of the shoulder girdle mechanism, including clinical descriptions of motion at the shoulder. Chapter 3 concentrates on the fundamental issues and theoretical aspects of three dimensional kinematics relevant to the thesis, while Chapter 4 presents a review of literature pertaining to relevant studies concerning the measurement of shoulder motion.

The materials and methods used within this study, including statistical techniques, are detailed in Chapter 5, while Chapter 6 presents the results of validating the measurement technique, examining inter-observer repeatability, inter-subject variability and the measurement error inherent in the system.

Chapter 7 details the development of the scapulohumeral kinematics model, including specifying the workspace over which the model is valid, and issues concerning the data collection and analysis.

Chapter 8 brings together the work and ideas contained within the thesis, and discusses the relevance and implications of the techniques developed and the results obtained, including comparisons with other published studies, while Chapter 9 presents the conclusions of these results, together with recommendations for future development.

Chapter 2

Introduction to the Shoulder Girdle Mechanism

The aim of this chapter is to introduce to the reader the fundamental issues regarding the structure and complexity of the shoulder girdle mechanism. Beginning with a brief introduction to clinical terminology, a description detailing the anatomy of the bones and joints involved is presented. Thereafter, clinical descriptions of motions are discussed, together with their associated inadequacies. The anatomy and function of the shoulder girdle mechanism is then assessed as a kinematic structure of articulations and links.

2.1 CLINICAL TERMINOLOGY

Within the field of medicine, axes and planes are defined in descriptions of anatomy. These axes and planes are also used in descriptions of motion, but this will not be discussed until later.

2.1.1 Anatomical Axes

The *superio-inferior* axis is a vertical axis passing through the body, the *superior* direction being vertically upward with regard to the body in the standing position, the *inferior* being vertically downwards (Figure 2.1).

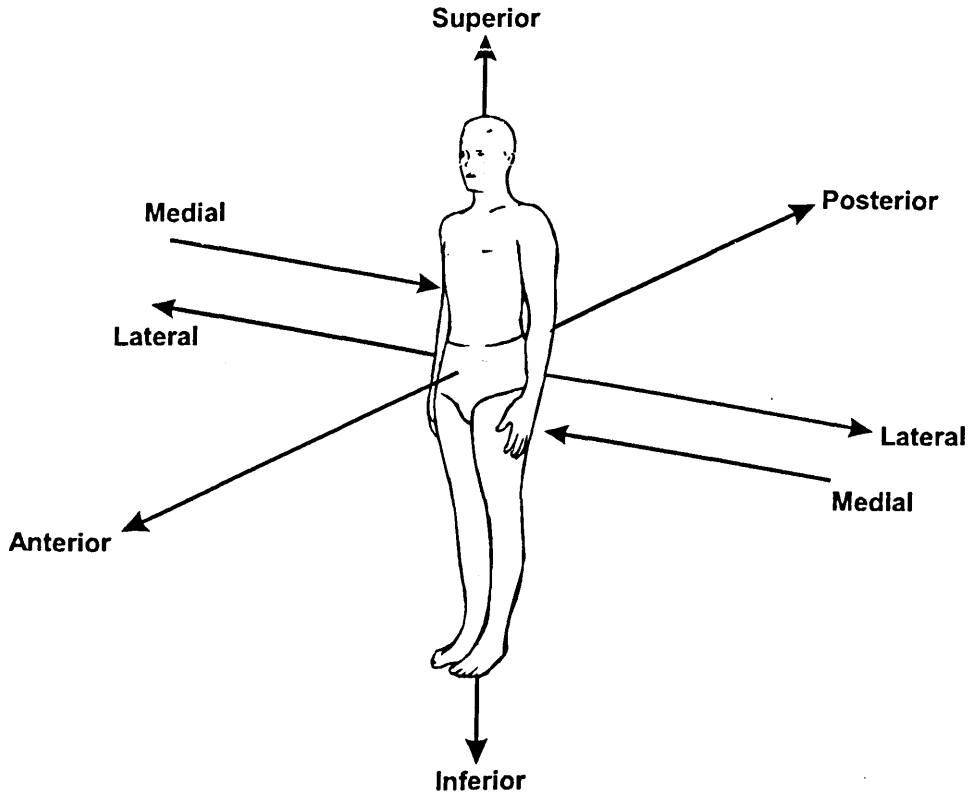


Figure 2.1: Axes of the body (Adapted from Luttgens and Wells, 1989)

The *anterio-posterior* axis is a horizontal axis passing through the body, the *anterior* direction being directly forwards with the body in the standing position, the *posterior* direction backwards (Figure 2.1).

The *medio-lateral* axis is a horizontal axis perpendicular to both the *anterio-posterior* and *superior-inferior* axes, and therefore has the direction of left to right (or *vice-versa*) with respect to the body in the standing position. The *lateral* direction is defined as that away from the centre line of the body, while the *medial* direction is that towards the centre line (Figure 2.1).

2.1.2 Anatomical Planes

The *transverse* (or *horizontal*) plane is any horizontal plane passing through the body normal to the *superior-inferior* axis (Figure 2.2).

The *sagittal* plane is any vertical plane passing through the body in an *anterio-posterior* direction, normal to the *medio-lateral* axis (Figure 2.2).

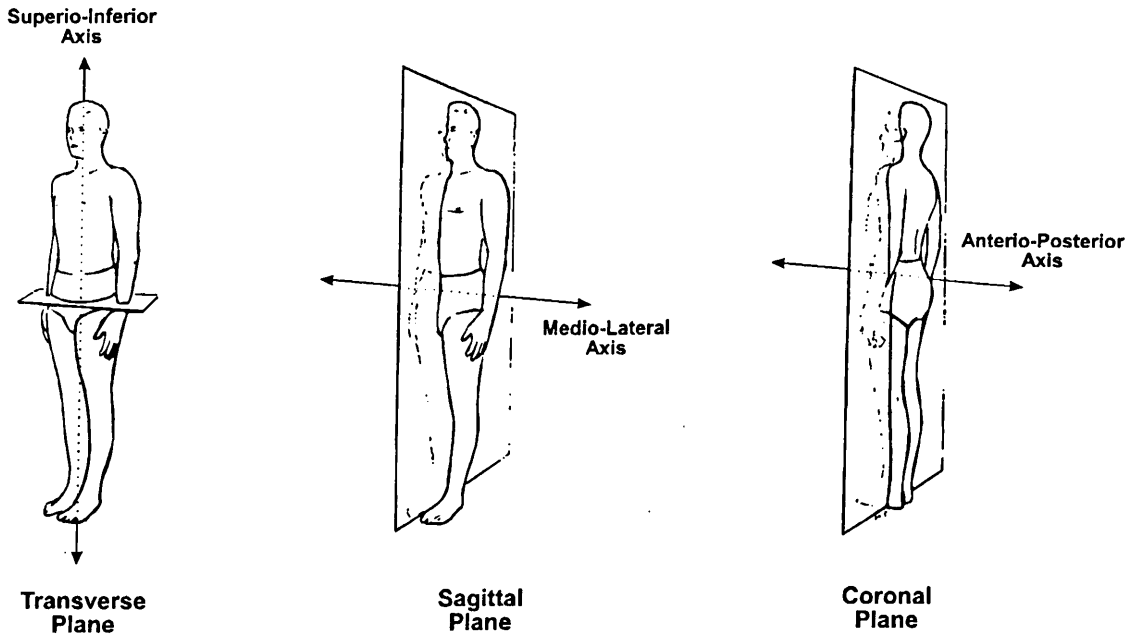


Figure 2.2: Planes of the body (Adapted from Luttgens and Wells, 1989)

The *coronal* (or *frontal*) plane is any vertical plane perpendicular to both the *sagittal* and *transverse* planes. It is therefore normal to the *anterior-posterior* axis (Figure 2.2).

A fourth plane, the *medial* plane, is often referred to. However, this is simply a *sagittal* plane passing through the midline of the body (that is, cutting the body into a left and right half).

2.2 SKELETAL STRUCTURE OF THE SHOULDER GIRDLE MECHANISM

2.2.1 Introduction

Issues concerning kinematic modelling of the shoulder are directly related to the motion of the hard tissues (that is, the bones) of the shoulder girdle mechanism. Considering active, as opposed to passive motion, it is the muscles across articulations which generate the forces necessary to achieve movement. However, this study is not directly concerned with what causes the articulations to move, but the results of these movements in terms of the kinematic structure of the system. As such, a complete anatomical description of the musculature of the shoulder girdle mechanism is not necessary. Besides, such descriptions may easily be found in a multitude of textbooks, and a repetition of these appears superfluous¹. An introduction

¹ For reference, such texts include Grant's Atlas of Anatomy (1983) and Palastanga *et al.* (1994)

to the function of the musculature around the shoulder girdle, in both normal and pathological conditions (due to facioscapulohumeral muscular dystrophy) may be found in the publication included in Appendix 1 (Barnett *et al.* 1996).

Considering the kinematic structure of the shoulder girdle mechanism, it can therefore be stated that the most important elements are those of the skeletal system, that is the bones and the articulations. However, ligaments also play an important role in skeletal kinematics, contributing to both the static and dynamic equilibrium of the structure, imposing constraints and limiting the range of motion at joints.

A description of the bones and introduction to the relevant articulations is hence presented. A detailed account of the articulations is presented later in terms of kinematic descriptions. A clinical description of the ligaments within the shoulder girdle mechanism is also included within the descriptions of the joints. Their kinematic effects are discussed further in Section 2.4.2.

2.2.2 The Bones and Joints of the Shoulder Girdle Mechanism

Regarding the skeletal system of the shoulder girdle mechanism, there are four main elements to consider:

- the sternum (chest bone), articulates at the sternoclavicular joint with,
- the clavicle (collar bone), articulates at the acromioclavicular joint with,
- the scapula (shoulder blade), articulates at the glenohumeral joint with,
- the humerus (bone of the upper arm.)

Together they form an open chain multi-link mechanism between the thorax and the arm (Figure 2.3). In addition to these, the geometry of the thorax must be considered, as it provides a “gliding plane” for the motion of the scapula. This is essentially a partial geometrical kinematic constraint and is discussed later in this context.

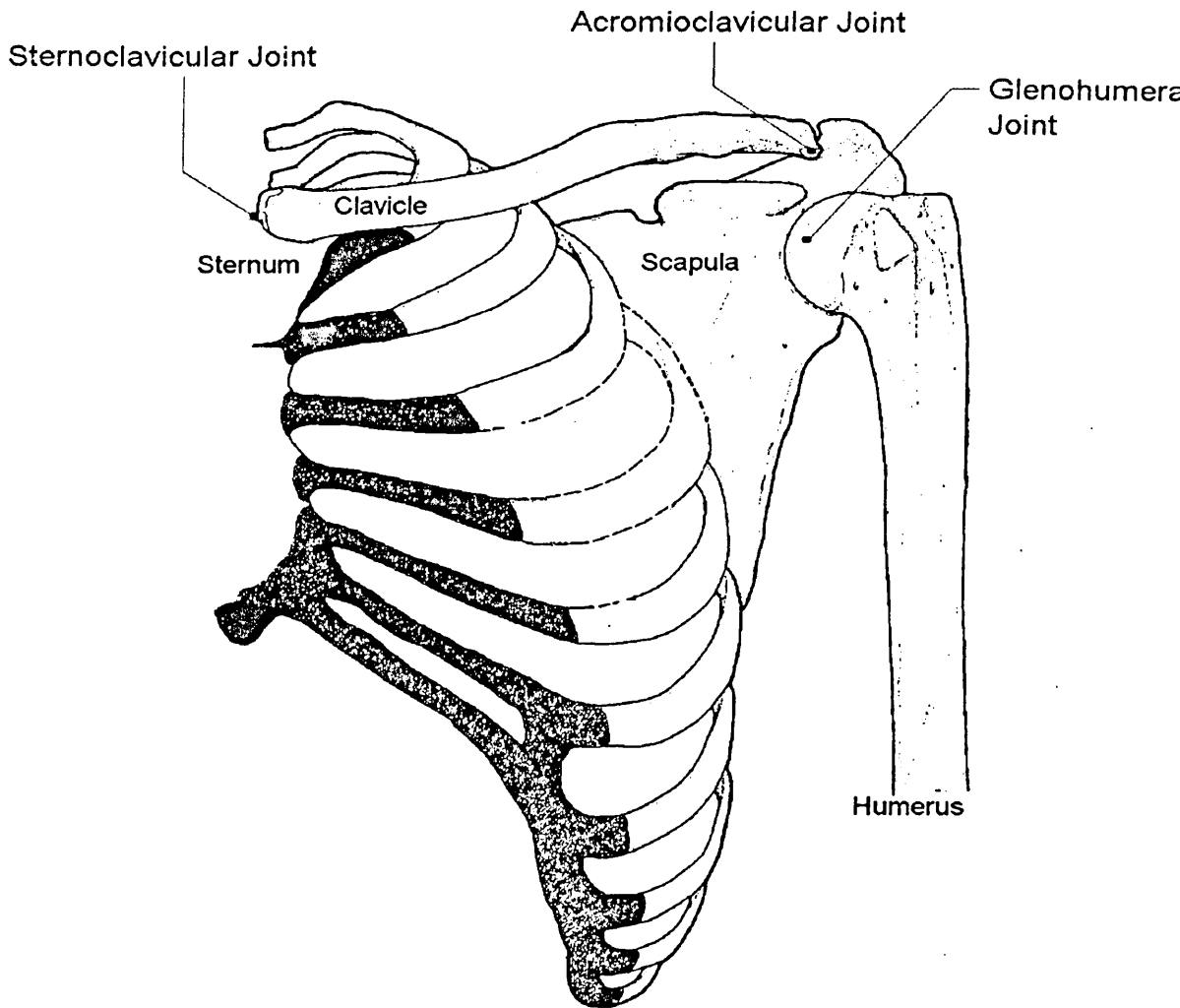


Figure 2.3: Skeletal system of the shoulder (Adapted from Palastanga et al., 1994)

The true definition of the term *girdle* actually refers to any encircling structure or part. In the case of the shoulder girdle, the constituent elements are the clavicle and scapula, so quoting Codman (1934):

“It takes two shoulder girdles to not quite girdle the body”.

For studies involving scapulohumeral kinematics, it is the motion of the shoulder girdle due to activities involving the upper limb which are of interest. To investigate these kinematics fully, both the origin of the motion (the trunk) and the motion of the limb itself must be considered, hence introducing the other elements into the description of the shoulder girdle mechanism.

2.2.2.1 The Sternum

The sternum is a flat narrow bone, situated in the medial line of the front of the chest. In adults, it consists of three pieces. The upper piece is termed the manubrium, and is of greatest concern with regard to upper limb mechanics. The remaining two pieces are termed the gladiolus and the xiphoid.

The superior border of the manubrium provides, at each side, an oval articular surface, for articulation with the sternal end of the clavicle forming the sternoclavicular joint.

The sternum acts as the base on the trunk for the hard tissues of the upper extremity.

2.2.2.2 The Clavicle

The clavicle forms the anterior (forward) portion of the shoulder girdle mechanism, originating from the sternum and lying almost horizontally at the upper part of the thorax, directly above the first rib. It is classed as a long bone, and has a characteristic "S" shape.

As suggested above, it forms the only bony link between the trunk and the upper extremity. Its medial end articulates with the sternum at the sternoclavicular joint while the lateral end joins the acromion of the scapula, forming the acromioclavicular joint.

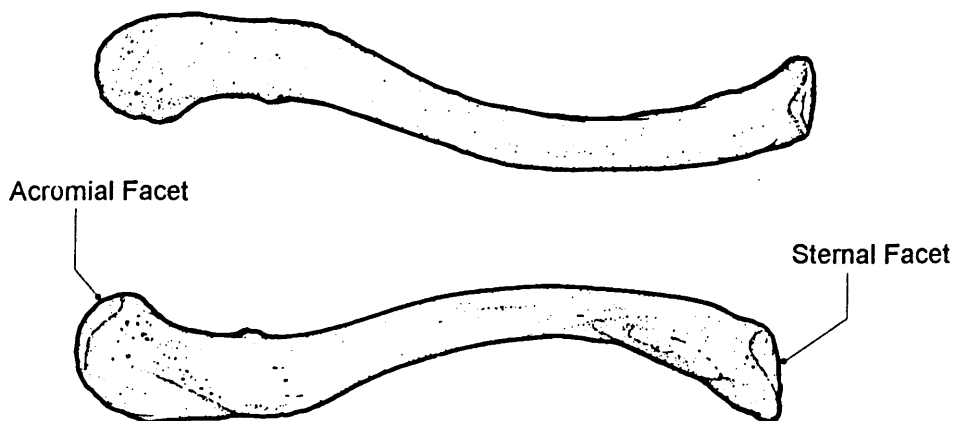


Figure 2.4: The clavicle (Adapted from Palastanga et al., 1994)

2.2.2.3 The Scapula

The scapula is a large, flat triangular bone forming the posterior part of the shoulder. It lies against the thorax, between the first and eighth ribs, with its *medial border* being

about an inch from, and nearly parallel to the spinous processes¹ of the vertebrae. Its other two borders are termed the *superior* and *lateral*, as illustrated in Figure 2.5 and Figure 2.6. Being of triangular form, it naturally possesses three corners, or *angles*, these being termed the *superior*, *inferior* and *anterior angles*. The last of these is sometimes referred to as the *head* of the scapula, and presents a shallow articular surface, known as the *glenoid cavity* or *glenoid fossa*² (Figure 2.6 and Figure 2.7). This is shaped rather like a comma, its vertical dimension being greater than its horizontal. It does not lie vertical, but is angled slightly upwards (by approximately 15°), offering support to the humeral head and forming the glenohumeral joint, the articulation with the humerus. Around the circumference of the glenoid is the labrum. This is a fibrous tissue which essentially deepens the glenoid cavity, offering additional support to the humerus.

The coracoid process protrudes forwards and upwards from the superior border of the scapula, just above the glenoid cavity (Figure 2.6).

The anterior surface of the scapula is slightly concave, uniform with the convex posterior thorax, and is termed the *subscapular fossa* (Figure 2.5).

¹ The term *process* is used in anatomy to refer to a bony prominence.

² The term *fossa* is used in anatomy to refer to a hollow or concave surface.

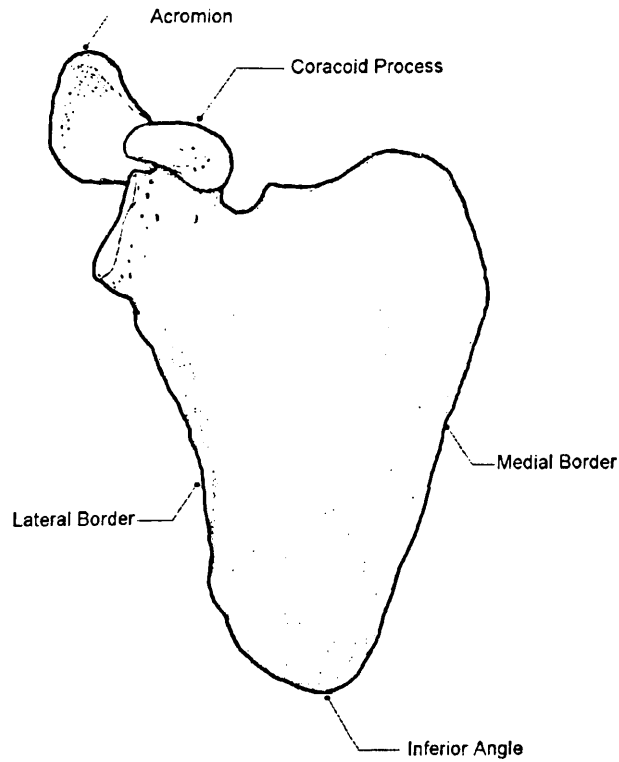


Figure 2.5: Anterior surface of the scapula (Adapted from Palastanga et al., 1994)

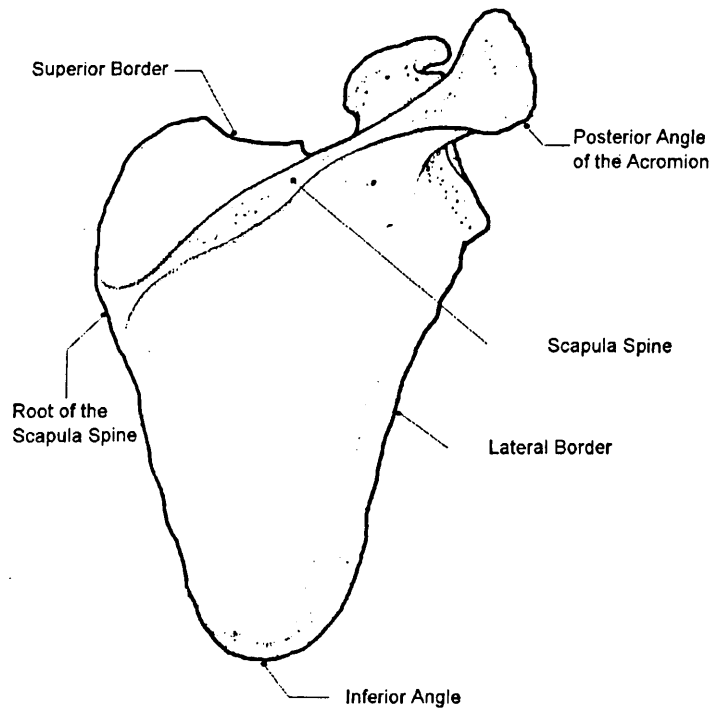


Figure 2.6: Posterior surface of the scapula, illustrating the spine of the scapula, the acromion and the anatomical landmarks (Adapted from Palastanga et al., 1994)

The posterior surface of the scapula reveals a noticeable ridge, rising to form the acromion at its lateral, uppermost edge (Figure 2.6). This is a free projection from the scapula, and provides the point of articulation with the clavicle at the acromioclavicular joint. The ridge itself, known as the *spine of the scapula*, forms a division in the posterior surface. The upper half (the smaller of the two), is termed the *supraspinatus fossa*, the lower part the *infraspinatus fossa*, both relating to muscles of similar names that lie within them.

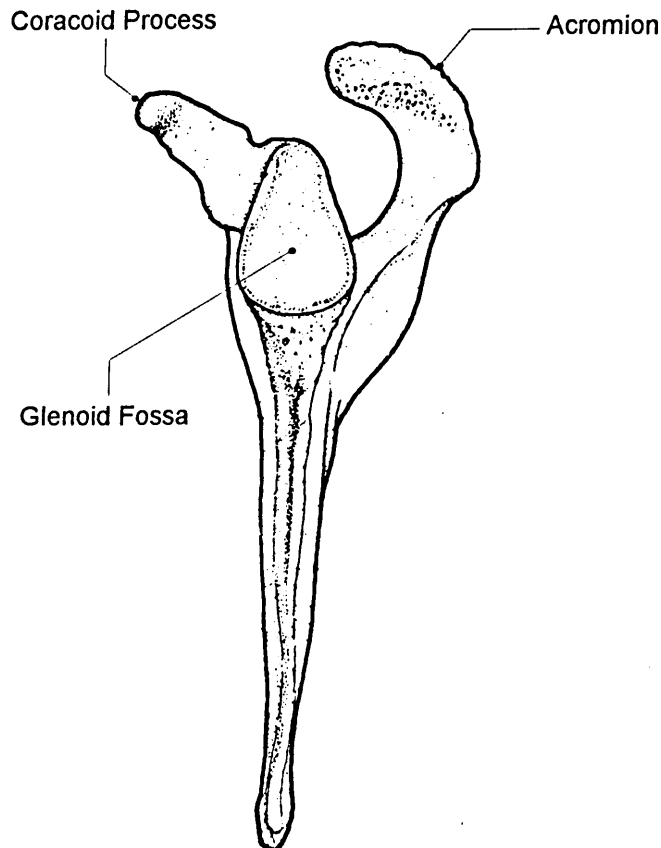


Figure 2.7: Lateral view of the scapula illustrating the glenoid fossa, acromion and the coracoid process (Adapted from Palastanga et al., 1994)

The main purpose of the scapula is to “articulate with the thorax”¹, in order to provide the humerus with a stable, yet mobile base. It is this mobility which allows the upper extremity such a wide range of motion, and gives rise to the term scapulohumeral rhythm.

¹ This term is used loosely, as it is not a true articulation, as discussed later.

2.2.2.4 The Humerus

The humerus is the longest and largest bone of the upper extremity. It consists of a long roughly cylindrical shaft, with an articular extremity at each end (Figure 2.8).

The upper end, which articulates with the scapula at the glenohumeral joint, is generally termed the *head* of the humerus and presents an almost hemispherical smooth surface, facing upwards, inwards and slightly backwards. Coated with cartilage, it forms the articular surface with the glenoid of the scapular.

The lower end of the humerus provides two surfaces for articulation at the elbow with the *radius* and *ulna* (bones of the forearm).

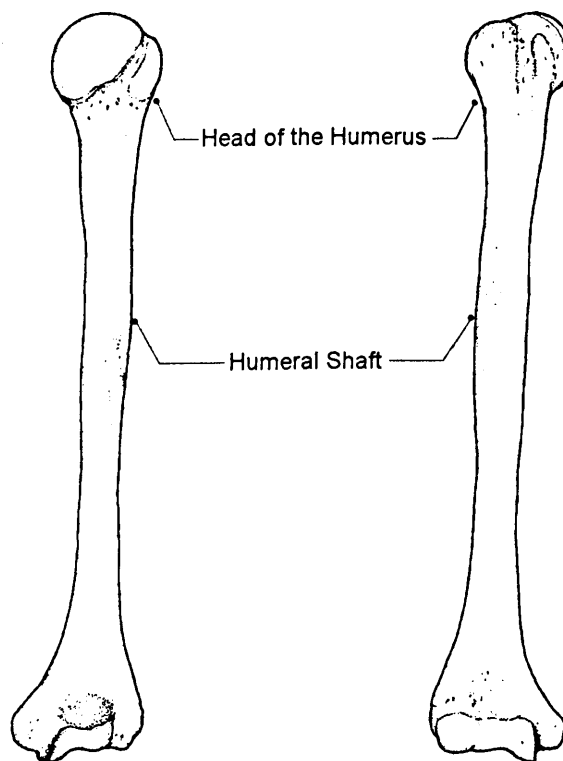


Figure 2.8: The humerus (Adapted from Palastanga et al., 1994)

2.3 CLINICAL DESCRIPTIONS OF MOTION

Throughout the clinical profession, human movement is generally described in terms of movements in the anatomical planes of the body (defined in Section 2.1.2). It is not difficult to show the inadequacies of these descriptions, and the need for alternative, more quantitative methods.

2.3.1 Abduction and Adduction

Abduction is defined as movement in the coronal plane in a direction away from the medial plane, for example, raising of the arm away from one's side, as viewed from in front or behind. By definition, this description of motion is only valid up to an abduction angle (that made by the limb and the medial plane) of 90° , after which point further raising of the arm brings it closer to the body once more.

The term elevation is used to describe raising the arm in any plane, up to or beyond 90° . Abduction above 90° may therefore be described as elevation in the coronal plane.

Adduction is movement in the coronal plane in a direction toward the medial plane, lowering of the arm from 90° abduction back to one's side (Figure 2.9).

2.3.2 Flexion and Extension

Flexion is applied to the movement which carries the limb forwards in the sagittal plane, or bends (flexes) the limb, for example, raising one's arm forward as viewed from the side.

Extension refers to the movement which carries the limb backwards. In the case of the elbow or knee, extension is used to describe the motion which straightens (extends) the limb from a flexed position.

In the shoulder girdle mechanism, flexion can occur in both the sagittal and transverse planes. In the latter case, the terminology applied is horizontal flexion and horizontal extension (Figure 2.9).

2.3.3 Rotation

Rotation of a limb is the term applied to movement in which the limb is turned around its own longitudinal axis. With regard to the shoulder girdle mechanism, this may be considered to occur in the clavicle and the humerus.

The scapula does not possess an obvious axis, and rotation is a complex motion which may be defined as a composite of three rotations about orthogonal axes. Such descriptions of motion are discussed further in Chapter 3.

Rotation of the humeral head in the glenoid is only obvious when the forearm is flexed, preferably to 90° . Without flexion of the elbow, humeral rotation cannot be distinguished from pronation/supination of the wrist when observing the final position of the hand.

Humeral rotation may be described as internal or external rotation, depending upon the direction of movement about the long axis of the bone. With the arm in its normal resting position by one's side and the elbow flexed to 90°, internal rotation turns the hand medially, towards the body, while external rotation turns the hand laterally, away from the body (Figure 2.9).

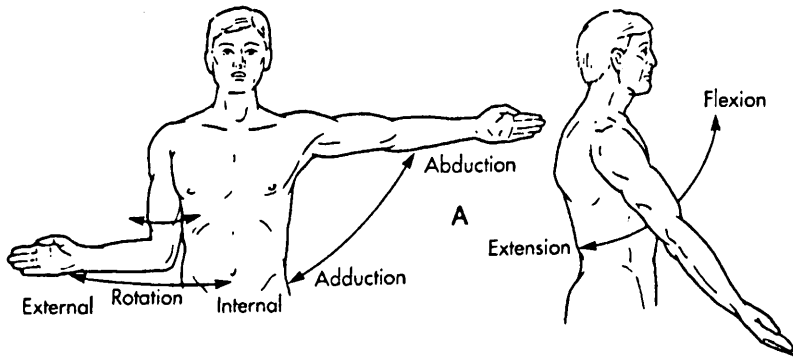


Figure 2.9: Clinical movements of the shoulder (Hollinshead, 1991)

2.3.4 Clinical Descriptions of the Motion of the Shoulder Girdle

Motion of the shoulder may be defined by the terms illustrated in Figure 2.10. Each of these terms are described below.

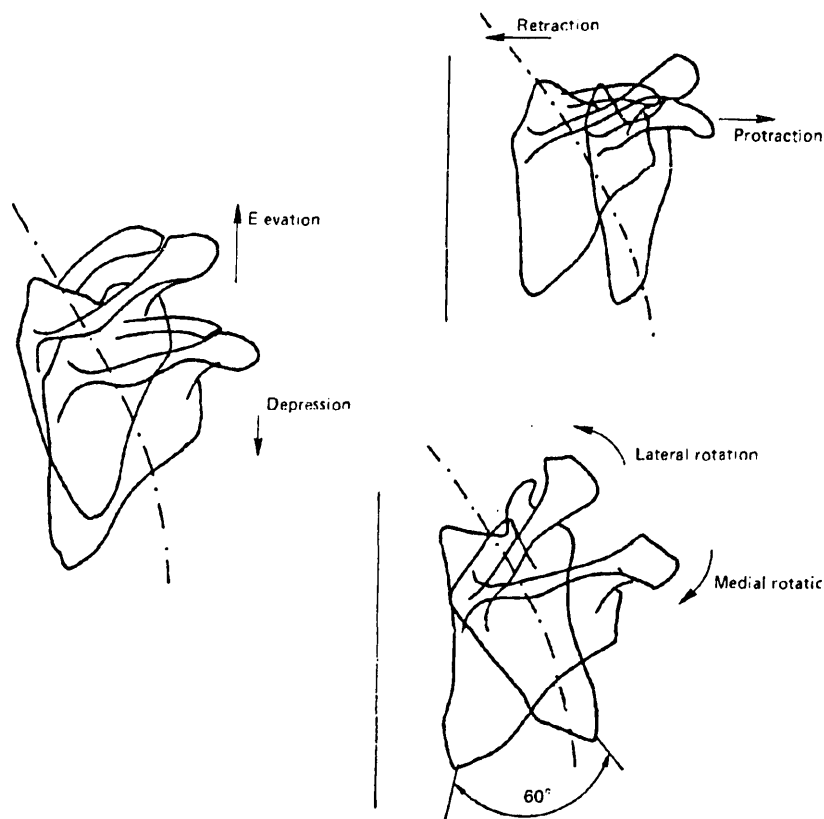


Figure 2.10: Clinical descriptions of the motions of the scapula (Palastanga et al., 1994)

Protraction is characterised by motion of the medial border of the scapula in a direction away from the vertebral column, while maintaining parallel to it. It therefore represents the scapula moving forwards and around the chest wall.

During retraction, the medial border of the scapula moves closer to the vertebral column, while maintaining parallel to it. The scapula therefore moves around the chest wall towards the medial plane.

Elevation is characterised by motion of the scapula in a superior (upwards) direction. Such motions occur, for example, during the shrugging motion, lifting the entire pectoral girdle, whereas depression involves the scapula moving in an inferior (downwards) direction. Also, elevation is connected with rotations of the scapula about a horizontal axis, or an axis along the scapula spine. Such rotations are generally referred to as tilting or tipping of the scapula.

What is commonly referred to as lateral rotation of the scapula is a complex motion in which the inferior angle moves laterally around the chest wall. The glenoid cavity is thus turned to face increasingly upwards. Such motion typically occurs during elevation of the arm or abduction.

During medial rotation, the inferior angle of the scapula moves medially around the chest wall. The glenoid cavity is thus turned to face increasingly downwards. Such motion typically occurs during adduction.

It is important to realise that these motions occur simultaneously during humeral motion. For example, during abduction of the arm, the scapula will tend to rotate laterally, while elevating and retracting. It may also tend to tip backward about an axis along the scapula spine, although clinical descriptions for this motion do not appear to exist.

2.3.5 Three Dimensional Finite Rotations and *Codman's Paradox*

Although the above descriptions may cover the movements available at the shoulder joint, it is difficult to specify precisely a position using these descriptions. This is further complicated due to the non-commutative nature of finite rotations. That is, when a rigid body is subjected to sequence of three finite rotations around three separate axes, the sequence of the rotations will effect the final position of the body. This and other issues regarding three dimensional rigid body kinematics are discussed further in Chapter 3.

The same may be said of the shoulder, and may be illustrated by *Codman's paradox* (Codman 1934). Beginning with the upper arm hanging vertically by the side, with the elbow flexed to 90° (forearm pointing directly forwards), the arm is raised away from the body in the coronal plane (abduction) to 90° . If the shoulder is then flexed in the horizontal plane so that the upper arm points forwards, and lowered in the sagittal plane (extension), the forearm will point laterally across the body when the arm returns to one's side. Hence, during this motion, an involuntary internal rotation of 90° has occurred. If the motion is repeated, but in the reverse order, the result will show an involuntary external rotation. This result is a consequence of the non-commutative nature of three dimensional rotations, and is therefore not a paradox at all, but demonstrates Codman's lack of appreciation of such rotations. Furthermore, it illustrates one of the many inadequacies of describing motions of the upper limb using the clinical terms.

Hence it can be seen that in a joint with three degrees of freedom, a more specific method of quantifying movements is desirable. Many descriptions have been presented in the literature, but most of them rely on the reader possessing a thorough knowledge of three dimensional rigid body kinematics. As such, these quantitative descriptions are discussed in the following chapter.

2.4 KINEMATIC DESCRIPTIONS OF ANATOMY

Considering the kinematics of the shoulder girdle mechanism, clinical anatomy serves as an introduction to the geometry of the structures involved. However, clinical descriptions of motion are inadequate as complete kinematic descriptions of motion as they do not define the possible combinations of motion available at each joint, and as such are limited in their application to kinematic analysis. A more useful approach is to examine the mechanics of each joint in terms of its degrees of freedom and kinematic constraints, providing an understanding of anatomical systems as mechanical linkages.

Before presenting such an analysis of the shoulder girdle mechanism, it is useful to introduce some kinematic aspects of the anatomical structures concerned.

2.4.1 Passive and Active Soft Tissues

Soft tissues may be broadly divided into two categories, those which contribute in active motion and those which contribute in passive motion. Active tissues consist of the muscles, while passive tissues include ligaments, joint capsules and fibrous cartilage. It must be stated however, that ligaments may also contribute in active motion. While not generating the motion themselves, their effect as kinematic constraints play an important role in the range and direction of motion available at joints.

It was stated earlier that in kinematic studies, the actions of muscles can largely be ignored. However, the tendinous insertions and origins of muscles often provide passive constraints to joint motion and hence have an effect on the kinematics of the system.

It is the passive structures which are hence of most interest.

2.4.2 Function of Passive Tissues

Ligaments are bands or sheets of tough, fibrous connective tissue. They have two primary purposes; firstly to inhibit movement beyond a certain range, thereby imposing a direct kinematic constraint, and secondly as connective tissues surrounding the articulations within the skeletal system.

The ends of bones entering a moveable joint are united by a strong flexible membrane, referred to as the joint capsule. This is a ligamentous structure which completely surrounds the joint, playing an important part in its kinematics. Although

the type of movement allowed at a joint usually depends primarily on the shape of the articular surfaces, ligaments offer a large degree of restraint, thereby imposing mechanical constraints on ranges and type of motion available to the joints by limiting the degrees of freedom available. This capsular restriction is illustrated in Figure 2.11. (a) shows the joint in a neutral position with the ligamentous capsule slack. When rotation occurs (b), the capsule becomes taut and limits motion.

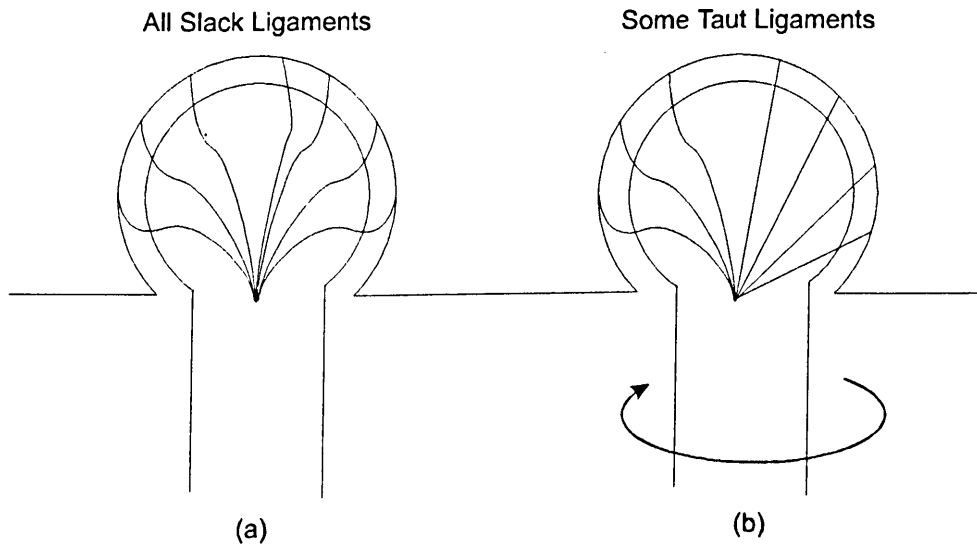


Figure 2.11: Ligamentous restriction of motion at joints

Ligaments also occur separately from joint capsules. However, their primary function remains the same, that is, to provide kinematic constraints and control on the range of movement.

2.4.3 Classification of Articulations

Articulations in the body fall under a number of classifications. Of greatest interest, and by far the most common of these are synovial joints. Here, the bearing surfaces are covered with firm, smooth articular cartilage, and slide on one another in a narrow cavity containing synovial fluid.

Synovial joints may be further subdivided into congruous and incongruous joints.

In a congruous joint, the concave surface is uniform with the convex surface, forming a true hinge or ball and socket joint in which the articular surfaces remain equidistant from each other at all points along the circumference (Figure 2.12).

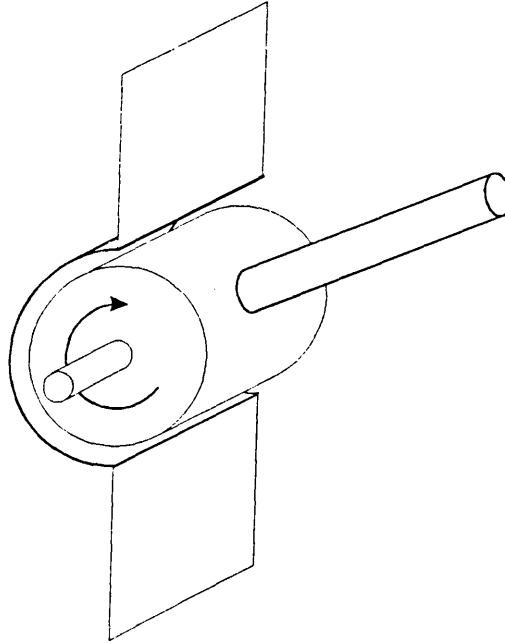


Figure 2.12: Illustration of a congruous joint with one degree of freedom

The elbow may be approximated to a hinge joint, in which the rotation occurs about a fixed axis and the joint possess just one degree of freedom.

A congruous ball and socket joint possess three degrees of freedom. This is the maximum number of degrees of freedom allowable for any congruous joint as translations of the "ball" within the "socket" are not possible due to the joint geometry.

In an incongruous joint, the concave surface is more shallow than that of the convex surface, forming what is sometimes referred to as a *cup and saucer* (rather than a ball and socket) joint. The distance between the articular surfaces therefore varies across the joint (Figure 2.13).

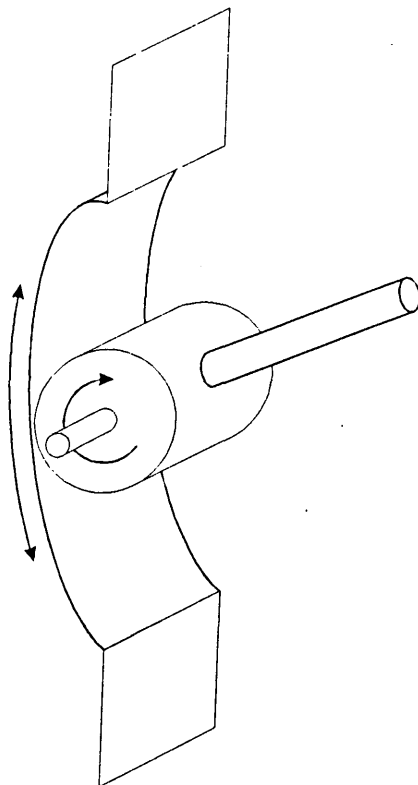


Figure 2.13: Illustration of an incongruous joint with two degrees of freedom

During articulation, the axis of rotation may shift, and the movements at the joint can comprise of ball "gliding" or sliding along the articular surface in addition to rolling. The joint may therefore possess up to six degrees of freedom. Rotation may be allowed about the three orthogonal axes within the joint, whilst the lack of geometrical constraints may also allow for translations of the articular surfaces relative to each other.

2.5 KINEMATIC ANATOMY OF THE SHOULDER GIRDLE MECHANISM

2.5.1 Introduction

A description of the kinematics of the shoulder girdle mechanism must include a description of the links, formed by the bony structures, and articulations within the system. The bones of the shoulder girdle mechanism have already been presented (Section 2.2), hence it remains to discuss the structural form of the connecting articulations between these bones, including a discussion on the degrees of freedom available at each joint, thereby defining the kinematics of the shoulder complex.

Beyond this, the nature of the rotations and translations allowed at the joints, together with the kinematic constraints imposed on these motions must be considered.

The clavicle, scapula and humerus, together with their base on the thorax, the sternum, form the rigid links of the shoulder girdle mechanism. Their kinematics require consideration of four articulations, these being;

- the sternoclavicular joint.
- the acromioclavicular joint.
- the glenohumeral joint.
- the scapulothoracic articulation.

The first three of these are true synovial joints. The fourth however, although not strictly a joint, must also be considered as it makes an important contribution to the kinematics of the shoulder girdle mechanism.

2.5.2 The Sternoclavicular Joint

This joint provides the only point of bony connection between the upper limb and the trunk. Although the joint is functionally a ball and socket joint, it does not have the form of such. The joint is not particularly congruous as the articular surfaces of the clavicle and sternum do not usually have similar radii of curvature. Congruency is partly provided by an inter articular fibrocartilaginous disc, mating the two surface more closely (Figure 2.14).

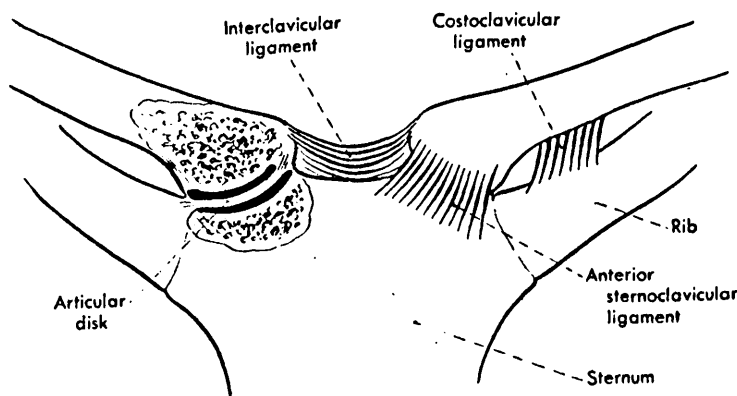


Figure 2.14: The sternoclavicular joint (Hollinshead, 1991)

In common with all synovial joints, a fibrous joint capsule surrounds the entire joint; attaching to the articular margins of both the sternum and the clavicle. Although the capsule is relatively strong, it is further reinforced anteriorly, posteriorly and medially by the anterior and posterior sternoclavicular ligaments and the interclavicular

ligament respectively. In addition to these, a further short, dense ligament attaches between the medial end of the clavicle and the first rib, the costoclavicular ligament. Its main function is to limit elevation of the clavicle, although it is also active in preventing excessive forwards or backwards movements of the medial end of the clavicle.

The joint allows the clavicle three degrees of freedom; elevation and depression, protraction and retraction and axial rotation. The lateral end of the clavicle may therefore describe an area represented by the surface of a sphere with a radius equal to the length of the clavicle.

2.5.3 The Acromioclavicular Joint

This incongruous joint connects the clavicle to the scapula. The articular surfaces involved are small, being oval in shape, with a flat or slight convex facet on the lateral end of the clavicle, and a similarly shaped flat or slightly convex facet on the acromion.

A relatively loose capsule surrounds the joint, this being thickened above the joint where it is reinforced by muscular fibres. The superior and inferior acromioclavicular ligaments also offer strength to the capsule above and below the joint (Figure 2.15).

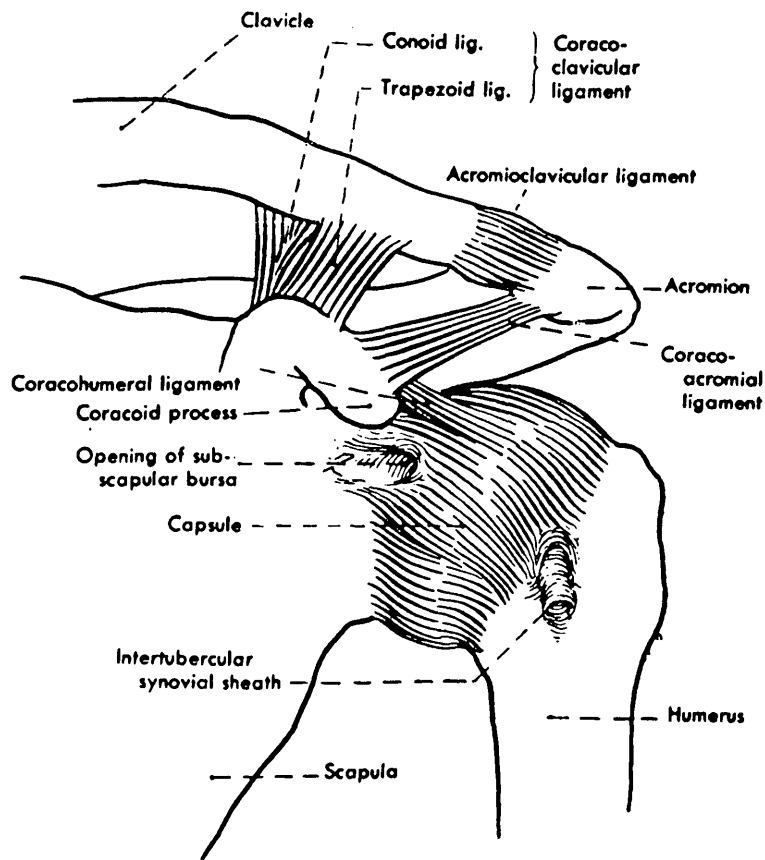


Figure 2.15: The acromioclavicular joint (Hollinshead, 1991)

The constraints at the joint are further increased by the coracoclavicular ligament. This extremely powerful ligament anchors the lateral end of the clavicle to the coracoid process of the scapula. It is split into two parts, these being termed the conoid (the more medial section) and the slightly more laterally placed trapezoid, named after their respective shapes (that is, conical and trapezoidal). Their function is to restrain rotations of the scapula with respect to the clavicle, while offering it support, as the scapula is suspended at two points by the clavicle, the acromioclavicular joint and the attachment of the coracohumeral ligament..

The joint allows the scapula three degrees of freedom, enabling it to rotate about a vertical (superior-inferior) axis, and about both horizontal axes (the anterior-posterior and medial-lateral axes).

Coupled with the three degrees of freedom available at the sternoclavicular joint, it would appear that the scapula is allowed a six degrees of freedom, three rotational components and three translational components due to the translations of the lateral end of the clavicle. However, the lateral end of the clavicle is constrained to move about the surface of a sphere defined by its length. The co-ordinates of the

acromioclavicular joint are therefore also constrained to this sphere, imposing a constraint equation on the kinematics of the scapula. The scapula hence possesses five degrees of freedom. However, due to the subject dependent nature of the kinematic constraint offered by the clavicle, it is still necessary to measure the kinematics of the scapula in six degrees of freedom. The extent of the constraint may be subsequently investigated by examining the x , y , z displacements of the acromion. The magnitude of these displacement vectors, relative to the sternoclavicular joint, may be directly compared with the length of the clavicle. Similarly, over a number of arm positions, these displacement vectors should all lie on the surface of a sphere. Using measured data, this will not be true for all points due to the error in the measurement system. However, the residual errors of performing the spherical surface fit may be investigated.

2.5.4 The Glenohumeral Joint

The glenohumeral joint is the articulation between the head of the humerus and the glenoid cavity of the scapula. It is an incongruous synovial joint capable of very large ranges of motion.

The articular surfaces of this joint are the relatively large, rounded head of the humerus, and the comparatively shallow glenoid cavity. Their union contributes little to the stability of the joint, some of which is provided for by the fibrous rim of the labrum around the edge of the glenoid cavity (Figure 2.16).

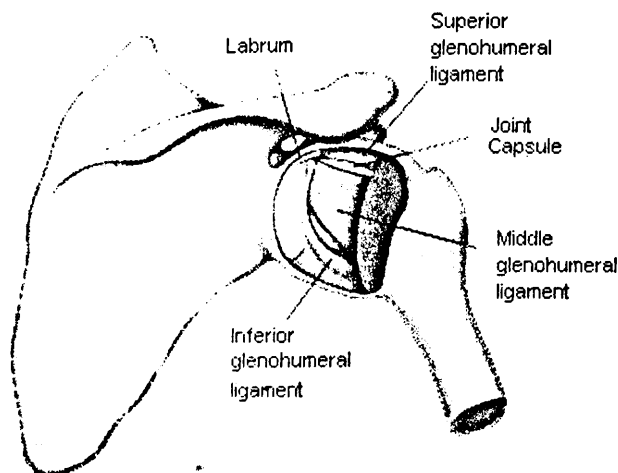


Figure 2.16: The glenohumeral joint (Adapted from Neer, 1990)

The fibrous capsule of the joint forms a loose cylindrical sleeve between the two bones. The anterior part of this capsule is strengthened by the presence of three

glenohumeral ligaments (superior, middle and inferior). The superoposterior (upper behind) part is strengthened by the coracohumeral ligament.

The majority of the stability of the joint is provided by the active tissues comprising the *rotator cuff* muscles. These are a group of four muscles which unite the humeral head with the scapula, providing dynamic control and stability.

Due to the incongruous structure of the joint, it possesses five degrees of freedom, being capable of rotation about any axis (three degrees of freedom) together with sliding of the humeral head within the glenoid both vertically and horizontally. It may be argued that a limited amount of motion is available in the lateral direction, pulling the two articular surfaces apart. However, this motion does not generally occur in normal joint motion, and as such is not considered as a sixth degree of freedom.

The glenohumeral joint may be considered as the final joint in the shoulder mechanism. Adding to this the six degree of freedom mobility of the scapula provided by the combination of the sternoclavicular joint and the acromioclavicular joint illustrates the complexity of the shoulder girdle mechanism, and demonstrates how the upper extremity can possess a range of motion capable of performing the excursions for which it is called upon. It also explains why the shoulder is regarded as the most complicated "joint" in the human body.

2.5.5 The Scapulothoracic Joint

The mobility of the clavicle allows the scapula not only rotational movements about the acromioclavicular joint, but also translation. This translation therefore requires articulation of the scapula upon the posterior wall of the thorax, giving rise to the scapulothoracic "joint". This may be more precisely defined as a gliding plane, as the scapula essentially slides upon the surface of the thorax which acts as a geometrical kinematic constraint. Although the scapulothoracic joint has no passive tissue stabilising its structure, the articular surfaces on both the anterior and posterior sides of the scapula are lined with fascia, a soft fibrous tissue providing a smooth surface for the gliding action of the scapula upon the thoracic cage.

2.6 CONCLUDING REMARKS

This chapter has introduced some elements of clinical terminology, together with an introduction to the structure and complexity of the shoulder girdle mechanism.

The freedom of movement allowed to the scapula and humerus are evident by analysing the degrees of freedom at each of the series of joints, and it should be reinforced that to describe fully the motions of the scapula requires measurement of all six degrees of freedom.

With regard to descriptions of motion, it is evident that clinical terminology alone is inadequate. As a consequence of these inadequacies, the following chapter investigates the development of kinematic descriptions of motion, and their application in describing human joint movements, specifically, that of the shoulder.

Chapter 3

Three Dimensional Kinematics

This chapter presents the fundamental issues and theoretical aspects of three dimensional kinematics relevant to this thesis.

Starting with an introduction to the concepts involved, the chapter continues to discuss various forms of representing orientation, including those relevant to describing anatomical kinematics. Further to this, complete kinematic descriptions are discussed, together with methods of co-ordinate transformations.

3.1 THREE DIMENSIONAL RIGID BODY MOTION

In order to measure the position of an object, a co-ordinate system needs to be defined to which measurements can be referred. This will consist of a set of three orthogonal axes, the intersection of which forms the origin of a three dimensional co-ordinate system. Beyond this, a set of rules governing the notation of measures needs to be stated. These rules, taken from Craig (1989) are defined as follows:

- 1 Usually variables written in uppercase represent vectors or matrices. Lowercase variables are scalars.
- 2 Leading subscripts and superscripts identify which co-ordinate system a quantity is written in. For example, ${}^A P$ represents a position vector written in co-ordinate system $\{A\}$, and ${}_B^A R$ is a rotation matrix that specifies the relationship between co-ordinate systems $\{A\}$ and $\{B\}$.
- 3 Trailing superscripts are used (as widely accepted) for indicating the inverse or transpose of a matrix, for example, R^{-1} , R^T .

The terms used above will become more clear in the following discussion.

3.1.1 Displacements: The Position Vector

With a defined co-ordinate system established, it is possible to specify the position of an object by means of a position vector. This is a three component column vector (3×1) labelled ${}^A P$, as it describes the position of P relative to the co-ordinate system $\{A\}$ (Figure 3.1).

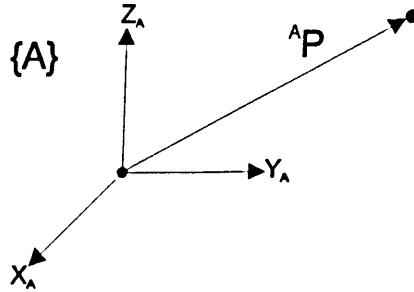


Figure 3.1: Position vector defined relative to co-ordinate system $\{A\}$

Each of the three elements of ${}^A P$ are the distances along the three axes of $\{A\}$, and can be represented as:

$${}^A P = \begin{bmatrix} p_x \\ p_y \\ p_z \end{bmatrix} \quad (3.1)$$

3.1.2 Orientations: The Rotation Matrix

Complete measurement of the position of a rigid body in three dimensional space requires knowledge not only of its displacement along prescribed axes, but also its orientation with respect to these axes, providing all six degrees of freedom. The position vector describes where a single point on a body lies. The body itself could be in any number of orientations about this point (Figure 3.2).

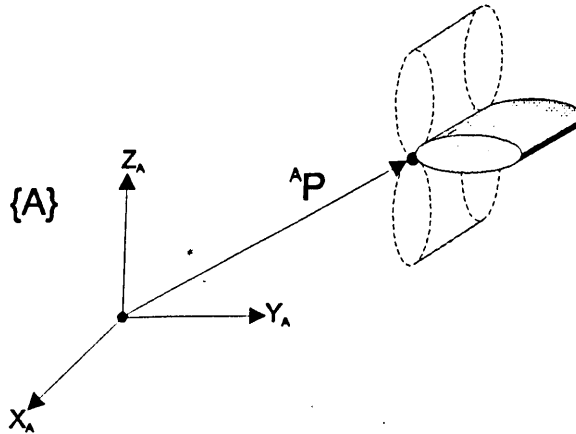


Figure 3.2: Possible orientations of an object with a known position vector

In order to define the orientation of a body with respect to the defined co-ordinate system, it is necessary to attach a co-ordinate system to the body itself. With this in place, it is possible to define a description of this co-ordinate system relative to the reference co-ordinate system $\{A\}$. This description consists of the direction cosines between each of the three axes of the body co-ordinate system $\{B\}$ and their equivalent axes in the reference system $\{A\}$. These are combined to form a nine element (3x3) rotation matrix.

The direction cosines of the axes can be determined by examining a unit vector in the direction of any of the axes. Considering, for example a unit vector ${}^B\hat{X}$ along the X axis of the body co-ordinate frame $\{B\}$ (Figure 3.3).

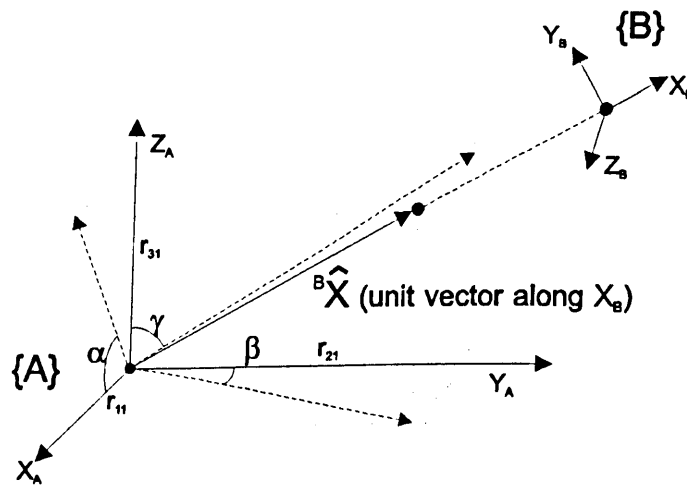


Figure 3.3: Direction cosines of a unit vector

The direction cosines of this vector, relative to the co-ordinate system $\{A\}$ are the cosines of the angles α , β and γ about the x , y and z axes respectively, or r_{11} , r_{21} and r_{31} if the scalar displacements are quoted rather than the angles ($\cos(\alpha)=r_{11}$ etc.). Hence the X axis of $\{B\}$ relative to the X axis of $\{A\}$ is described by the relationship;

$${}^B\hat{X} = \begin{bmatrix} \cos(\alpha) \\ \cos(\beta) \\ \cos(\gamma) \end{bmatrix} = \begin{bmatrix} r_{11} \\ r_{21} \\ r_{31} \end{bmatrix} \quad (3.2)$$

Similar relationships may be obtained for the Y and Z axes of $\{B\}$. Combining these single axis definitions yields the rotation matrix which describes the orientation of $\{B\}$ relative to $\{A\}$, ${}^A_R{}^B$. Hence,

$${}^A_B R = \begin{bmatrix} {}^A\hat{X}_B & {}^A\hat{Y}_B & {}^A\hat{Z}_B \end{bmatrix} = \begin{bmatrix} r_{11} & r_{12} & r_{13} \\ r_{21} & r_{22} & r_{23} \\ r_{31} & r_{32} & r_{33} \end{bmatrix} \quad (3.3)$$

It is also possible to perform transformations between co-ordinate systems using these relationships. That is, the orientation of $\{A\}$ or $\{B\}$ may be described relative to any other known co-ordinate system. This important concept is discussed further in Section 3.1.4.

3.1.3 Displacements and Orientations : The Frame

It has been shown how to specify (i) the position and (ii) the orientation of a body in three dimensional space, relative to a defined co-ordinate system. The combination of these two descriptions fully describes the whereabouts of a rigid body, and is termed the Frame. It may be represented as a 4x4 matrix (Denavit and Hartenberg, 1955), in which the first 3x3 elements are the rotation matrix, followed by the 3x1 position vector as shown below.

$${}^A_B T = \begin{bmatrix} {}^A_B R & {}^A_B P \\ 0 & 1 \end{bmatrix} = \begin{bmatrix} r_{11} & r_{12} & r_{13} & p_x \\ r_{21} & r_{22} & r_{23} & p_y \\ r_{31} & r_{32} & r_{33} & p_z \\ 0 & 0 & 0 & 1 \end{bmatrix} \quad (3.4)$$

However, within this text, such representations are not necessary. The purpose of this is to make the reader aware that the motions of one frame quoted relative to another frame provides a complete description of the rotations and displacements between the two entities.

3.1.4 Co-ordinate Transformations

In Section 3.1.2, the concept of transforming rotations from one frame to another was introduced. Such transformations may be applied to both rotations and displacements.

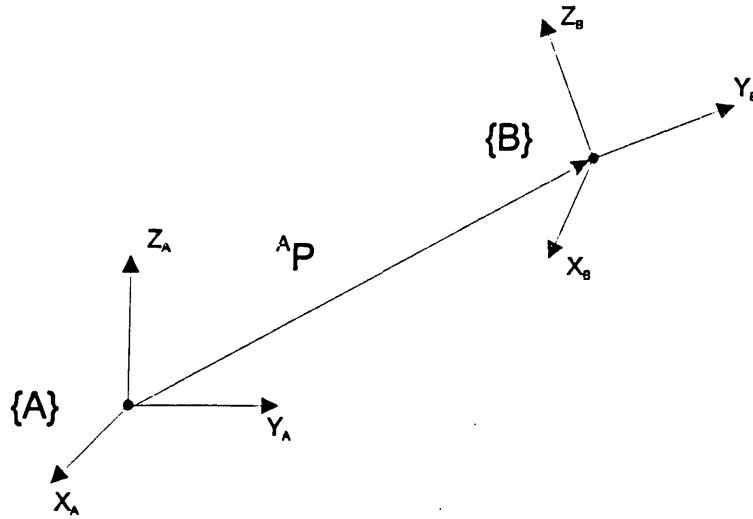


Figure 3.4: Co-ordinate transformations between two frames

The vector AP in Figure 3.4 defines the position of the origin of $\{B\}$ in the frame of $\{A\}$. The rotation matrix describing the rotation of $\{B\}$ relative to $\{A\}$ is ${}^A_B R$. The rotation matrix which describes the orientation of $\{A\}$ relative to $\{B\}$, ${}^B_A R$ is simply the transpose of this:

$${}^B_A R = {}^A_B R^T \quad (3.5)$$

Similarly, a vector BP , describing the position of the origin of $\{A\}$ in the frame of $\{B\}$ may be defined as

$${}^BP = -{}^A_B R^T \cdot {}^AP \quad (3.6)$$

These concepts may be applied to more general cases, where compound transformations between one or more frames are necessary, as is the case for investigating the three dimensional kinematics of scapulohumeral rhythm.

3.2 REPRESENTATION OF ORIENTATION

3.2.1 Introduction

Although rotation matrices provide a full mathematical description of the orientation of a body in three dimensional space, they do not allow for convenient visualisation or representation of objects. An alternative representation of orientation presents itself as a sequence of three rotations about defined axes. However, whereas translations along three mutually perpendicular axes are relatively easy to visualise, rotations are

far less intuitive. One of the reasons for this is that sequential rotations about axes are non-commutative. That is, a fixed rotation about the X , then Y , then Z axes does not give the same result as the same rotation about an axes sequence Y, Z, X . As such rotations are derived from rotation matrices, this result is not altogether surprising, as matrix multiplication is generally non-commutative also.

Nevertheless, three angle rotations sequences provide a more obvious method of representing orientation than the rotation matrices themselves. As such, these, together with other methods of describing orientation are discussed in the subsequent sections.

3.2.2 Euler Angles

Euler angles are probably the most frequently used method of representing orientation in biomechanics. They may be defined relative to any axis sequence (providing at least two axes are used), but for this discussion the sequence Z, Y', X'' will be used, conforming to the Polhemus[®] descriptions and that used by Goldstein (1980). This and other sequences will be adopted throughout this thesis.

Given a reference frame $\{A\}$, and a body attached frame $\{B\}$, the Euler angle rotations between the two frames may be described as follows:

Starting with $\{A\}$ and $\{B\}$ coincident, rotate $\{B\}$ about Z_B by an angle α , then rotate about Y_B by an angle β and finally about X_B by an angle γ (Figure 3.5)

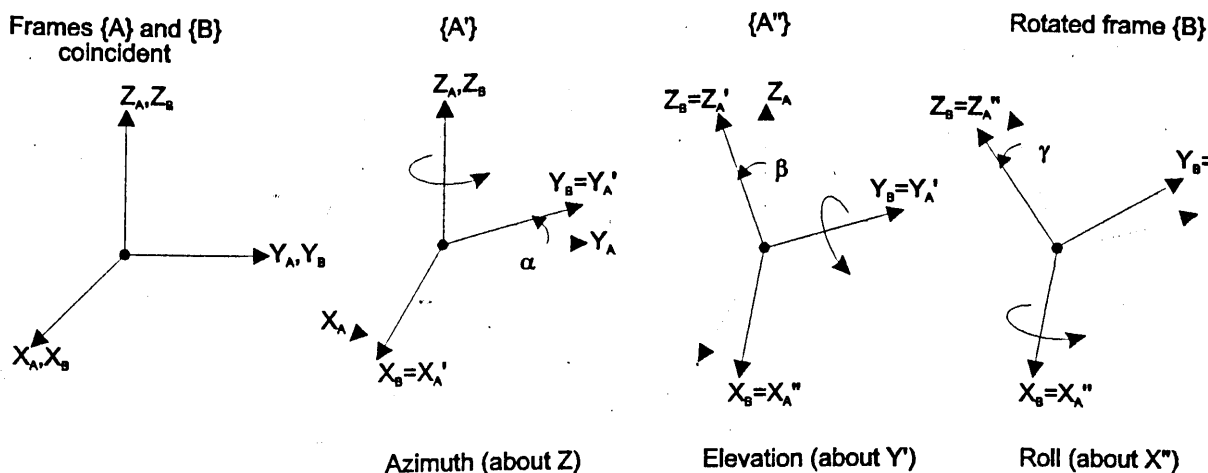


Figure 3.5: Euler angle definitions

It is important to note that each rotation occurs about an axis of the moving frame $\{B\}$ (or rather one of the intermediate frames $\{A'\}$ or $\{A''\}$) and not the fixed or reference frame $\{A\}$. Hence the position of the axis of the second rotation is determined by the

magnitude of the first rotation. That is, the second rotation occurs about the axis Y_B , the position of which depends upon the rotation α . Similarly, the position of the axis of the final rotation X_B is dependent on the magnitude of rotations α and β , illustrating the sequence dependency of three dimensional rotations.

As each rotation illustrated in Figure 3.5 occurs about a defined axis, the rotation matrix ${}^A_B R$ describing $\{B\}$ relative to $\{A\}$, can be written in the equivalent form of ${}^A_B R = {}^A_B R_{Z,Y',X''}(\alpha, \beta, \gamma)$. This may be expanded to provide a rotation matrix comprised of the three constituent rotations, α about the Z axis, β about the Y' axis and γ about the X'' axis:

$${}^A_B R_{Z,Y',X''}(\alpha, \beta, \gamma) = R_Z(\alpha) \cdot R_{Y'}(\beta) \cdot R_{X''}(\gamma) \quad (3.7)$$

Expanding this into matrix form, and multiplying out:

$$\begin{aligned} {}^A_B R_{Z,Y',X''}(\alpha, \beta, \gamma) &= \begin{bmatrix} \cos \alpha & -\sin \alpha & 0 \\ \sin \alpha & \cos \alpha & 0 \\ 0 & 0 & 1 \end{bmatrix} \begin{bmatrix} \cos \beta & 0 & \sin \beta \\ 0 & 1 & 0 \\ -\sin \beta & 0 & \cos \beta \end{bmatrix} \begin{bmatrix} 1 & 0 & 0 \\ 0 & \cos \gamma & -\sin \gamma \\ 0 & \sin \gamma & \cos \gamma \end{bmatrix} \\ &= \begin{bmatrix} \cos \alpha \cdot \cos \beta & \cos \alpha \cdot \sin \beta \cdot \sin \gamma - \sin \alpha \cdot \cos \gamma & \cos \alpha \cdot \sin \beta \cdot \cos \gamma - \sin \alpha \cdot \sin \gamma \\ \sin \alpha \cdot \cos \beta & \sin \alpha \cdot \sin \beta \cdot \sin \gamma + \cos \alpha \cdot \cos \gamma & \sin \alpha \cdot \sin \beta \cdot \cos \gamma - \cos \alpha \cdot \sin \gamma \\ -\sin \beta & \cos \beta \cdot \sin \gamma & \cos \beta \cdot \cos \gamma \end{bmatrix} \end{aligned} \quad (3.8)$$

Given a rotation matrix of the general form

$${}^A_B R = \begin{bmatrix} r_{11} & r_{12} & r_{13} \\ r_{21} & r_{22} & r_{23} \\ r_{31} & r_{32} & r_{33} \end{bmatrix} \quad (3.9)$$

it is now possible to extract the equivalent Z, Y', X'' axis rotations by solving Equation 3.8 for α, β , and γ . Hence:

$$\beta = \text{Atan2}\left(-r_{31}, \sqrt{r_{11}^2 + r_{21}^2}\right) \quad (3.10)$$

$$\alpha = \text{Atan2}\left(\frac{r_{21}}{\cos \beta}, \frac{r_{11}}{\cos \beta}\right) \quad (3.11)$$

$$\gamma = \text{Atan2}\left(\frac{r_{32}}{\cos \beta}, \frac{r_{33}}{\cos \beta}\right) \quad (3.12)$$

3.2.2.1 Examples from the Literature

As stated earlier, Euler angles are widely used throughout the field of biomechanics and kinematics generally. Many of the studies discussed later in Chapter 4 employ kinematic descriptions in terms of Euler angles, although the sequence of rotations often varies, as illustrated in Table 3.1. These variations generally stem from the desire to define rotation sequences to be comparable with clinical descriptions of motion.

Author	Euler angle sequence
Langrana (1981)	x, y', z''
An <i>et al.</i> (1991)	x, y', x''
Hogfors (1991)	x, y', z''
Moriwaka (1992)	z, y', x''
Johnson <i>et al.</i> (1993)	y, z', x''
van der Helm and Pronk (1995)	y, z', x''
McQuade <i>et al.</i> (1995)	x, y', z''
Barker <i>et al.</i> (1995)	x, y', z''

Table 3.1: Euler angle sequences used by various authors investigating upper limb kinematics

It should be stated that all of these selected studies involved measurement of either total shoulder motion or motion of the scapula. Many more examples would be included if considering the kinematics of other joints.

Interestingly, out of all of the studies in Table 3.1, only An *et al.* (1991) used a two axes system, with all other authors preferring to employ all three orthogonal axes. The study of An *et al.* (1991), concentrating on the measurement of humeral motion, defined a local co-ordinate system within the humerus. The first and third rotations were then used to define the plane of elevation and the axial rotation of the humerus, both along the long axis of the humerus, defined as the x axis, while the second rotation described the amount of elevation (Figure 3.6).

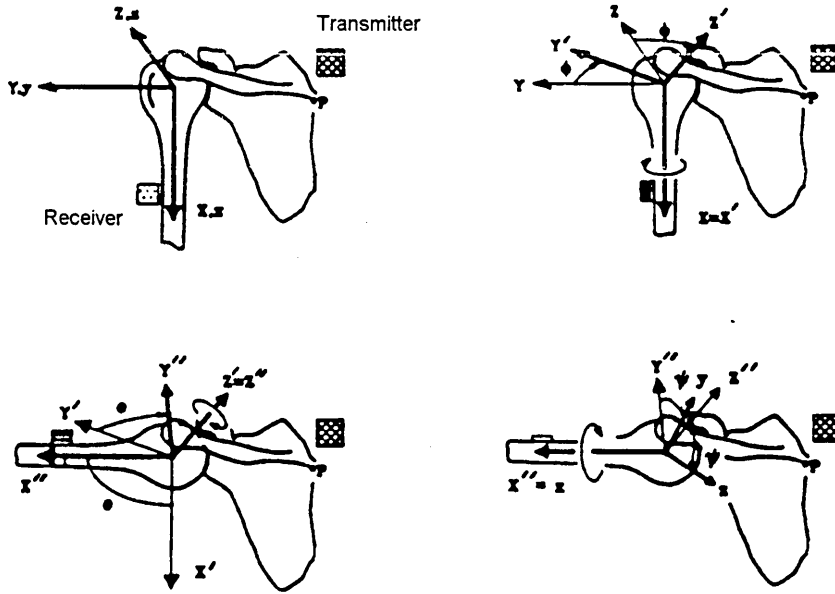


Figure 3.6: Humeral co-ordinate system and rotation sequence defined by An et al. (1991). Isotrak[®] transmitter mounted in a laboratory co-ordinate system with the receiver on the humerus

Although unclear from the text, this definition could lead to erroneous results if the humerus was not perfectly vertical at the start of the motion, as all subsequent rotations are defined relative to this local frame. If the humerus was not initially vertical, the first two rotations would not occur about a vertical and horizontal axis respectively, but about an arbitrary orthogonal axes set offset from a global frame. To avoid this problem, the rotations may be defined relative to a remote global, fixed reference frame.

Considering measurement of humeral motion, a convenient system describing rotations in this manner is provided by the *azimuth*, *elevation* and *roll* system discussed in Section 3.2.4.

3.2.3 The Floating Axis System

An alternative form of Euler angle representation was presented by Grood and Suntay (1983). This system, termed the Joint Co-ordinate System, is a three axis Euler rotation sequence often referred to as a floating axis technique. It differs from a standard Euler sequence in that only one of the rotation axes is fixed in the moving body, rather than all three axes being fixed in this frame.

The first rotation occurs about an axis fixed in the reference body, and the third about an axis fixed within the moving body. The second rotation occurs about the floating axis, formed by the common perpendicular to the other two rotation axes (Figure 3.7)

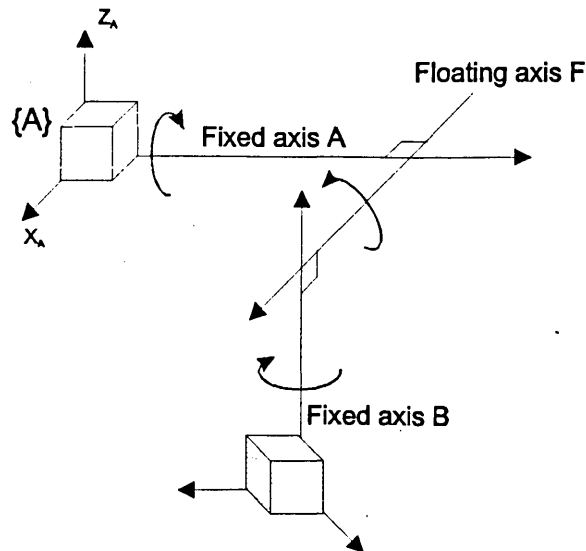


Figure 3.7: Grood and Suntay's "Floating axis" Euler system (1983).

The principal advantages of this system is that it removes the sequence dependency of the rotations inherent in all other Euler angle definitions.

3.2.4 Azimuth Elevation and Roll

Very similar to the floating axis system, this method for representing orientation is more familiar to the field of robotics, and is surprisingly little used in biomechanics. Various papers on upper limb task analysis have used this system (Buckley, 1996), probably due to its suitability for describing the large excursions of the shoulder joint.

It is a specific form of Euler angle rotation sequence in which the rotations of the moving body are expressed not relative to a co-ordinate frame within that body, but relative to a remote co-ordinate system, generally in a global or laboratory orientation.

One of the main advantages of this system is that it allows for a spherical representation of rotations akin to global navigation.

The terms latitude and longitude are frequently used to describe a position on a globe. However, measures of latitude and longitude are not the same as lines of latitude and longitude, which are different again to lines of constant latitude and constant longitude. It can easily be seen that discussions using these terms often lead to confusion, or worse, misunderstanding. The more Western terms of meridians and parallels are hence used instead. A meridian is an imaginary line which passes North to South around the circumference of a global sphere, for example, the Greenwich Meridian. A meridian is therefore the same as a line of longitude. Any number of similar circles around the sphere may be defined, creating sectors rather like those of an orange. Parallels are imaginary lines perpendicular to the meridians forming

horizontal circles around the sphere, for example the Equator and the Tropics of Cancer and Capricorn. A parallel is therefore the same as a line of latitude. The centres of these circles all lie on the polar axis (Figure 3.8).

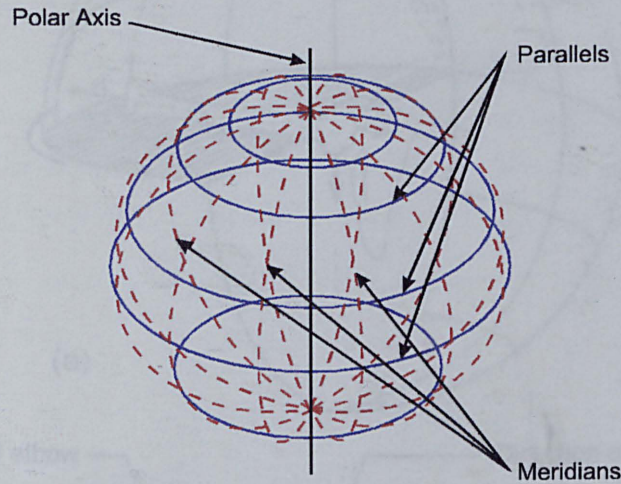


Figure 3.8: Meridians and Parallels

Angles of azimuth identify specific meridians, while angles of elevation specify parallels. Quantifying both defines a single point on the globe.

Considering motion of the upper limb, an imaginary sphere with a radius equal to the length of the humerus may be centred at the shoulder. The position of the elbow may be described on this sphere in terms of azimuth and elevation.

In navigation, a third quantity is used to describe direction of travel on the earth's surface. This is generally referred to as the bearing or heading. Applying this to the upper limb, this quantity is used to describe humeral rotation or roll along the long axis of the humerus (Figure 3.9). Also see Figure 3.12 and Figure 3.13 on page 43.

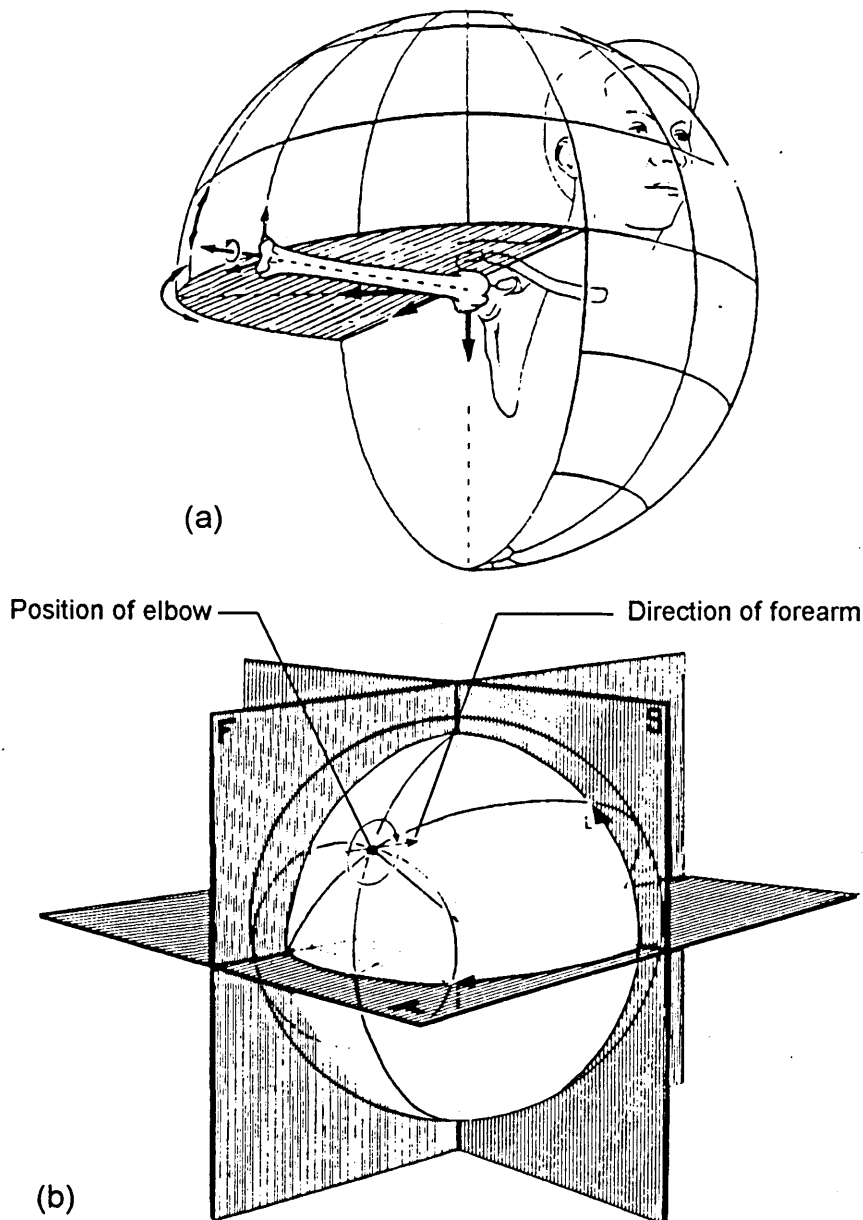


Figure 3.9: Spherical representation of shoulder rotations (a) An et al. (1991),
(b) Kapandji, (1980)

By appropriate selection of axes, this system is computationally identical to the z, y', x'' Euler system discussed earlier. The z axis must form the polar axis, about which the azimuth rotation occurs. The subsequent rotation, elevation, is about the y' axis, which is still horizontal. These two rotations specify the position of the elbow on the sphere. The final rotation, roll, occurs about the x'' axis and describes the humeral rotation.

However, when using the Isotrak®II system as described in later in Chapter 5, the vertical axis of the global frame (the sternal sensor) is the x axis. Hence to determine

the rotations of the humerus in terms of azimuth, elevation and roll, the rotation sequence x, y', z'' is required, where x will be the polar axis. Fortunately, this is quite simple to achieve and may be explained as a rotation of the reference co-ordinate system.

Consider the rotation matrix $[R_{polar\ x}]$ describing the rotation of the humerus with respect to the sternal sensor. Extraction of the co-ordinates of the humerus from Equations 3.10 - 3.12 would not provide the azimuth, elevation and roll co-ordinates as presented here. Instead, the azimuth would occur about the horizontal z axis¹.

In order to achieve the desired rotations, $[R_{polar\ x}]$ must be pre-multiplied by a rotation of 90° about the y axis.

$$R_{polar\ z} = \begin{bmatrix} \cos(90) & 0 & \sin(90) \\ 0 & 1 & 0 \\ -\sin(90) & 0 & \cos(90) \end{bmatrix} \cdot R_{polar\ x} \quad (3.13)$$

This effectively rotates the frame of reference, swapping the x and z axes, thereby making the z axis a vertical polar axis (Figure 3.10).

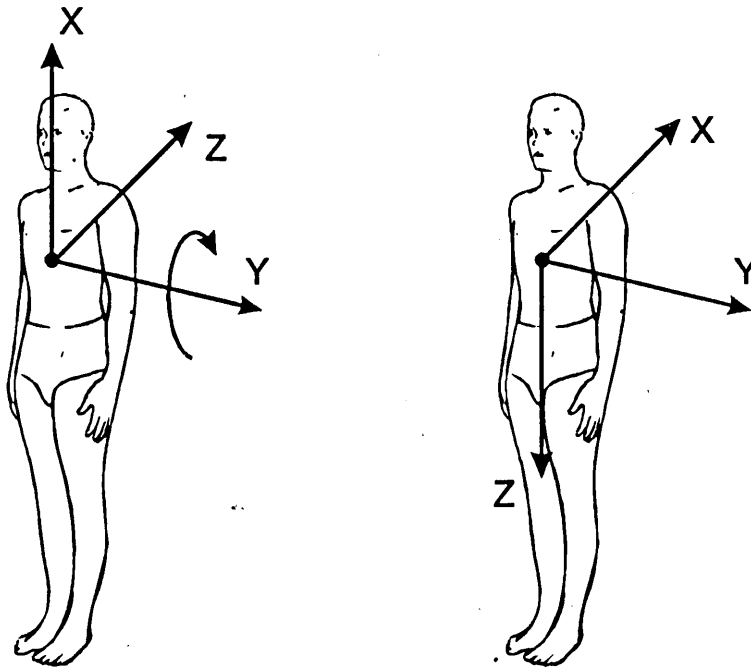


Figure 3.10: Rotating the reference frame

Equations 3.10 - 3.12 may now be applied to Equation 3.13 to extract the humeral co-ordinates in terms of azimuth, elevation and roll.

¹ The consequences of this are discussed further in Section 3.2.5 where comparisons are drawn between this and the Kapandji system of representing humeral position.

The positions of zero azimuth, elevation and roll together with direction of positive rotations are illustrated in Figure 3.11.

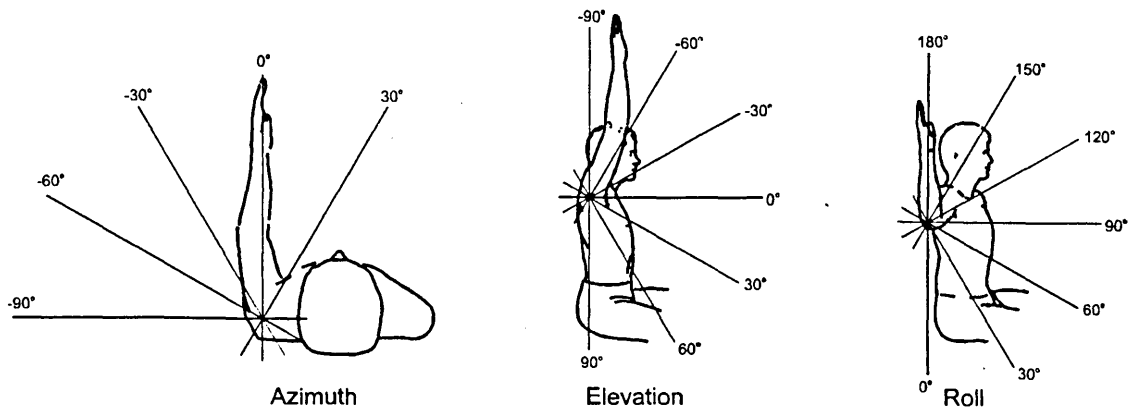


Figure 3.11: Definitions of zero azimuth, elevation and roll.

This system of representing humeral position bears close similarities to the Kapandji system presented in Section 3.2.5. The main difference lies in the orientation of the polar axis which in Kapandji's system is horizontal rather than vertical. The implications of this are discussed further in Section 3.2.5.

The principal advantages of this system are threefold:

- 1 It allows visual representation and comprehension of humeral motion. This is extremely useful when requesting subjects unfamiliar with three dimensional kinematics to perform upper limb tasks.
- 2 With the appropriate feedback software, this system allows humeral movement along any meridian (plane of elevation) or parallel (plane of azimuth or horizontal flexion/extension) to be easily monitored and controlled.
- 3 Derivations of the three angles of azimuth, elevation and roll are computationally identical to deriving the three Euler angles α , β , and γ .

The system however is not perfect. At the poles, a singularity exists where the axes of azimuth and roll are coincident. Accurate interpretation of these two co-ordinates is hence impossible as any amount of azimuth may be measured, but compensated for by the roll component, giving somewhat spurious results. This phenomenon is often referred to as the *Gimbal-Lock* problem.

In practise, this effect hinders data collection through an area of approximately 20° of elevation, from the pole (0°) to about 70° elevation. However, using the Isotrak®II system in the manner described later (Chapter 5), this problem may be overcome by a

technique best described by example. When the humerus is at 90° azimuth and 90° roll, at any level of elevation, the sensor on the arm splint is always in plane with the reference frame on the sternum. The sum of the azimuth and roll co-ordinates is hence either 0° or 180° , depending on which shoulder is being measured. Knowledge and control of this quantity therefore allows for controlled humeral motion along the meridian specified by 90° azimuth. Similarly, motion along any other meridian at a constant azimuth and roll may be achieved by calculating the sum of these first and third rotations and using it as a controlling factor.

The azimuth, elevation and roll system is hence used throughout this thesis for measures of humeral position.

3.2.5 Other Defined Systems

Various other kinematic representations of orientation have been presented in the literature. Kapandji's system (1982)¹ bears close similarity to the definitions of azimuth, elevation and roll presented earlier. Movements of the elbow are presented on an imaginary sphere, with positions specified by angles of latitude and longitude. The term bearing is also used to define humeral rotation.

The principal difference between this and the descriptions of azimuth, elevation and roll is in the direction of the polar axis which in Kapandji's system is horizontal, lying in a medio-lateral direction (Figure 3.12 and Figure 3.13).

¹ First published in 1970

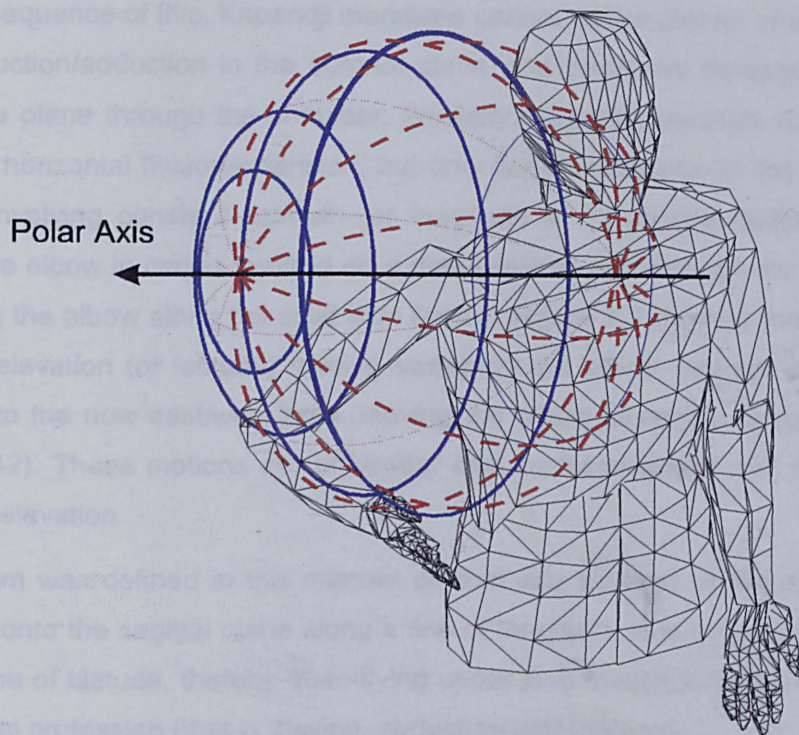


Figure 3.12: Polar axis in Kapandji's system (meridians in broken red lines, parallels in solid blue lines)

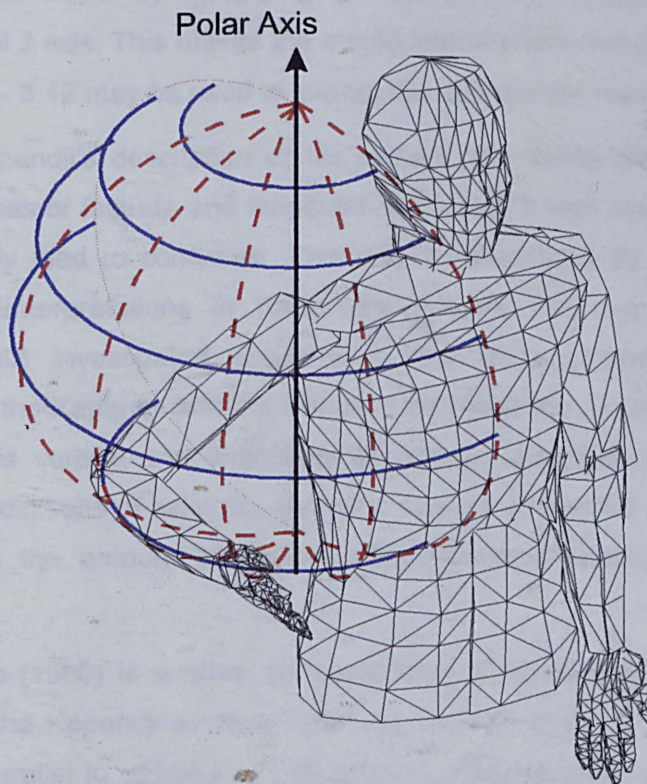


Figure 3.13: Polar axis in the azimuth, elevation and roll system (meridians in broken red lines, parallels in solid blue lines)

As a consequence of this, Kapandji meridians cannot define planes of elevation, apart from abduction/adduction in the coronal plane and horizontal flexion/extension in a transverse plane through the shoulder. Similarly, Kapandji parallels cannot describe planes of horizontal flexion/extension, but only flexion/extension in the sagittal plane. Motions involving constant azimuth (or longitude in Kapandji's description) involve moving the elbow in circles centred on a medio-lateral axis through the shoulder (that is, moving the elbow along the solid blue lines in Figure 3.12), while motions involving constant elevation (or latitude) involve sweeping the elbow through an arc along a meridian to the now east/west pole (moving the elbow along the broken red lines in Figure 3.12). These motions are unfamiliar and uncharacteristic with descriptions of planes of elevation.

The system was defined in this manner so that any position of the elbow could be projected onto the sagittal plane along a line of longitude, and onto the coronal plane along a line of latitude, thereby quantifying upper limb motion in terms which satisfied the medical profession (that is, flexion, abduction and rotation).

Similar definitions to these can be achieved using the azimuth, elevation and roll system described earlier by multiplying the rotation matrix $[R_{polar\ x}]$ by a 90° rotation about the global z axis. This makes the medio-lateral y axis the polar axis from which Equations 3.10 - 3.12 may be used to extract the appropriate rotations.

Throughout Kapandji's description of his system, the terms latitude and longitude, together with lines of latitude and longitude, are used. It was stated earlier that such terms can easily lead to confusion. This may be illustrated by referring to authors adopting their interpretations of Kapandji's system. For example, Johnson and Anderson (1990) investigated upper limb kinematics comparing two forms of representation, the Kapandji and the Benati (1980) systems. In his "Kapandji" system, the polar axis is vertical and definitions of latitude, longitude and bearing appear similar to the definitions of azimuth, elevation and roll presented earlier. They are not used to define the amount of flexion, abduction and rotation as Kapandji had intended.

Benati's system (1980) is another spherical form of representing orientation and is very similar to the Kapandji system. However, instead of using the intersection of a meridian and parallel to define humeral position, the intersection of two meridians is employed, one from a vertical axis and one from a horizontal axis (Figure 3.14).

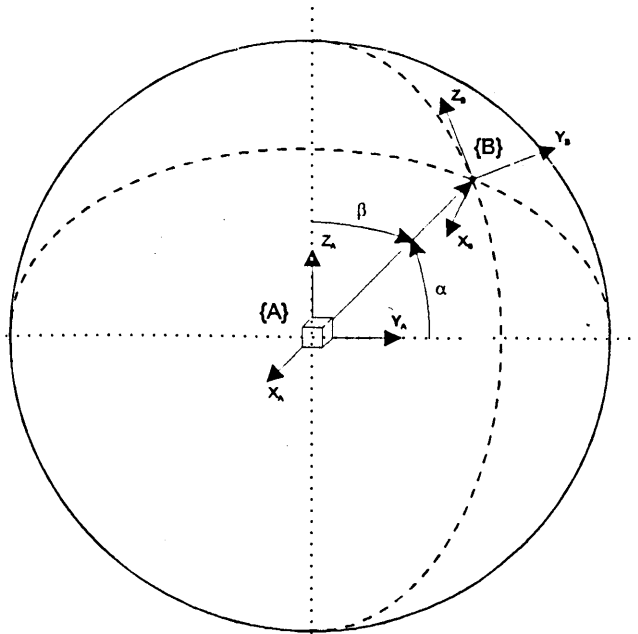


Figure 3.14: Definition of humeral position using the Benati system (1980).

This system was proposed to allow upper limb kinematics to be studied in terms of the traditional clinical angles (that is, flexion, abduction and rotation), and provide a means of determining these from the rotation matrix. This may again demonstrate the lack of understanding or comprehension of the basis of the Kapandji system which was defined to provide the same information.

Other spherical representations of orientation include Engin and Chen's (1986) Globographic system in which the Cartesian co-ordinates of the elbow are projected onto the now familiar sphere centred at the shoulder. Pearl *et al.* (1992) also used a spherical system similar to the azimuth, elevation and roll system.

Moving away from spherical representations of orientation, various other kinematic descriptions of rotation have been presented. It has already been shown that only three independent quantities are needed to specify the orientation of a rigid body. However, for some applications the use of four quantities is preferred.

The Cayley-Klein, or closely related Euler parameters are four parameter methods of representing orientation. Similar, and indeed closely related to, Hamilton's quaternions, they are much better adopted for computational use, and as such are often used in the field of robotics (Spring, 1986). However, their use is not suitable for describing motion in terms of generalised co-ordinates, thereby hindering their use when communicating findings to the uninitiated, which may include clinicians who often represent the end user of information resulting from biomechanical studies.

Descriptions of rotations in terms of these four parameter sets are therefore not employed within this thesis.

Another description of rotation is provided by Euler's Theorem, which states that the general displacement of a rigid body *with one point fixed* can be described as a rotation about some single axis. Although a useful theorem, the limitations imposed by the requirement of one point of the moving body to remain fixed have limited its use in the field of biomechanics. However, it does provide the basis for the more general screw theory discussed a little later in Section 3.3.3.

3.3 COMPLETE KINEMATIC DESCRIPTIONS

3.3.1 Introduction

Complete description of the position of a rigid body in three dimensional space requires knowledge of not only its orientation but also the translation of a point on or within the body. All descriptions of orientation discussed above therefore require additional descriptions of the translational components to provide complete kinematic definitions.

Although three rotation, three displacement descriptions are widely used and understood, various other complete kinematic techniques exist.

3.3.2 The Finite Centre of Rotation

Reuleaux (1875) demonstrated that the planar motion of a rigid body between two finite positions can be described as a rotation about a single point. This point, often incorrectly referred to as the instantaneous centre of rotation, is known as the finite centre of rotation and is an approximation to the instantaneous centre of rotation which is a differential quantity, being the point of zero velocity within or projected from the moving body. It should be stressed that the technique developed by Reuleaux concerned the finite centre of rotation, not the instantaneous centre.

Reuleaux's graphical method for determining this point involved finding the intersection of the perpendicular bisectors of displacement vectors for two points on the body (Figure 3.15). Mathematical techniques for determining this point have also been presented (Spiegelman and Woo, 1987).

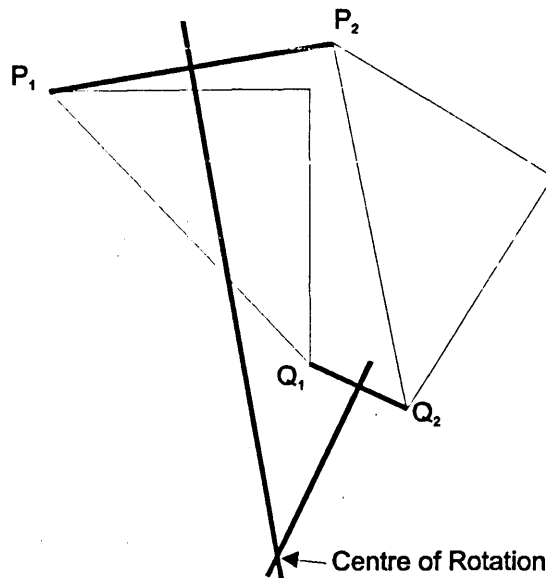


Figure 3.15: Reuleaux's method for determining the finite centre of rotation.

Although a useful two dimensional technique, it cannot be directly translated into three dimensions. This is because it relies on the body being rigid in the two dimensional plane, whereas two dimensional projections of three dimensional rigid body movement give rise to distortions in the shape of the body due to foreshortening and perspective.

However, if the finite centre of rotation is regarded as an axis normal to the plane, and hence represented as a single point on the plane, and this axis is allowed to change in direction, the technique becomes similar to Euler's Theorem of three dimensional rotations discussed earlier. Expanding further upon this provides the basis of the finite helical axis, or screw theory.

3.3.3 The Finite Helical Axis

Chasles' Theorem¹ states that the general displacement of a rigid body can be expressed as a translation and a rotation along a common axis. A mathematical interpretation of this, using vector algebra, is presented by Bisshop (1969) employing what is commonly referred to as the Rodrigues' formula². The underlying theory of this system is relatively easy to explain.

When a rigid body, in an initial position and orientation described by $\{A\}$, is subject to a finite motion, its new position and orientation are described by $\{B\}$ (Figure 3.16).

¹ Presented in Routh, 1891.

² Goldstein (1980) states that attributing this commonly used formula to Rodrigues is incorrect, crediting Gibbs (1901) with its first use, although the underlying form is probably much older.

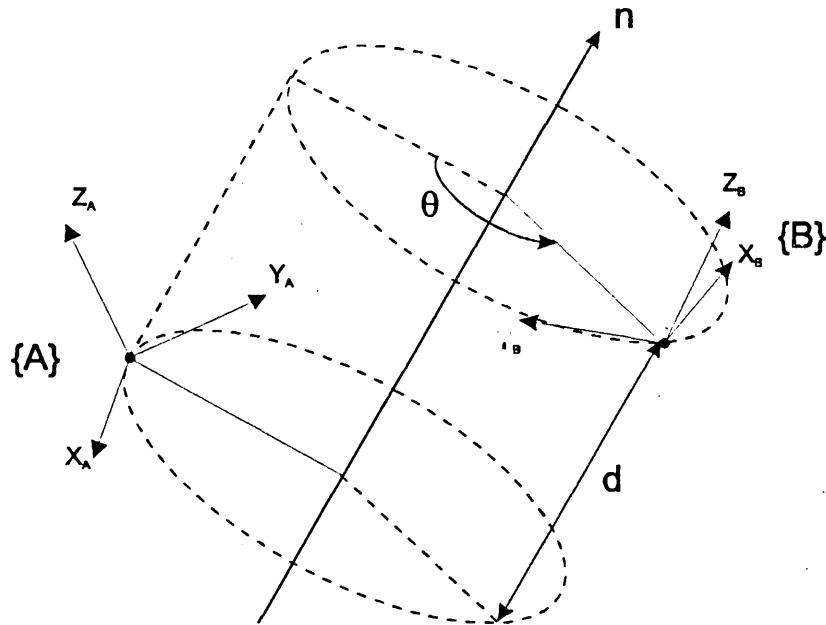


Figure 3.16: Illustration of the finite helical axis

This motion may easily be described using the methods presented earlier as a three component position vector p , combined with three rotations to describe the change in orientation between $\{A\}$ and $\{B\}$. Alternatively, applying Chasles' Theorem, the motion may be represented as a single displacement d along the finite helical axis n , combined with a single rotation θ about this axis. By knowledge of the start and end points, determination of the position and direction of the axis, together with the displacement d and the rotation θ completely describe all six degrees of freedom of the motion of the body between $\{A\}$ and $\{B\}$.

Much work has been presented on both the theoretical aspects of applying the helical axis technique to measure human motion (Kinzel 1972, Spoor and Veldpaus 1980, Woltring 1985, Veldpaus *et al.* 1988, de Lange *et al.* 1990) and also its application in the measurement of human motion (Panjabi *et al.* 1981, Dimnet and Guinguand 1984, Moore *et al.* 1993, Sennwald *et al.* 1993, Woltring *et al.* 1994, Fuss 1994 among others).

Although providing a very useful, and somewhat elegant technique, the finite helical axis method is not without its shortcomings. Woltring (1985) stated that in the determination of the position and the direction of the axis, stochastic errors frequently occur, having magnitude inversely proportional to the finite rotation magnitude between the two frames. However, sequential static measurements are often used to approximate continuous motion, and in performing such approximations it is essential

that the incremental size between measurements is not so large as to miss the underlying characteristics.

Additionally, the position of the finite helical axis, although important in specifying the kinematics of the moving body, is often not related to the mechanical structure of the joint itself, thereby contributing to difficulties in communicating this system to the clinical world.

As a result of these difficulties, the finite helical axis method has not been used in the analysis and presentation of results within this thesis. However, a method has been developed to determine the helical axis parameters from the position vector and rotation matrix. This method is included in Appendix 2.

Chapter 4

Review of the Literature Regarding Measurement of Shoulder Motion

This chapter presents a review of literature pertaining to relevant studies concerning the measurement of shoulder motion. Beginning with an introduction to the history of shoulder anatomy and biomechanics, the chapter continues to present a review of techniques for the measurement of body segment motion and total shoulder motion. Following this, a discussion on the difficulties associated with measuring scapulohumeral rhythm is presented, together with a review of techniques previously employed in the measurement of this specific motion.

4.1 INTRODUCTION

4.1.1 History

Prior to the beginning of the Renaissance era around the 15th century, there is little published evidence of the scientific study of humans. Before such times, anatomical studies were hindered due to religious and personal proscriptions against the dissection of human cadavers, and different philosophical ideas regarding the laws of nature (Jobe, 1990). However, despite these constraints it is known that studies were undertaken.

One of the earliest descriptions of the structure of the shoulder was performed by Sustruta in India and dates back to the sixth century BC (Hoernle, 1907). Around the same time, full descriptions of human bones were presented by Atroya. However, due to a lack of subsequent work, the significance of these findings was lost, and it was

left to Hippocrates in the fifth century BC to lay the foundations on the anatomy of the shoulder (Rasch, 1959). His discussions on articulations began with the shoulder and much of his work focused on this joint.

What may be referred to as the first scientific approach to descriptive anatomy took place around 300 BC. Herophilus, the father of anatomy, dissected approximately 600 cadavers for purposes of description and not just pathological analysis (Persaud, 1984).

Little more was revealed through the next few centuries and into Roman times due to the continued prohibition on human dissection, which intensified greatly after Christianity was adopted as the dominant religion of the Roman empire. Similarly, no substantial contributions to this knowledge were made during the subsequent Dark and Middle Ages.

It took until the Renaissance era around the 15th century before the frontiers of anatomy and science in general began to expand once more. The Renaissance painters, in particular Leonardo da Vinci (1452-1519), were extremely interested in anatomy in order to produce accurate representations in their work. Indeed, da Vinci became a keen student of anatomy, producing numerous drawings of his own dissections with striking accuracy (Persaud, 1959).

Between the sixteenth and nineteenth century, areas of anatomical knowledge expanded steadily. The development of electrical equipment made the dynamic study of muscles possible, with work starting in the early nineteenth century, and developing rapidly to the extensive work of Duchenne's *Physiology of Motion* (1867). However, the subsequent development of electromyographical techniques used in the observation of muscular activity is beyond the scope of this work.

Meanwhile, kinematic studies of motion were beginning to evolve. In the late nineteenth century, Muybridge (1957)¹ published a series of rapid-sequence photographs of a horse in motion. Later, he published similar photographs of human motion, opening a new chapter in the measurement and analysis of human motion. Similar studies were also being undertaken by Marey (1885).

¹ Originally published 1872

In 1895, Braune and Fischer developed an active marker motion tracking system. By attaching tethered light sources to body segments, they studied body segment motion from multiple synchronised cameras at rates of up to 25 Hz. By reconstructing the three dimensional co-ordinates of the markers, both the spatial orientations and time derivatives of the light sources were determined, allowing estimation of these properties for the underlying body segments.

Since the turn of the century, numerous techniques have been employed to study human motion.

The measurement of body segment motion is generally facilitated by the application and fixation of an external device. The nature of this external measuring device may take many forms, for example, stereophotogrammetry (Cappozzo, 1984), Moire fringe interference patterns (Shoup 1976, Jonsson *et al.* 1987), two and three dimensional goniometers and electrogoniometers (Kinzel 1972, Chao 1980, Nicol 1987, 1989), sonic emitters (Engin and Peindl 1987) and electromagnetic systems (An *et al.* 1988).

4.1.2 Difficulties in Measurement of Scapulohumeral Rhythm

Despite the variety of measurement techniques available, measurement of scapulohumeral kinematics has proven rather difficult. Unlike the motion of a limb, where a measurement device may be physically attached to the moving limb, the motion of the scapula occurs beneath the skin, inhibiting the fixation of any externally applied measurement system.

Additionally, the motion of the scapula during humeral movements is three dimensional, comprising of not only lateral rotation, but also protraction/retraction and forward/backward tip. These motions are illustrated Figure 2.10. Further to this, the scapula possesses five degrees of freedom, as demonstrated in Chapter 2, and is therefore capable of not only rotational movements but translations also. These three dimensional characteristics of scapular motion have been overlooked by many investigators, as discussed in Section 4.2.

Radiographic techniques overcome many of these difficulties. Rapid sequence bi-planar radiography would allow the three dimensional motions of the scapula to be investigated. However, the effect of the ionising radiation is harmful and hence unethical for studies of normal subjects. Such systems also require intense calibration procedures, which, even if undertaken would impose restrictions on the geographical mobility of subjects as the system would hardly be portable. Similar restrictions exist in the use of computer axial tomography scans (CAT or CT scans), and magnetic

resonance imaging (MRI), particularly with regard to subject mobility due to the restricted size of the apparatus. Also, such measurements can only produce a sequence of images in static positions, and not dynamic motions.

Despite all of these difficulties, numerous studies have been performed on the observation and measurement of scapular motion.

4.2 MEASUREMENT OF SCAPULAR MOTION

4.2.1 Qualitative Observations of Scapular Motion

Prior to the turn of the century, the movements of the shoulder girdle mechanism had attracted the interest of anatomists. Duchenne (1867) discussed the lateral rotation of the scapula, describing its necessity to allow elevation of the humerus above the point where the arm is horizontal.

Cleland (1881) presented a comprehensive discussion of his observations of the shoulder girdle, paying great attention to the movements at each of the articulations of the shoulder complex. Unfortunately, he did not expand upon these individual movements to provide an overall picture of shoulder motion.

Soon afterwards, Cathcart (1884) summarised the current thinking of the time, and offered his opinions from studies of his own. Combining the descriptions offered by Duchenne (1867) and Quains' *Elements of Anatomy* (1882), he described the "ordinary view" of shoulder motion to consist of two stages. The first stage comprised arm elevation up to the horizontal, during which the scapula did not move, and the humeral head articulated in the fixed glenoid. He continued to describe the second stage during which no relative motion occurred between the scapula and the humerus, and further elevation of the arm was made possible by the rotation and elevation of the scapula on the thoracic cage. While not explicitly disagreeing with this description, Cathcart went on to offer his rather different account of shoulder motion. In this, he described the rotation of the scapula as occurring throughout the whole range of arm movement, and not just in elevation above the horizontal. Furthermore, he describes the motion of the humerus with respect to the scapula occurring at levels of humeral elevation above the horizontal. Continuing his descriptions, he stated that during abduction of the arm, lateral rotation of the scapula began at an abduction of approximately 30°, a finding later supported by the measurements of Inman *et al.* (1944). Within this study, Cathcart was the first to openly discuss the concept of

synchronous movements of the humerus and scapula throughout the range of humeral elevation.

In 1934, Codman published his book *The Shoulder*. Despite being the only book to be published on the shoulder at the time, Codman was quick to claim it as the best and most comprehensive book in the field. However, criticism of such boasts should not detract from this eminent piece of work. He coined the term *scapulohumeral rhythm* to describe the synchronous motion of the humerus and scapula, and his observations on the mechanics and pathology of the shoulder complex have been widely accepted and highly regarded among the surgical profession, providing the preface to nearly every book written on the shoulder since.

Codman was the first author to provide a detailed account of the motions at each individual joint within the shoulder complex. His appreciation of the complexity of the combined motion is probably best illustrated by Figure 4.1.

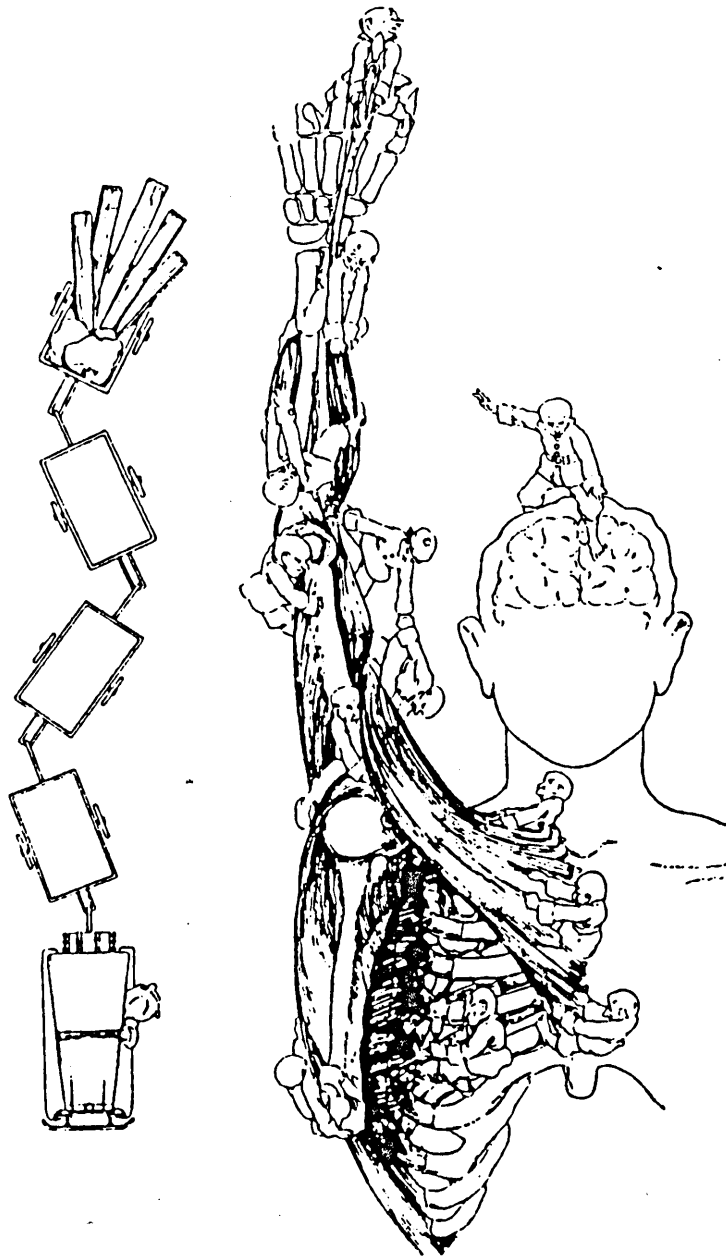


Figure 4.1: "Complex motion at the shoulder", from Codman (1934)

In 1937, Johnston presented further contributions to the discussions on movements of the shoulder joint. Citing Fick (1911), he introduced the "plane of the scapula", and requested the adoption of this plane as the reference plane for the movements of the glenohumeral joint. However, as pointed out by Saha (1950):

"[The] Scapular plane is not a fixed one. [The] Scapula rotates about a vertical axis...So any reference to this unstable structure would be useless. Scapular planes at the beginning of abduction or flexion and at the end of these movements are not the same."

This important concept has unfortunately been overlooked in many two dimensional studies of scapulohumeral rhythm which have insisted on measuring rotations in “the plane of the scapula”. Such studies are discussed later.

Although undoubtedly important and significant pieces of work, these studies concerned the observation rather than the measurement of scapular motion. Quantitative analysis of scapular motion did not occur until beyond the turn of the century and the application of radiographic techniques, discovered accidentally by the German physicist Roentgen in 1895.

4.2.2 Two Dimensional Radiographic Techniques

In 1929, Flecker conducted what appears to be the first quantitative investigation into the rotations of the scapula during movements of the arm. By taking coronal plane radiographs of three subjects during abduction, he determined the two dimensional rotations of the scapula in the plane of projection. The angle between a medial vertical plane (depicted by the spinous processes of the thoracic vertebrae) and the glenoid cavity was measured from tracings obtained from the radiographs. Similarly, the angle made by the humerus relative to the medial plane was measured. From the tabulated data quoted, it is possible to plot the angle of rotation of the scapula against the abduction angle of the arm.

Despite each subject displaying individual variation, a definite trend may be identified (Figure 4.2).

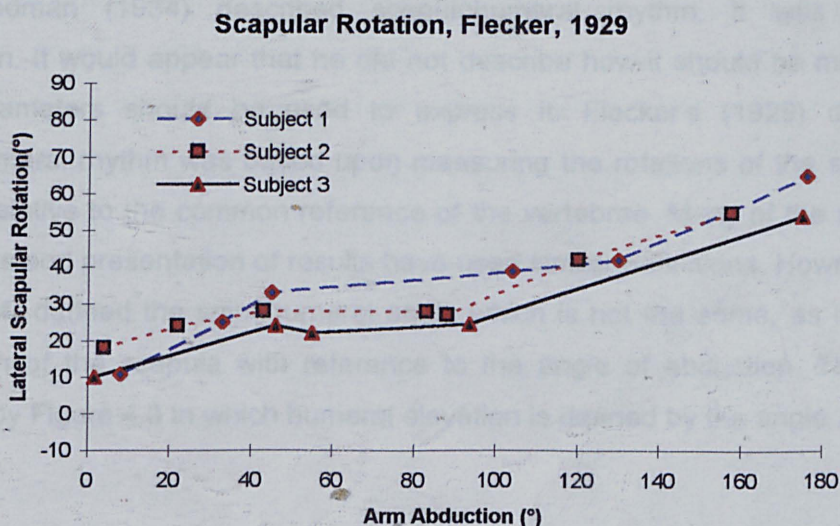


Figure 4.2: Graphical representation of lateral rotation of the scapula during humeral abduction, measured by Flecker (1929)

Soon afterwards, Lockhart (1930) presented a more simple series of radiographs, investigating shoulder motion in normal and pathological subjects. The images from the normal subject illustrated the position of the scapula with the arm in the normal vertical position, elevated to the horizontal in the coronal plane, and at an elevation of approximately 160° , again in the coronal plane. This once more demonstrated the synchronous motions of the scapula and humerus, nearly four years before Codman's now ubiquitous description of scapulohumeral rhythm was published.

In 1944 the classic paper of Inman *et al.* was published. This comprehensive study brought together a variety of measurement techniques to investigate and measure the motions of the shoulder girdle mechanism, including radiographs, insertion of pins into the bones and electromyography (EMG) to observe muscular activity.

Rotations of the scapula during abduction between 30° and 70° in the coronal plane were measured from tracings taken from the radiographs. As in the earlier studies, the radiographs were taken in the coronal plane, hence the results represent the projection of the rotations onto this plane. Unfortunately, the publication does not state how many measurements were taken between this range, nor how many subjects were examined.

They defined the spinohumeral angle as the angle between the spine of the scapula and the long axis of the humerus, and expressed scapulohumeral rhythm as the changes in this angle during elevation of the arm, which introduces an important and often overlooked concept.

When Codman (1934) described scapulohumeral rhythm, it was based on observation. It would appear that he did not describe how it should be measured, or which parameters should be used to express it. Flecker's (1929) definition of scapulohumeral rhythm was based upon measuring the rotations of the scapula and humerus relative to the common reference of the vertebrae. Many of the subsequent descriptions and presentation of results have used similar definitions. However, Inman *et al.* (1944) defined the spinohumeral angle which is not the same, as it measures the rotation of the scapula with reference to the angle of abduction. This may be illustrated by Figure 4.3 in which humeral elevation is defined by the angle λ .

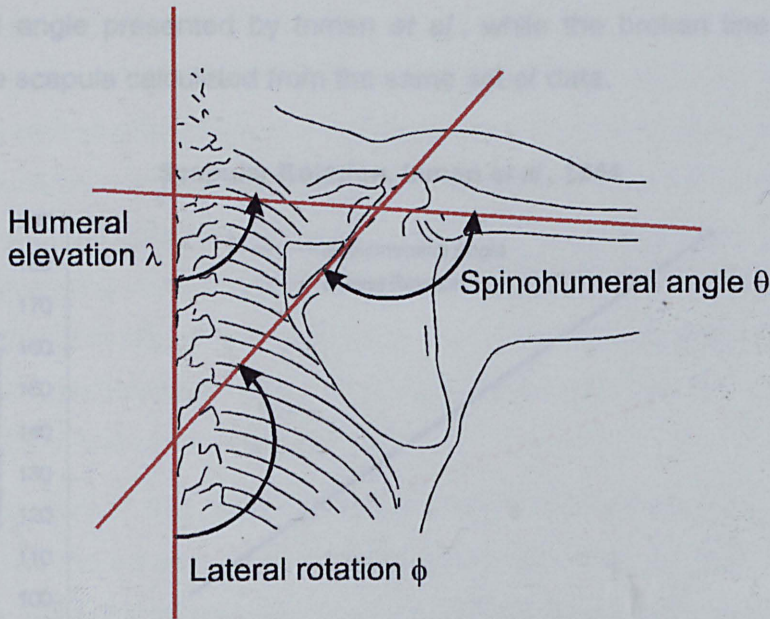


Figure 4.3: Differences in the definition of the spinothumeral angle and lateral rotation of the scapula

The spinothumeral angle defined by Inman *et al.* (1944) is represented by θ , while the rotation of the scapula measured relative to the vertical is defined by the angle ϕ . By considering the geometry, the relationship between θ and ϕ may be expressed as:

$$\phi = \lambda + (180 - \theta) \quad (4.1)$$

The angle ϕ hence represents the angle between the spine of the scapula and a vertical reference. Measurement of changes in this angle during abduction therefore represent scapulohumeral rhythm in the same manner as measurement of the angle between the medial border of the scapula and the meridian plane, or the glenoid and the meridian plane, although the absolute values will obviously differ.

The degree to which this anomaly has been overlooked by authors since Inman *et al.* (1944) is surprising. Inman's work is almost always cited in studies involving motion of the shoulder girdle mechanism, and most studies involving the measurements of scapulohumeral rhythm refer and compare their work to that of Inman *et al.*. However, it would appear that no other author has highlighted the differences between the spinothumeral angle and lateral rotation of the scapula.

The overall effect of these differences is to apparently exaggerate the rotations of the scapula. Figure 4.4 illustrates the effect of determining the lateral rotation of the scapula from the results presented by Inman *et al.* (1944). The solid line is the

spinohumeral angle presented by Inman *et al.*, while the broken line is the lateral rotation of the scapula calculated from the same set of data.

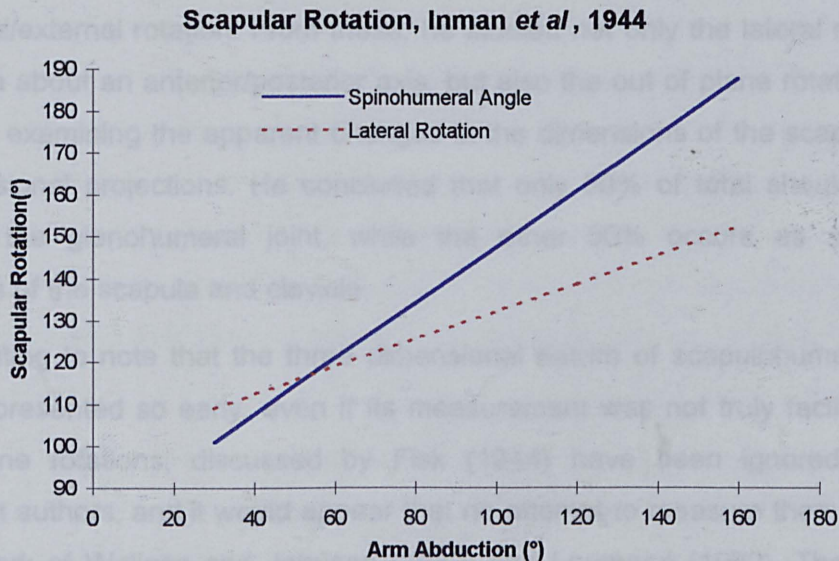


Figure 4.4: Spinohumeral angle during humeral abduction, measured by Inman *et al.* (1944), together with the corresponding lateral rotation of the scapula

Their results present what they term as two *phases* of scapular motion. The first phase occurs with arm abduction angles of up to around 30°, and is termed the *setting phase*. During this phase, the motion of the scapula was said to exhibit great variability between individuals, without rotating by a great amount, but stabilising itself to act as a base for the humerus. It has since been suggested (Freedman and Munro, 1966) that during this phase, the scapula is aligning with the plane of abduction.

The second phase identified by Inman *et al.* occurs with abduction angles between approximately 30° to 170° (nominal maximum abduction). This was found to represent the most consistent motion of the scapula, with approximately 1° of scapula rotation to each 3° of humeral elevation. This is presented as a glenohumeral to scapulothoracic ratio of 2:1, that is, for each 3° of humeral elevation, 2° occurs at the glenohumeral joint and 1° occurs through scapula rotation on the thorax. However, for the purposes of this discussion and in presenting the ratios from other authors, the *scapulohumeral ratio* is defined as the ratio of humeral elevation to scapular rotation, and was hence found by Inman *et al.* to be 3:1. It would appear more logical to measure this parameter, as humeral motion may be measured independently of scapular motion. This second phase is supported by data, as presented above (Figure 4.4). However, there are no data relating to or illustrating the motion during the first phase.

Shortly after the publication of Inman *et al.* (1944), Fisk (1944) presented another radiographic study concerning scapulohumeral rhythm. He published a series of ten coronal plane radiographs of the shoulder girdle at a number of positions of elevation and internal/external rotation. From these, he studied not only the lateral rotations of the scapula about an anterior/posterior axis, but also the out of plane rotations of the scapula by examining the apparent changes in the dimensions of the scapula on the two dimensional projections. He concluded that only 50% of total shoulder motion occurs at the glenohumeral joint, while the other 50% occurs as a result of movements of the scapula and clavicle.

It is interesting to note that the three dimensional nature of scapulohumeral rhythm had been presented so early, even if its measurement was not truly facilitated. The out of plane rotations, discussed by Fisk (1944) have been ignored by many subsequent authors, and it would appear that no attempt to measure them was made until the work of Wallace and Johnson (1982) and Laumann (1982). These studies are discussed in greater depth later (see Section 4.2.4).

In 1956, Jones published his results on the movements of scapular motion during abduction. He performed a series of radiographs and measured the elevation of the humerus and the rotation of the medial border of the scapula relative to a vertical copper wire which was used as a plumb line during the radiography. Graphical interpretation of the results is illustrated in Figure 4.5.

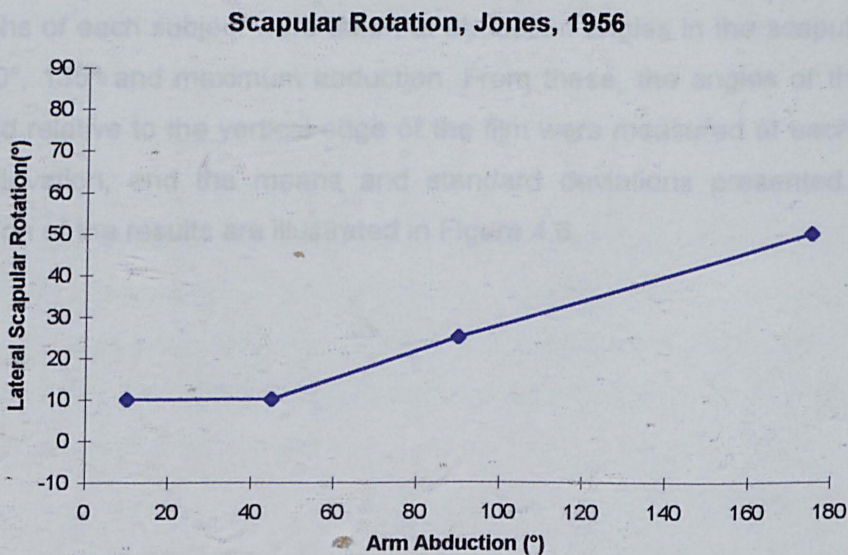


Figure 4.5: Lateral rotation of the scapula during humeral abduction, measured by Jones (1956)

Jones (1956) concluded that these findings “differ considerably” from those published by Inman *et al.* (1944) in both the size of the “setting phase” and in the ratio of scapular to humeral movement. It is clear from Figure 4.5 that the setting phase measured by Jones was present up to 45° degrees of humeral elevation compared to that of 30° measured by Inman *et al.*. However, the scapulohumeral ratio is very similar to that measured by Inman *et al.* (3:1 from Inman *et al.* compared to approximately 3.27:1 from Jones). It would appear that Jones compared his results to the spinohumeral angle measured by Inman *et al.*, which as already discussed, is not the same as the lateral rotation of the scapula. Taking this into account, the results of Jones compare well with those of Inman *et al.*, contrary to what Jones actually states himself.

Further two dimensional radiographic studies of scapulohumeral rhythm were conducted by Freedman and Munro (1966) and Poppen and Walker (1976), who both measured the lateral rotation of the scapula during abduction of the arm in the scapula plane (defined at an angle of 30° to the coronal plane). As has been stated earlier, this definition must be a compromise as the scapula does not remain in the same plane throughout elevation of the arm (Saha, 1950). Indeed, this approximation is accepted by Freedman and Munro. Nevertheless, the results from these studies are based on the two dimensional projection of the scapula onto this plane, and are still worthy of discussion.

Freedman and Munro (1966) measured the motion of 52 right male shoulders. Radiographs of each subject were taken at abduction angles in the scapular plane of 0°, 45°, 90°, 135° and maximum abduction. From these, the angles of the humerus and glenoid relative to the vertical edge of the film were measured at each interval of humeral elevation, and the means and standard deviations presented. Graphical interpretation of the results are illustrated in Figure 4.6.

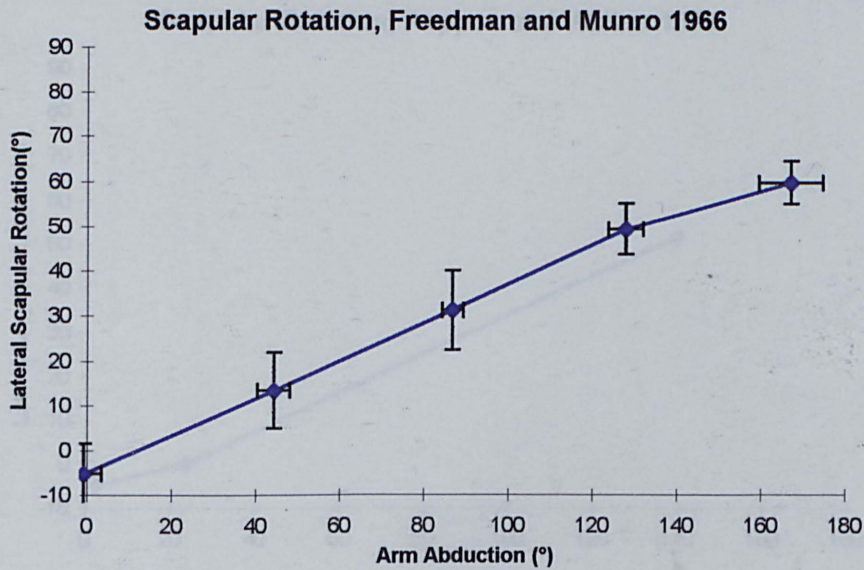


Figure 4.6: Lateral rotation of the scapula during humeral abduction, measured by Freedman and Munro (1966). Error bars are ± 1 standard deviation for measures of both scapular and humeral angles

Unlike Inman *et al.* (1944), the results of Freedman and Munro (1966) do not illustrate a setting phase of the scapula at the lower levels of arm elevation. Instead, their results show an almost linear relationship up to approximately 130° of humeral elevation, above which point they found the ratio of scapular rotation to humeral elevation decreased, as illustrated in Figure 4.6. The respective ratios in these two intervals are 2.4° of total humeral elevation for each 1° of scapula rotation for the first phase and 3.8° of total humeral elevation for each 1° of scapula rotation for the second phase. These are calculated in terms of the scapulohumeral ratio discussed earlier, rather than the ratio of glenohumeral to scapula rotation as quoted by the authors.

Poppen and Walker (1976) conducted a similar study to Freedman and Munro (1966). Examining the radiographs taken from twelve normal subjects, they measured the rotations of the scapula in the scapula plane during abduction in this plane. As can be seen from the graphical interpretation of their results (Figure 4.7), they agree closely with those of Freedman and Munro.

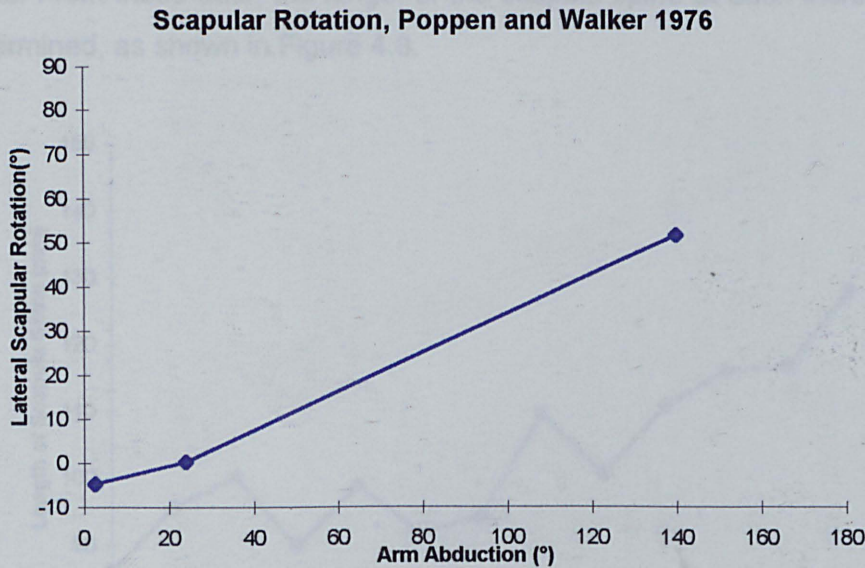


Figure 4.7: Lateral rotation of the scapula during humeral abduction, measured by Poppen and Walker (1976)

Unlike Freedman and Munro (1966), Poppen and Walker (1976) detected a slight setting phase of the scapula, described by Inman *et al.* (1944). Beyond this, the ratio of scapular rotation to total humeral elevation was very similar to that of Freedman and Munro, at 2.3:1 (compared to 2.4:1 from Freedman and Munro). As the two experiments were performed in an almost identical manner, the similarities in these results are not too surprising. However, despite suggesting a reliability of the measurement technique, it is important to realise that both studies were not without their shortcomings, and they do not provide an accurate measure of scapulohumeral rhythm.

Poppen and Walker (1976) continued their study with an attempt to determine the finite centres of rotation of the scapula between each measured position. However, as discussed in Section 3.3.2, determination of such a point is not valid due to the three dimensional nature of scapulohumeral rotations.

A similar study was undertaken by Dvir and Berme (1978), measuring the rotations of the scapula from coronal plane radiographs at 15° increments of humeral abduction, from 0° to maximum elevation (stated as 180°). Using the data obtained from these radiographs, together with that previously published, they modelled the motions of the shoulder girdle using a mechanism approach first introduced by Dempster (1955). The publication quotes data for the co-ordinates of the root of the scapula spine and the acromioclavicular joint throughout a range of arm elevation from 0° to 180° in 15°

increments. From these data, the length of the scapula spine at each increments has been determined, as shown in Figure 4.8.

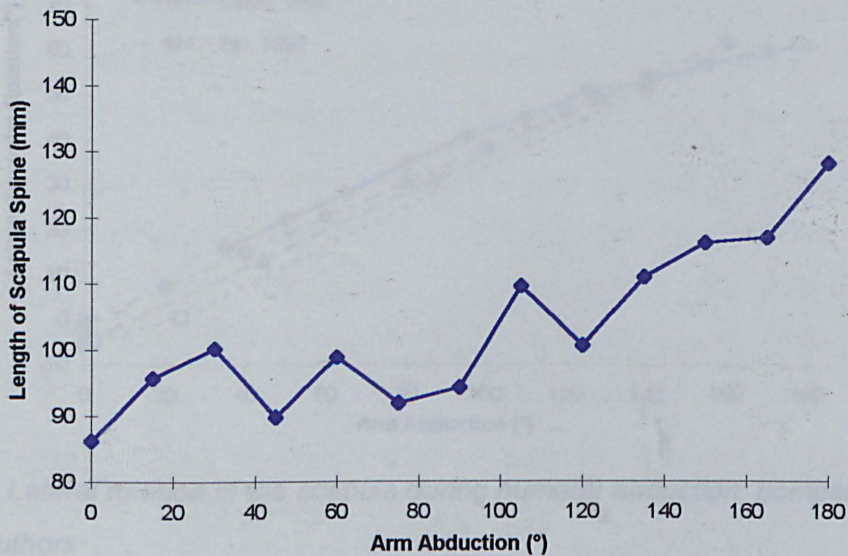


Figure 4.8: Changes in the projected length of the scapula, Dvir and Berme 1978

Beside the amount of noise present in this data, it is interesting to note the amount of variation in the projected length of the scapula spine. Much of this variation may be accounted for as a result of out of plane rotations of the scapula. For example, if the scapula was parallel with the plane of projection at an arm abduction of 180°, then the real length of the scapula spine is approximately 130mm. An out of plane rotation of approximately 40° during the range of abduction would mean that this dimension would appear approximately 100mm in the plane of projection with the arm at 0°. However, the more recent three dimensional studies of Pronk (1991) and Johnson *et al.* (1993) have found that the out of plane rotations are not of such magnitudes. This suggests that the co-ordinate data presented by Dvir and Berme (1978) may be somewhat erroneous, illustrating larger out of plane rotations than actually exist.

Ozaki (1989) used a technique similar to that of Freedman and Munro to investigate the shoulder movements of subjects with glenohumeral instability. Despite using cine-radiography, he does not state whether the rotations of the scapula were measured during dynamic or sequential static arm movements, although due to the general applications of cine-techniques, it is likely that dynamic motions were studied. Within this study, he measured the scapular motion of thirty normal shoulders. Analysis and presentation of his data reveal findings similar to those presented by Freedman and Munro and Poppen and Walker (Figure 4.9).

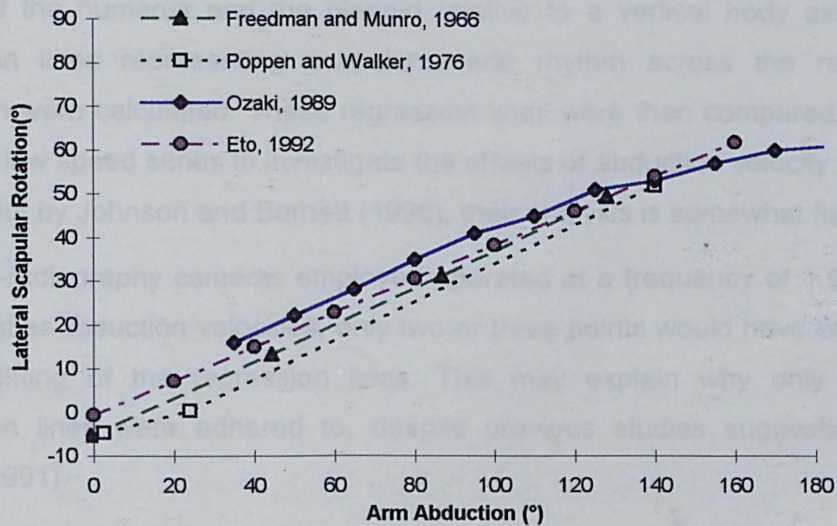


Figure 4.9: Lateral rotation of the scapula during humeral abduction: comparisons between authors

Eto (1991) also conducted a two dimensional radiographic study of scapulohumeral rhythm, investigating the effects of periarthritis scapulohumeralis on the relative movements of the scapula and humerus. Within this, seven normal subjects were analysed and the results presented. Graphical representation of these results again shows a close similarity to the results presented by other authors (Figure 4.9).

More recently, Michiels and Grevenstein (1995) investigated the effects of abduction velocity and external load on the kinematics of the scapula. Using two dimensional cine-radiography, their intention was to study the dynamic behaviour of the scapula during arm abduction in the scapular plane, rather than the sequential static measurements performed by previous authors. They claimed that no similar studies had been undertaken to measure scapula kinematics dynamically. However, the work of Ozaki (1989) discussed above probably measured scapular kinematics dynamically in two dimensions while Wallace (1982) performed a similar dynamic investigation. Additionally, Wallace and Johnson (1982) and Hogfors *et al.* (1991) have performed bi-planar radiography in dynamic shoulder motions to investigate the three dimensional kinematics of the scapula. These studies are discussed further in Section 4.2.4.

The study of Michiels and Grevenstein (1995) involved requesting subjects to abduct their arm repeatably at a "high speed" and again at a "low speed". From the resulting radiographs, the average angular velocities of the arm were determined. In the low speed series, the mean angular velocity over the whole range of abduction was

34.34° s⁻¹, while the mean in the high speed series was 70.00° s⁻¹. By determining the angles of the humerus and the glenoid relative to a vertical body axis, first order regression lines representing scapulohumeral rhythm across the range of arm abduction were calculated. These regression lines were then compared between the high and low speed series to investigate the effects of abduction velocity. However, as pointed out by Johnson and Barnett (1996), their analysis is somewhat flawed.

The cine-radiography cameras employed operated at a frequency of 1.92 Hz. Hence at the higher abduction velocities, only two or three points would have been available for the fitting of the regression lines. This may explain why only single order regression lines were adhered to, despite previous studies suggesting otherwise (Pronk, 1991).

Nevertheless, it is interesting to note that although the authors found a statistically significant difference in the slope of the regression lines between the high and low speed series (slope of 0.654, SD=0.056 and 0.670, SD=0.054 respectively), they discounted this as of no physical significance.

Their results therefore suggest that the speed of abduction has little or no effect on the dynamic kinematics of the scapula. However, it is unfortunate that they did not perform a series of sequential static radiographs as performed by previous authors such as Poppen and Walker (1976) in order to investigate the differences in scapular kinematics between dynamic and sequential static arm movements.

4.2.3 Other Two Dimensional Measurement Techniques

In addition to single plane radiography, a number of other two dimensional techniques to measure scapulohumeral rhythm have been developed.

Doody *et al.* (1970a) developed their "scapulo-humeral goniometer" to measure the planar rotations of the scapula during abduction of the arm. This device consisted of three transparent sections joined by two 360° protractors (Figure 4.10).

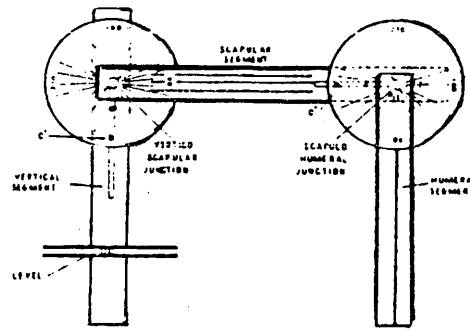
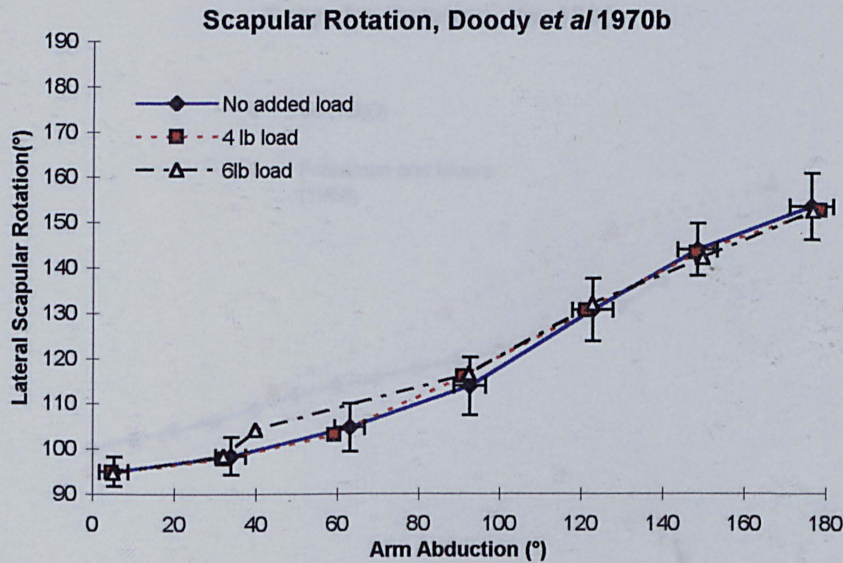


Figure 4.10: Scapulo-humeral goniometer developed by Doody et al. (1970a)

One of the sections was held vertical, while the centre section was positioned over the scapula spine, thereby measuring its rotation relative to the vertical section. The final section was placed over the humerus to measure humeral abduction.

Using this instrument, they studied the motion of the scapula during abduction in the now familiar scapular plane (Doody *et al.*, 1970b). Measurements were taken from twenty five subjects (one shoulder examined on each), with significant differences being found between subjects. Unlike the previous studies, they found a definite non-linearity in scapulohumeral rhythm across the range of abduction tested.

They also investigated the effect on the motions of the scapula of carrying hand loads by performing the tests unloaded and with four pound and six pound hand loads. As can be seen from a graphical interpretation of their results (Figure 4.11), these effects appear slight, although the authors claim these differences are not due to measurement error but represent real changes in the pattern of scapulohumeral rhythm between the loaded and unloaded cases.



*Figure 4.11: Lateral rotation of the scapula during humeral abduction; the effect of hand loads, measured by Doody *et al.* (1970b). Error bars are ± 1 standard deviation for measures of both scapular and humeral angles on the unloaded test only*

More recently, Youdas *et al.* (1994) investigated the inter-observer reliability of the scapulohumeral goniometer. Based on a study of 45 subjects, they concluded that repeated measurements of scapular and glenohumeral rotations made by the same physical therapist did not compare well. Similarly, measurements between therapists had a poor correlation.

Ito (1980) presented a dynamic method of recording the two dimensional rotations of the scapula during arm elevation using an electrogoniometer comprising two potentiometers. One of these was mounted on a metal plate and fixed to the posterior of the upper arm, while the second was mounted to a tube fixed to the scapula spine. Both fixations were non-invasive, consisting of adhesive tape and bandages. With an intermediate structure coupling the two potentiometers, the relative rotations between them were determined.

Considering the degree of scapular movement beneath the skin, together with the constraints of motion provided by the necessary quantities of fixing tape and bandages, it is not surprising that the rotations measured by Ito (1980) are smaller than those presented in earlier studies.

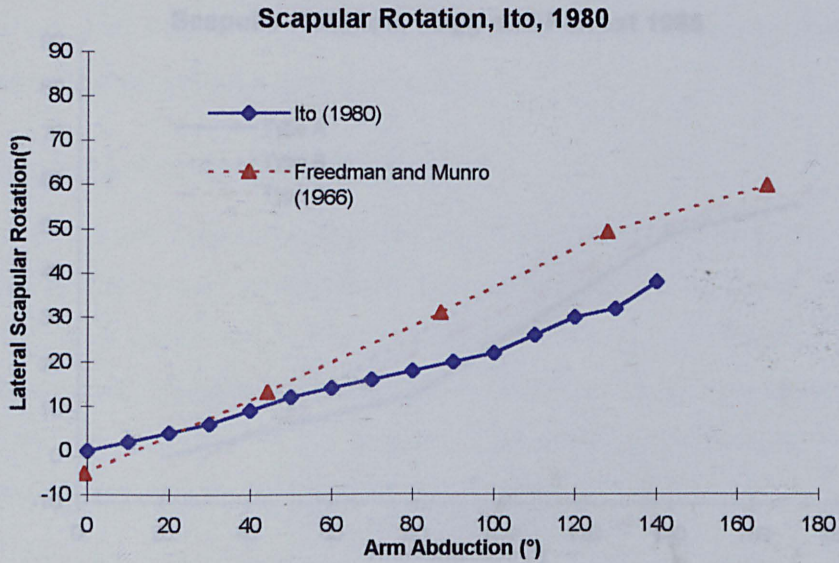


Figure 4.12: Lateral rotation of the scapula during humeral abduction measured by Ito (1980)

In 1988 Bagg and Forrest presented a technique to measure scapulohumeral rhythm involving identification and stereo-photogrammetric recording of the positions of anatomical landmarks palpable beneath the skin. The acromial angle, inferior angle and root of the scapula spine, together with two vertebrae were marked and photographed at 15° intervals of arm abduction in the scapula plane. Analysis of these data for twenty one subjects (one shoulder examined on each) revealed what Bagg and Forrest termed type A, B and C patterns of scapulohumeral rhythm (Figure 4.13).

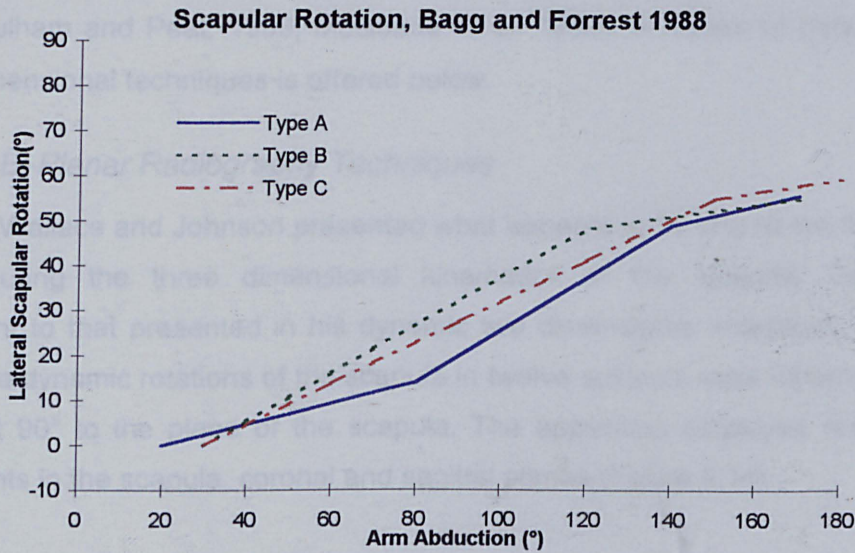


Figure 4.13: Characteristic types of lateral scapular rotation identified by Bagg and Forrest (1988)

Type A was the most commonly observed (twelve subjects), possessing three definite phases, with the greatest contribution of scapular motion occurring in the second phase. Types B and C differ only slightly. In type B, identified in four subjects, the scapular contribution to arm elevation is greater up to approximately 130°. Elevation beyond this point took place mainly at the glenohumeral joint. Type C however, identified in four subjects, shows a more linear relationship between glenohumeral and scapulothoracic rotations, akin to the results of Inman *et al.* (1944), Freedman and Munro (1966) and Poppen and Walker (1976).

Large variations in scapulohumeral rhythm between subject had been identified by most previous authors.

Oddly, only twenty out of the twenty one subjects measured were classified as belonging to these types. The remaining subject appears to have been forgotten, perhaps preferring to remain classless?

4.2.4 Three Dimensional Measurement Techniques

Considering that the three dimensional nature of scapulohumeral rhythm had been discussed in the early forties (Fisk, 1944), it is surprising that no measurement techniques were presented until much later. It was not until the early eighties before three dimensional measurements of scapulohumeral rhythm were presented (Wallace and Johnson, 1982, Laumann, 1982). A variety of techniques have been published since, many relying on the development and application of new three dimensional

measurement devices such as electromagnetic digitising systems (Johnson *et al.*, 1993, Culham and Peat, 1993, McQuade *et al.* 1995). A review of these and other three dimensional techniques is offered below.

4.2.4.1 Bi-Planar Radiography Techniques

In 1982, Wallace and Johnson presented what appears to be one of the first attempts at measuring the three dimensional kinematics of the scapula. Using similar equipment to that presented in his dynamic two dimensional investigation (Wallace, 1982), the dynamic rotations of the scapula in twelve subjects were determined during flexion at 90° to the plane of the scapula. The apparatus employed restricted arm movements in the scapula, coronal and sagittal planes (Figure 4.14).

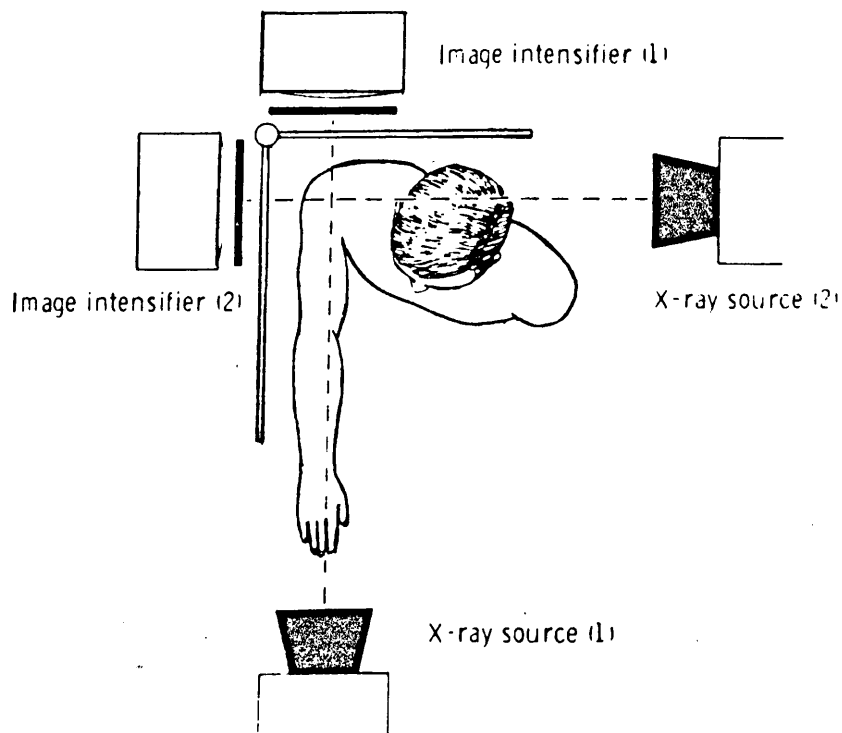


Figure 4.14: Experimental set-up used by Wallace and Johnson (1982)

The resulting rotations are presented as projections onto three orthogonal views; an anterior-posterior view (front to back), plan view and lateral view (from the side), as shown in Figure 4.15.

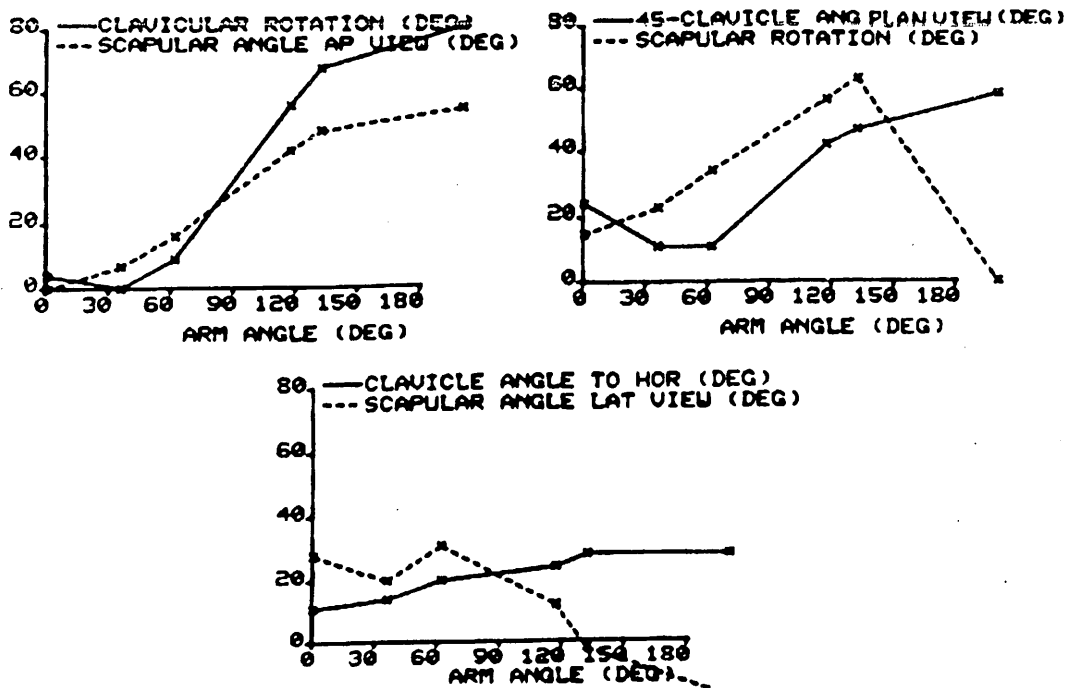


Figure 4.15: Rotations of the scapula measured by Wallace and Johnson (1982)

The results, although somewhat erratic, show a definite combination of all three rotations throughout the range of motion.

Kondo *et al.* (1984) performed a bi-lateral radiographic investigation of scapulohumeral rhythm. This involved taking two images of the scapula along the same axis but from different distances. Subsequently, images were taken at 40° to the coronal plane at arm elevations of 90°, 150° and maximum elevation. Hence, this study was based on sequential static measurements rather than dynamic arm elevation as observed by Wallace and Johnson (1982). From the resulting images, the three dimensional rotations or “tilts” of the scapula were determined and presented as angles relative to orthogonal axes (Figure 4.16 and Table 4.1).

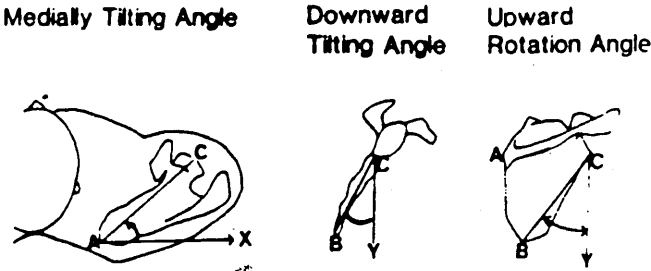


Figure 4.16: “Tilting angles of the scapula” (Kondo et al. 1984)

Arm Position	Medial tilting angle	Downward tilting angle	Lateral rotation
Resting position	38.29	12.64	51.97
90° elevation	39.86	-0.55	20.59
150° elevation	40.53	-7.17	-0.05
Max. elevation	47.46	-11.80	-8.67

Table 4.1: Rotations of the scapula measured by Kondo et al. (1984)

Although these rotational components may be reasonable, the study continues to depict the motions of the scapula using the X, Y, Z co-ordinates calculated in the study (Figure 4.17).

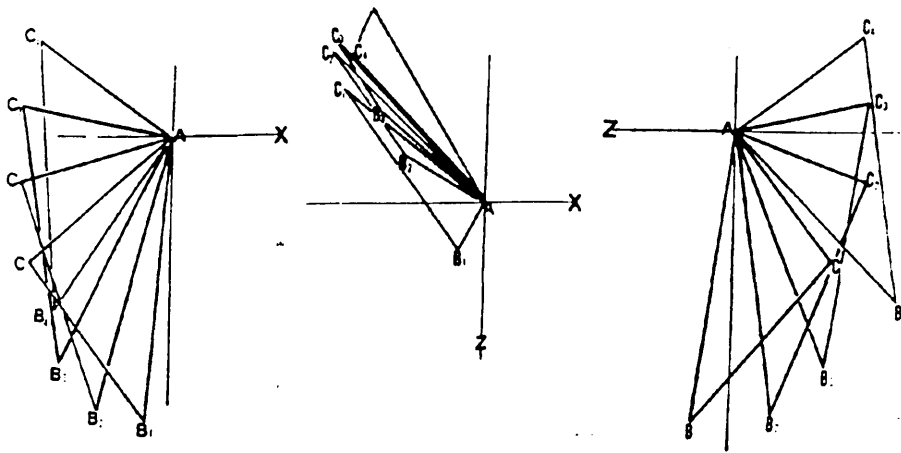


Figure 4.17: Anterior, superior and lateral views of the scapula during elevation of the arm (Kondo et al. 1984)

It is somewhat surprising to see that the point A representing the root of the scapula spine remains in a fixed position throughout the range of elevation observed.

From the table of results, the authors concluded that the plane of the scapula is exactly 40° to the coronal plane. In a two dimensional study of scapulohumeral rhythm, such claims are understandable as the out of plane rotations cannot be measured. However, in a three dimensional investigation, statements such as this should be used with caution. The results do indicate that with the arm in the resting position and at 90° and 150° elevation the scapula is at approximately 40° to the coronal plane. However, as no measurements were taken between these levels of arm elevation, it is not possible to state whether the scapula remained in this plane. Admittedly, such arguments could be raised whatever increment size in arm elevation was adopted. This presents a problem analogous with aliasing, where the increment

size must be small enough to estimate the underlying signal. The previous work of Wallace and Johnson (1982), and the two dimensional work of Doody *et al.* (1979b) suggest that an increment size of 90° is indeed too large to estimate the underlying trends, especially in the out of plane rotations presented by Wallace and Johnson (see Figure 4.15).

In 1991, Hogfors *et al.* presented a comprehensive investigation of scapulohumeral rhythm, or the shoulder rhythm as they preferred to refer to it. They describe a technique developed by Selvik (1972), in which small radiographic opaque metallic markers are implanted into the bones. By performing a normal dose stereo radiograph, the positions of these markers were recorded and used in defining co-ordinates systems for each of the bones in which they are implanted. Thereafter, low dose bi-planar radiography was employed, in which only the markers need to be identified.

Four tantalum balls of radius 0.8mm were inserted into the proximal humerus, the lateral acromion and the lateral clavicle of three subjects. After a few days rest period to overcome the soreness, bi-planar radiographs were taken at a rate of four exposures per second during dynamic motions of the arm. An unusual arm movement was requested of the subjects during measurements. Being described as a "spiral form arm-lifting movement", it is best described by the authors' text:

"The movement started from a position with the upper arm abducted 65° and outward rotated 90° . The elbow angle was kept constant as the upper arm was flexed 90° horizontally, further flexed 10° vertically and the extended horizontally to the starting position".

The reasons why this movement was used are not stated. Unfortunately, such motions make comparisons between this and other studies difficult.

Each subject performed the test three times; once without any additional loading, once with a 1kg hand load and one with a 2kg hand load. The Euler angle rotations of the clavicle, scapula and humerus were subsequently determined.

The authors concluded that the shoulder rhythm was subject dependent, exhibiting significant difference between subjects, thereby agreeing with previous work (Bagg and Forrest, 1988). They also concluded that the rhythm of an individual was essentially unaffected by small hand loads, confirming the earlier work of Doody *et al.* (1970b).

More interestingly, they found their results compatible with the static technique used by Poppen and Walker (1976), and suggested that there are no significant differences in the kinematics of the scapula between sequential static and dynamic arm motions.

4.2.4.2 Three Dimensional Digitisation Techniques

While the use of radiographic techniques has become increasingly uncommon due to the harmful effects of the ionising radiation, non-invasive techniques for measuring scapulohumeral rhythm have become more prevalent.

In 1991, Pronk and van der Helm presented a three dimensional measurement device. Named the Palpator, the device composed an open chain, four link mechanism, connected by three hinges, each of which incorporated a potentiometer. With its base secured to a known fixed origin, the position of the end point of the device in three dimensional space could be determined, allowing its use as a digitising probe.

Using palpation techniques, seven anatomical landmarks were identified around the shoulder of eighteen subjects (Pronk 1991, van der Helm and Pronk 1995). The landmarks used are illustrated in Figure 4.18.

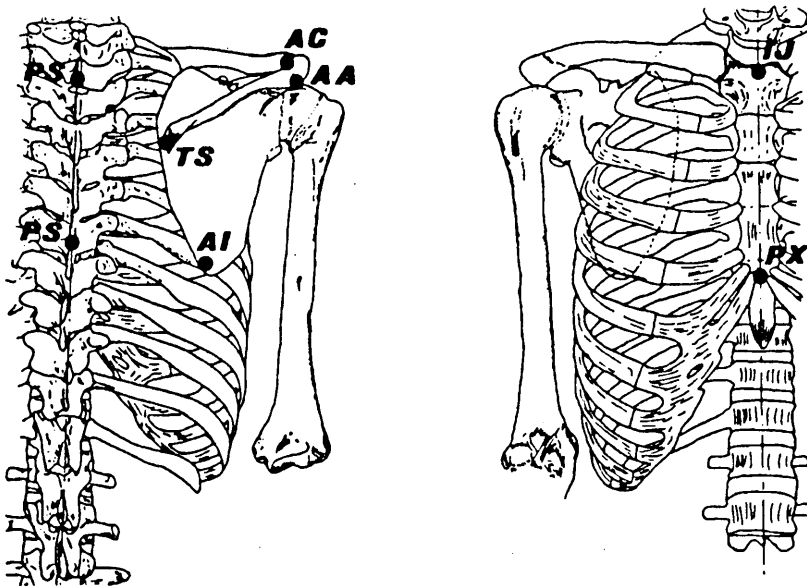


Figure 4.18: Anatomical landmarks identified by Pronk (1991)

These landmarks were then sequentially digitised through a range of abduction and forward flexion from rest to maximum elevation, in approximately 30° increments. Regression lines corresponding to the Euler angle rotations of the scapula were presented, as shown in Figure 4.19.

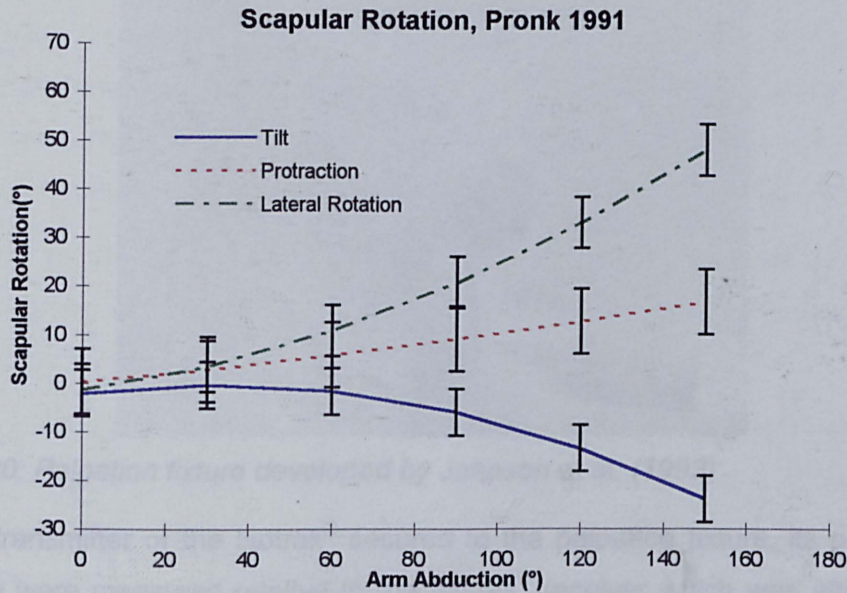


Figure 4.19: Three dimensional rotations of the scapula, measured by Pronk (1991)

By projecting data of the scapula spine and the humerus onto the coronal plane, Pronk compared his measurements of scapulohumeral rhythm with those of Inman *et al.* (1944). He found the regression lines from his study to be comparable to those of Inman *et al.*, although Pronk's 95% confidence interval for the measurements of lateral rotation of the scapula was slightly higher at 25° compared to a width of 22° from Inman *et al.*.

The advantage of this method is that it is completely non-invasive. However, digitising each of the seven individual landmarks at each level of abduction is time consuming and hence induces fatigue in subjects. Also, to standardise measurements between individuals, the subjects had to stand within a rigid frame in which their feet, hips and head were fixed. As all measurements were taken from an origin remote to the subject, the frame was necessary to ensure that upper body movements were minimised.

To overcome these problems, Johnson *et al.* (1993) developed a rigid three legged fixture which adjusted to fit over three palpable anatomical landmarks of the scapula; the posterior angle of the acromion, the root of the scapula spine and the inferior angle (see Figure 2.5 and Figure 2.6). Once set for a single subject, the fixture provided a frame external to the body which could be applied over the scapula with the arm in any position, and its whereabouts measured. The position and orientation of the fixture were measured using a Polhemus® Isotrak® six degree of freedom electromagnetic measurement system.

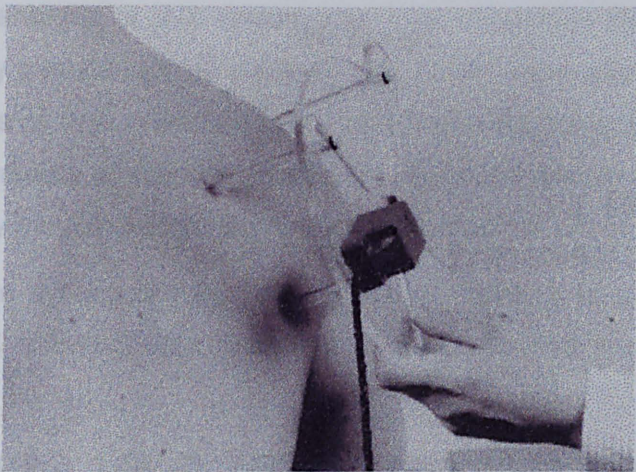


Figure 4.20: Palpation fixture developed by Johnson et al. (1993)

With the transmitter of the Isotrak[®] secured to the palpation fixture, its position and orientation were measured relative to the Isotrak[®] receiver which was attached over the manubrium sterni with adhesive tape.

Two observers measured the motion of the right shoulder of fifteen normal male subjects during abduction in the coronal plane. The palpation fixture was applied with the arm at rest (0°) and elevated to 55°, 90° and 120°, measured with a fluid filled goniometer. Euler angle rotations of the scapula were subsequently determined using the same rotation sequence as that used by Pronk (1991), and correspond well with his results (Figure 4.21).

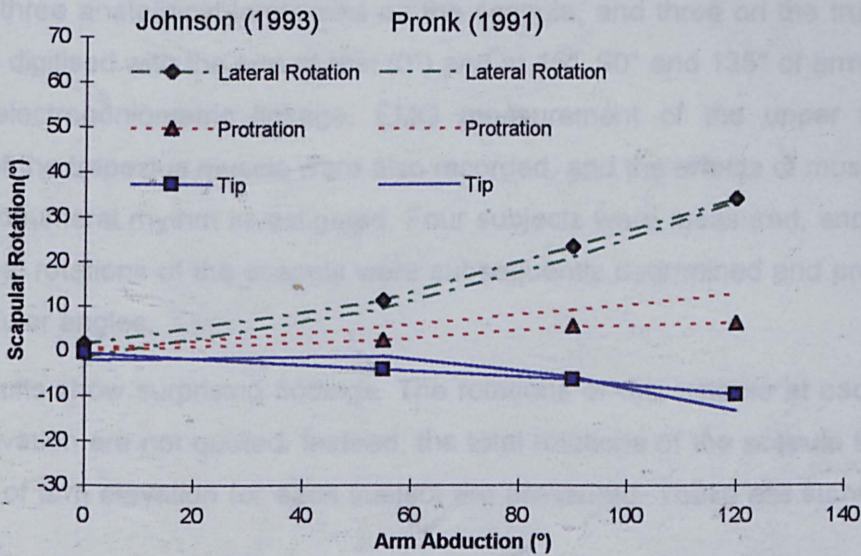


Figure 4.21: Rotations of the scapula measured by Johnson (1993), and comparisons with Pronk (1991)

The principal advantages of this system over that developed by Pronk (1991) are twofold. Firstly, by simultaneously digitising the three landmarks of the scapula, it makes the process of data collection more swift, reducing subject fatigue. Secondly, all of the measurements of scapular motion are recorded relative to the upper body. Hence, upper body movements during data collection do not affect the resulting data.

Additionally, as the system requires no calibration frame, it is small enough to be easily transported, allowing data collection to be performed conveniently within a clinical setting.

Culham and Peat (1993, 1994 and 1995) have also used the Isotrak[®] system in their studies of shoulder posture. Employing a digitising stylus, they recorded the static posture of the upper spine and shoulder complex for both normal and pathological subjects, investigating the differences between the two groups. However, as no motion studies were undertaken, their work is not wholly relevant to the discussion presented here, other to conclude that they found the accuracy of the system to be suitable for the application.

More recently McQuade *et al.* (1995) presented a single point digitising technique for measuring scapulohumeral rhythm during arm elevation in the plane of the scapula, which they boldly (and incorrectly) claim to be only the second three dimensional investigation of scapulohumeral rhythm, citing Hogfors *et al.* (1991) as the only other published technique. Using a technique very similar to that of Pronk (1991), they identified three anatomical landmarks on the scapula, and three on the trunk. These were then digitised with the arm at rest (0°) and at 45°, 90° and 135° of arm elevation, using a electrogoniometric linkage. EMG measurement of the upper and lower sections of the trapezius muscle were also recorded, and the effects of muscle fatigue on scapulohumeral rhythm investigated. Four subjects were measured, and the three dimensional rotations of the scapula were subsequently determined and presented in terms of Euler angles.

These results show surprising findings. The rotations of the scapula at each position of arm elevation are not quoted. Instead, the total rotations of the scapula throughout the range of arm elevation for each subject are presented. These are summarised in Table 4.2.

Subject	Total Scapular Rotations (°)		
	Backward tilt	Protraction	Lateral rotation
1	43.9	103.1	60.9
2	20.9	57.3	19.3
3	37.0	54.8	27.3
4	21.8	55.7	19.3

Table 4.2: Rotations of the scapula measured by McQuade et al. (1995)

It seems most surprising that in all subjects, the rotation corresponding to protraction is the greatest. It is generally accepted that the largest rotations of the scapula are in the lateral direction, as observed in all two dimensional studies mentioned earlier. The three dimensional studies reviewed above all reinforce this view, as illustrated by the results of Pronk (1991) and Johnson *et al.* (1993), shown in Figure 4.21. Additionally, it is unlikely that a rotation of over 100° about a vertical axis through the scapula is anatomically possible, yet such rotations are reported to occur on Subject 1, a normal subject.

As the measurement technique is very similar to that used by Pronk, it is surprising that the results are so contrasting. It is accepted that McQuade *et al.* used a different axis sequence in the calculations of the scapular rotations, but even taking this into account, the results appear somewhat atypical, and are more likely to be due to errors in the analysis of the data.

4.2.4.3 Other Three Dimensional Techniques

Laumann (1982 and 1987) employed stereo-photogrammetry techniques to measure the dynamic motion of the scapula during elevation of the arm in the coronal (frontal) and sagittal planes. Little is stated about how the motions were observed using this technique. It is assumed that either markers were placed on the skin, and their motion tracked, or that the contours of the skin were used directly to estimate the underlying positions of the scapula. Considering the degree of movement of the scapula under the skin, it is unlikely that the first of these methods would have provided sufficient information. Along with the early three dimensional studies of Wallace and Johnson (1982), the results clearly illustrate the previously unmeasured out of plane rotations of the scapula. A similar photogrammetric technique was employed by Runciman (1993), although the measurements were based on sequential static rather than dynamic motions of the arm.

Sidles *et al.* (1991) used a rather more direct approach of measuring the motions of the shoulder complex. Inserting pins through the skin, fixing into the bones of the scapula and humerus, they measured the motion of these bones externally from the pins, using the Isotrak[®] electromagnetic measurements system. The authors do not state the whereabouts of the origin of the measurements. The focus of the work, like that of Pronk (1991), was to investigate the implications of fusion positions in glenohumeral arthrodesis (fusion of the scapula and humerus). Unfortunately, the results and discussion are concerned with these implications, hence position and orientation data for the scapula are not quoted.

Moriwaka (1992) also used an Isotrak[®] in his investigation of three dimensional scapulohumeral rhythm. The Isotrak[®] transmitter was strapped to the front of the thorax, similar to the positioning of the receiver in the study of Johnson *et al.* (1993). The receiver was then mounted on the hand of an observer who grasped the scapula spine of the subject. With the observer grasping firmly, the subject moved his arm, and the kinematics of the scapula were recorded via the observer's hand. The results suggest that the out of plane rotations of the scapula were not detected, which, considering the limitations on scapula movement which would be imposed by such a technique, is not altogether surprising.

4.3 SUMMARY OF RELEVANT FINDINGS

As can be seen, an extensive number of techniques have been developed to investigate the motions of the shoulder girdle mechanism. However, drawing comparisons between the results of these studies is difficult due to the variety of different motions investigated, the various parameters measured and the choice of methods used to present the resulting data. Nevertheless, the key points identified by these studies which are relevant to the work presented in this thesis should be highlighted.

Firstly, it has been quite clearly shown that scapular motion is not planar. Rotations of the scapula during movements of the arm occur in three dimensions, although the "out of plane" rotations are of a smaller magnitude to the lateral rotations of the scapula measured in the two dimensional studies.

Furthermore, the majority of the two dimensional studies and most of the three dimensional studies have identified the setting phase of the scapula, first discussed by Inman *et al.* (1944). It has been stated that the scapula aligns itself with the plane

of arm elevation during this setting phase (Steindler 1962, Dvir and Berme 1978), although this statement appears not to have been proven. However, more recently the linearity of scapulohumeral rhythm beyond the setting phase has been shown by both two dimensional and three dimensional methods to be only an approximation to underlying non-linear characteristics (Doody *et al.* 1970b, Hogfors *et al.* 1991, Pronk 1991, Johnson *et al.* 1993).

The inter-subject variability between subjects has also been widely discussed (Flecker 1929, Bagg and Forrest 1988, Hogfors *et al.* 1991), although it would appear that no theories pertaining to these variations have been proposed. Similarly, the effect of hand loads on scapulohumeral rhythm has been investigated and shown to be small if not negligible.

Possibly of most interest are the differences in the measurements of scapulohumeral rhythm between studies involving dynamic and sequential static arm movements. Hogfors *et al.* (1991) determined the rotations of the scapula in the plane of projection used by Poppen and Walker (1976), and found the results to be compatible. Similarly, the dynamic results obtained by Wallace and Johnson (1982) and Laumann (1982 and 1987) appear to be of a similar magnitude to the sequential static results of Pronk (1991) and Johnson (1993), although due to discrepancies in the determination of the rotations between the different studies, accurate comparisons are impossible. Also, the two dimensional dynamic study of Michiels and Grevenstein (1995) quotes a mean value of 0.662 for the gradient for a regression line expressing the tilt of the glenoid relative to humeral abduction. This is equivalent to the spinohumeral angle determined by Inman *et al.* (1944), from which they determined a comparable gradient of 0.66.

In order to gain a complete understanding of the kinematics of the shoulder girdle mechanism, it is necessary to determine not only the rotations of the relevant bones, but also the translations. None of the studies presented here investigate the full six degrees of freedom of scapular motion. The two dimensional studies only consider one rotational degree of freedom, while the three dimensional studies generally pay no attention whatsoever to the three translational components of scapular kinematics. The exceptions to this are the work of Kondo *et al.* (1984) and Laumann (1987). However, Laumann only considered one translational component, measuring the distance between the medial border and the vertebrae, which is not independent of the rotations. Considering the work of Kondo *et al.*, the calculated co-ordinates of the

anatomical landmarks on the scapula appear erroneous due to the fixed centre of rotation at the root of the scapula spine, as illustrated in Figure 4.17 on page 73.

It must also be pointed out that many of the measurement techniques presented pay little attention to the repeatability of the results or the inherent measurement errors of the systems. Such validation procedures are essential in the assessment of the system and in the interpretation of the results.

In conclusion, it may be stated that despite the apparent multitude of published techniques for the measurement of scapulohumeral rhythm, there is a definite lack of validated, non-invasive, portable, six degree of freedom techniques suitable for use in both research and as a clinical diagnostic tool. It is the purpose of this work to develop and validate such a method, and employ the technique to develop a three dimensional, six degree of freedom, mathematical model of scapulohumeral kinematics.

Chapter 5

Materials and Methods

This chapter presents the material and methods used throughout the progress of the work, including design of a new measurement system and associated hardware and software development. The chapter continues to describe the more involved statistical techniques employed. Standard statistical techniques such as the Students t-test and the calculation of standard deviations are assumed to be understood by the reader.

5.1 INTRODUCTION

5.1.1 Criteria for a Suitable Measurement Technique

In the development of a new scapulohumeral measurement system, a set of criteria were defined. These may be summarised by stating that the system must be:

- non-invasive
- capable of measuring the three dimensional rotations and displacements of the scapula
- capable of measuring the position of the scapula across a wide range of humeral positions, and not just elevation in the coronal or sagittal planes
- portable to allow its use in clinics and not just within the research laboratory
- relatively simple and quick to use, for the benefit of both subjects and observers

Additionally, any new measurement system must be validated to determine the inherent measurement error (intra-observer) and to investigate the inter-observer repeatability.

Considering these criteria, no system for the measurement of scapulohumeral rhythm presented in Chapter 4 fulfils all of them, and some are not covered by any published technique (including, interestingly, the issue of validation). All of the radiographic studies are invasive and do not possess portability or simplicity of use (Flecker 1929, Fisk 1944, Inman 1944, Jones 1965, Freedman and Munro 1966, Poppen and Walker 1976, Wallace and Johnson 1982, Kondo 1984, Ozaki 1989, Hogfors 1991, Eto 1991, Michiels and Grevenstein 1995). Doody's scapulohumeral goniometer (1970) fulfils the requirements of portability and apparently ease of use, but only measures the rotations of the scapula in two dimensions, and like all other studies cited above, does not consider the translational components at all.

It is the techniques involving digitisation of anatomical landmarks which appear to offer the most scope. Although the results are not quoted, Pronk's Palpator (1988) must have revealed the translations of the scapula as well as the rotations. However, the system is not portable, and appears slow to use due to the number of individual landmarks which need to be digitised for each increment.

Johnson's palpation fixture (1993) overcomes this problem by simultaneous digitisation of a number of landmarks. However, the technique proved to be too inaccurate to determine the translations of the scapula due to the difficulties in repeatably placing the fixture over the anatomical landmarks. Despite this, this system fulfils many of the criteria listed above, with the exception of providing a means of controlling or measuring humeral position.

Acknowledging these difficulties, it was decided to focus on this technique, but to redesign the palpation fixture completely and analyse all sources of error to develop a new, more repeatable system.

5.1.2 Progression of Research

Following an introduction to the fundamental aspects of the measurement technique developed, all of the materials used throughout every stage of the work are presented. Subsequently, all analytical and statistical methods employed are discussed.

Such descriptions often lack explanations of why specific tools or techniques were developed, leaving this to be deciphered from the subsequent presentation of results. This often brings confusion and a general lack of continuity to the reader, making the progression of the work difficult to follow. The discussion below aims to reduce this problem by briefly describing how the research progressed in terms of materials and methods development.

As stated, the immediate requirement was a fundamental redesign of Johnson's palpation fixture in order to improve the repeatability and also the ease of use of the system. The development of this fixture, termed the *Locator* is discussed further in Section 5.4.

With this completed, preliminary testing and validation could begin following the methods discussed in Section 5.2.1. As first attempts (or even second) are rarely perfect, further developments to the technique, including standardisation of the method for positioning the Isotrak® receiver over the sternum were needed, together with general improvements in the necessary hardware as discussed in Section 5.5.

Subsequent to further testing, a validation study was performed, the results of which are presented in Chapter 6.

At this stage, the system was capable of measuring scapulohumeral kinematics only in humeral elevation. That is, humeral azimuth or rotation could not be measured or accurately controlled. Incorporating a two channel Isotrak®II, the system allowed these factors to be considered. This required slight modifications to the hardware, including some additional components, as discussed in Sections 5.4.7 and 5.5. Software developments were also necessary, including changes to the data collection software, and the development of a data analysis suite capable of performing the necessary co-ordinate transformations and representations. These aspects are discussed in Section 5.6.

A further validation study was then performed using the methods discussed in Section 5.2.2. The results of this are presented in Chapter 6.

The system was then deemed to be a valid measurement technique, and work progressed to modelling scapulohumeral kinematics more generally, as discussed in Chapter 7.

5.2 INTRODUCTION TO THE MEASUREMENT TECHNIQUE

5.2.1 Initial "Single Channel" Studies

Measurement of the position and orientation of a rigid body in three dimensional space requires knowledge of the co-ordinates of at least three non-collinear points on or within that body.

For measurement of scapular position and orientation, three palpable landmarks may be identified; the posterior angle of the acromion, the root of the scapular spine and the inferior angle¹ (Johnson *et al.* 1993). If a rigid, three legged fixture is applied over these landmarks, its position and orientation may be measured and used to determine the kinematics of the underlying scapula.

Employing a single channel Polhemus® Isotrak®, the transmitter of the system was mounted on the rigid palpation fixture (the Locator), and its position and orientation measured relative to the Isotrak® receiver which is mounted on an adjustable support and taped over the manubrium sterni.

For collection of the data, a standard test was defined for the subjects. This involved abduction of the arm in the coronal plane from 0° to 90° in 10° increments, measured with a fluid filled goniometer. During this motion, all subjects were instructed to keep their elbow flexed at 90° with their forearm pointing directly forwards at all times. This position was adopted to discourage rotation of the humerus about its long axis which may alter the rotations of the scapula. At each increment, the Locator was applied (Figure 5.1) and a record of scapular position taken by pressing the space bar on the keyboard of the host computer, or using the hand held push button which was constructed for this purpose.

¹ These landmarks are illustrated in Figure 2.5 and Figure 2.6.

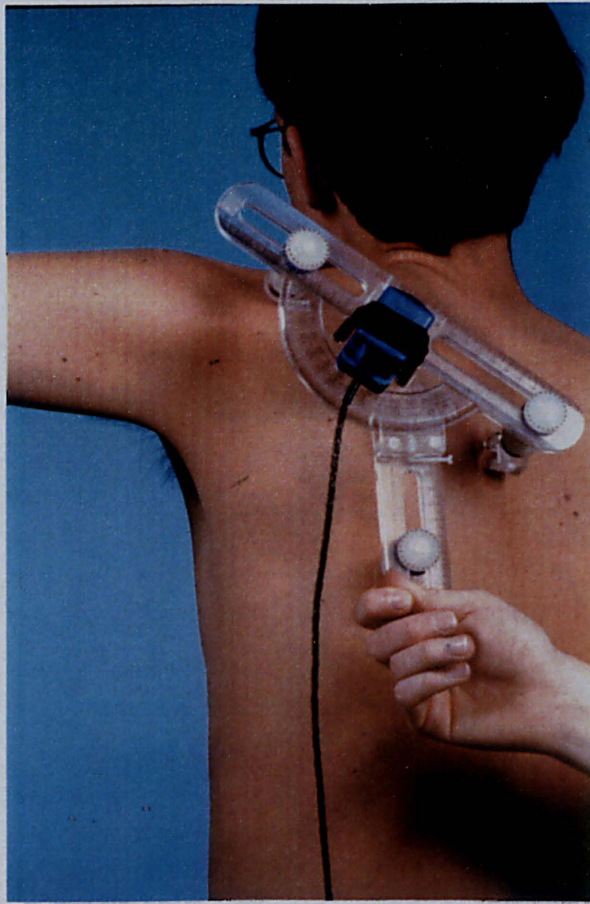


Figure 5.1: Collecting data with the Locator using the single channel Isotrak®

The displacements of the scapula, together with the Euler angle rotations were subsequently determined.

5.2.2 “Two Channel” Studies

Although demonstrated to be valid, the single channel Isotrak® technique involved the use of a fluid filled goniometer to measure arm position, limiting the application to measurements involving only elevation of the arm. Horizontal flexion (or *azimuth*) and internal/external rotation of the arm could not be controlled. In addition, it was found that during the data collection, the unavoidable time lag between measuring the position of the arm, and then measuring the position of the scapula caused inconsistencies in the results, affecting repeatability.

In order to address these problems, a two channel Isotrak®II was employed. While one channel is used to measure the position of the scapula (as in the single channel study), the second channel is mounted on an arm splint to accurately record the three dimensional position of the arm in a similar manner to that performed by Johnson and Anderson, 1990 (Figure 5.2 and Figure 5.3).

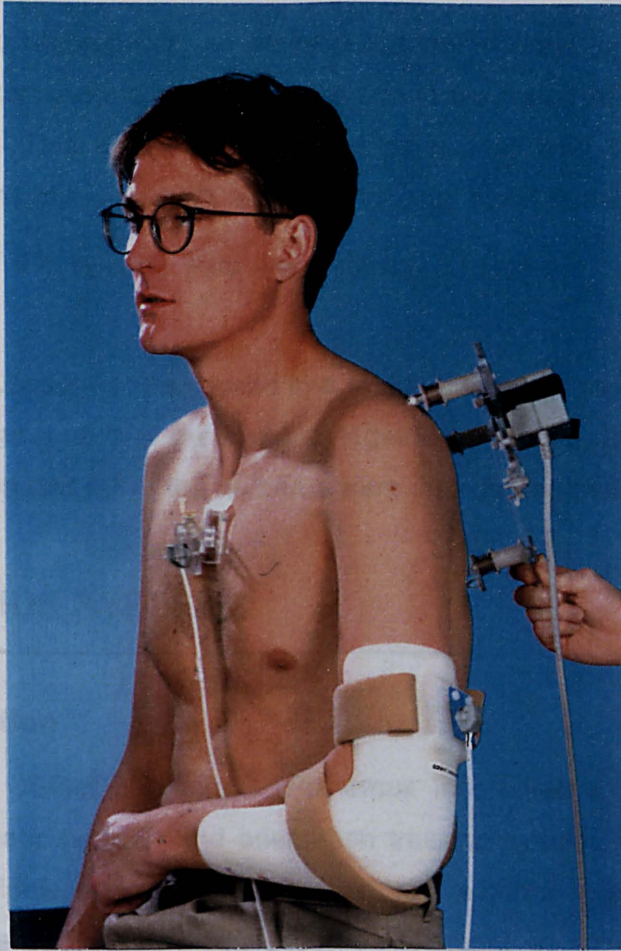


Figure 5.2: Arrangement of hardware for collecting data with the Locator using the two channel Isotrak®II

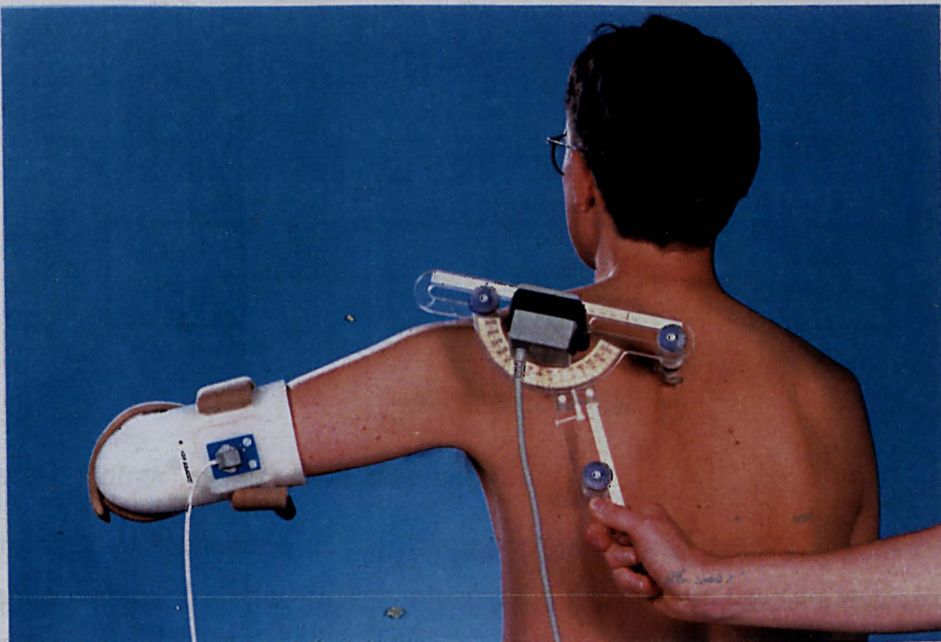


Figure 5.3: Collecting data with the Locator using the two channel Isotrak®II

Incorporating the appropriate co-ordinate transformations, custom software was developed to determine the position of the arm in the frame of the receiver mounted on the sternum. This was then displayed as a real time feedback during data collection, in terms of the azimuth, elevation and roll of the humerus.

For validation of the system, data were collected using the “standard test” defined above.

The data were subsequently analysed in a similar manner to the single channel study, yielding the displacements of the scapula, together with the Euler angle rotations. The azimuth, elevation and roll of the humerus were also determined.

5.3 POLHEMUS SYSTEMS

5.3.1 Introduction

The Polhemus® 3SPACE® Isotrak® (Polhemus Incorporated, Colchester, Vermont, USA) is a magnetic position and orientation tracking system, comprising of a three axis magnetic dipole source (or transmitter) and a three axis magnetic sensor (or receiver), together with the related electronic equipment, as shown in Figure 5.4.

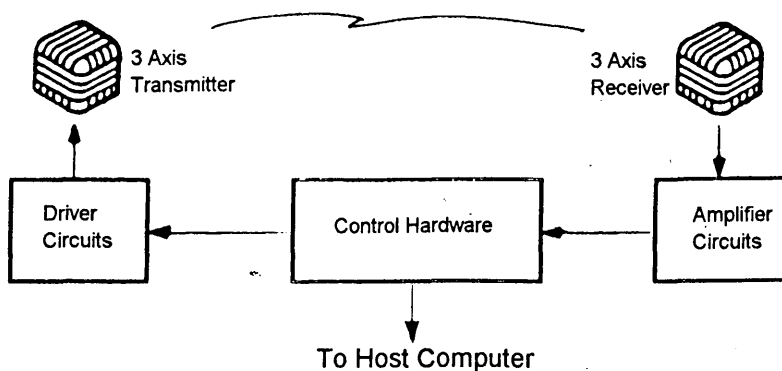


Figure 5.4: Isotrak® system block diagram

The transmitter generates a low frequency magnetic field composed of three sequential excitation states, each of which produces an independent excitation vector. The resultant of three receiver output vectors contains information sufficient to determine both the position and the orientation of the receiver relative to the transmitter, thereby providing all six degrees of freedom.

Both the position and orientation of the receiver are determined by considering the relative rotations between it and the transmitter, and employing the coupling inherent in the magnetic dipole field (Raad, 1979). The azimuth, elevation and roll system presented in Section 3.2.4 may be used to illustrate this. Representation of the orientations of the receiver employ this system directly. The position of the receiver may be represented in a similar manner by considering the rotation of frame $\{B\}$ about the axes of frame $\{A\}$, where the origins of the two frames are not coincident (Figure 5.5).

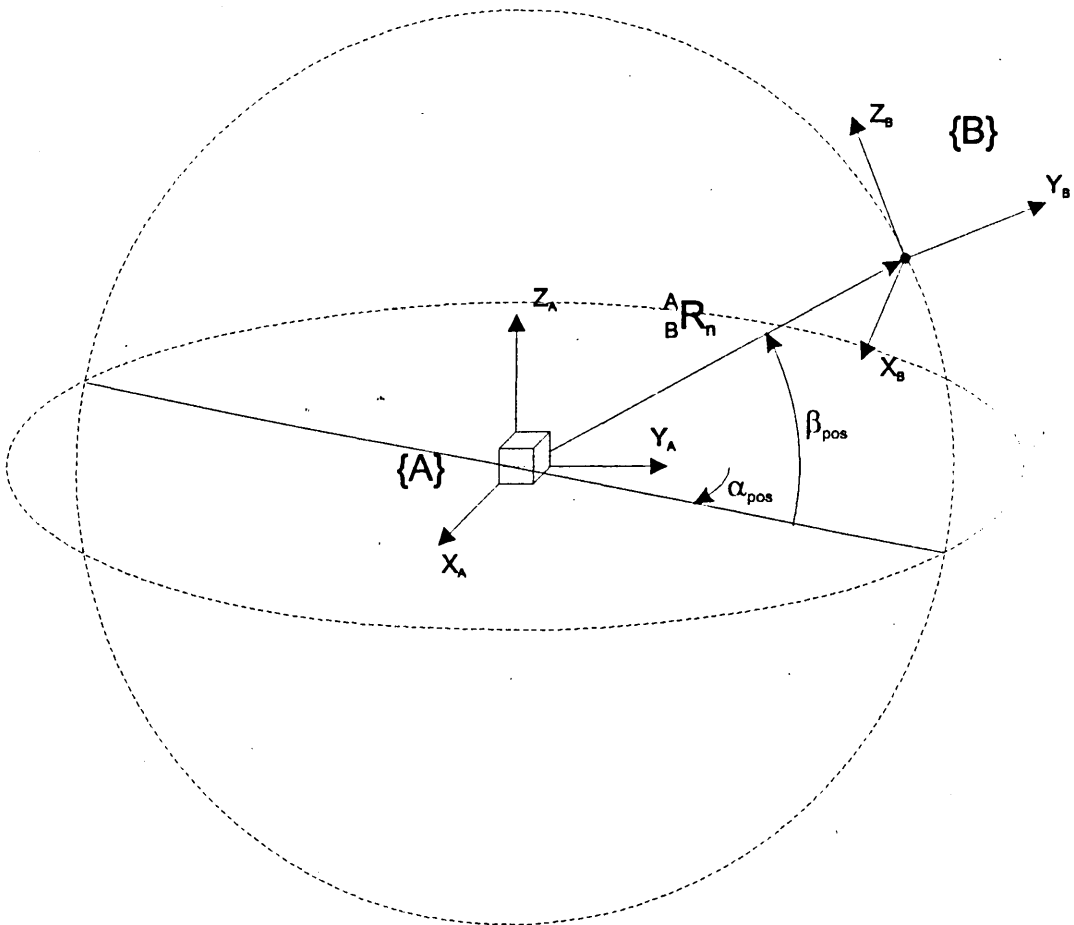


Figure 5.5: Position of the receiver relative to the transmitter

Hence, a rotation of frame $\{B\}$ about the Z axis of frame $\{A\}$ causes not only a rotation of $\{B\}$, but also a translation as it describes an arc along the perimeter of a circle centred of the Z axis of $\{A\}$. This motion is described as position azimuth (illustrated in Figure 5.5 as α_{pos}), and when combined with position elevation (β_{pos}) about the floating Y axis of $\{A\}$ together with knowledge of the radii of the arcs, specifies the position of the receiver in three dimensional space.

5.3.2 Specification of Systems Used

A single channel Isotrak[®] was used throughout the initial validation study, measuring scapular position with respect to the thorax as described in Section 5.2.1. This comprises of a Systems Electronics Unit (SEU), one receiver and one transmitter. The interface to the host computer is through a single RS-232 cable, operating through the COM1 or COM2 (serial) port. The system operates up to a maximum frequency of 60Hz.

For the second study and all of the subsequent modelling work, a two channel Isotrak[®]II was employed, the second channel allowing measurement of humeral position as discussed in Section 5.2.2. This system comprises a Systems Electronics Unit (SEU), two receivers and one transmitter. The interface to the host computer is identical to the single channel system. The system may be used with either one or two receivers and operates up to a maximum frequency of 60Hz when using one receiver, and up to 30Hz when using two receivers.

The static accuracy of the system is 2.4mm RMS for the x, y or z receiver position, and 0.75° RMS for the receiver orientation angles. These figures apply within the optimal range of the system, which is when the receivers are located within a hemisphere with a radius of approximately 100mm to 710mm from the transmitter. This range was adhered to throughout all data collection.

5.3.3 Host Computer

For the majority of the data collection throughout the thesis, an Elonex 486 DX33 computer with 4MB (and later 8MB) of RAM was used, running MSDOS[®]6.2. However, any IBM compatible computer with a 286 processor or above, running MSDOS[®]4.0 or above would suffice.

5.3.4 Important Warning Regarding Pacemakers

Due to the low frequency electro-magnetic signal generated by the Polhemus[®] systems, their use is not recommended for collecting data from or by anyone with an artificial cardiac pacemaker. Interference to such a device by excitation due to an Isotrak[®] or similar system has not been proven. However, in a personal communication with Polhemus[®], they stated their systems had not been tested in such situations and strongly discouraged their use.

5.4 DEVELOPMENT OF THE LOCATOR

5.4.1 Assessment of the Current Fixture

The palpation fixture used by Johnson *et al.* (1993) demonstrated the possibility of measuring the rotations of the scapula by measurement of an external frame placed over anatomical landmarks located under the skin.

However, determination of the translational co-ordinates is essential for a full understanding of scapulohumeral kinematics. Analysis of the data collected with Johnson's system (1993) showed that its design was not appropriate with such requirements. It is believed that the reasons for this stemmed predominately from the approximate location of the three pointers of the fixture which were positioned over the palpable landmarks. Each of these pointers were identical, being a perspex rod tapered to an approximately 2mm radius point at the end, which were difficult to place repeatably over an anatomical landmark on the scapula. Location of the angle of the acromion was not a great problem as it too may be identified as a single point. However, both the root of the scapula spine and the inferior angle are palpable as relatively large areas, hence precise and repeatable location of these landmarks by each pointer of the fixture was extremely difficult.

In addition to this, the palpation fixture was somewhat inflexible with regard to both measuring the dimensions between the pointers (required for the subsequent calculation of the co-ordinates of each anatomical landmark), and in moving the pointers themselves in order to accommodate testing scapulae of different sizes. Measurement of the distances between the pointers had to be performed separately for each one, using a rule external to the device. Adjustment of the pointers for repositioning required loosening the screws which secure them to the main body. This then allowed them to be moved within slots in the body of the fixture, increasing or decreasing the appropriate dimensions as appropriate for the scapula being tested, followed by tightening of the screws once more. Performing this adjustment while holding the fixture and palpating the landmarks required extreme dexterity and patience!

A revised device to replace the original fixture was therefore designed: the Locator. The fundamental design requirements of this over the original fixture were hence to improve the accuracy and therefore the repeatability, and to make the device more simple to use.

5.4.2 Anatomy of the Locator

The aim of the Locator is to provide a representation of the position and orientation of the scapula in a structure external to the body, the kinematics of which may then be measured. As stated earlier, measurement of the position and orientation of a rigid body in three dimensional space requires knowledge of the co-ordinates of a minimum of three non-colinear points on or within that body. For non-invasive measurement of scapular kinematics, these points must be palpable through the skin, enabling their location to be determined. The most palpable landmarks on the scapula are undoubtedly those used by Johnson *et al.* (1993), that is the posterior angle of the acromion, the root of the scapula spine and the inferior angle of the scapula (see Figure 2.5 and Figure 2.6). It is hence logical to design the Locator to "locate" over these landmarks.

An illustration of the Locator in its final form is shown in Figure 5.6. The purpose of this is to introduce the main elements of its design, which are discussed in the following sections.

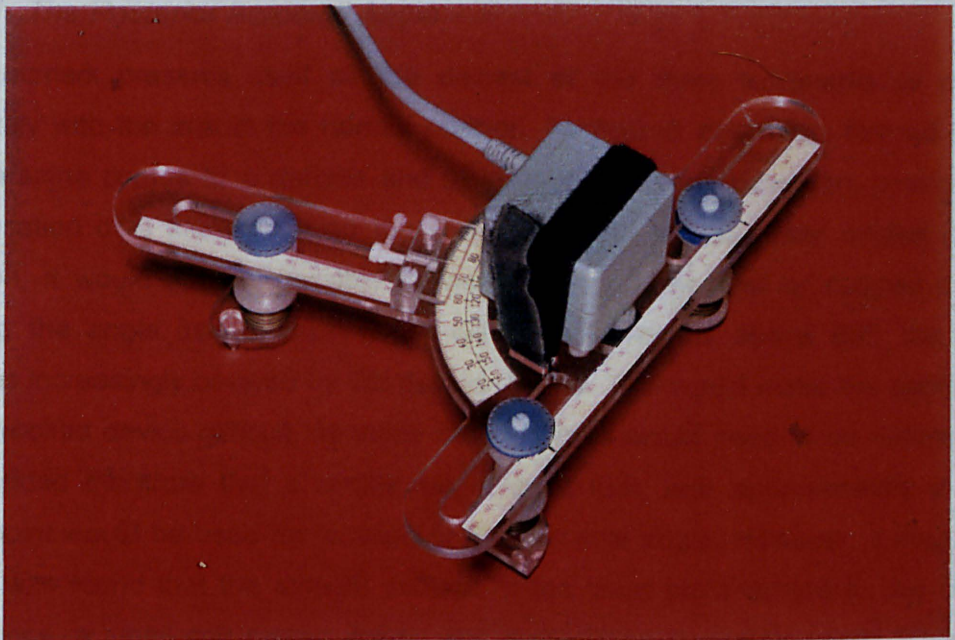


Figure 5.6: Illustration of the Locator in its final form

The *main body* of the Locator is comprised of two parts; the upper symmetrical flat perspex sheet to which the Isotrak[®] transmitter is fastened, and the lower swinging *arm*. The arm is fastened to the upper main body by a central bolt with a friction washer to maintain its position. A twist clamp is also fitted to the arm to provide an additional restraint against movement.

The Locator has three *legs*, one in each of the slots on the main body. At the end of each leg are the *feet* of the Locator, the shape of which are specific to the landmark over which they locate.

The three slots in the main body (two in the upper part and one in the arm) allow the legs to be adjusted to accommodate different size scapulae.

5.4.3 Design of the Locator Feet

In order to improve the repeatability in positioning the fixture over the anatomical landmarks, the Locator feet which position directly onto the skin (over the landmark) have been designed to *fit* over each specific landmark. Both live subjects and cadavers in various stages of dissection were used to develop an understanding of the contours of the landmarks and how their identification is affected by various muscles throughout ranges of humeral motion. This led to the development of customised feet for the three landmarks, each of which are discussed below.

5.4.3.1 *The Posterior Acromial Angle*

This landmark presents itself as the easiest of the three landmarks to palpate accurately with the arm in the normal position. Its distinct angularity, formed as the scapula spine comes to a definite end at its union with the acromion, provides for easy location of a blunt point on the surface of the skin. At lower angles of arm elevation, it would appear possible to locate a slightly hooked or cupped device, covering the angle itself. However, as elevation increases above 90°, the angle becomes increasingly covered by the deltoid muscle. This would make the application of any hooked device difficult, as many muscle fibres would need to be deformed. It was decided therefore that a simple single point foot, with approximately a 4mm radius point would be used for location of the acromial angle. However, during initial tests, it was found that the smooth surface of the blunt point tended to slip on the skin. Hence, a small soft rubber insert, with a diameter of approximately 2mm was fitted into the end of the point. This increased the coefficient of friction between the Locator and the skin making the foot stay more firmly in place over the acromial angle. The final arrangement for this foot is illustrated in Figure 5.7.

5.4.3.2 *The Root of the Scapula Spine*

This landmark is palpated by tracing the path of the scapula spine from the easily identifiable angle of the acromion, medially across the scapula until the medial border is encountered. Its most characteristic feature is the distinct contour of this border,

which allows the positioning of some form of locating device against it. A restraint must also be incorporated into the device to rest against the surface of the scapula, slightly lateral to the medial border (that is, directly over the root of the scapula spine). This ensures that the perpendicular distance between the surface of the skin, and hence the scapula via the landmark, and the body of the Locator is kept constant.

A three pegged device arranged in a triangular formation was therefore designed as the foot locating over the root of the scapula spine. The two medial pegs are slightly longer (approximately 5mm) than the lateral peg, allowing them to be positioned against the medial border, while the shorter (lateral) peg ensures that the Locator remains in a plane parallel to that of the scapula. Initially, all of the pegs were mounted parallel to the main legs of the Locator. However, it was found that a better overall *fit* was achieved if the pegs were mounted at an angle inclined towards the scapula, encouraging the Locator to almost grasp the scapula spine at both ends. This arrangement can be seen in Figure 5.7.

The feet for the acromial angle and the root of the scapula spine are interchangeable to enable measurement of both left and right scapulae.

5.4.3.3 *The Inferior Angle*

This landmark may be palpated by following the medial border downwards until its union with the lateral border. Generally, with the arm in the normal position, this angle is quite obvious as the overlying layers of muscle are few. However, in some cases the latissimus dorsi muscle has an attachment to the inferior angle, making palpation more difficult.

Of the three angles of the scapula, the inferior angle is by far the most acute, and as such the design of a device to locate over it is made relatively simple. As with the root of the scapula spine, pegs may be located against the borders of the scapula, in this case one against the medial border and one against the lateral border. A third peg, resting on the surface of the skin directly over the inferior angle is also used in a manner to that described above, that is, to position the body of the Locator in a plane parallel to that of the scapula. This arrangement is illustrated in Figure 5.7.

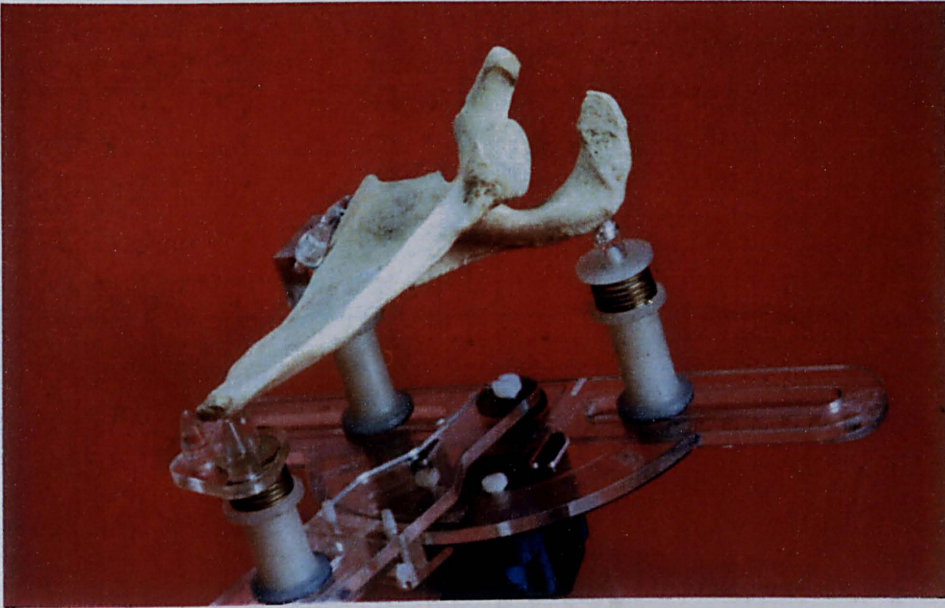


Figure 5.7: Illustration showing the details of the Locator feet and how they fit around each anatomical landmark

5.4.4 Improving the Simplicity of Use

5.4.4.1 Adjustment of the Locator Leg Positions

In order to measure different scapulae, it is necessary for the Locator to be easily adjustable to accommodate differing sizes. As stated earlier, Johnson's palpation fixture necessitated the loosening and tightening of screws, while holding the fixture and palpating the landmarks - at least a three handed job! Some form of quick release mechanism was therefore desired.

To achieve this, each leg of the Locator incorporates a sliding sprung collar. When this collar is pulled away from the main body towards the foot, the leg will slide easily. Upon its release, the leg is again held in place. It was found that to maintain the fixed position, extra friction between the main body and the collar was needed. This was provided by bonding Dycem™¹ washers to the surface of the collar in contact with the main body of the Locator, thereby increasing the coefficient of friction between the two surfaces.

This arrangement is illustrated in Figure 5.8.

¹ Dycem™ is a synthetic material possessing a high friction coefficient.

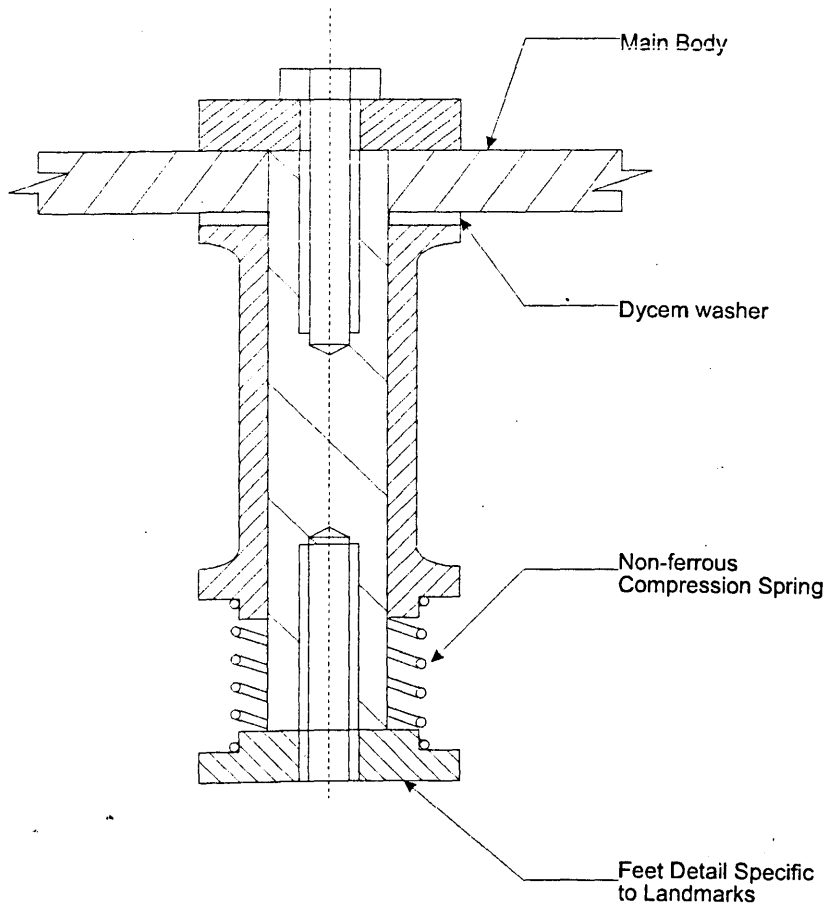


Figure 5.8: Sprung collar of Locator legs for rapid and easy adjustment

5.4.4.2 Measurement of Scapula Dimensions

To aid speed and accuracy of data collection it is advantageous to be able to take the principal dimensions of the scapula¹ directly from the Locator. To perform such a task it is necessary to have a visible scale apparent on the device from which to read the distances between the legs. However, it would be somewhat cumbersome to use a linear scale for each. Hence for the dimension between the acromion angle and the root of the scapula spine a linear scale is used, while the inferior angle is expressed as a polar co-ordinate from a point a fixed distance from the acromial angle leg. The acromial angle leg was set to a fixed position on the body of the Locator. The dimensions between the legs may be entered into the data analysis software (discussed in Section 5.6.2) to provide the co-ordinates of the three feet of the Locator, and hence the underlying anatomical landmarks on the scapula in the frame of the fixed sternal receiver (measurement error notwithstanding). The measurement scales may be seen in the illustration of the Locator on page 93 (Figure 5.6)

¹ The principal dimensions are defined as the distances between the three anatomical landmarks.

5.4.5 Other Design Considerations

When using electro-magnetic measurement equipment, no ferrous, and preferably no metallic objects should be within the working range of the equipment (up to 0.7m for optimal accuracy). The main structure of the Locator was therefore constructed in perspex, with the legs and some of the feet details being made from Nylon 66. Nylon nuts and bolts were used throughout.

To achieve the necessary displacements and restoring forces in the sprung collar mechanism used in the Locator legs, metallic springs had to be used as no other material could be found to fulfil the criteria. However, the springs were made from non-ferrous beryllium copper with a wire diameter of under 1mm. It was found that such a small quantity of a metallic material had no noticeable effect on the Isotrak® systems.

The Isotrak® system is designed with the intention of fixing the transmitter to a reference base and measuring the position of the moving receiver relative to it. However, the reference base in this application is the thorax, or more specifically the manubrium sterni. Securing the transmitter to the skin over this would be difficult due to its size and weight (100g for the Isotrak® and 270g for the Isotrak®II). However, the receivers are relatively small and light (17g) allowing them to be easily fixed on the skin with adhesive tape. As the weight of the Locator is never taken by the subject, but supported by the observer, securing the transmitter to the Locator was not a problem.

5.4.6 Illustrations of the Prototype Locator

The initial Locator is shown in Figure 5.9. The single channel Isotrak® transmitter can be seen mounted on the main body, secured with the Velcro™ strap. The scales for measuring the distances between the Locator legs were constructed from standard flat faced rules and a 180° protractor with a radius of 75mm.

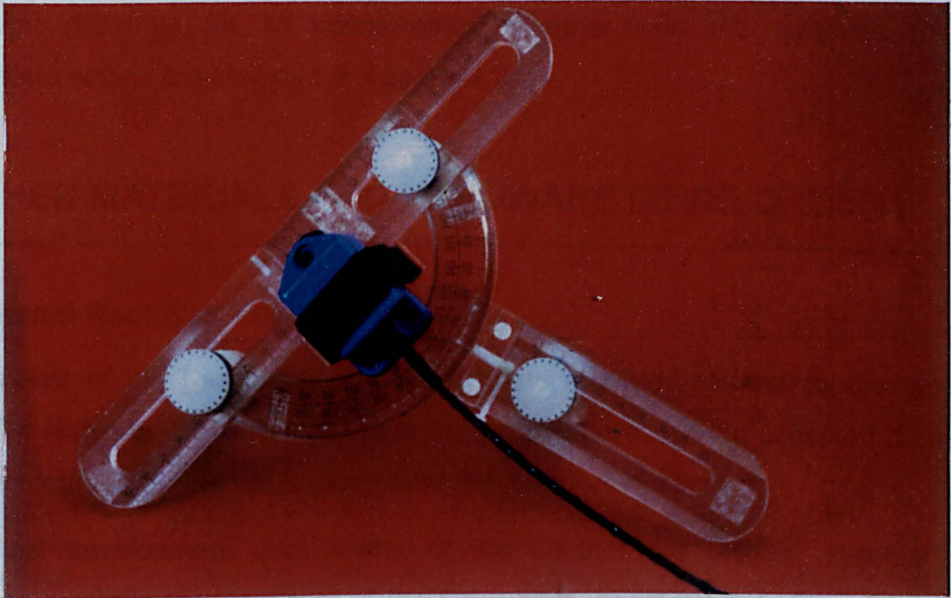


Figure 5.9: Illustration of the prototype Locator

5.4.7 Modifications for Two Channel System

Very few modifications in design were necessary to allow the Locator to be used with the two channel Isotrak®II. The most important consideration was in the location of the Isotrak®II transmitter.

The data from the Isotrak® provide a position vector from the electrical centre of the transmitter to the electrical centre of the receiver. In order to determine the coordinates of the Locator feet, it is essential to know the vectors describing the position of the Locator feet relative to the electrical centre of the Isotrak® transmitter mounted on the Locator. Hence for the Isotrak® and the Isotrak®II to provide equivalent results, the electrical centre of the transmitter must remain in the same position relative to the fixed leg for the acromial angle. Although any such differences could easily be controlled in the data analysis software, changes to the design of the hardware are more permanent, and less likely to be overlooked by others who may develop further software in the future.

The only other differences between the revised Locator and the prototype were in measurement scales used for measuring inter-leg distances. Instead of using the plastic rules and protractor, which required machining to be suitable, a printed template was constructed and applied using clear self adhesive film.

The final version of the Locator may be seen in Figure 5.6 on page 93.

The design drawings for all components, together with the template for the measurement scales are included in Appendix 3.

5.5 OTHER MATERIALS AND HARDWARE DEVELOPMENT

5.5.1 Sternal Receiver Mount

Measurements of the position of the Locator are recorded relative to the Isotrak® receiver. To eliminate the effect of upper body movements on the collected data, the receiver is mounted on the upper body over the manubrium sterni.

During initial development and testing of the Locator the Isotrak® receiver was mounted on a 40mm square sheet of flexible rubber, approximately 2mm thick. This provided an area to apply the adhesive tape (Leukofix) necessary to secure the receiver on the skin.

Although this provided an adequate fixture in the early prototyping studies, it was not suitable for comparisons between subjects due to the variations in the inclination of the sternum.

Instead, an adjustable support was developed which allows the orientation of the receiver to be adjusted after application on the sternum. A bubble level mounted within the support allows the receiver to be positioned vertically with respect to a global (laboratory) frame.



Figure 5.10: Illustration of the sternal receiver mount

Design drawings for this mount are included in Appendix 3.

5.5.2 Fluid Filled Goniometer

For all data collected with the single channel system, measurement of humeral elevation was performed using a fluid filled goniometer (MIE Medical Devices, Leeds, UK). A method for attaching a strap to the goniometer was also constructed. This allowed the goniometer to be fixed to the upper arm throughout the data collection.

The goniometer/strap assembly is illustrated in Figure 5.11

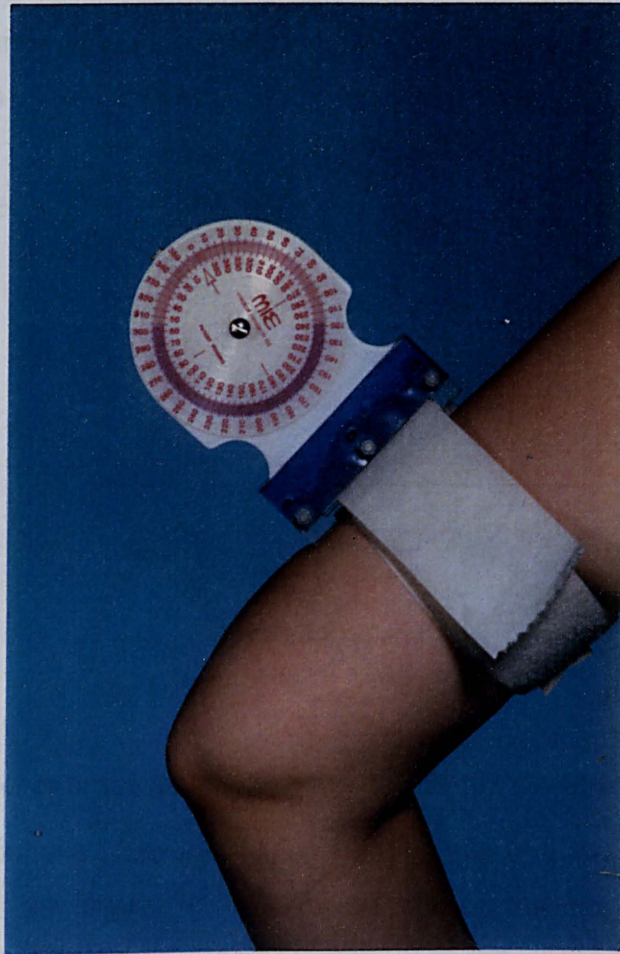


Figure 5.11: Fluid filled goniometer and arm strap

5.5.3 Arm Splint

Three dimensional measurement of humeral position was made possible by employing the second receiver of the Isotrak®II system. The receiver was attached to the arm via a moulded polythene arm splint (J. C. Peacock and Son Ltd., Newcastle upon Tyne, UK). The arm splint was moulded with the elbow flexed to 90° to ensure internal/external rotation of the humerus was observed, and was secured in place using Velcro™ straps.

A flat surface was moulded into the posterior of the upper arm of the splint to provide a fixing area for the Isotrak® receiver. However, it was found that this surface was not normal to the direction of the lower arm of the splint, which would lead to errors in the determination of humeral angles relative to the sternal receiver. Although these errors would be of a fixed magnitude, their effect on the measured humeral angles would be in an opposite sense for the left and right arms. For example, Figure 5.12 illustrates the effect of an error in the mounting. The orientation of the receivers mounted on the

left and right arms is identical with respect to a medio-lateral axis. However, it is obvious that the orientation of the arm is different in each case.

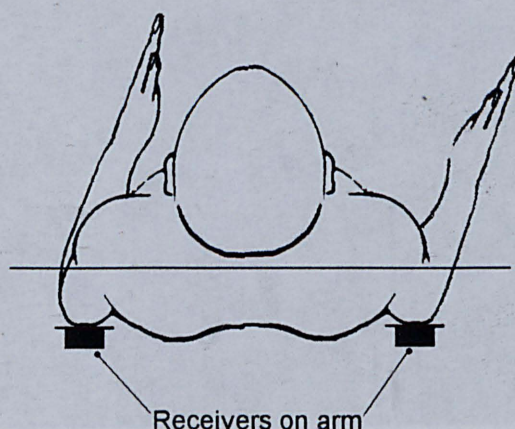


Figure 5.12: Effect of errors in mounting the receiver on the arm splint

An additional mounting plate was hence incorporated onto the splint, which allowed the orientation of the receiver to be adjusted, making the mounting plane normal to the direction of the forearm.

5.5.4 Data Collection Switch

Using data collection software previously developed (see Section 5.6.1), an Isotrak[®] record (containing orientation and displacement parameters) was obtained upon pressing the space bar on the host computer. In practice, this proved difficult to perform, especially when working solo, as the reaching movements of the observer in pressing the space bar often caused slight movements in the Locator.

A remote push button was therefore obtained (RS Components Ltd., UK), which was mounted on the Locator, and communicated with the host computer via the LPT1 (parallel) port. This enabled each record to be taken without the need for the observer to reach to a keyboard, making data collection faster, easier and more accurate.

5.5.5 Calibration Rig

A calibration rig was designed and built for use in assessing data analysis routines (Figure 5.13).

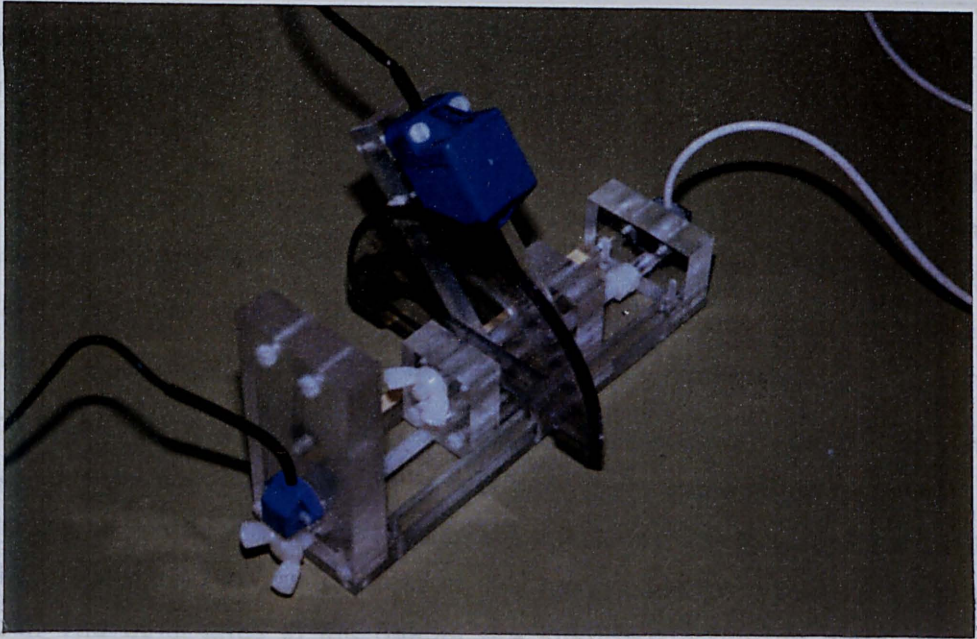


Figure 5.13: Isotrak[®] calibration rig

This consisted of a flat tray, approximately 300mm long, with a fixed support at either end providing mountings for Isotrak[®] receivers or transmitters. Within the tray is a carriage which can be moved along the length of the tray by rotation of a central threaded drive. The carriage itself incorporates a rotating arm which may be clamped at any angle between $\pm 90^\circ$ from vertical. The arm also provides mountings for Isotrak[®] receivers or transmitters.

Linear and rotational scales were gauged to 1mm and 0.5° respectively.

Design drawings of this rig are included in Appendix 3.

5.6 SOFTWARE

5.6.1 Data Collection Software

An application for collecting data using the single channel Isotrak[®] system had been previously developed and used by Johnson *et al.* (1993). This application was used for all single channel studies, although slight modifications were necessary to allow the use of the push button.

The program prompts the user for details about the subject (name, age, height, weight, gender), and saves all of this information in a three line header of the resulting data file (*.dat.), the name of which may be chosen by the user. The kinematic data is

saved in the file in terms of the transposed rotation matrices (oddly) and displacement vectors of the receiver in the frame of the transmitter.

In order to use the two channel Isotrak[®]II system, the application had to be upgraded to take account of the increased record size, being two rotation matrices and two displacement vectors for each recorded position instead of just one. The resulting application, iso2.exe, also required "real-time" visual feedback of the co-ordinates of the arm in terms of the azimuth, elevation and roll of the humerus.

The format of the *.dat data file for both 3dmove and iso2 was changed to store the non-transposed rotation matrices of the receivers in the frame of the transmitter. Also, allowance was made for a 35 line header which included a field stating the number of receivers used during the data collection, this being used for subsequent analysis of the data. The other lines in the header are intended to provide more information regarding data collection in future revisions of the software. This is now the standard CREST¹ format for Isotrak[®] data files.

Both 3dmove and iso2 run on a IBM compatible PC running MSDOS[®]4.0 or above.

At the time of writing a new data collection application was being developed, being capable of handling single channel Isotrak[®] systems, together with the Isotrak[®]II and three and four channel Fastrak[®] systems. This system, when completed, will run under Microsoft[®] Windows[™] 3.1 or above.

Due to concentrating on the data analysis routines, the author was not directly involved in the development of the data collection applications, although contributed the algorithms for the co-ordinate transformations necessary to provide the azimuth, elevation and roll of the humerus in the frame of the sternal receiver for iso2.

5.6.2 WinMat Data Analysis System

Although software had been previously developed for analysis of scapular kinematics using the single channel system (newang.exe and scappos.exe), nothing was available for performing more complicated co-ordinate transformations necessary for all two channel studies. Also, the existing software, although accurate, was poorly documented and not particularly intuitive to use, and did not take account of the rather odd transposed rotation matrix format of the Isotrak[®] data file.

A completely new data analysis system was therefore developed. As it was desirable for the software to operate under Microsoft[®] Windows[™], the C++ computing language

¹ CREST is the Centre for Rehabilitation and Engineering Studies, the institution of the author.

was used. Upon learning the language and developing an understanding of “programming for Windows™”, an application was designed which would be suitable for use with the single channel Isotrak® system, together with the two channel Isotrak®II and the three and four channel Fastrak® systems. The resulting application, WinMat (Windows Matrices), is hence compatible with the new data collection software under development at the time of writing.

WinMat uses Isotrak® data files (*.dat, CREST format, 3 or 35 line header) as its input, and outputs a text file containing headed lists of rotations and displacements (*.out).

Its primary purpose is to perform various co-ordinate transformations on the input data, and calculate the rotation angles and displacements of the system being measured.

It includes a number of options for specifying a desired orientation format, including global frame and local frame Euler angles, and azimuth, elevation and roll systems about any of the orthogonal axes of the global co-ordinate frame (Figure 5.14). The kinematic description of these representations are discussed in Chapter 3.

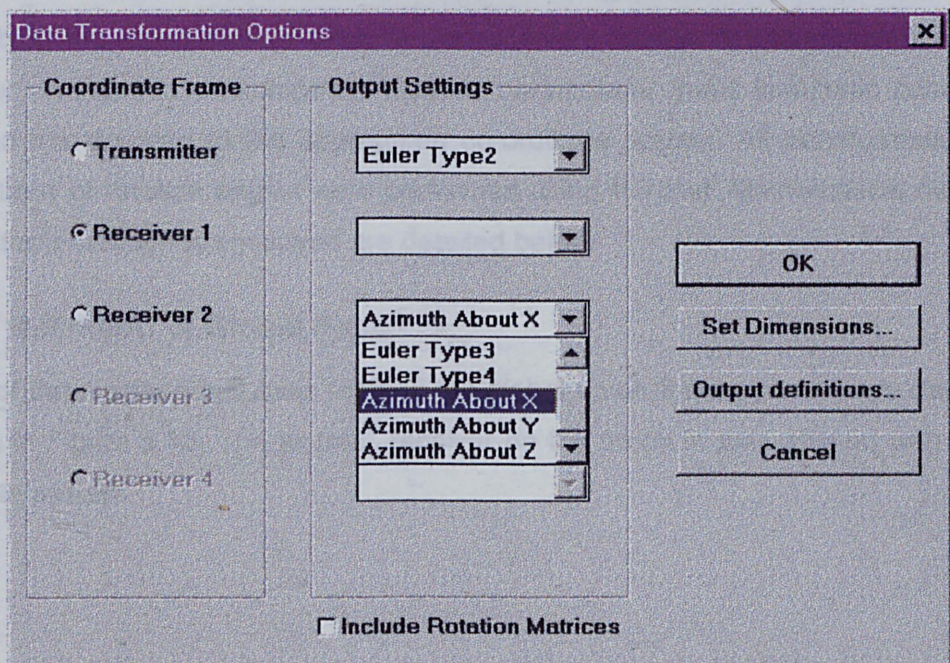
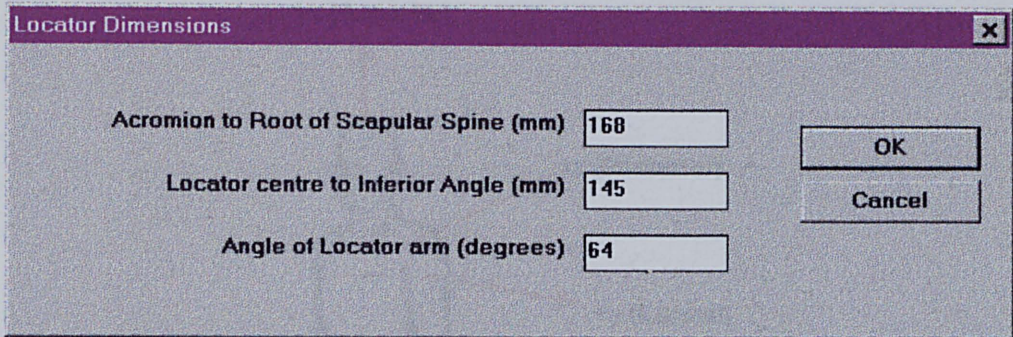


Figure 5.14: Data transformation options for a two channel file (one transmitter, two receivers) being analysed in WinMat

The system also allows the dimensions of the scapula, taken from the Locator, to be entered directly, and determines the co-ordinates of the feet of the Locator in the specified co-ordinate frame Figure 5.15.

A screenshot of a software dialog box titled "Locator Dimensions". It contains three input fields with the following labels and values: "Acromion to Root of Scapular Spine (mm)" with value "168", "Locator centre to Inferior Angle (mm)" with value "145", and "Angle of Locator arm (degrees)" with value "64". To the right of the input fields are two buttons labeled "OK" and "Cancel". The dialog box has a standard Windows-style title bar with a close button (X) in the top right corner.

Acromion to Root of Scapular Spine (mm)	168
Locator centre to Inferior Angle (mm)	145
Angle of Locator arm (degrees)	64

Figure 5.15: Entering the dimensions of the scapula into WinMat

A User Guide to WinMat has been written, describing the transformation options which includes a step-by-step guide to analysing a data file using the application. Mathematical definitions of all co-ordinate transformations, for rotations and displacements are also presented. This guide is included in Appendix 5.

5.7 DATA ANALYSIS

The CREST format Isotrak[®] data file contains rotation matrices and position vectors describing the kinematics of each of the receivers relative to the transmitter on the Locator. In order to determine the desired parameters, these kinematic descriptions needed transforming to the appropriate co-ordinate system. All transformations and derivations of rotation angles were performed using WinMat. Mathematical definitions of the transformations employed are detailed below.

5.7.1 Definition of Global Axes

A set of three orthogonal axes forming the global co-ordinate system were defined as shown in Figure 5.16. The Isotrak[®] receiver on the sternum was aligned with this co-ordinate system.

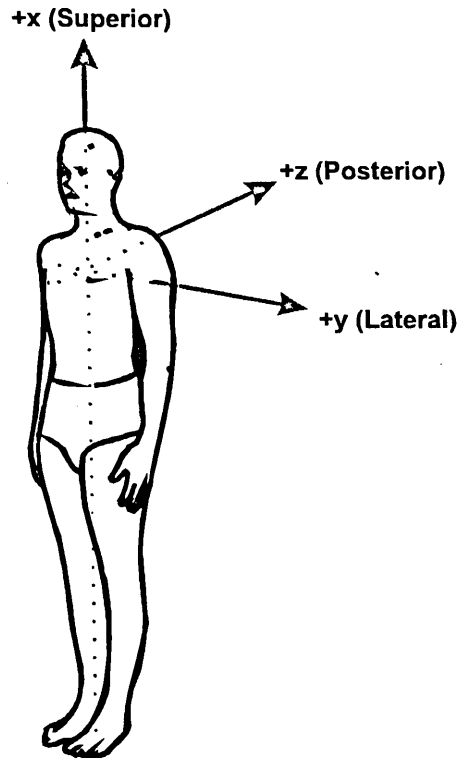


Figure 5.16: Global co-ordinate system

The co-ordinates of the humerus were determined using the azimuth, elevation and roll system presented in Chapter 3, where the polar axis is the global x axis. Hence, the co-ordinate system for the humerus consists of a vertical axis through the head of the humerus (the azimuth axis), a horizontal axis through the head of the humerus (the elevation axis) and an axis coincident with the longitudinal axis of the humerus itself (the roll axis). This is referred to in WinMat as "Azimuth About X" for Receiver 2, the global co-ordinate system being specified by Receiver 1 (see Figure 5.14).

The co-ordinate transformations necessary to provide the rotation matrix describing the orientation of receiver 2 in the frame of receiver 1 may be presented with the aid of Figure 5.17.

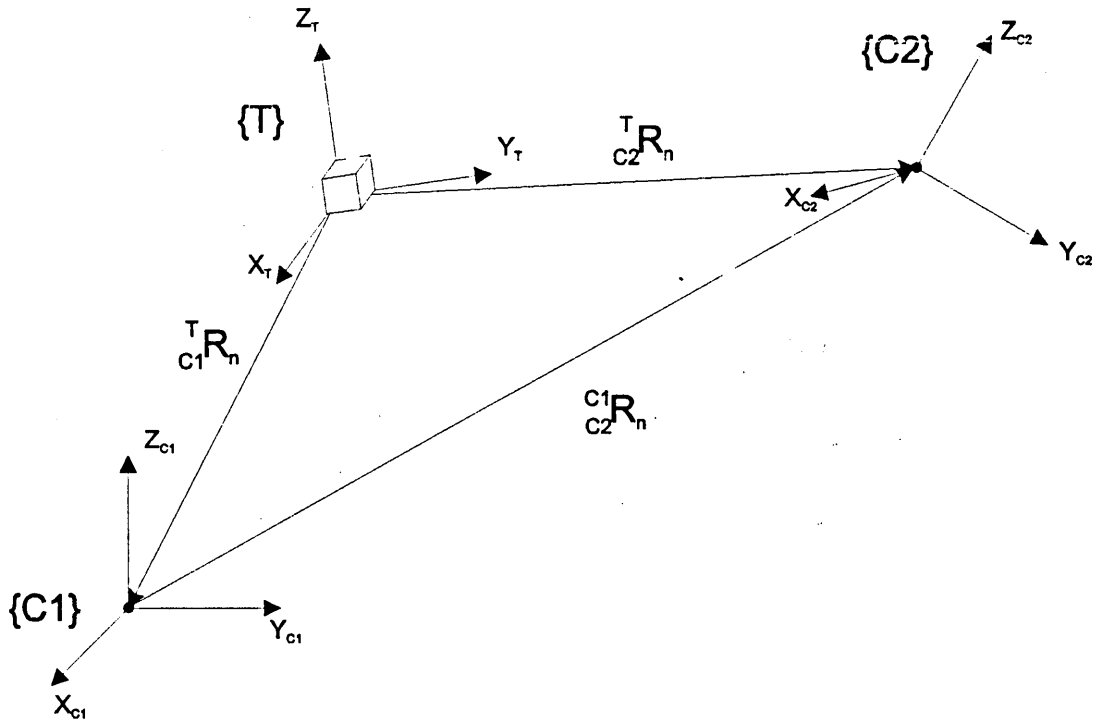


Figure 5.17: Rotations of Receiver 2 (C2) in the frame of Receiver 1 (C1)

Using the notation introduced in Chapter 3, ${}^{T}_{C1}R_n$ is the rotation matrix describing Receiver 1 (C1) in the frame of the Transmitter (T), while ${}^{T}_{C2}R_n$ is the rotation matrix describing Receiver 2 (C2) in the frame of the Transmitter (T). The rotation matrix describing C2 in the frame of C1 is given by:

$${}^{C1}_{C2}R_n = {}^{T}_{C1}R_n^T \cdot {}^{T}_{C2}R_n \quad (5.1)$$

However, as discussed in Chapter 3, the default polar axis is the z axis, so extraction of the azimuth, elevation and roll directly from ${}^{C1}_{C2}R_n$ would lead to confusing results.

The rotation matrix ${}^{C1}_{C2}R_n$ needs to be transformed by a $+90^\circ$ rotation about the y axis to make the x axis the polar axis. Hence,

$${}^{C1}_{C2}R_n{}^{Polar\ x} = \begin{bmatrix} 0 & 0 & 1 \\ 0 & 1 & 0 \\ -1 & 0 & 0 \end{bmatrix} \cdot {}^{C1}_{C2}R_n \quad (5.2)$$

The co-ordinates of the humerus may now be extracted as discussed in Chapter 3.

5.7.2 Definition of Scapula Axes

A co-ordinate system for the scapula was defined as shown Figure 5.18. This system is aligned with the Isotrak[®] transmitter mounted on the Locator.

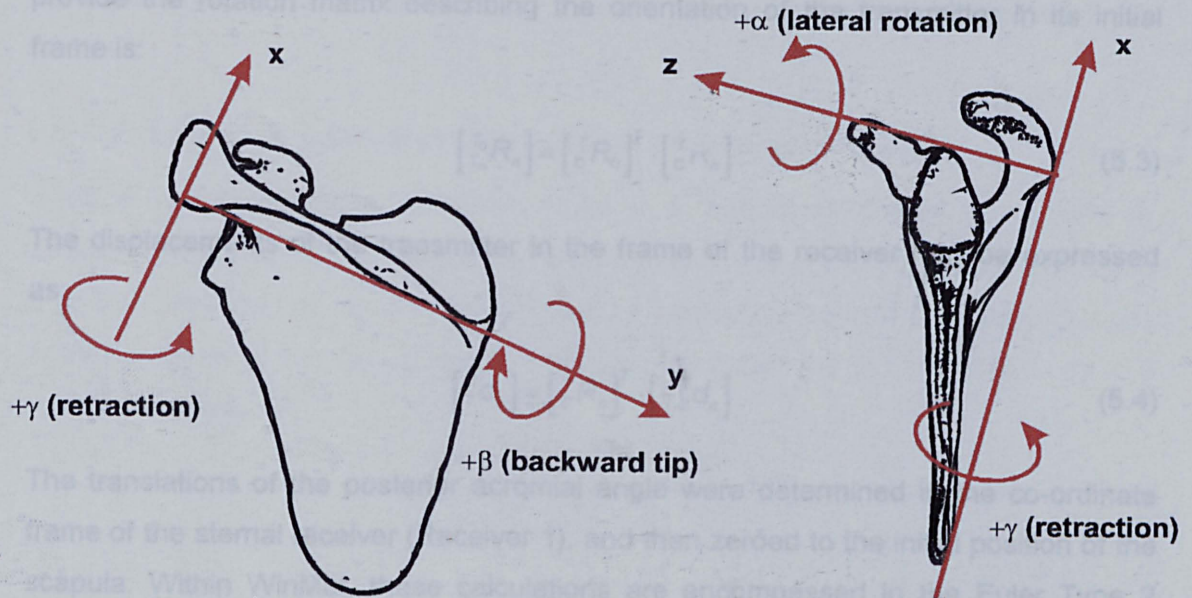


Figure 5.18: Scapula co-ordinate system

As an attempt to account for anthropometric differences between subjects, the Euler angle rotations of the scapula were determined in the local co-ordinate frame of the scapula at rest for each test. This corresponded to the humerus in the neutral position, which was initially defined as zero abduction, flexion and neutral rotation. When the two channel system was implemented and the position of the humerus could be accurately controlled, the neutral position was defined as -90° azimuth, 80° elevation (that is, 10° abduction), and 90° roll (that is neutral internal/external rotation). Figure 3.11 illustrates the definitions of zero and directions of rotation for humeral motion.

The scapular rotations were defined in the following sequence: γ about x (protraction/retraction), then α about z' (lateral rotation), and finally β about y'' (forward/backward tip), conforming to the sequence used by Pronk (1991) and Johnson *et al.* (1993). This is referred to in WinMat as "Pronk Sequence" for the Transmitter, the global co-ordinate system being specified by Receiver 1 (see Figure 5.14). The rotations were also determined using the sequence: α about z (lateral rotation), β about y' (forward/backward tip) and γ about x'' (protraction/retraction), conforming to the definitions of Goldstein (1980) and Polhemus[®]. Results in this rotation format are included in Appendix 4. This is referred to in WinMat as "Euler

Type 2" for the Transmitter, the global co-ordinate system being specified by Receiver 1.

Using the same notation as above, the co-ordinate transformation necessary to provide the rotation matrix describing the orientation of the transmitter in its initial frame is:

$$\begin{bmatrix} {}^T_0R_n \end{bmatrix} = \begin{bmatrix} {}^T_cR_0 \end{bmatrix}^T \cdot \begin{bmatrix} {}^T_cT_n \end{bmatrix} \quad (5.3)$$

The displacements of the transmitter in the frame of the receiver may be expressed as:

$$\begin{bmatrix} {}^c_\tau d_n \end{bmatrix} = \begin{bmatrix} {}^T_cR_n \end{bmatrix}^T \cdot \begin{bmatrix} -{}^T_c d_n \end{bmatrix} \quad (5.4)$$

The translations of the posterior acromial angle were determined in the co-ordinate frame of the sternal receiver (Receiver 1), and then zeroed to the initial position of the scapula. Within WinMat, these calculations are encompassed in the Euler Type 2 definition.

Rotations and displacements of the scapula were also determined in the global, non-zeroed, frame (defined as Euler Type 1 in WinMat).

5.8 VALIDATION TECHNIQUES

5.8.1 Introduction

Any new system of measurement, regardless of its application, requires validation. This procedure is essential in order to gain an understanding of the accuracy (or precision) and the repeatability of the system in question. It is an important consideration that both of these criteria are fulfilled. For example, a rule made of a thin elastic material may be accurate on one occasion but not on another, while a non-elastic rule marked with an incorrect scale will be repeatable but consistently inaccurate, unless calibrated. These examples illustrate that fulfilment of just one of the above criteria does not lead to a valid technique.

However, when measuring a quantity for which there is no defined or standard value, it is difficult, and arguably somewhat subjective to assess the accuracy of the measurement tool. In such situations, obtaining a single point estimate of the

unknown quantity is not sufficient. Instead, an interval within which the unknown quantity lies must be determined.

This interval is generally referred to as a *Confidence Interval*. The accuracy or precision of the system may then be gauged by assessment of the width of this interval.

5.8.2 Confidence Interval and Prediction Interval Estimation

Given a population with an unknown mean μ , a random sample of size n may be obtained. The mean of this sample, \bar{x} , is a point estimate of the population mean μ . It is unlikely that the two values μ and \bar{x} will be identical. However, it is likely that the unknown mean μ will fall within an interval determined by the distribution of the sample (Figure 5.19).

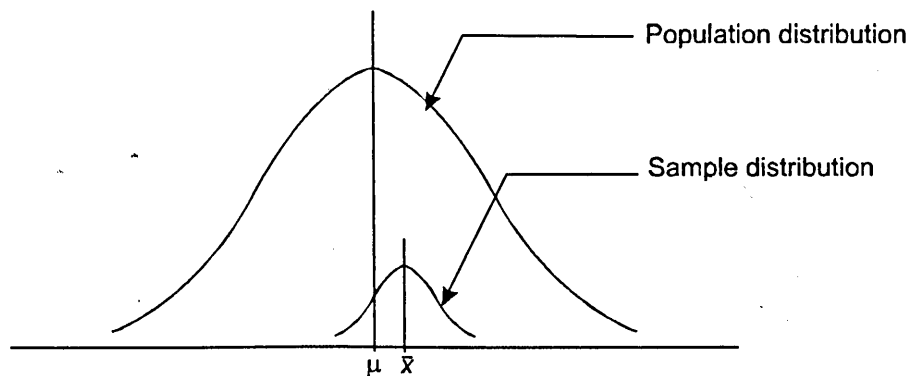


Figure 5.19: Distribution of a sample drawn from a population of mean μ

An interval estimation of the unknown parameter μ is an interval of the form $L \leq \mu \leq U$ where the end points L and U depend upon the variance of the sample s , which is related to the underlying population variance σ .

The level of confidence for which the calculated interval applies may be specified at any value, although for most applications, the 95% level is chosen. The interpretation of this is that if an infinite number of random samples is collected from a single population, and a 95% confidence interval for μ computed from each sample, then 95% of these intervals will contain the true value of μ . This situation is illustrated in Figure 5.20 which shows ten 95% confidence intervals calculated from samples drawn from a population with a mean μ . The dots at the centre of the interval represent \bar{x} , the point estimate of μ . It can be seen that one of the ten intervals shown fails to contain the true value of μ . For 95% confidence intervals, in the long term, one in twenty of the intervals would fail to contain μ .

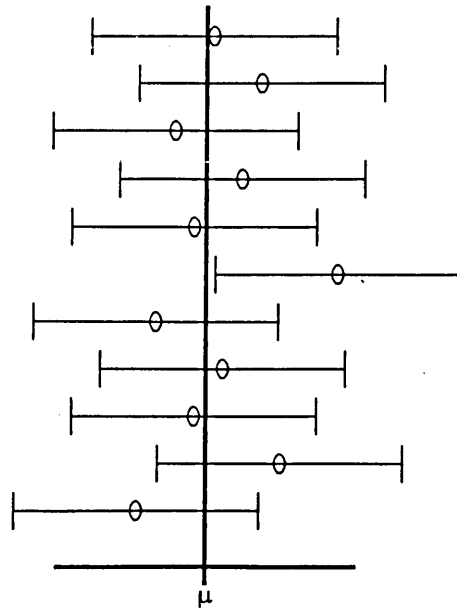


Figure 5.20: Repeated construction of confidence intervals for a population mean μ

Calculation of the confidence interval requires knowledge of the mean of the sample, and either the variance of the sample or of the population. If the variance of the underlying population is known, a slightly better estimate of the population mean can be obtained from the sample mean. This is because use of the sample variance assumes that it is representative of the population variance, which although generally true, may not always be the case. Statistically, these differences are distinguished by the shape of the assumed distribution. If only the sample variance is known (s), the t -distribution must be employed, which tends to be flatter and wider than the z -distribution which would be used if the population variance σ was known (Figure 5.21). The effect of this is to widen the confidence interval slightly, although the effect is very small.

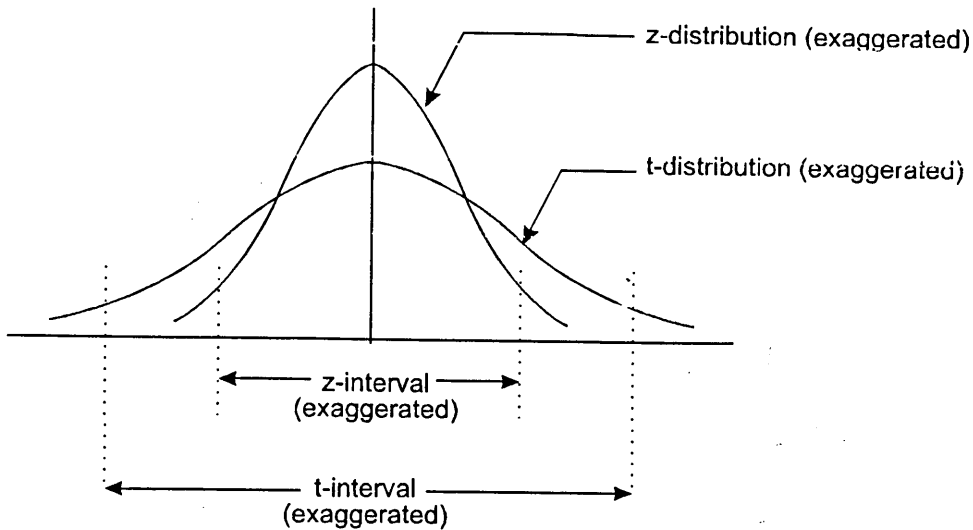


Figure 5.21: Differences in shape between the [exaggerated] t-distribution and z-distributions and their effect on the interval size

The t-distribution of the sample can be expressed as a normal distribution in the form:

$$T = \frac{\bar{X} - \mu}{\left(s \cdot \sqrt{\frac{1}{n}} \right)} \quad (5.5)$$

Re-arranging Equation 5.5 for μ , an interval estimation may be determined, of the form:

$$\bar{X} - t_{95\%} \cdot s \cdot \sqrt{\frac{1}{n}} \leq \mu \leq \bar{X} + t_{95\%} \cdot s \cdot \sqrt{\frac{1}{n}} \quad (5.6)$$

Another type of interval that is often misinterpreted and confused with the confidence interval is the prediction interval. Whereas a confidence interval is an estimation of an unknown population mean based on a sample taken from the population, the prediction interval is an estimation of a future observed response. Prediction intervals are used in the development of the scapulohumeral kinematic model, and may be determined from Equation 5.7.

$$\bar{X} - t_{95\%} \cdot s \cdot \sqrt{1 + \frac{1}{n}} \leq \mu \leq \bar{X} + t_{95\%} \cdot s \cdot \sqrt{1 + \frac{1}{n}} \quad (5.7)$$

Calculation of confidence and prediction intervals from samples drawn from a single population such as those discussed is a relatively simple task as the variance within the sample data is easily determined. However, in many cases variations in the data

may not occur purely due to experimental error, but also due to experimental factors which may be controlled, for example in the investigation of differences between groups of subjects, or due to employing different observers to collect the data. In such situations it is essential to account for these factors in the analysis of the data by attributing components of variance to each of them. The full effect of each of these experimental factors may then be investigated separately using the analysis of variance (ANOVA) technique.

5.8.3 Factorial Experimental Design

In order to validate a measurement system, design of a suitable experiment and the identification of the key factors involved play a fundamental role. For measurement of scapulohumeral kinematics and validation of a technique, a number of factors must be considered.

At the most simple level, measurement of one degree of freedom of scapular position may be performed with the humerus in a single fixed position. Repeating this measurement at the same humeral position provides a sample of data from which a confidence interval may be determined, thereby quantifying the measurement error of the system. However, this error will only be valid at the humeral position tested and not across a number of positions spanning a range of humeral motion.

It is obvious that the scapula will not remain in the same position across a range of humeral motion, hence if measurements of scapular position are taken at a variety of humeral positions, the variance in the sample data is not solely due to measurement error, and hence cannot be directly used in the estimation of this error. A factor must therefore be introduced into the experimental analysis to account for the variability in the data due to measurements being taken at different humeral positions. Using this, it becomes possible to determine the measurement error of the system across a range of humeral motion.

Graphical representation of this form of factorial analysis is illustrated in Figure 5.22. It can be seen that the introduction of the factor creates a form of hierarchy in the analysis of the sample data (or response), ensuring that the correct comparisons are drawn.

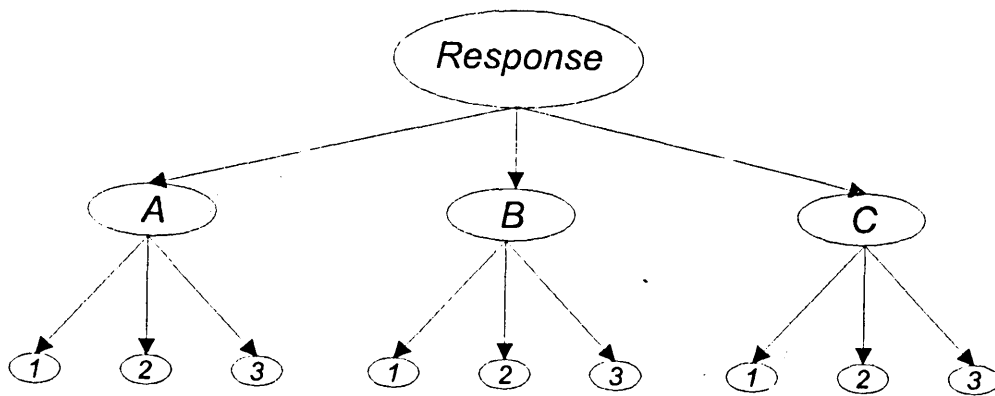


Figure 5.22: Hierarchical structure of a single factor model

Here, group A represents three replicate measures of data collected at one level of humeral elevation, while groups B and C are sets of data collected at other levels of humeral elevation. The factorial structure of the model allows a variance component to be calculated within the groups, pertaining to the measurement error, while also providing a measure of the variability between the groups allowing the effect of different levels of humeral elevation to be investigated.

The mathematical interpretation of this model is given in Equation 5.8 (Montgomery, 1994), where Y represents any single observation within the response, μ represents a mean value for that observation, γ is the humeral position factor (possessing k levels, one for each humeral position), and ε represents the measurement error inherent in the system (based upon I observations).

$$Y = \mu + \gamma_k + \varepsilon_i \quad (5.8)$$

Another factor may be introduced by considering the effect on the response of employing a different observer to collect the data. By including a factor to control and account for this in the analysis, the inter-observer variation can be investigated. This can again be discussed as a hierarchical model, where the addition of the observer factor introduces another level above the humeral position factor, again ensuring that the correct comparisons are drawn.

The model can be developed further still, to investigate the changes in the response between subjects. Data across a number of subjects may be collected at a number of different humeral positions by a number of observers. By introduction to the statistical model of a factor to control for differences between subjects, the inter-subject variability may too be quantified. Again, this introduces yet another level into the hierarchy, as illustrated in Figure 5.23.

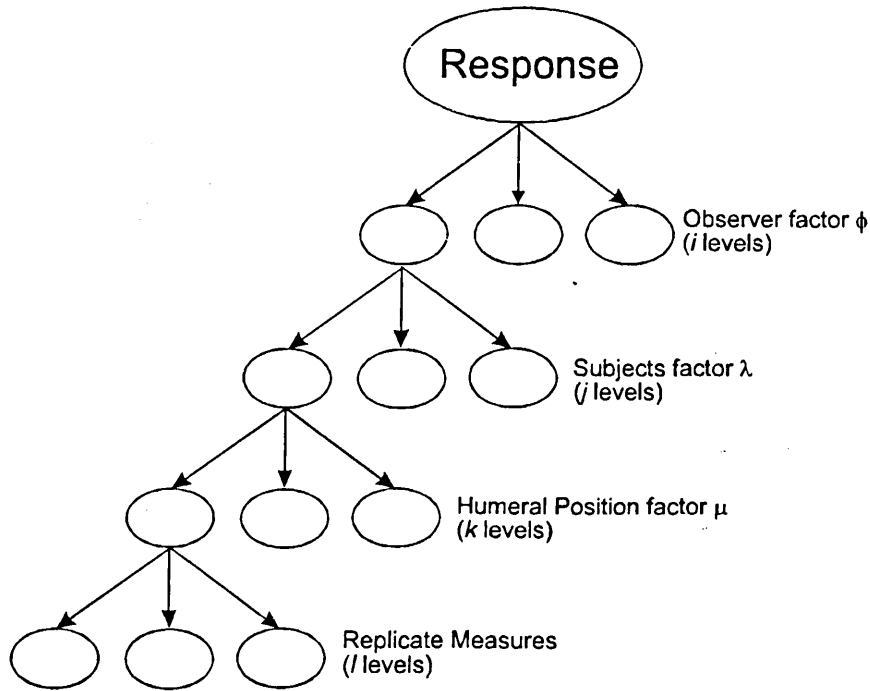


Figure 5.23: One branch of the hierarchical structure of a three factor model

The mathematical interpretation of this three factor statistical model is given in Equation 5.9.

$$Y_{ijkl} = \mu + \phi_i + \lambda_j + \mu_k + (\phi\lambda)_{ij} + (\phi\mu)_{ik} + (\lambda\mu)_{jk} + (\phi\lambda\mu)_{ijk} + \varepsilon_{l(ijk)} \quad (5.9)$$

where:

$Y \equiv$ any single observation

$\mu \equiv$ overall mean for that observation

$\varepsilon \equiv$ measurement error, based upon l observations

$\phi \equiv$ observers (i observers)

$\lambda \equiv$ subjects (j subjects)

$\mu \equiv$ humeral positions (k positions)

After collecting suitable sets of data encompassing all of these factors, this statistical model was employed to validate the system. It allows the components of variance attributable to each of the individual factors to be determined, allowing a full investigation of the effects of each. Subsequently, the 95% confidence intervals were calculated using Equation 5.6.

5.9 DATA SMOOTHING AND INTERPOLATION TECHNIQUES

5.9.1 Introduction

The preceding discussion on validation techniques introduced the concept of statistical variation within sets of measured data. This important issue deserves further discussion due to the consequences of its effect on measured data, and the analytical techniques which must be employed to account for these effects. Before identifying these consequences, it is important to discuss the characteristics of a “noisy” signal and the necessity of data smoothing.

The motivation behind smoothing techniques is that the data is subject to error, but that some underlying relationship between the x and y co-ordinates exists, possessing certain properties not apparent in the perturbed data. For example, there may be a good reason to believe that there is an underlying function $y(x)$ that has a slope varying only slowly with x . However, an error in the measurements is likely to be a random error, distributed normally either side of the slope. The size of the error will depend on the variability in the sample, but its effect may be to introduce a high frequency variation over the lower frequency signal, resulting in the underlying trend of the data becoming disguised or even lost completely. The aim of smoothing is to “filter out” this high frequency error component, leaving the underlying signal to describe the characteristics of the system, which may then be employed in further analysis or modelling.

Describing the error component as a high frequency element on top of a generally low frequency signal implies that frequency domain filters are used as a smoothing technique. Although this is a somewhat simplified description, many filtering techniques can be thought of in this way. Indeed, in many applications where measurements are recorded against a time scale, for example gait analysis or recording any form of position data with respect to time, the perturbed signal is transformed to the frequency domain and subject to a low pass filter. The resulting smoothed data may then be integrated with respect to time to provide information on the velocity and acceleration of the system in question.

However, considering scapulohumeral kinematics, the positions are not measured at equal intervals of the single variable of time, but at a number of positions of the humerus, which may be at irregular intervals and, in experiments involving more than just elevation of the arm, may be two or three dimensional. The need therefore

presents itself for alternative smoothing techniques to those based in the time and frequency domains.

Smoothing the data however is only one element in the analysis. As alluded to above, the smoothed data allows trends to be investigated. The process of interpolation employs these trends in the estimation of data in between the points where the measurements were taken. However, the processes of smoothing and interpolation may be combined by fitting trends directly to the noisy data, although the order of such trends must be closely controlled to ensure that the trend is an estimation of the underlying signal and not the signal including the noise.

Whether the appropriate context is smoothing or trend analysis, the “quality of fit” is often used as a measure of the degree to which the trend or the smoothed curve fits the data. This quality of fit is generally assessed by determination of R^2 , a measure of the sum of the residuals between the fitted and measured data. R^2 is defined in the region $0 \leq R^2 \leq 1$. When $R^2 = 1$, every point of the measured data lies on the smoothed curve, and there is no residual component. This does not mean that the signal contains no error component, but that if it is present, the trend includes a fit to the error as well as the underlying signal. Piecewise polynomial or spline fits are examples of such a trend, where the fitted curve may interpolate between the absolute measured values at all points. Generally, single polynomial fits do not interpolate for all points, but perform a “best-fit”, generally in a least squares sense (that is to minimise the sum of the squares of the residuals, thereby maximising R^2). However, in the presence of a relatively high signal to noise ratio, the residual components may cause R^2 to be well below unity, but the resulting fit may be a good estimation of the underlying system characteristics.

For fitting trends to scapulohumeral kinematics over a range of humeral motions including changes in azimuth, elevation and roll, single variable relationships are not sufficient. Instead, four dimensional surfaces must be fitted to each degree of freedom of scapula motion (one dimension for the degree of freedom being examined, and one for each of the co-ordinates of the arm). Although spline routines are capable of performing such analysis, multiple linear regression provides a more simple, although less flexible technique. However, due to the trend fitting (and hence noise reduction) inherent in fitting polynomial relationships, there use is preferred.

5.9.2 Repeated Measures and Superposition

Probably the most simple of all smoothing techniques is that of superposition. By measuring a variable or trend a number of times, the error at each measured interval will, in an infinite number of measurements, sum to zero due to its normal distribution about the true value.

Essentially, this is exactly the same as using a mean and confidence interval to estimate a value. Estimation of a number of values across a range of another variable provides a series of mean values, through which a trend may be established. Because the trends are based on smoothed data, relatively high values of R^2 are expected.

This form of smoothing obviously requires replicate measures. As such, it has been employed in the validation studies for visual examination of trends between and within observers and subjects, as presented in Chapter 6.

Polynomial trends were determined using multivariate linear regression techniques, discussed below.

5.9.3 Multiple Linear Regression

Linear relationships require the definition of two constants. Generally, these are expressed as a function of the form $y=mx+c$, in which an input variable x is used to predict an output variable or response y . Many applications involve situations where there is more than one input variable contributing to affect the output. In such situations the above linear relationship may be expanded to allow modelling of a response with more than one independent input or regressor variables. In general, the dependent variable, y , may be related to k regressor variables by use of a general regression model of the form:

$$Y = \beta_0 + \beta_1 \cdot x_1 + \beta_2 \cdot x_2 + \dots + \beta_k \cdot x_k + \varepsilon \quad (5.10)$$

The regressor variables are x_n ($n = 0, 1, \dots, k$), while the parameters β_n ($n = 0, 1, \dots, k$) are the regression coefficients. ε is the error term of the model.

Multiple linear regression models are generally used, and are used within this thesis, as approximating functions. That is, the true mathematical relationship between Y and x_1, x_2, \dots, x_n is unknown, but over certain ranges of measured data, the model may be employed to provide an adequate approximation.

Despite being termed linear regression, models such as these may be applied to a variety of modelling situations including those of higher order problems. For example, a cubic polynomial takes the form:

$$Y = \beta_0 + \beta_1 \cdot x + \beta_2 \cdot x^2 + \beta_3 \cdot x^3 + \varepsilon \quad (5.11)$$

If $x_1 = x$, $x_2 = x^2$ and $x_3 = x^3$, then Equation 5.11 may be rewritten as:

$$Y = \beta_0 + \beta_1 \cdot x_1 + \beta_2 \cdot x_2 + \beta_3 \cdot x_3 + \varepsilon \quad (5.12)$$

which is a multiple linear regression model with three regressor variables.

Precise definitions of input and output parameters for each regression model employed are given in the appropriate chapters.

5.10 CONCLUDING REMARKS

This chapter has discussed a variety of physical materials, together with their application and associated theoretical techniques for collection and analysis of data.

Following the protocols established within this chapter, the following chapter details the results obtained through preliminary testing of the apparatus, and investigations into the validity of both the single channel and two channel measurement techniques.

Chapter 6

Validation of the Measurement Technique

Employing the materials and methods presented in Chapter 5, this chapter details the design, analysis and results of experiments for determining the accuracy and validity of the measurement technique developed.

Beginning with the results of data collection during initial testing and prototyping of the Locator, the chapter continues to provide a detailed account of the validation studies undertaken for both the single channel and two channel measurement systems.

6.1 PRELIMINARY RESULTS

Over a period of approximately one month, thirty sets of data were collected from one subject. For each set of data, the subject performed the “standard test” discussed in Section 5.2.1. This involved abduction of the arm in the coronal plane from 10° to 90° in 10° increments. This abduction was measured with a fluid filled goniometer. At each increment, the Locator was applied and the position and orientation of the scapula measured.

As these measurements were taken on one subject, by one observer, the resulting data could not be used to investigate inter-subject and inter-observer differences. These analyses are left to the validation studies presented in Sections 6.2 and 6.3. However, this aside, this preliminary data may be used in examining the effects of gaining familiarity with the measurement technique.

The Euler angle rotations of the scapula (x , z_α , y_β sequence), together with the displacements of the acromial angle were calculated for each measurement within the thirty sets of data. These data were then divided into six groups, each containing five

sets of data. Group 1 contained the first five data sets to be collected (1-5), group 2 the second five data sets (6-10) and so on until group 6, containing the final data sets 26-30. For each group, a mean value and variance were calculated for each degree of freedom, at each level of humeral abduction. Comparison of the degree of variance in each group provides a measure relating to the effects of "learning" the measurement technique.

Figure 6.1 to Figure 6.6 illustrate these comparisons for each degree of freedom. Each column represents a normalised mean variance across the range of abduction for each group of data. The solid lines are linear trends across the groups.

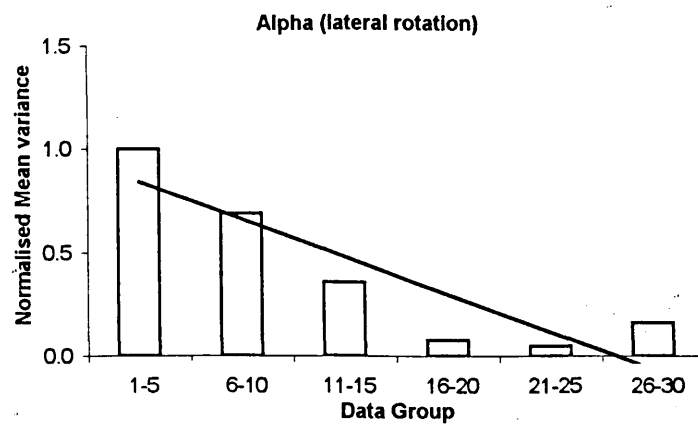


Figure 6.1: Changes in mean variance in alpha over 30 repeated tests on one subject

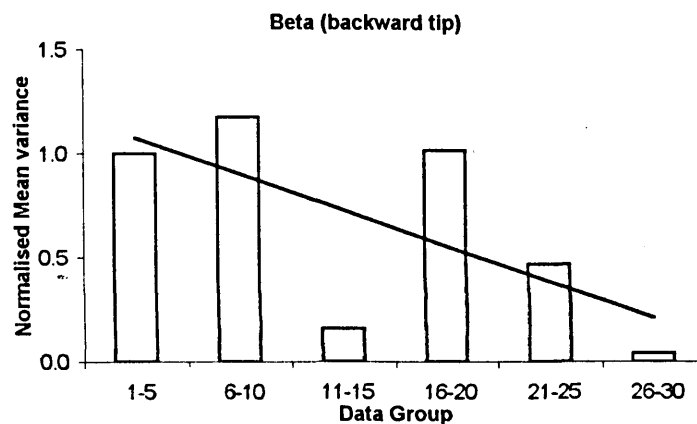


Figure 6.2: Changes in mean variance in beta over 30 repeated tests on one subject

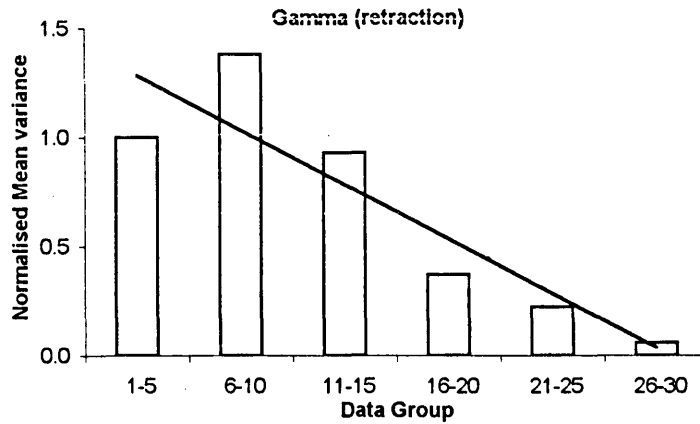


Figure 6.3: Changes in mean variance in gamma over 30 repeated tests on one subject

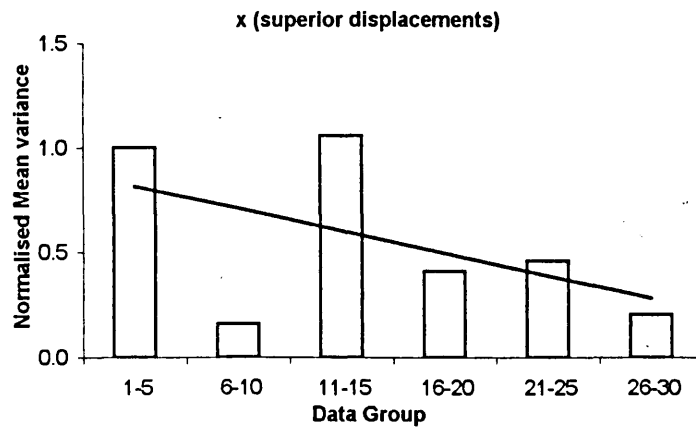


Figure 6.4: Changes in mean variance in x over 30 repeated tests on one subject

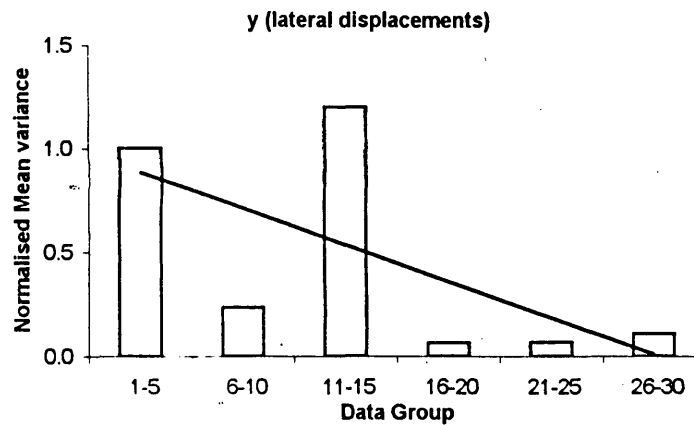


Figure 6.5: Changes in mean variance in y over 30 repeated tests on one subject

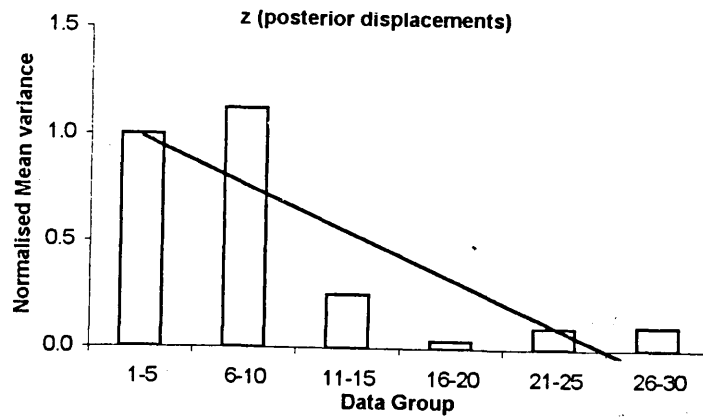


Figure 6.6: Changes in mean variance in z over 30 repeated tests on one subject

These results show that the mean level of error in the measured data was reduced over the thirty tests. This indicates that a learning technique exists in performing the measurements, although it is not possible to state whether this arises through using the apparatus or in the identification of the anatomical landmarks. These issues are discussed further in Chapter 8.

6.2 SINGLE CHANNEL VALIDATION STUDY

6.2.1 Design of the Experiment

To perform a thorough investigation into the validity of the measurement system, an experiment was designed to analyse the inter-observer repeatability and inter-subject variability, and also to quantify the measurement error inherent in the system.

Two observers each recorded five replicate measurements of scapular motion over a range of arm abduction in the coronal plane on each of five subjects. The range of arm abduction examined was again that defined by the standard test (10° to 90° in 10° increments). Throughout this motion, all subjects were instructed to keep their elbow flexed at 90° with their forearm pointing directly forwards at all times. This position was adopted to discourage rotation of the humerus about its long axis which may have altered the rotations of the scapula. At each increment, the Locator was applied and a record of scapular position and orientation taken.

Euler angle rotations of the scapula were determined in the local co-ordinate frame of the scapula at rest for each test, as illustrated Figure 5.17. The rotations were determined in both rotation sequences presented in Section 5.7.2, that is the $x_\gamma, z_\alpha', y_\beta''$ sequence (retraction, lateral rotation, tip), corresponding to the work of Pronk

(1991), and the $z_\alpha, y_\beta', x_\gamma''$ (lateral rotation, tip, retraction) sequence, in which the dominant lateral rotation is first.

The translations of the posterior acromial angle were determined in the co-ordinate frame of the sternal receiver, and then zeroed to the initial position of the scapula.

For statistical analysis of the data, a three factor mixed model ANOVA design was employed as discussed in Section 5.8.3. The statistical model is expressed in Equation 6.1.

$$Y_{ijkl} = \mu + \phi_i + \lambda_j + \mu_k + (\phi\lambda)_{ij} + (\phi\mu)_{ik} + (\lambda\mu)_{jk} + (\phi\lambda\mu)_{ijk} + \varepsilon_{l(ijk)} \quad (6.1)$$

where:

$Y \equiv$ any single observation

$\mu \equiv$ overall mean for that observation

$\varepsilon \equiv$ measurement error, based upon l replicate measures ($l = 1, \dots, 5$)

$\phi \equiv$ observers ($i = 1, 2$)

$\lambda \equiv$ subjects ($j = 1, \dots, 5$)

$\mu \equiv$ humeral positions ($k = 1, \dots, 9$)

Beyond this, the 95% confidence intervals for each degree of freedom of scapular motion were determined.

6.2.2 Results

The following graphs illustrate the resulting rotations and displacements of the scapula at each of the humeral positions tested. Figure 6.7 to Figure 6.9 show the rotations of the scapula using the rotations sequence $x_\gamma, z_\alpha', y_\beta''$. The x, y, z displacements of the scapula are shown in Figure 6.10 to Figure 6.12. In all cases the error bars represent the 95% confidence intervals on the data, based on any observer obtaining five replicate measures on any subject

The rotations of the scapula using the $z_\alpha, y_\beta', x_\gamma''$ rotation sequence are presented in Appendix 4.

6.2.2.1 Rotations of the Scapula ($x_\gamma, z_\alpha', y_\beta''$ sequence)

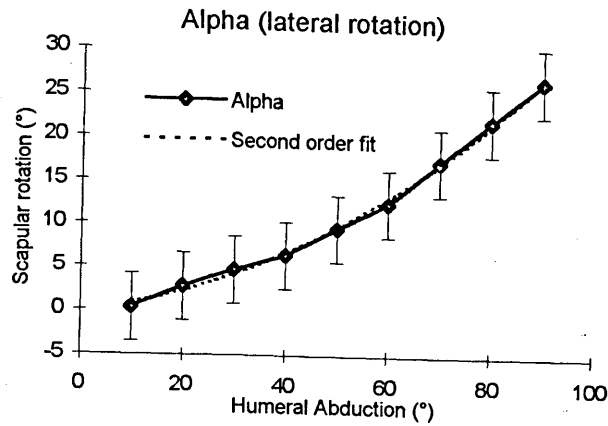


Figure 6.7: Rotation angle α during humeral abduction, $x_\gamma, z_\alpha', y_\beta''$ one channel study

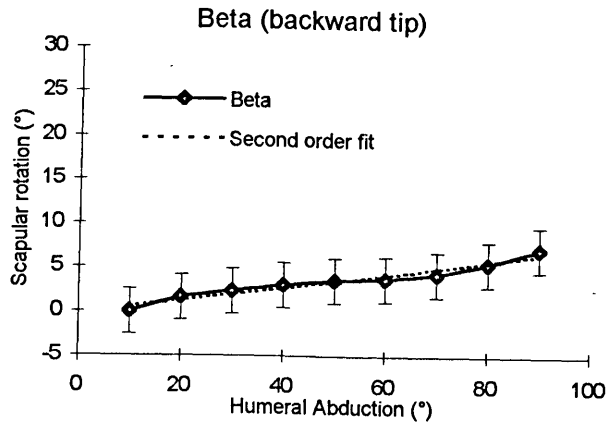


Figure 6.8: Rotation angle β during humeral abduction, $x_\gamma, z_\alpha', y_\beta''$ one channel study

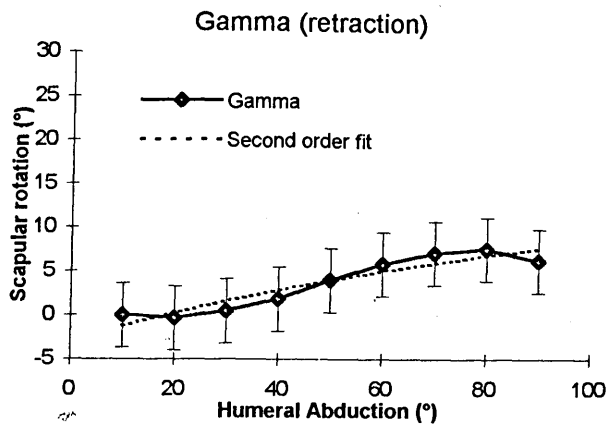


Figure 6.9: Rotation angle γ during humeral abduction, $x_\gamma, z_\alpha', y_\beta''$ one channel study

6.2.2.2 Displacements of the Scapula

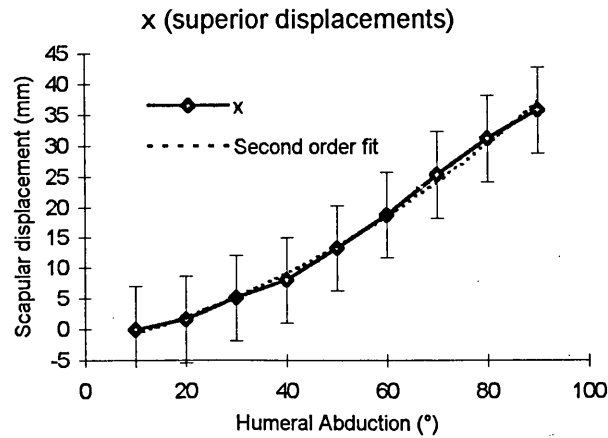


Figure 6.10: Scapular x displacements during humeral abduction, one channel study

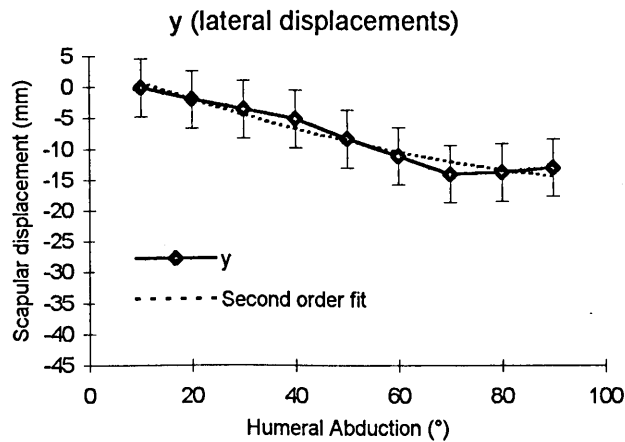


Figure 6.11: Scapular y displacements during humeral abduction, one channel study

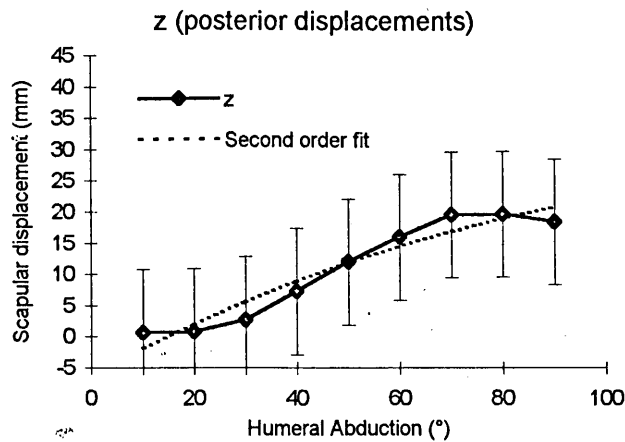


Figure 6.12: Scapular z displacements during humeral abduction, one channel study

6.2.2.3 Regression Coefficients

Table 6.1 details the regression coefficients and values of R^2 for the second order polynomials on the measured data illustrated in the graphs.

	x^2	x	constant	R^2
Alpha	0.0026	0.0638	-0.0425	0.998
Beta	0.0001	0.0640	-0.1198	0.950
Gamma	-0.0005	0.1556	-2.7448	0.896
x	0.0029	0.1837	-2.8448	0.996
y	0.0012	-0.3093	3.7748	0.954
z	-0.0014	0.4255	-6.0309	0.933

Table 6.1: Regression coefficients and R^2 's for second order polynomial fits to data, one channel study

6.2.2.4 Statistical Interpretation

The results from applying the statistical model, in terms of components and proportions of variance for each of the factors, are quoted in Table 6.2. The resulting confidence intervals on the data are also given.

Degree of Freedom	Variance components σ^2 or mm^2 (%)			95% Confidence Intervals
	Observer	Subject	Error	
α (lateral rotation)	0.0 (0%)	6.1 (6%)	2.6 (3%)	3.85°
β (backward tip)	0.0 (0%)	0.77 (9%)	1.6 (18%)	2.55°
γ (retraction)	0.5 (2%)	4.0 (16%)	2.2 (9%)	3.63°
x (superior)	0.0 (0%)	16.6 (7%)	8.9 (4%)	7.01mm
y (lateral)	0.2 (0%)	9.6 (16%)	3.5 (6%)	4.64mm
z (posterior)	4.0 (2%)	48.3 (25%)	13.8 (7%)	10.08mm

Table 6.2: Components and proportions of variance, and 95% confidence intervals for single channel study

6.2.3 Conclusions

The aim of the single channel validation study was to determine whether the palpation method using the Locator would provide data adequate for kinematic modelling. That

is, the data relating to all six degrees of freedom should exhibit characteristics suggesting that an underlying signal has been observed rather than simply noise. It was also of great importance to ensure that two observers could measure the same motion on each of the subjects.

From the components of variance pertaining to the measurement error and observer variation, these two criteria were sufficiently fulfilled to advance the technique to the stage of measuring scapular and humeral positions simultaneously, using the two channel Isotrak[®]II system.

It was acknowledged that there were difficulties in measuring both arm and scapular position using different apparatus. It is also believed that the lack of experience of one of the observers could have contributed to larger observer variations than would have otherwise have been the case. These issues are discussed further in Chapter 8.

6.3 TWO CHANNEL VALIDATION STUDY

6.3.1 Design of the Experiment

This second validation study follows almost exactly the same methods as the single channel study, with the exception of the associated hardware and software developments as discussed in Chapter 5. These developments allowed real time feedback of the position of the arm, in the frame of the receiver mounted on the sternum, in terms of the azimuth, elevation and roll of the humerus.

Two observers each recorded five replicate measurements of scapular motion over a range of arm abduction in the coronal plane on each of five subjects. The range of arm abduction examined was again that defined by the standard test (10° to 90° in 10° increments). Throughout this motion, the internal/external rotation of the arm (roll), together with changes in the plane of elevation (changing azimuth) were monitored, and only allowed to vary within defined limits of $\pm 5^\circ$. At each increment, the Locator was applied and a record of scapular position taken.

The rotations and displacements of the scapula were determined in the same manner as those in the single channel study, and the same statistical analysis of the data was employed.

6.3.2 Results

The following graphs illustrate the resulting co-ordinates of the humerus together with the rotations and displacements of the scapula at each of the humeral positions tested. Figure 6.13 and Figure 6.14 show the mean values for the measured co-ordinates of the humerus for each position tested during the studied motion. The expected values are also shown for comparison.

Figure 6.15 to Figure 6.17 show the rotations of the scapula using the rotations sequence $x_y, z'_\alpha, y''_\beta$. The x, y, z displacements of the scapula are shown in Figure 6.18 to Figure 6.20.

Unless otherwise stated, the error bars represent the 95% confidence intervals on the data, based on any observer obtaining five replicate measures on any subject

The rotations of the scapula using the $z_\alpha, y'_\beta, x''_\gamma$ rotation sequence are presented in Appendix 4.

6.3.2.1 Measurements of Arm Position

Figure 6.13 and Figure 6.14 present the rotations of the humerus during data collection. The ten humeral positions along the x axis of each graph refers to each incremental measurement of humeral position across the standard test performed by the subjects.

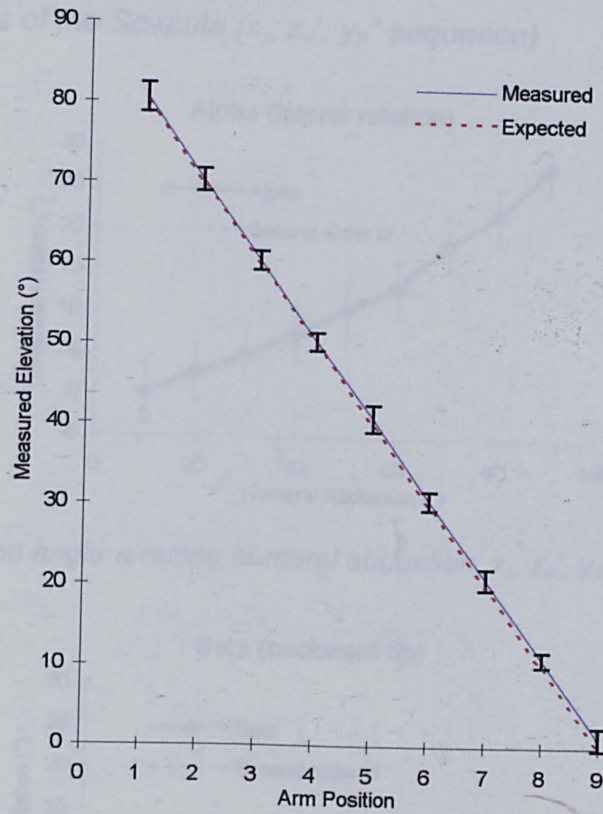


Figure 6.13: Measured humeral elevation against expected elevation at each arm position. Error bars represent ± 1 standard deviation

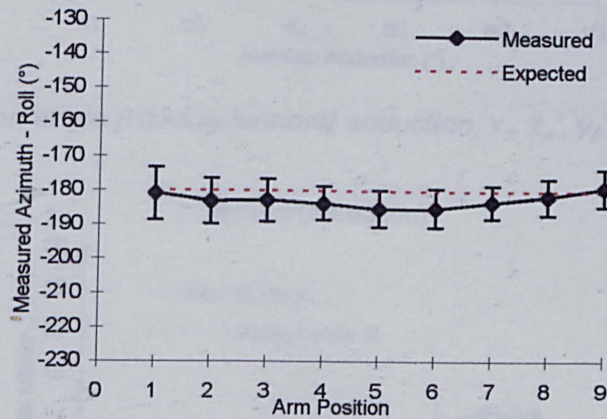
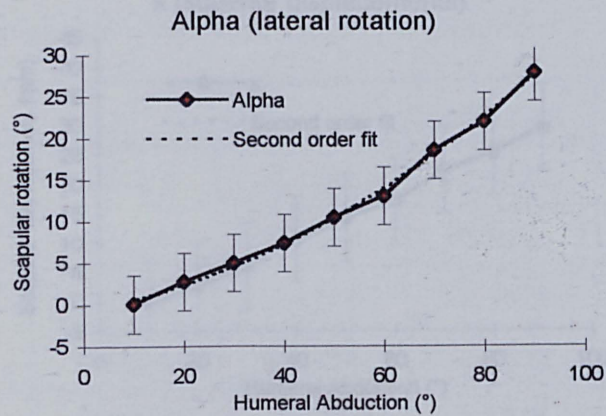
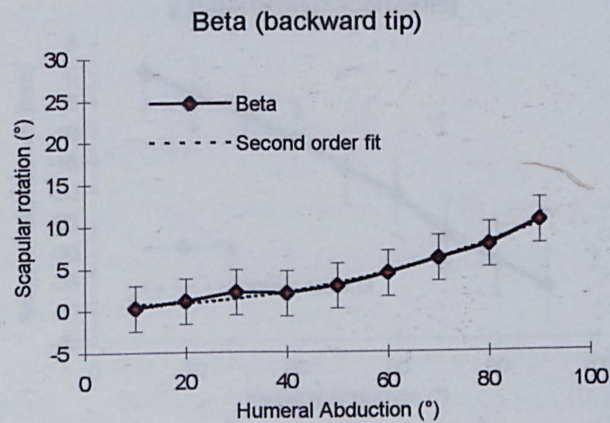
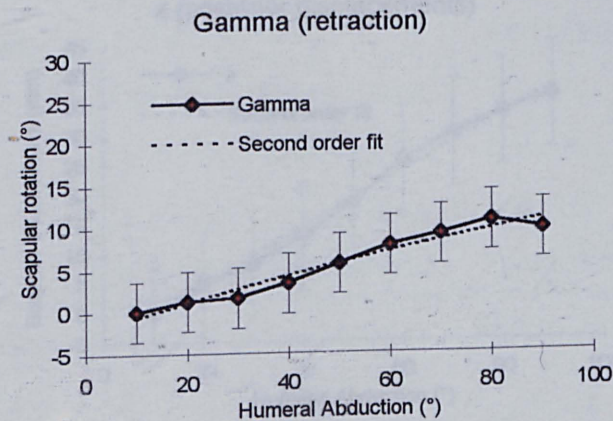


Figure 6.14: Measured humeral (azimuth - roll) against expected (azimuth - roll) at each arm position. Error bars represent ± 1 standard deviation

6.3.2.2 Rotations of the Scapula ($x_\gamma, z_\alpha', y_\beta''$ sequence)Figure 6.15: Rotation angle α during humeral abduction, $x_\gamma, z_\alpha', y_\beta''$ two channel studyFigure 6.16: Rotation angle β during humeral abduction, $x_\gamma, z_\alpha', y_\beta''$ two channel studyFigure 6.17: Rotation angle γ during humeral abduction, $x_\gamma, z_\alpha', y_\beta''$ two channel study

6.3.2.3 Displacements of the Scapula

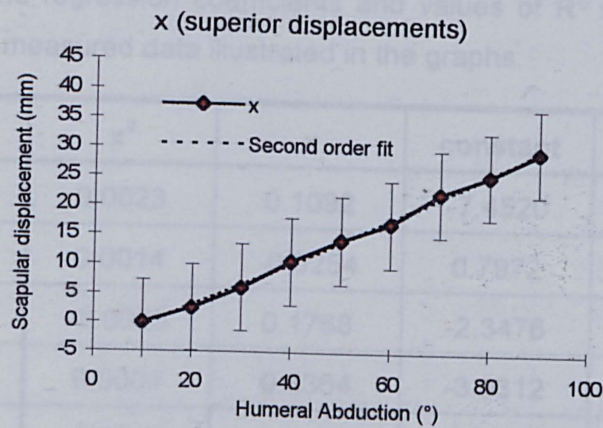


Figure 6.18: Scapular x displacements during humeral abduction, two channel study

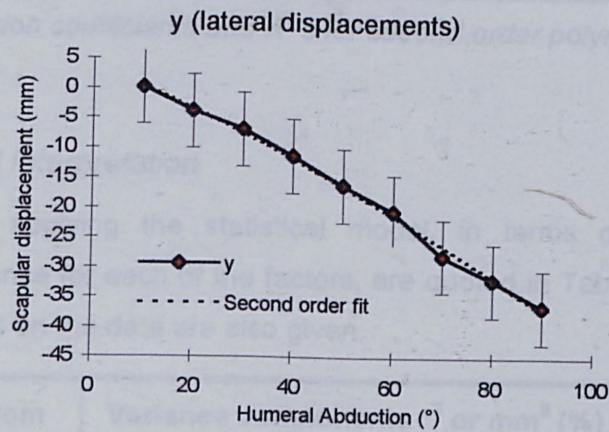


Figure 6.19: Scapular y displacements during humeral abduction, two channel study

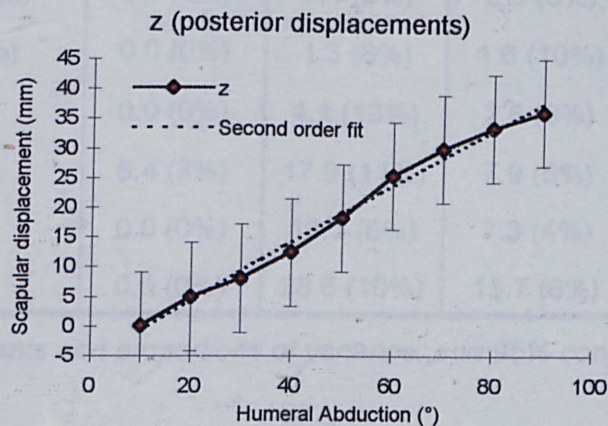


Figure 6.20: Scapular z displacements during humeral abduction, two channel study

6.3.2.4 Regression Coefficients

Table 6.3 details the regression coefficients and values of R^2 for the second order polynomials on the measured data illustrated in the graphs.

	x^2	x	constant	R^2
Alpha	0.0023	0.1092	-7.4520	0.997
Beta	0.0014	-0.0254	0.7972	0.987
Gamma	-0.0003	0.1768	-2.3476	0.955
x	0.0004	0.3364	-3.9312	0.998
y	-0.0014	-0.3337	3.7811	0.997
z	-0.0003	0.5113	-0.7568	0.990

Table 6.3: Regression coefficients and R^2 's for second order polynomial fits to data, two channel study

6.3.2.5 Statistical Interpretation

The results from applying the statistical model, in terms of components and proportions of variance for each of the factors, are quoted in Table 6.4. The resulting confidence intervals on the data are also given.

Degree of Freedom	Variance components σ^2 or mm^2 (%)			95% Confidence Intervals
	Observer	Subject	Error	
α (lateral rotation)	0.4 (0%)	0.1 (0%)	2.9 (3%)	3.47°
β (backward tip)	0.0 (0%)	1.3 (8%)	1.6 (10%)	2.72°
γ (retraction)	0.0 (0%)	4.1 (13%)	2.5 (8%)	3.57°
x (superior)	5.4 (3%)	17.9 (11%)	7.9 (5%)	7.45mm
y (lateral)	0.0 (0%)	13.3 (6%)	7.3 (4%)	6.20mm
z (posterior)	0.0 (0%)	28.6 (10%)	15.7 (6%)	9.08mm

Table 6.4: Components and proportions of variance, and 95% confidence intervals for two channel study

6.3.3 Conclusions

These results demonstrate that it is possible to measure reliably both rotations and translations of the scapula, while simultaneously monitoring and recording the position

of the arm. It is interesting to note that the differences arising from the statistical analysis of the data are small between the single channel and two channel studies, even though the subjects were not the same group in the two studies. This, and other issues arising from these results are discussed further in Chapter 8.

6.4 CONCLUDING REMARKS

Considering the statistical results, in all cases the variations between observers is small compared to that between subjects. Indeed, in the two channel study, the differences in the measured data due to observer variation accounted for less than 1% of the total variation in the data for five out of the six degrees of freedom measured, and for only 3% in the sixth degree of freedom.

Similarly, the measurement error is responsible for, at the very most, 10% of the variation in the data, and generally much less than this. Furthermore, it can be seen from the graphical results, and the high values of R^2 on the polynomial fits, that definite trends have been observed, which are not obscured by noise.

In conclusion, this technique has been proven to be more valid than any other previously developed technique for the measurement of, and investigation into scapulohumeral kinematics. Measuring both humeral and scapular kinematics allows a comprehensive set of data to be collected investigating the kinematics of the scapula over a defined workspace of the arm, and not just elevation in the coronal or frontal planes. It also allows, for the first time, the effects of humeral rotation on the kinematics of the scapula to be investigated.

A study considering these factors is presented in the subsequent chapter.

Chapter 7

Modelling of Three Dimensional Scapulohumeral Kinematics

With a suitable measurement system developed the possible applications of such a tool start to become a reality. Such applications include clinical measurements for diagnostic purposes, and studies involving the analysis of shoulder girdle motion in normal subjects. Within this, modelling techniques may be employed to make use of available or obtainable data, allowing prediction of scapulohumeral kinematics more generally. This could allow scapulohumeral motion patterns to be characterised quantitatively over various ranges of motion.

This chapter details the development of such a model.

7.1 OBJECTIVES

The aim of this study was to develop a mathematical model capable of predicting the position of the scapula in three dimensional space for a given arm position. Using such a model a sequence of arm positions describing a specific upper limb task may be defined and the accompanying motion of the scapular investigated.

The immediate complexity of this presents itself as the identification of a “useful” workspace of the arm over which such a model will be valid. Once this is identified, it is possible to collect representative sets of data encompassing this workspace, and apply various mathematical techniques to develop and validate a predictor model. Each of these issues will be dealt with in turn, followed by a discussion on graphical representation of scapulohumeral kinematics in three dimensions.

7.2 DEFINING THE WORKSPACE

7.2.1 Workspace Representation

It has already been stated on numerous occasions that the shoulder is unique as a joint complex, being capable of such a wide and stable range of motion. This range of motion is possibly best illustrated by Kapandji's *Cone of Circumduction* (1982), representing a workspace for the hand assuming an extended elbow (Figure 7.1).

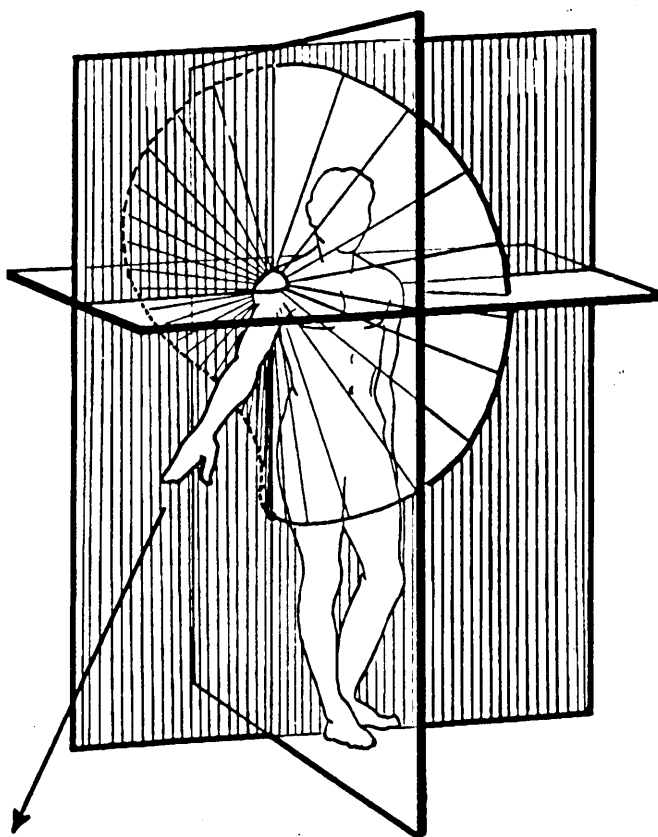


Figure 7.1: Kapandji's cone of circumduction (Kapandji, 1982)

Although referred to as a cone, having a principal axis identified by the solid arrow, it is more correct to refer to this workspace as a spherical section centred at the shoulder, the radius of which is the length of the arm from the shoulder to the fingertips with the elbow extended. The periphery of the sphere which can be touched with the fingers falls within the workspace, while that which cannot be reached is obviously outside the workspace. It is important to realise that this is not the same as the dextrous workspace, which allows elbow flexion to affect the final position of the hand.

Despite providing a useful illustration of the flexibility of the shoulder, this representation offers little as a quantitative description of shoulder motion, as without flexion of the elbow, humeral rotation cannot be distinguished from pronation/supination of the wrist when observing the final position of the hand. This is due to an excess number of degrees of freedom caused by redundancies in the shoulder/elbow/wrist mechanism, where humeral rotation in one direction can be compensated for by pronation or supination in the opposite direction, while the final position and orientation of the hand remains the same.

Kapandji also presented a method of quantifying shoulder motions using spherical coordinates to measure the position of the elbow. Engin and Chen (1986), An *et al.* (1991) and Pearl *et al.* (1992) have presented similar systems of spherical representations of arm position.

The kinematic descriptions of these systems, which include definitions of rotation of the humerus are discussed in greater detail in Chapter 3. The workspaces which they present are discussed later in Section 7.2.3, Functional Workspace Representation.

An alternative representation, presented by Dempster (1965), involves plotting the workspace of the humerus alone, thereby discounting any effects of rotation below the elbow. These workspaces are termed the *joint sinus* of the shoulder complex, and have also been used by other authors (Engin and Tümer, 1989)

Although these global representations are relatively easy to interpret, they do not lend themselves to two dimensional presentation particularly well. For a workspace encompassing a large range of motion, it is often necessary to display two orthogonal views of the globe to ensure complete description. An alternative method is offered here in terms of a Mercator style projection of a global workspace onto a flat two dimensional "map". This method of representation is widely used in cartography, and is derived through an "inside-out" projection of features from a sphere onto a bounding cylindrical space. This cylinder may then be unrolled and laid flat, thereby providing the two dimensional view (Figure 7.2).

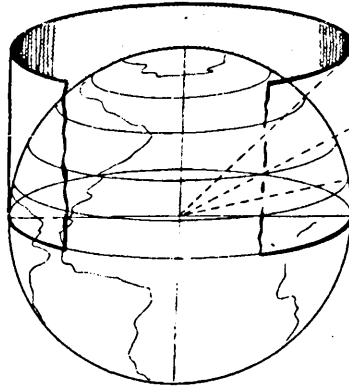


Figure 7.2: Derivation of the Mercator projection (RYA, 1994)

A similar representation was presented by Brown *et al.* (1990), although it was limited to a small range of motion, and the analogy between it and any cartographic schemes was not identified. It was used however as a planar representation of humeral motions similar to that presented here.

Such a projection incurs distortions in vertical distances as lines of latitude become progressively further apart away from the equator. An alternative and more simple representation, also subject to distortions, is known as the plane chart or Plate Carrée. It is sometimes referred to as the equirectangular chart as it has regular intervals of longitude (Robinson *et al.* 1995).

Within the representations illustrated in this text, all intervals of latitude and longitude (or azimuth and elevation) will be regular as in the Plate Carrée projection.

Using these projections, or *workspace maps*, any workspace of the upper arm, or an individual task may be identified as an area upon it

Once again, such techniques make use of the analogies between the measures of longitude and latitude and azimuth and elevation respectively. A bearing in degrees (analogous with the rotation or roll of the humerus) may also be represented as an angle between vectors representing the start and end points of the range of motion, assuming constant latitude and longitude.

An approximation to the workspace presented in Kapandji's *cone of circumduction* is illustrated in Figure 7.3 as an example of this form of representation (without the rotational components). This may be directly compared to Figure 7.1.

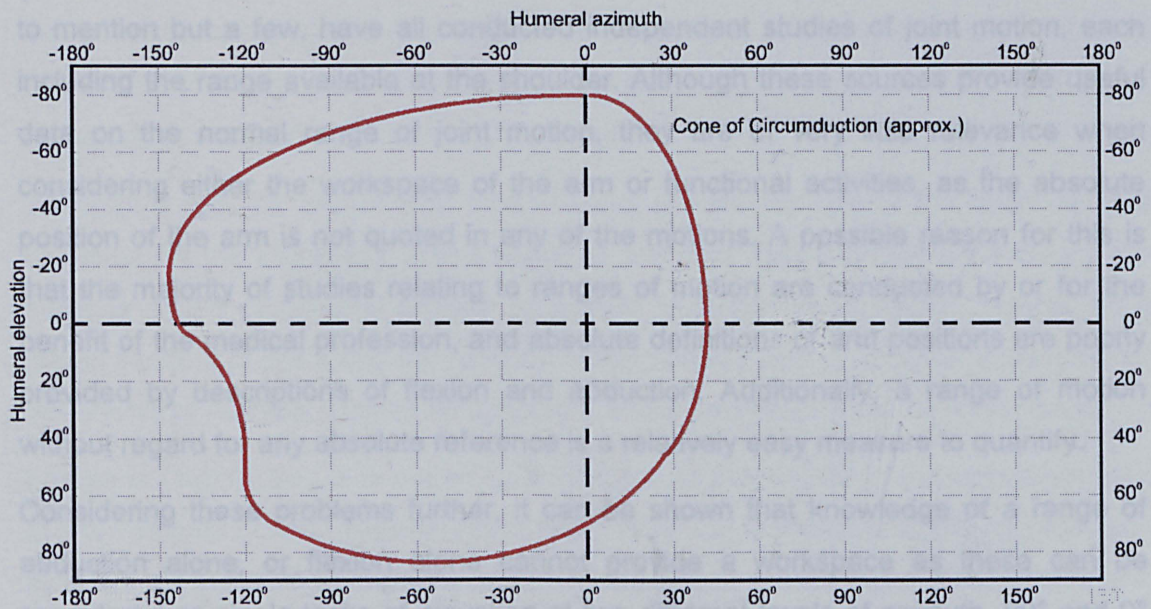


Figure 7.3: Workspace map representation of Kapandji's cone of circumduction

This representation will be used for all further workspace illustrations.

7.2.2 Issues Concerning Modelling of the Workspace

With a method for workspace representation established, a range of humeral motion needs to be defined for which the model will be valid. Ideally, this workspace would encompass every physically possible combination of azimuth, elevation and roll, thereby describing the position of the scapula for any configuration of arm position. However, due to the practicalities of collecting data, in terms of the time demands imposed on investigators and especially on subject volunteers, developing a model over such a complete workspace would necessitate such large increments between each measurement that the accuracy of any resulting model would be in some doubt.

A compromise has therefore to be sought in which a range of motion wide enough of interest is covered, while not being too large to become impractical.

A useful workspace may be defined as one which contains a variety of activities of everyday living, such as eating and drinking, or grooming. A model which is valid over such a workspace may then be used in characterisation of scapulohumeral rhythm in such activities. This can then be developed with respect to muscle sites of attachment and moments to predict individual muscle and reaction forces, following a similar pattern to the research undertaken regarding the lower limb (Winter, 1987). However, unlike the lower limb, kinematic data for activities involving the arm is scarce.

Many authors have discussed the range of motion available at the shoulder joint. Allander *et al.* (1974), together with Salter and Darcus (1953) and Boone *et al.* (1979),

to mention but a few, have all conducted independent studies of joint motion, each including the range available at the shoulder. Although these sources provide useful data on the normal range of joint motion, they are of very little relevance when considering either the workspace of the arm or functional activities, as the absolute position of the arm is not quoted in any of the motions. A possible reason for this is that the majority of studies relating to ranges of motion are conducted by or for the benefit of the medical profession, and absolute definitions of arm positions are poorly provided by descriptions of flexion and abduction. Additionally, a range of motion without regard for any absolute reference is a relatively easy measure to quantify.

Considering these problems further, it can be shown that knowledge of a range of abduction alone, or flexion alone cannot provide a workspace as these can be considered as single tasks of elevation at two different levels of azimuth, 90° and 0° respectively. No information of the range of elevation between or outside of these azimuth positions are quoted. On the workspace map, they would appear as just two single lines, and not define a surface.

Similarly, a range of humeral rotation is restricted to a certain range of elevation and azimuth, as the amount of humeral rotation available varies considerably across the workspace.

Few studies exist involving absolute representation of arm position, especially during functional activities. A review of the literature by Buckley (1996) provides a comprehensive resource, identifying the small number of key papers in this field.

7.2.3 Functional Workspace Representation

The work of Kapandji, Engin and Chen (1986), An *et al.* (1991) mentioned earlier attempts to identify a complete workspace for the arm encompassing all possible combinations of azimuth, elevation and roll. Further studies by Johnson and Gill (1987) and Lenaric and Umick (1994) have investigated total workspace for the hand. Within these studies, the relationship between arm kinematics and activity performance has not been considered.

Dol'nikov (1965) performed what appears to be the first investigation of upper arm kinematics during activities of everyday living¹. Seven activities were identified, four being described as domestic activities (pouring from a bottle, drinking from a glass, eating with a spoon and combing the hair), and three as work activities (using a screwdriver a hammer and a file). Each activity was performed wearing an

instrumented orthosis, and joint angles, velocities and accelerations were measured for shoulder flexion, abduction and humeral rotation, together with four other measures concerning the elbow and the wrist.

Although it may be argued that these results are lacking due to the absence of a definition for the starting or zero position of the arm, they illustrate quite clearly the sizeable extent of humeral rotation compared to flexion or abduction. Hence, for a model capable of predicting the motions of the scapula during activities of daily living, the effects of humeral rotation on scapulohumeral kinematics must be investigated.

Langrana (1981) used a bi-planar video method to investigate upper limb kinematics in just one activity, the "diagonal reach task". Euler angle rotations of the shoulder and elbow of six subjects were measured. The importance of defining a start position and its consistent use for comparisons between subjects is highlighted, although unfortunately this start position is not defined numerically, contributing to difficulties in interpreting the results.

More recently, Safaee-Rad *et al.* (1990) studied whole arm function for feeding activities using a bi-planar video method. Ten subjects were studied performing three activities, namely, eating with a spoon, eating with a fork and drinking from a cup. The results, unfortunately quoted in terms of flexion, abduction and rotation show relatively small motions at the shoulder joint with the largest occurring in flexion through an arc of just 28.3°. However, as all of the activities studied were of a similar nature, these results are not too surprising.

Pearl *et al.* (1992) presented a more comprehensive study of upper arm motion analysis using an Isotrak[®] system to measure humeral position with respect to the thorax. Eight subjects were studied, performing a total of nine activities, four of which may be considered as activities of everyday living; washing the axilla, eating, combing hair and reaching the perineum. The remaining five activities involved measuring maximal ranges of elevation and/or rotation. This study differs from those mentioned above in that shoulder motion is observed without any regard for motion of the elbow or the wrist. Although of little use for studying the workspace of the hand, this study provides useful data on the kinematics of the upper arm during these activities.

Possibly the most comprehensive study to date involving the kinematics of the upper limb was conducted by Romille *et al.* (1994). Within this study, twenty-two standard activities were identified, consisting of four eating and drinking activities, six reaching

¹ or "everyday chores" as quoted by the author.

activities, nine daily living activities and three personal hygiene activities. Six subjects were studied performing each of these activities and the data presented in terms of azimuth, elevation and roll of the shoulder, although with a different zero position to the one used throughout this thesis.

7.2.4 Model Workspace Identification

Comparison of the results from all of the studies mentioned above is hindered due to the differences in angle formats and presentations adopted by each author. Also, the data within the aforementioned studies are presented in terms of the maximum, minimum or average values of shoulder angles across a range of motion, rather than describing the path actually taken. Despite this, ranges of humeral motion most functionally used have been identified, and a bounding workspace defined. It is this functionally useful workspace which is used in the development of the scapulohumeral kinematic model.

7.3 DATA COLLECTION AND ANALYSIS

After dealing with the theoretical aspects of where to collect data, the practicalities of collecting and analysing representative data from a set of subjects take priority.

7.3.1 Task Identification

For the purpose of investigating scapulohumeral kinematics, a *task* is defined as any number of sequential humeral positions in which only one co-ordinate describing humeral position changes. Hence, elevation tasks represent changes in humeral elevation at a constant azimuth and rotation, while a rotation task would consist of various levels of humeral rotation at a constant azimuth and elevation.

By defining a variety of individual tasks within the desired workspace, data to describe a complete picture of scapulohumeral kinematics within this workspace may be sequentially collected over a period of time.

The method of collecting scapulohumeral data developed thus far is a static technique, whereby the position of the scapula is measured at a series of discrete arm positions. In developing a mathematical model of scapulohumeral rhythm, it is necessary to collect data in a series of arm positions that will allow reliable interpolation between these points in order to predict scapulohumeral kinematics more

generally. The spacing or increment size between each arm position is hence an issue of great importance.

In the validation studies presented in Chapter 6, the incremental step of humeral elevation between measurements was 10° . From the data collected, polynomial regression curves were obtained which were used to describe scapulohumeral kinematics across the range of humeral elevation in the measured task.

Increasing the incremental step between humeral positions would reduce the size of the data sets required, thereby lowering the demands placed upon subjects and investigators. With this aim, similar regression curves to those discussed above were generated for the same data, but at 20° increments of arm elevation. Comparison of the data obtained from these relationships to that obtained from the regression relationships at 10° increments shows no significant differences between the two models ($p > 0.05$). Graphical comparisons confirm this, as seen in Figure 7.4.

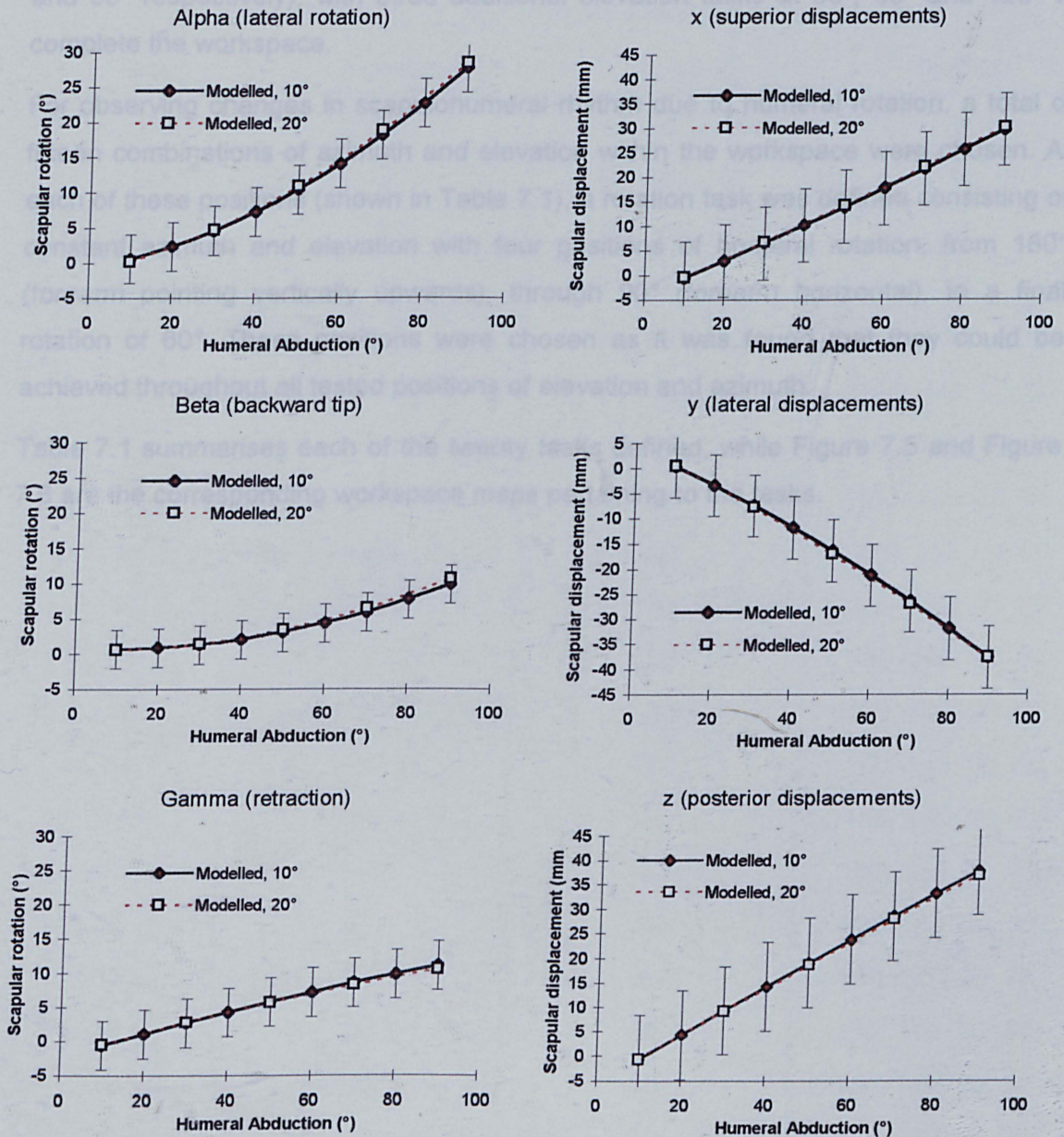


Figure 7.4: Comparisons between two channel validation study data modelled at 10° and 20° increments

An elevation task is hence defined as a sequence of arm positions at constant humeral azimuth and rotation separated by 20° increments in humeral elevation.

An elevation task on the workspace map is represented by a single vertical line at any position of azimuth. Definition of a number of elevation tasks at various levels of azimuth will hence provide an approximation to the workspace of interest.

An increment size of 30° azimuth was used to separate each elevation task, allowing data to be collected in both the sagittal and coronal planes (elevation at azimuth of 0°

and 90° respectively), with three additional elevation tasks at 30° , 60° and 120° to complete the workspace.

For observing changes in scapulohumeral rhythm due to humeral rotation, a total of fifteen combinations of azimuth and elevation within the workspace were chosen. At each of these positions (shown in Table 7.1), a rotation task was defined consisting of constant azimuth and elevation with four positions of humeral rotation, from 180° (forearm pointing vertically upwards), through 90° (forearm horizontal), to a final rotation of 60° . These positions were chosen as it was found that they could be achieved throughout all tested positions of elevation and azimuth.

Table 7.1 summarises each of the twenty tasks defined, while Figure 7.5 and Figure 7.6 are the corresponding workspace maps pertaining to the tasks.

Task	Approximate Arm Position (degrees)		
	Azimuth	Elevation	Rotation
1	0	40, 20,..., -20	90
2	-30	60, 40,..., -20	90
3	-60	80, 60,..., -20	90
4	-90	80, 60,..., -20	90
5	-120	60, 40,..., -20	90
6	0	90	180, 145, 90, 60
7	-30	90	180, 145, 90, 60
8	-60	90	180, 145, 90, 60
9	-90	90	180, 145, 90, 60
10	-120	90	180, 145, 90, 60
11	0	-20	180, 145, 90, 60
12	-30	-20	180, 145, 90, 60
13	-60	-20	180, 145, 90, 60
14	-90	-20	180, 145, 90, 60
15	-120	-20	180, 145, 90, 60
16	0	30	180, 145, 90, 60
17	-30	30	180, 145, 90, 60
18	-60	30	180, 145, 90, 60
19	-90	30	180, 145, 90, 60
20	-120	30	180, 145, 90, 60

Table 7.1: Tasks defining the measured workspace

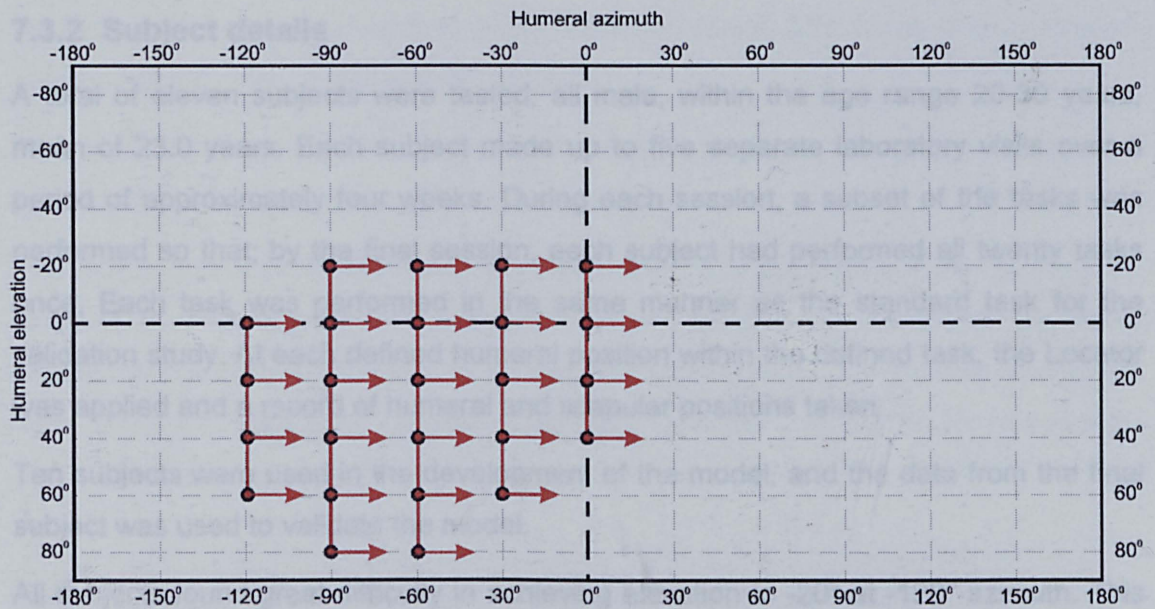


Figure 7.5: Workspace map representation of the five defined elevation tasks. The position of the elbow is denoted by the circle, while the arrow represents the direction of the forearm, thereby specifying the rotation of the humerus

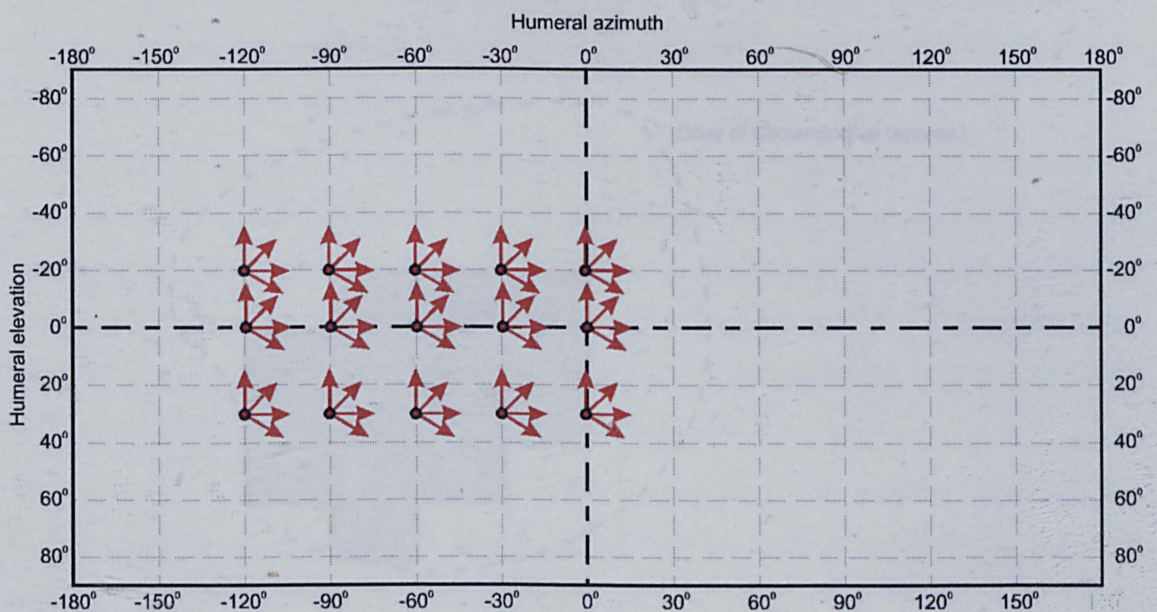


Figure 7.6: Workspace map representation of the fifteen defined rotation tasks. The position of the elbow is denoted by the circle, while the arrow represents the direction of the forearm, thereby specifying the rotation of the humerus

It should be noted that the arm positions defined here are approximate positions requested of the subjects during data collection. It is extremely difficult to obtain these numbers precisely while collecting data.

7.3.2 Subject details

A total of eleven subjects were tested, all male, within the age range 20-30 years, mean of 23.0 years. Each subject made up to five separate laboratory visits over a period of approximately four weeks. During each session, a subset of the tasks was performed so that, by the final session, each subject had performed all twenty tasks once. Each task was performed in the same manner as the standard task for the validation study. At each defined humeral position within the defined task, the Locator was applied and a record of humeral and scapular positions taken.

Ten subjects were used in the development of the model, and the data from the final subject was used to validate the model.

All subjects found great difficulty in achieving elevation to -20° at -120° azimuth. This affected the last position in Task 5 and all of Task 20. These positions were therefore removed from the model to give a final workspace as shown below, including rotation from 180° to 60° throughout.

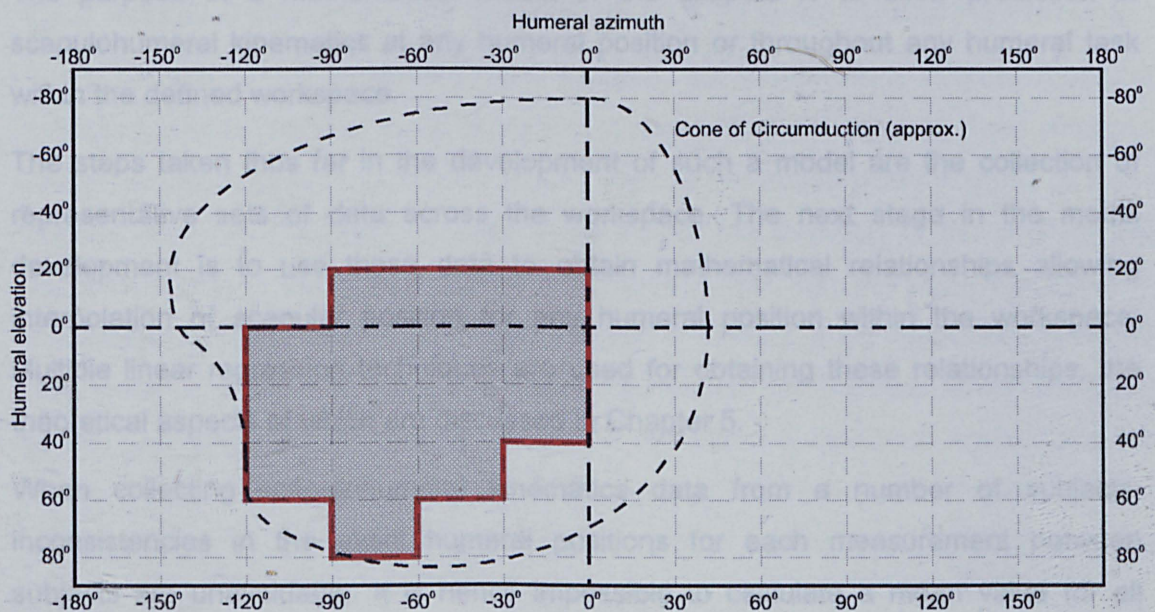


Figure 7.7: Final modelled humeral workspace.

The data was collected using the Isotrak[®] II system in exactly the same manner as in the two channel validation study presented in Chapter 6.

7.3.3 Co-ordinate Frame Specification

The data was analysed in WinMat, again in the same manner as in the validation study, to yield Euler rotations of the scapula relative to its initial position. The displacements of the scapula were determined in the global frame of the sternal

receiver, and then zeroed to their initial value to reduce differences arising through anthropometric differences between subjects.

The co-ordinates of the arm were determined in terms of azimuth, elevation and rotation of the humerus in the global (sternal) frame.

The resulting data provides measured static positions of the humerus and scapula for each of the 86 approximate humeral positions defined in the tasks. By fitting polynomial surfaces to this data, all six degrees of freedom of the scapula have been determined at regular finite intervals of azimuth, elevation and rotation for all subjects, and a generic model developed.

7.4 DEVELOPING THE SCAPULOHUMERAL KINEMATIC MODEL

7.4.1 Introduction

The purpose of a mathematical model of the scapula is to allow prediction of scapulohumeral kinematics at any humeral position or throughout any humeral task within the defined workspace.

The steps taken thus far in the development of such a model are the collection of representative sets of data across the workspace. The next stage in the model development is to use these data to obtain mathematical relationships allowing interpolation of scapular position for any humeral position within the workspace. Multiple linear regression techniques are used for obtaining these relationships, the theoretical aspects of which are discussed in Chapter 5.

When collecting scapulohumeral kinematics data from a number of subjects, inconsistencies in the exact humeral positions for each measurement between subjects are unavoidable. It is hence impossible to calculate a mean value for all subjects for each degree of freedom of the scapula, for each humeral position, directly from the collected data. It is necessary therefore to model the data individually for each subject. Upon validation of these models, it is possible to obtain data at a number of finite humeral positions for all subjects, and to use this data to develop an overall, subject independent, mathematical model of scapulohumeral kinematics.

The subsequent sections detail the progression through each of these stages.

7.4.2 Summary of Regression Procedures

Linear relationships require the definition of two constants. Generally, these are expressed as a function of the form $y=mx+c$, in which an input variable x is used to predict an output variable or response y .

Recalling from Chapter 5, this relationship may be expanded to allow modelling of a response with more than one independent input or regressor variable by use of the general model

$$Y = \beta_0 + \beta_1 \cdot x_1 + \beta_2 \cdot x_2 + \dots + \beta_k \cdot x_k + \varepsilon \quad (7.1)$$

possessing k regressor variables. Despite being termed linear regression, models such as these may be applied to a variety of modelling situations including those of higher order problems. This concept, discussed in Chapter 5, is employed in the modelling of scapulohumeral kinematics presented here.

7.4.3 Issues Concerning the Modelling of Three Dimensional Kinematics

For prediction of the motions of the scapula, six independent outputs must be modelled, one for each of the six degrees of freedom of the scapula; three rotations and three displacements. It may be argued that, as the rotations are in terms of Euler angles, dependencies exist between them in that the direction of the axis for the second rotation is dependent on the magnitude of the first rotation. This effect is compounded for the third rotation, the direction of its axis being dependent upon the magnitude of the first and second rotations. However, as pointed out by Goldstein (1980) and Gupta (1988), among others, the extraction of the Euler angles from the rotation matrix eliminates the dependencies in their presentation. It is the elements of the rotation matrix which contain the dependencies, not the derived Euler rotations themselves.

Six separate regression models are hence needed to define a complete scapulohumeral kinematics model, one for each degree of freedom of scapular motion.

The input variables for the final scapulohumeral kinematics model are the co-ordinates of the arm in terms of the azimuth, elevation and rotation of the humerus. However, the use of these three linear parameters alone in the regression models is inadequate. The non-linearity inherent in scapulohumeral rhythm has already been identified and illustrated in Chapter 6 where quadratic relationships of humeral

elevation were used in modelling the motion of the scapula. Although these models provided a faithful representation of three dimensional scapulohumeral rhythm in the *standard test*, little is known about the characteristics of scapulohumeral motion outside elevation in the coronal plane, which may contain characteristics necessitating the use of higher order polynomials. Cubic models have hence been used in the development of the scapulohumeral kinematics model. Quadratic models are also investigated as they provide a far more simple model. The results from both are compared to investigate the effects of increasing the order of the regression.

7.4.4 Input and Output Parameters for Regression Models

Considering the input parameters for the regression models, three base inputs exist (the co-ordinates of the arm). The cubic regressions hence require nine regression variables; azimuth, elevation and rotation together with the quadratic and cubic terms for these, giving the model,

$$Y = \beta_0 + \beta_1 \cdot a + \beta_2 \cdot a^2 + \beta_3 \cdot a^3 + \beta_4 \cdot e + \beta_5 \cdot e^2 + \beta_6 \cdot e^3 + \beta_7 \cdot r + \beta_8 \cdot r^2 + \beta_9 \cdot r^3 + \varepsilon \quad (7.2)$$

where $Y \equiv$ the response variable (any one of the degrees of freedom),

$a \equiv$ humeral azimuth

$e \equiv$ humeral elevation

$r \equiv$ humeral rotation

$\beta_k \equiv$ regression coefficients

and $\varepsilon \equiv$ error term

The more simple quadratic regressions possess six regressor variables; azimuth, elevation and rotation, together with their quadratic terms, giving the model,

$$Y = \beta_0 + \beta_1 \cdot a + \beta_2 \cdot a^2 + \beta_3 \cdot e + \beta_4 \cdot e^2 + \beta_5 \cdot r + \beta_6 \cdot r^2 + \varepsilon \quad (7.3)$$

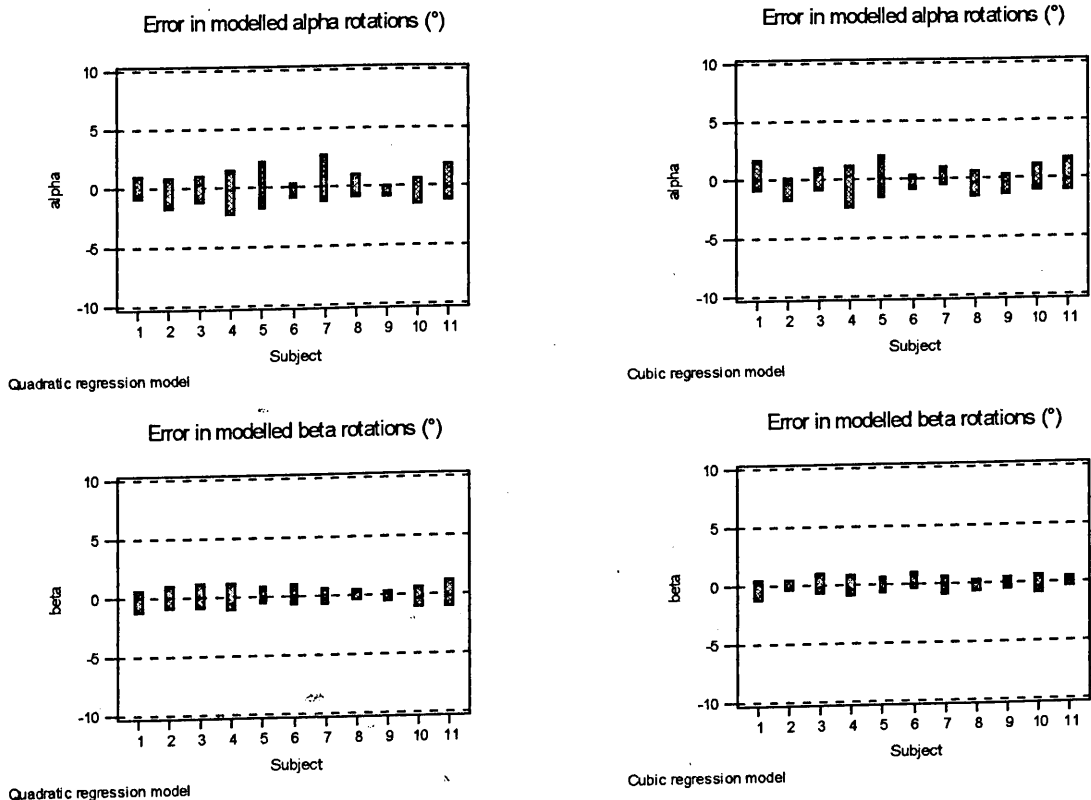
Definitions of variables is identical to Equation 7.2.

The regression analysis was performed using both Microsoft Excel and Minitab to ensure consistent results between the two software packages. Results from these were identical and all further analysis was performed using Excel.

7.4.5 Validation of Subject Models

In order to investigate the accuracy of the relationships obtained from the regression analysis, scapular position data were generated for the humeral positions collected for each subject. These model generated data were then compared directly with the collected scapular position data and the differences investigated using the paired t-test.

In all degrees of freedom, for all subjects, no significant differences existed between the measured and predicted data for either the quadratic or cubic regression models ($p > 0.05$). However, knowledge of this alone does not provide a useful indicator for assessing the effects of increasing the order of the regression. As an alternative to comparing p-values, the 95% confidence intervals resulting from the t-test of the error were investigated. If no error were present, the 95% confidence intervals would have zero magnitude. As the error increases, so do the confidence intervals. Figure 7.8 shows these results for each degree of freedom, for each subject. The graphs to the left are the 95% confidence intervals of the error for the quadratic regression, while those on the right are for the cubic regression.



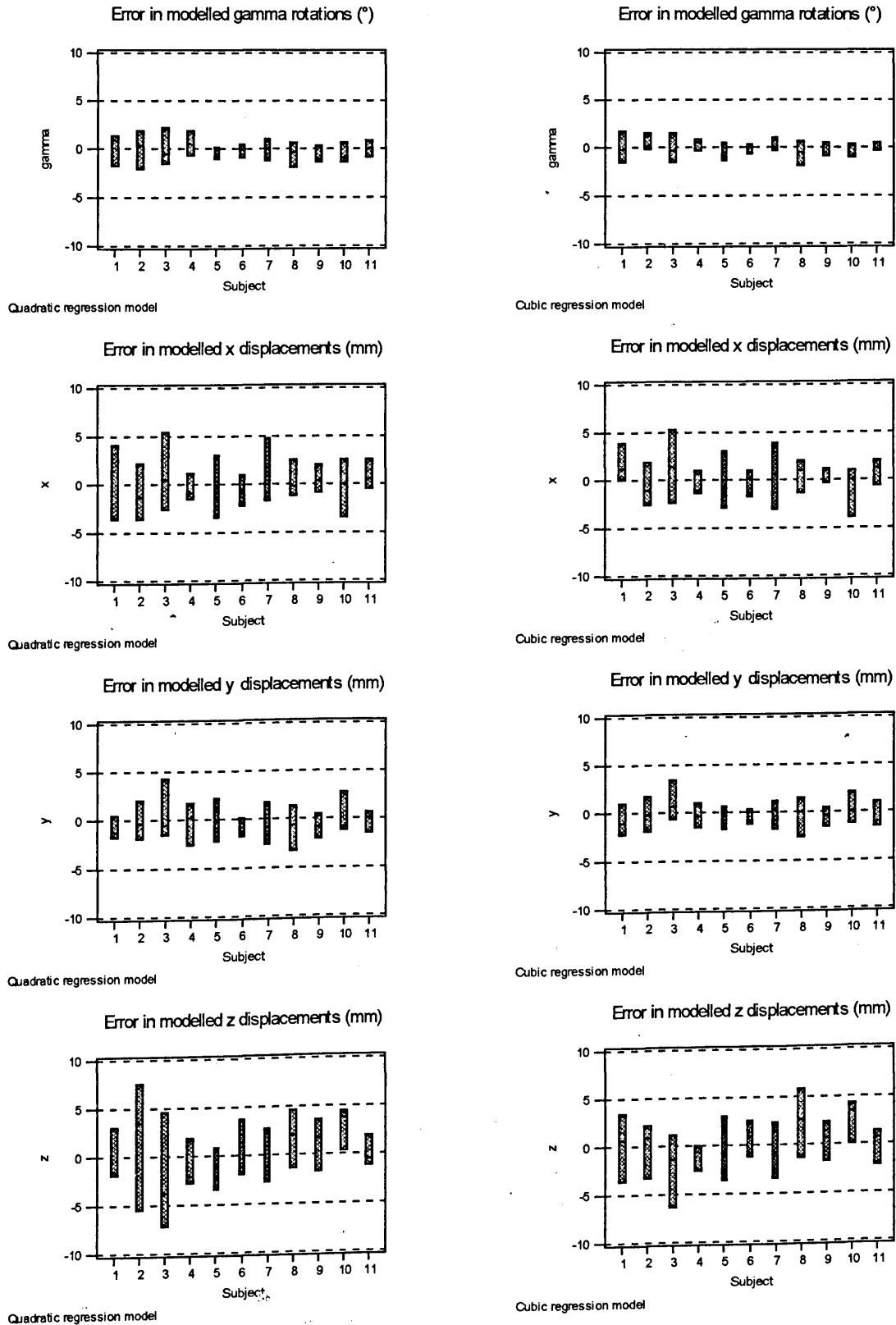


Figure 7.8: Comparisons of 95% confidence intervals for errors between measured and predicted data in quadratic and cubic regressions.

It can be seen quite clearly from these results that increasing the order of the regression from a quadratic to a cubic model has little effect in terms of the residual error between measured and predicted data. However, the quadratic regression models simplify the final model, and have already been shown to provide a good approximation to the measured data presented in Chapter 6. Quadratic regression models were hence used in prediction of scapulohumeral kinematics from each subject.

7.4.6 Development of a Generic Model

The analysis discussed thus far has been concerned with the development of mathematical models of each degree of freedom of scapular motion, for each subject across the defined workspace. Hence, at this point, it would be possible to investigate the scapulohumeral kinematics of each subject and the differences between them. However, using these subject specific models, it is also possible to obtain scapulohumeral kinematic data from all subjects at identical humeral positions. The mean values of these data may then be determined and used in the development of a generic, subject independent model of scapulohumeral kinematics. The variation between subjects may also be determined and incorporated in to the model, providing confidence or prediction intervals on the resulting motion patterns.

As this work is an investigation into general scapulohumeral kinematics, the latter of these options has been taken. This is considered to be advancing the study further, rather than analysis of the results obtained up to this point. However, the regression coefficients of the individual subject models are included in Appendix 4, should the reader wish to investigate these further.

The first stage in the modelling process was to define the humeral positions at which scapulohumeral kinematic data were generated. All modelled positions must lie within the defined workspace, hence this issue is more concerned with defining the size of the incremental steps between positions of humeral azimuth, elevation and rotation. To avoid the possibility of any weighting effects, a common increment of 10° was defined across all parameters describing humeral position. Hence, at every 10° increment of azimuth, elevation or roll, the position and orientation of the scapula were calculated.

Applying this incremental size to the defined workspace gave a total of 1469 humeral positions at which all six degrees of freedom of scapular motion were modelled for each subject. At all of these positions, the mean value between subjects of each

degree of freedom was calculated. This provided a final set of data to which the regression analysis was again applied to develop a set of generic constraint equations describing scapulohumeral kinematics.

The regression analysis was again performed using Microsoft Excel, with quadratic relationships determined for each degree of freedom of scapular motion.

7.5 A MODEL OF THREE DIMENSIONAL SCAPULOHUMERAL KINEMATICS

7.5.1 Governing Constraint Equations

The quadratic regression analysis provides the β_k coefficients in Equation 7.3. From these the explicit constraint equations are presented for each degree of freedom of scapular motion (Equations 7.4-7.9). These governing equations of scapulohumeral kinematics are valid across the workspace identified in Figure 7.7. The definitions of these rotations and displacements are given in Chapter 5 (Section 5.7). These relationships refer to the rotations of the scapula in the local scapular co-ordinate system, using the $x_\gamma, y_\alpha', z_\beta''$ rotation sequence. The displacements of the scapula in the global co-ordinate system are zeroed to the initial position of the scapula.

The coefficients of these constraint equations using the $x_\alpha, y_\beta', z_\gamma''$ rotation sequence in both the local scapular, and global co-ordinate systems are included in Appendix 4.

Lateral rotation, α :

$$\alpha = 24.72 - 0.01 \cdot a + 9.74 \times 10^{-5} \cdot a^2 - 0.27 \cdot e - 6.48 \times 10^{-4} \cdot e^2 + 0.002 \cdot r - 106 \times 10^{-4} \cdot r^2 \quad (7.4)$$

Backward tip, β :

$$\beta = -6.21 - 0.08 \cdot a - 4.40 \times 10^{-4} \cdot a^2 + 0.14 \cdot e - 2.16 \times 10^{-4} \cdot e^2 - 0.13 \cdot r + 4.36 \times 10^{-4} \cdot r^2 \quad (7.5)$$

Retraction, γ :

$$\gamma = 12.35 + 0.08 \cdot a - 4.64 \times 10^{-4} \cdot a^2 + 0.09 \cdot e + 6.78 \times 10^{-4} \cdot e^2 - 0.22 \cdot r + 7.90 \times 10^{-4} \cdot r^2 \quad (7.6)$$

Superior acromial displacements, x :

$$x = -51.95 + 0.31 \cdot a + 1.27 \times 10^{-3} \cdot a^2 + 0.27 \cdot e + 2.78 \times 10^{-3} \cdot e^2 + 0.49 \cdot r - 1.51 \times 10^{-3} \cdot r^2 \quad (7.7)$$

Lateral acromial displacements, y :

$$y = -0.74 - 0.12 \cdot a - 7.64 \times 10^{-4} \cdot a^2 - 0.17 \cdot e - 2.27 \times 10^{-3} \cdot e^2 - 0.25 \cdot r - 1.21 \times 10^{-3} \cdot r^2 \quad (7.8)$$

Posterior acromial displacements, z :

$$z = 19.24 + 0.11 \cdot a - 1.45 \times 10^{-3} \cdot a^2 + 0.18 \cdot e + 2.90 \times 10^{-3} \cdot e^2 - 0.60 \cdot r + 2.38 \times 10^{-3} \cdot r^2 \quad (7.9)$$

where:

a = azimuth in degrees,

e = elevation in degrees,

r = roll in degrees,

based on the definitions given in Figure 3.11.

7.5.2 Model Validation

To validate the results generated by the scapulohumeral kinematic model, it is necessary to compare predicted data to measured data which was not used in the model development. The eleventh subject was used as the resource for this data.

Four tasks have been analysed to compare the model with subject 11. These are:

- 1 Elevation between 80° and 0° at -90° azimuth and 90° roll (abduction in the coronal plane)
- 2 Elevation between 80° and 0° at 0° azimuth and 90° roll (flexion in the sagittal plane)
- 3 Azimuth between 0° and -120° at 0° elevation and 90° roll (horizontal flexion)
- 4 Humeral rotation between 180° and 60° at -90° azimuth and 0° elevation.

Figure 7.9 to Figure 7.12 illustrate the comparisons between the model and subject 11 for each of these tasks. It can be observed that the measured data lies within the 95% confidence intervals of the model.

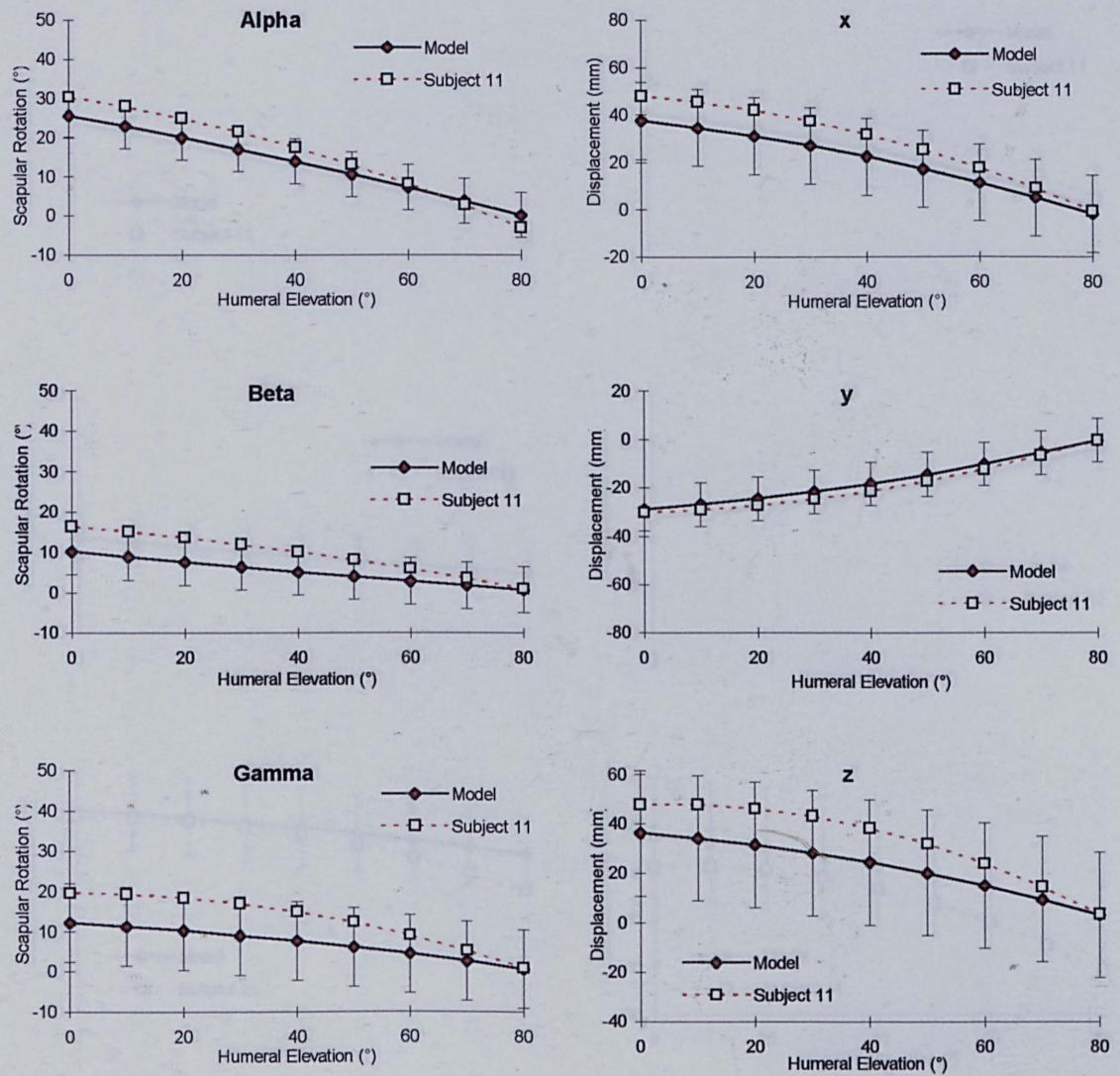


Figure 7.9: Comparisons between measured and predicted data for each degree of freedom, task 1 (abduction in the coronal plane)

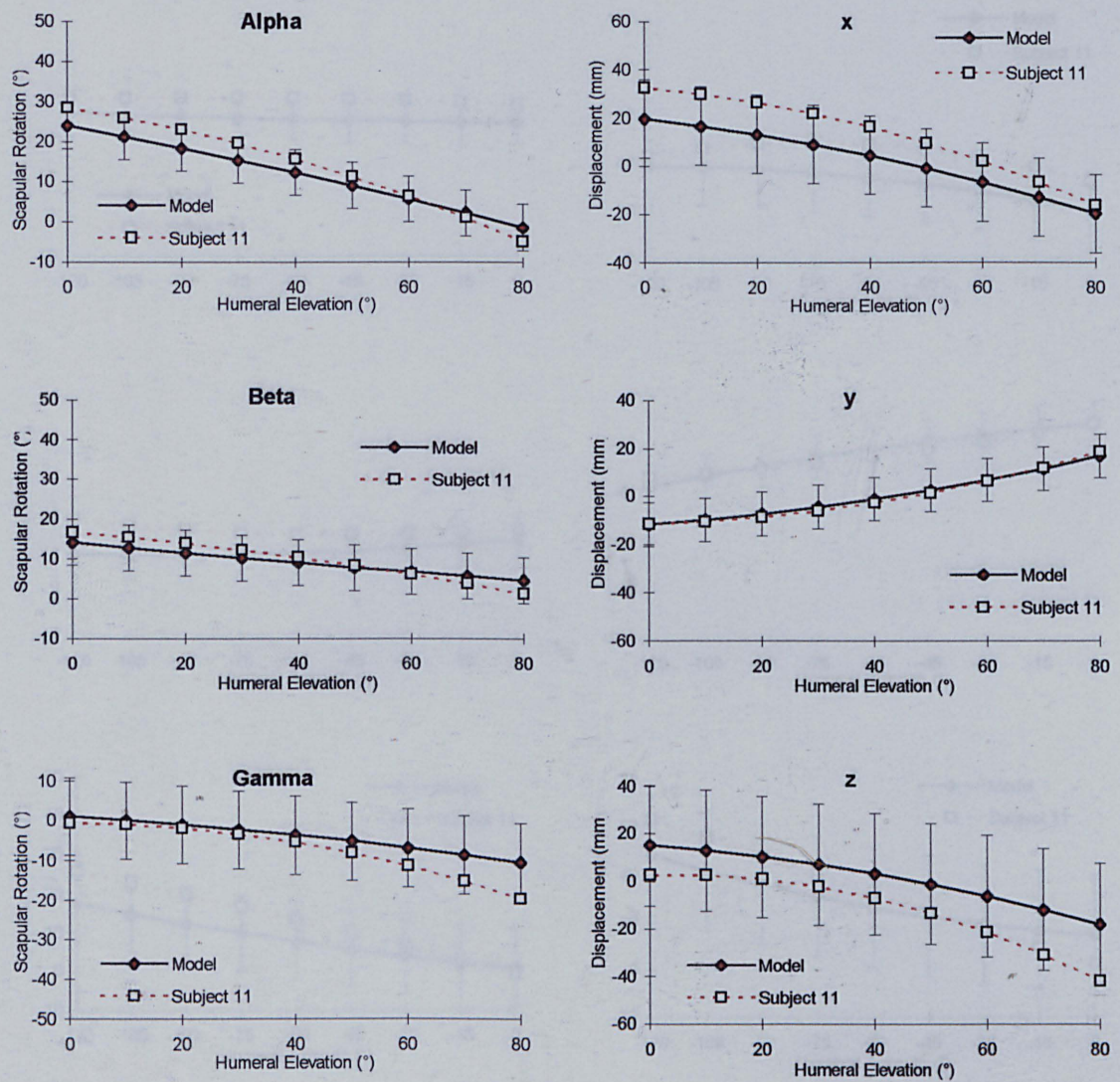


Figure 7.10: Comparisons between measured and predicted data for each degree of freedom, task 2 (flexion in the sagittal plane)

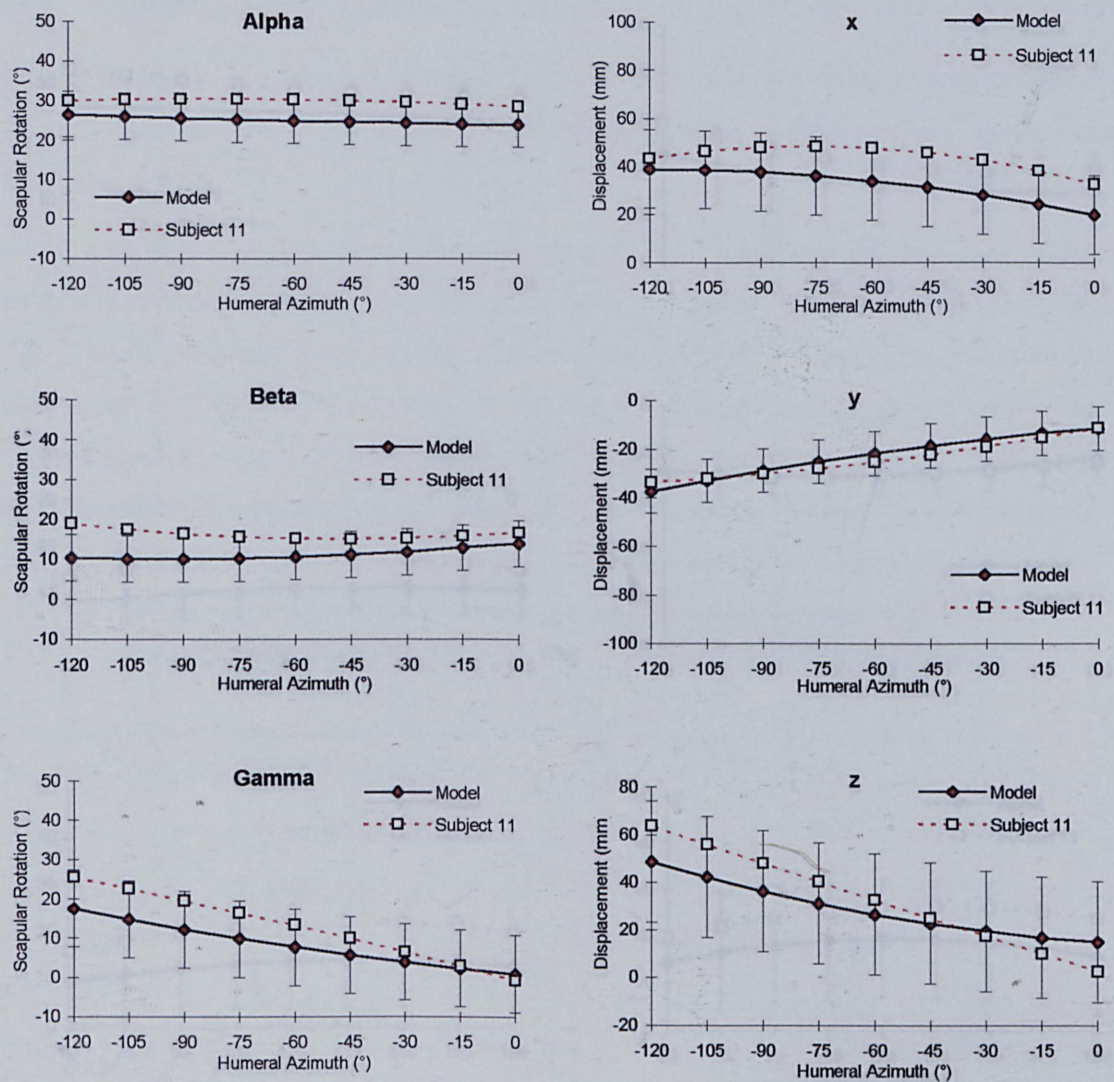


Figure 7.11: Comparisons between measured and predicted data for each degree of freedom, task 3 (horizontal flexion)

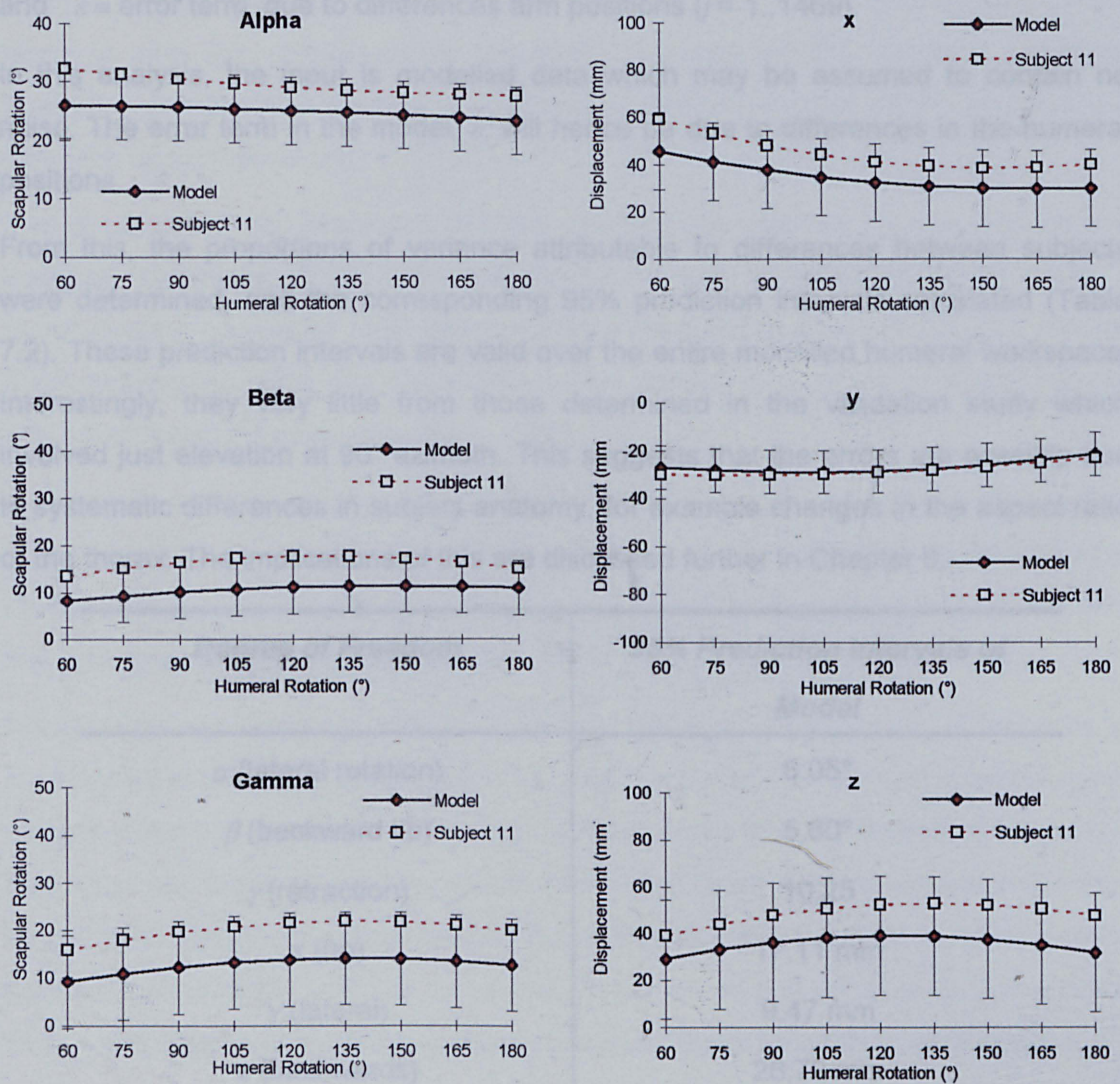


Figure 7.12: Comparisons between measured and predicted data for each degree of freedom, task 4 (humeral rotation)

7.5.3 Subject Variation

To quantify the variations in scapulohumeral kinematics between subjects a single factor analysis of variance was performed, using the following model.

$$Y = \mu + \alpha_i + \varepsilon_j \quad (7.10)$$

where:

$Y \equiv$ any single reading,

$\mu \equiv$ a mean value for that reading,

$\alpha \equiv$ effect of subjects ($i = 1..11$),

and ε = error term, due to differences arm positions ($j = 1..1469$).

In this analysis, the input is modelled data which may be assumed to contain no noise. The error term in the model, ε , will hence be due to differences in the humeral positions.

From this, the proportions of variance attributable to differences between subjects were determined, and the corresponding 95% prediction intervals calculated (Table 7.2). These prediction intervals are valid over the entire modelled humeral workspace. Interestingly, they vary little from those determined in the validation study which involved just elevation at 90° azimuth. This suggests that the errors are possibly due to systematic differences in subject anatomy, for example changes in the aspect ratio of the thorax. The implications of this are discussed further in Chapter 8.

<i>Degree of Freedom</i>	<i>95% Prediction Intervals of Model</i>
α (lateral rotation)	6.05°
β (backward tip)	5.60°
γ (retraction)	10.25
x (up)	17.11 mm
y (lateral)	9.47 mm
z (backwards)	26.72 mm

Table 7.2: 95% Prediction Intervals for model

7.6 REPRESENTATION OF SCAPULOHUMERAL KINEMATICS

The multivariate nature of scapulohumeral kinematics creates difficulties when considering presenting any useful graphical representations. It is not practical to consider plotting all six degrees of freedom of scapular motion on one chart. The duplicated demands on axes, combined with the amount of information needed would lead to a complex, cluttered representation which would be almost, if not completely, impossible to interpret.

Considering any one degree of freedom separately reveals more fundamental difficulties.

Each constraint equation contains four variables; the three co-ordinates of the humerus and the corresponding kinematic response of the scapula. Graphical illustration of this across a range of all three humeral co-ordinates would require a four dimensional representation.

Two dimensional representations of three variables are relatively easy to produce and interpret. Generally, x , y pairs are plotted in two dimensional plane while a corresponding z value for each pair provides a measure of depth. Such plots provide a two dimensional view of a three dimensional surface in what are often termed two and a half dimensional models (Marr, 1982).

A pseudo fourth dimension may be added to these models by allowing multiple values of z for each x , y pair. Such representations are frequently used in topology, illustrating the depth of layering of rock formations, or thermodynamics where the heat flow across an irregular surface may be colour mapped to a corresponding key.

Representations similar to this have been applied to each degree of freedom of scapular kinematics. For each plot, rotation is fixed and azimuth and elevation pairs replace x and y . For each of these pairs a value of the specific degree of freedom is calculated and plotted along the vertical z axis. The result yields a surface in the form of the 2½-D models discussed earlier. Repeating this at n levels of humeral rotation generates n surfaces. Although these may be plotted on one set of axes, it was found to be more clear to avoid this and display a separate plot for each level of rotation.

Using this form of representation, Figure 7.13 to Figure 7.18 (a-c) illustrate the results generated by the model. The results from three levels of rotation are displayed; 180° in (a), 90° in (b) and 60° in (c).

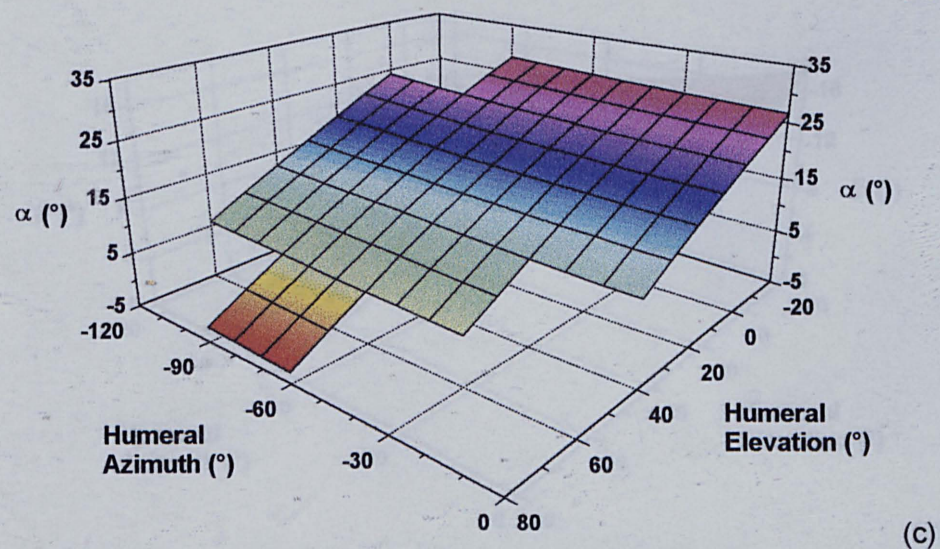
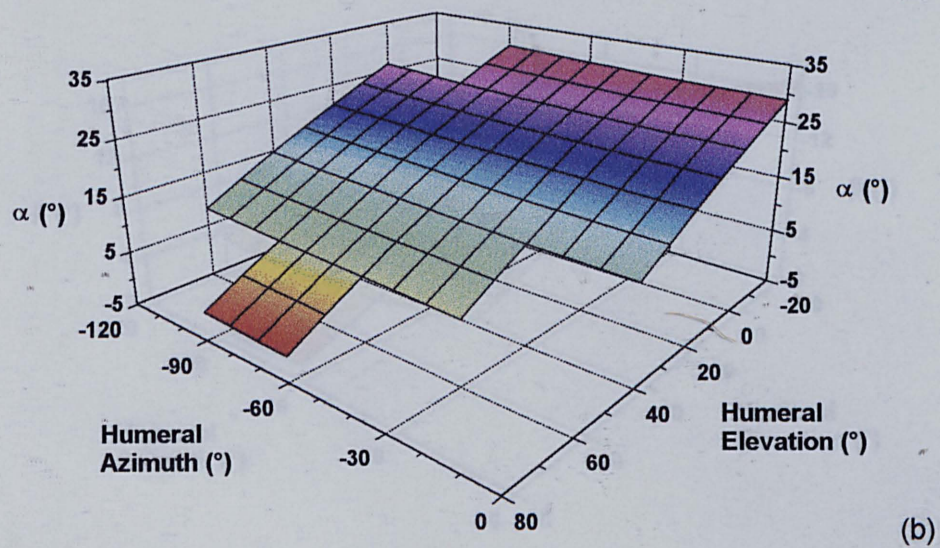
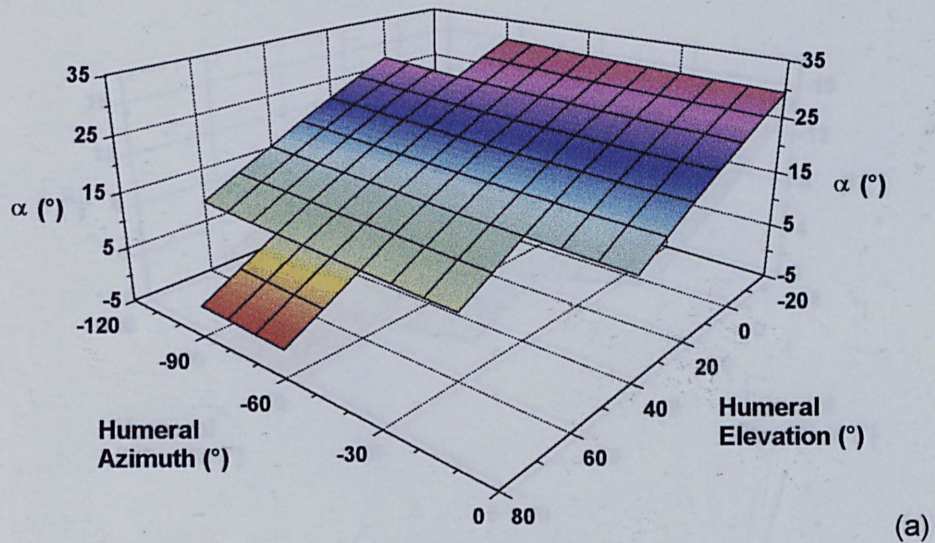


Figure 7.13: Variations in scapular rotation angle α (lateral rotation) due to humeral azimuth and elevation. (a) at 60° humeral rotation, (b) at 90° humeral rotation and (c) at 180° humeral rotation.

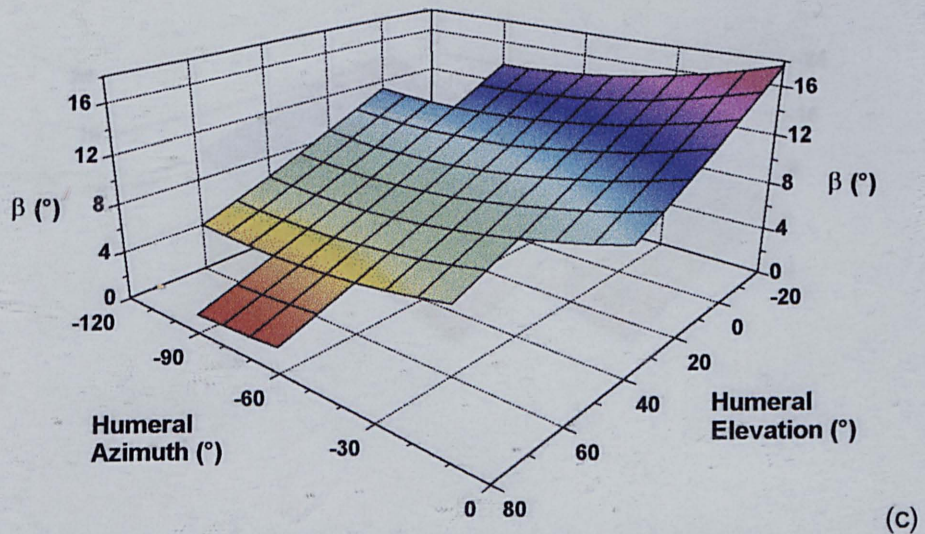
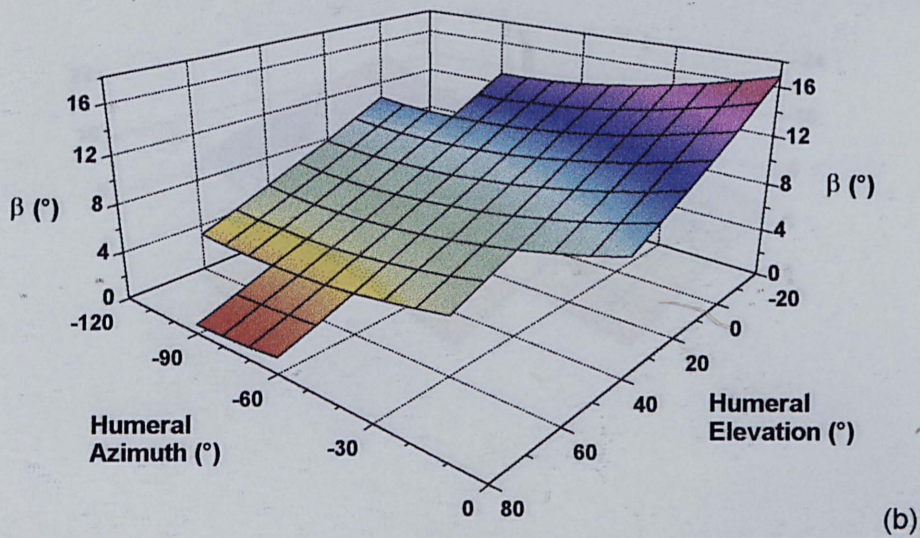
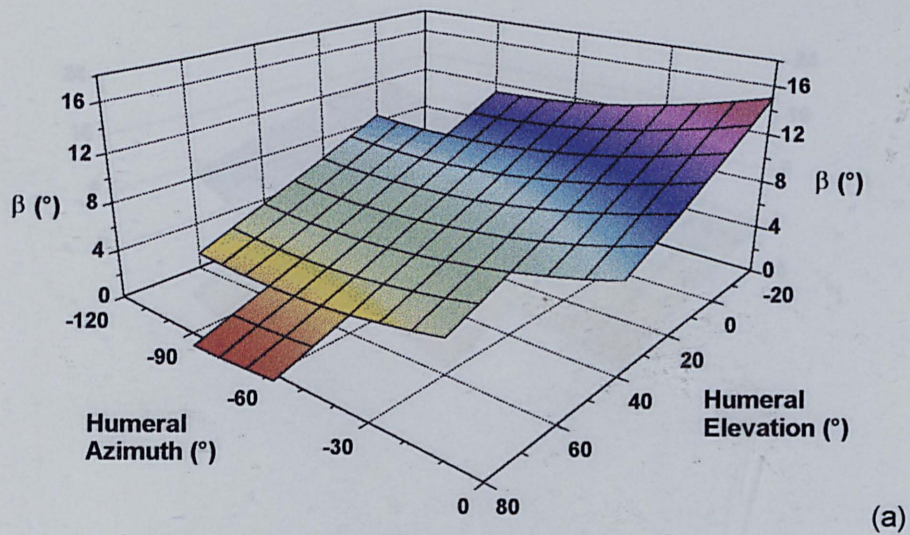


Figure 7.14: Variations in scapular rotation angle β (backward tip) due to humeral azimuth and elevation. (a) at 60° humeral rotation, (b) at 90° humeral rotation and (c) at 180° humeral rotation.

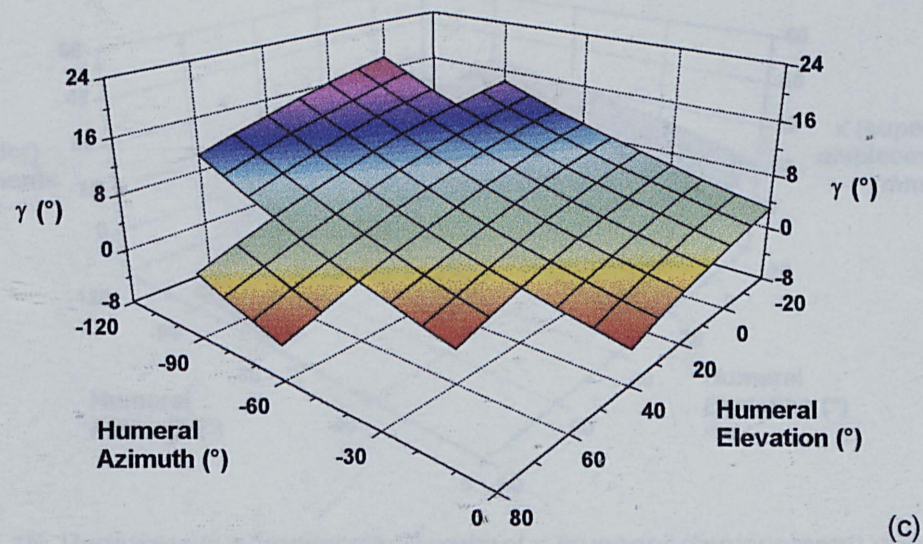
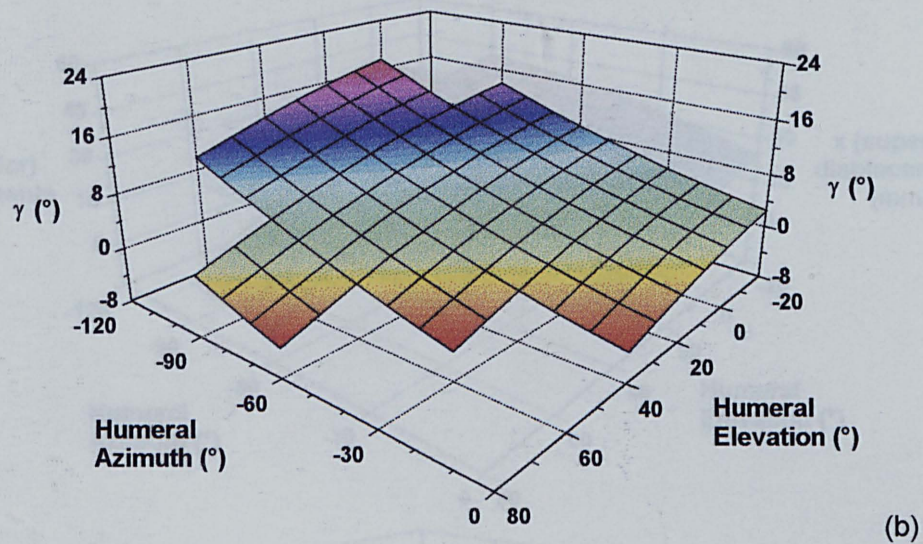
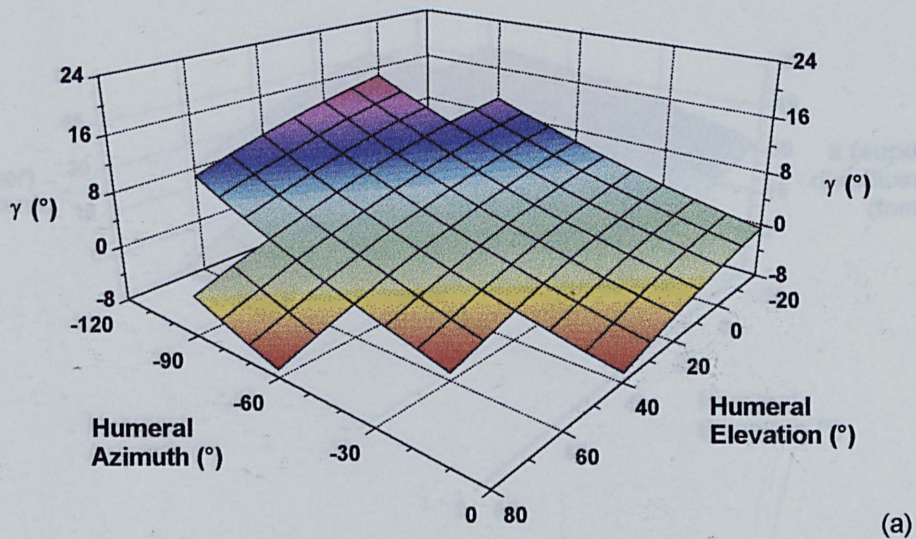


Figure 7.15: Variations in scapular rotation angle γ (retraction) due to humeral azimuth and elevation. (a) at 60° humeral rotation, (b) at 90° humeral rotation and (c) at 180° humeral rotation.

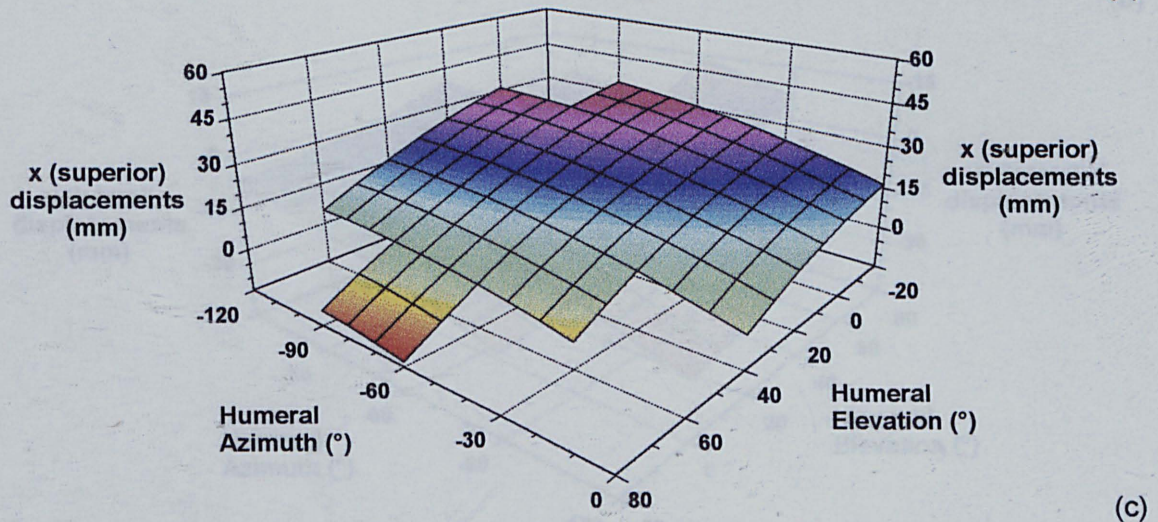
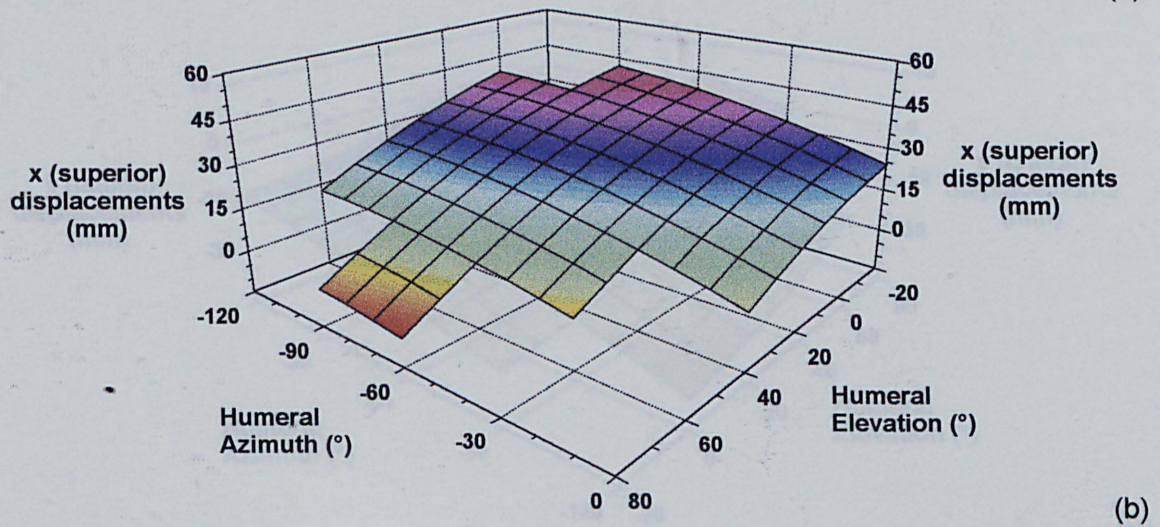
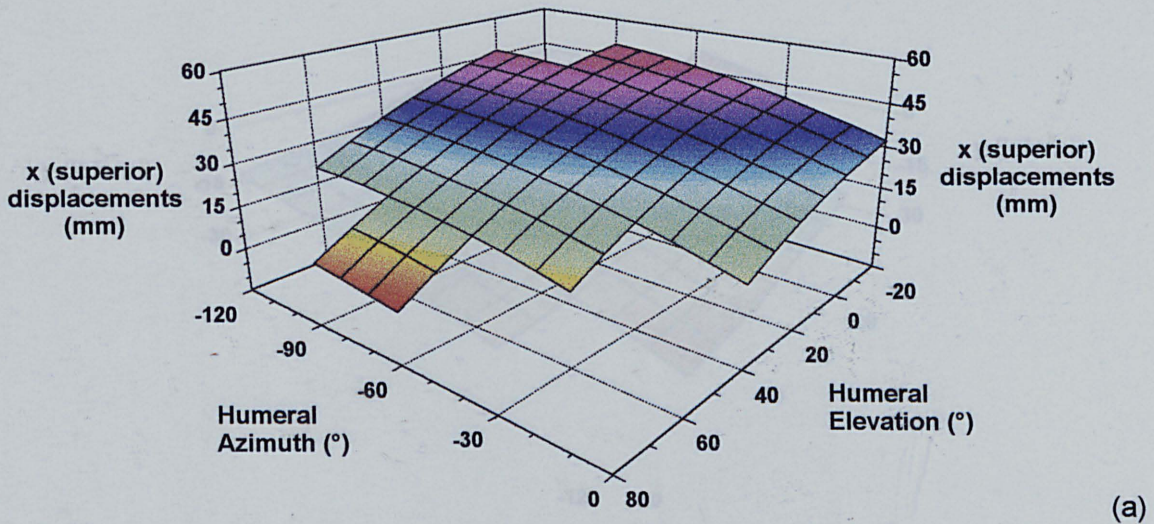


Figure 7.16: Variations in acromial displacement x (superior displacement) due to humeral azimuth and elevation. (a) at 60° humeral rotation, (b) at 90° humeral rotation and (c) at 180° humeral rotation.

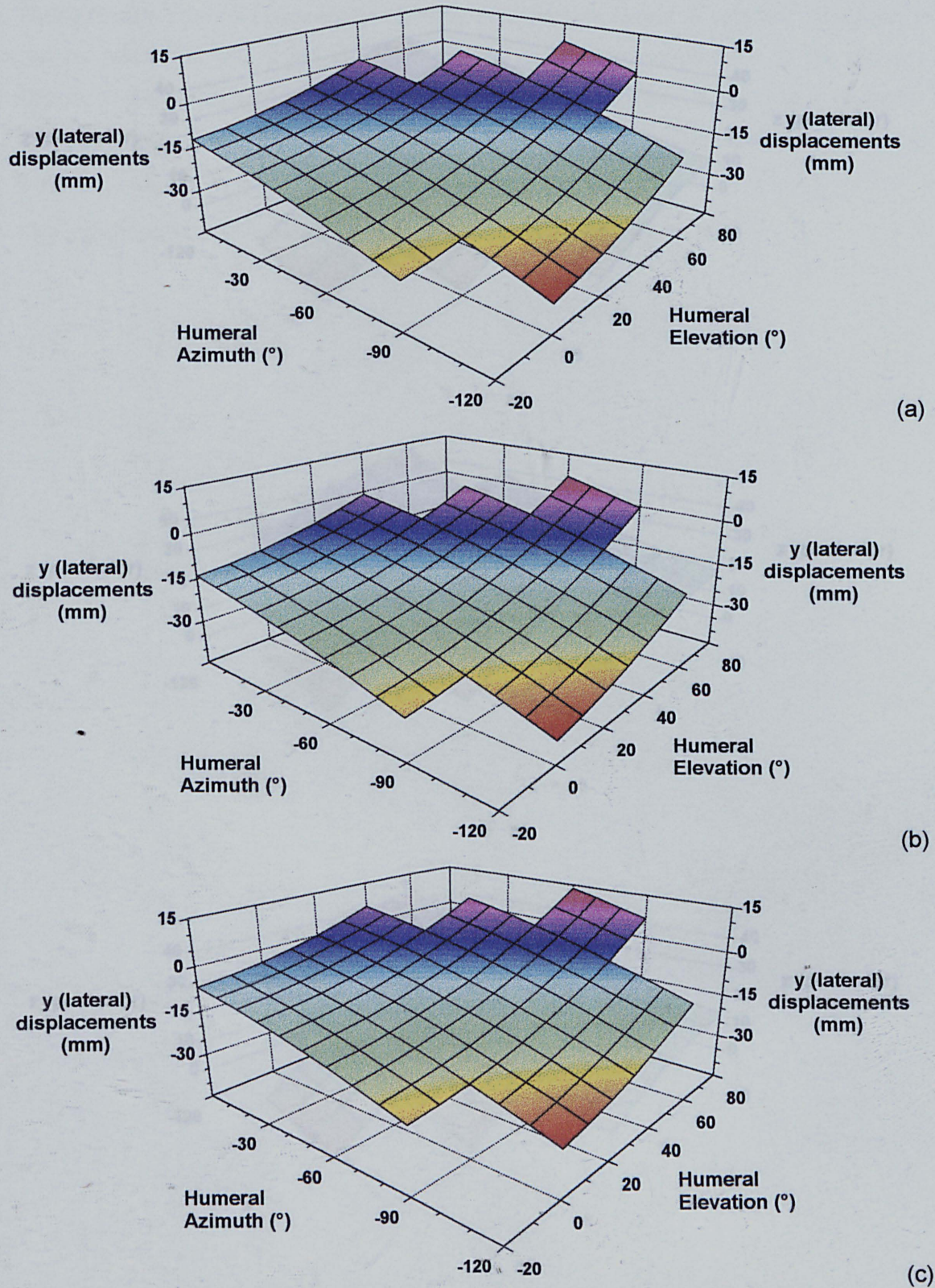


Figure 7.17: Variations in acromial displacement y (lateral displacement) due to humeral azimuth and elevation. (a) at 60° humeral rotation, (b) at 90° humeral rotation and (c) at 180° humeral rotation.

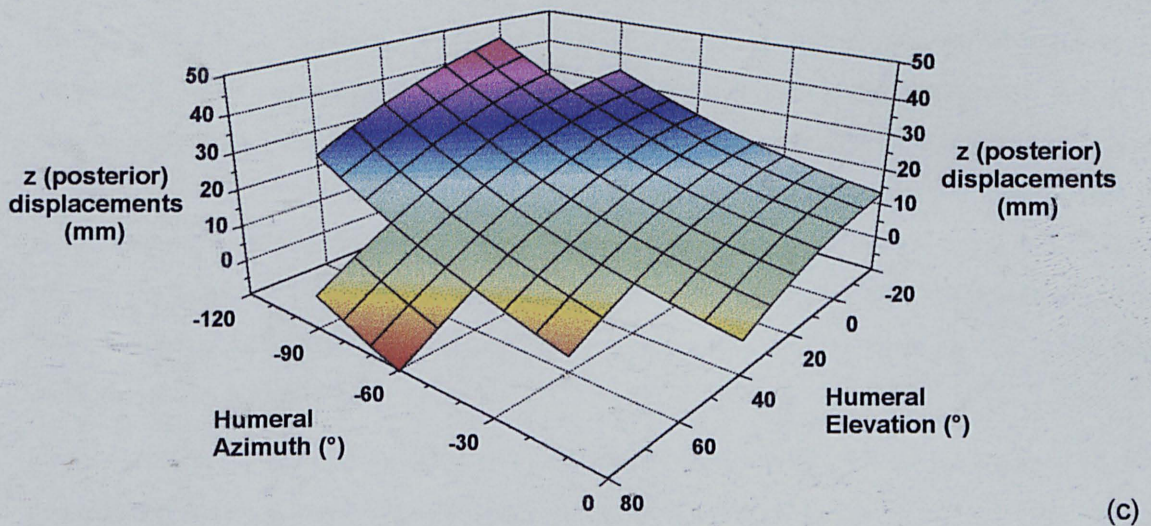
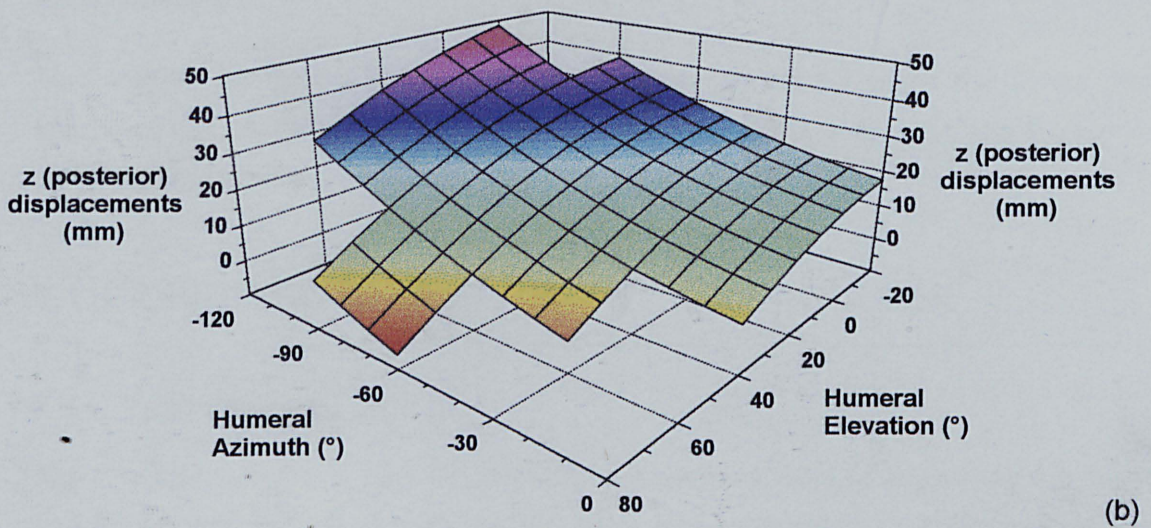
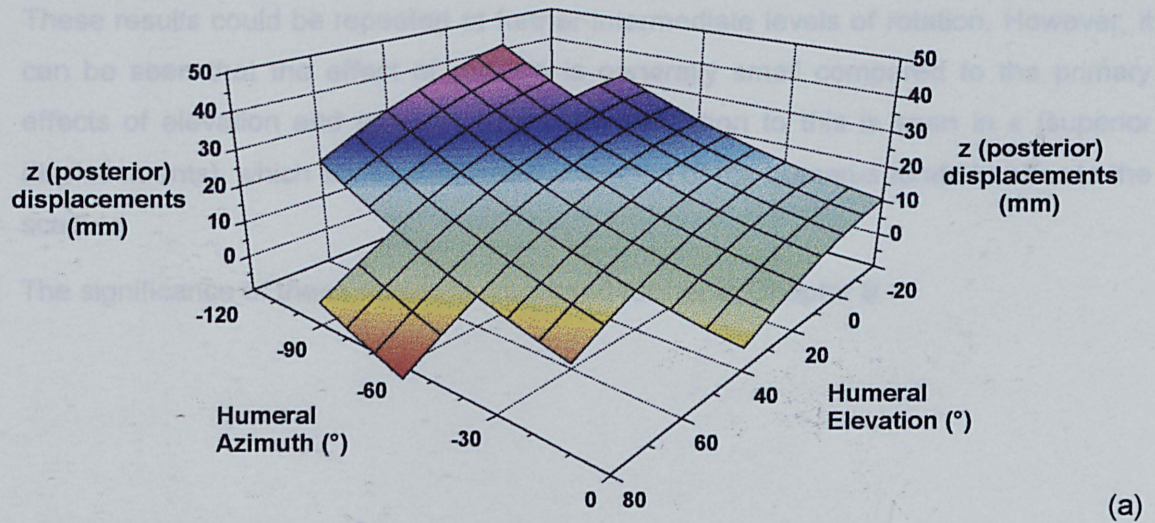


Figure 7.18: Variations in acromial displacement z (posterior displacement) due to humeral azimuth and elevation. (a) at 60° humeral rotation, (b) at 90° humeral rotation and (c) at 180° humeral rotation.

These results could be repeated at further intermediate levels of rotation. However, it can be seen that the effect of rotation is generally small compared to the primary effects of elevation and azimuth. The main exception to this is seen in x (superior displacements), which shows that internal rotation of the humerus tends to elevate the scapula.

The significance of these results is discussed further in Chapter 8.

Chapter 8

Discussion

This chapter brings together the work and ideas contained within the thesis, and discusses the relevance and implications of the techniques developed and the results obtained, including comparisons with other published studies.

8.1 DESCRIPTIONS OF MOTION AT THE SHOULDER

8.1.1 Total Shoulder Motion

The shoulder complex is a highly developed system capable of supporting the upper limb throughout an extensive range of motion, while maintaining stability and control. Due to this range of motion, clinical descriptions of shoulder motion, introduced in Chapter 2, have been criticised as inadequate for describing the motions of the arm. The descriptions of shoulder flexion and rotation can only describe a limited number of motions, and combinations of these terms without common interpretations lead to confusing results. Indeed, Dumas's paradox may be explained as not a paradox at all, but an example of a poor understanding of the sequence dependence in three-dimensional rotations, coupled with inadequate descriptions of the observed motions at the shoulder.

In comparison, kinematic descriptions allow motions to be precisely specified. By quantifying motions over the complete range of motion of the arm, rather than in just two planes, they eliminate many of the shortcomings apparent in the clinical descriptions. However, the accurate definitions and clear descriptions of kinematic systems are essential, especially when communicating a particular system to other researchers, whether in the clinical or biomedical fields. It was illustrated in Chapter

Chapter 8

Discussion

This chapter brings together the work and ideas contained within the thesis, and discusses the relevance and implications of the techniques developed and the results obtained, including comparisons with other published studies.

8.1 DESCRIPTIONS OF MOTION AT THE SHOULDER

8.1.1 Total Shoulder Motion

The shoulder complex is a highly developed system, capable of supporting the upper limb throughout an expansive range of motion, while maintaining stability and control. Due to this range of motion, clinical descriptions of shoulder motion, introduced in Chapter 2, have been shown to be inadequate for describing the motions of the arm. The descriptions of abduction, flexion and rotation can only describe a limited number of motions, and combinations of these terms without common interpretations lead to confusing results. Indeed, Codman's paradox may be explained as not a paradox at all, but an example of a poor understanding of the sequence dependence inherent in three dimensional rotations, coupled with inadequate descriptions of the observed motions at the shoulder.

In comparison, kinematic descriptions allow arm positions to be precisely specified. By quantifying motions over the complete range of motion of the arm, rather than in just two planes, they eliminate many of the shortcomings apparent in the clinical descriptions. However, the accurate definitions and clear descriptions of kinematic systems are essential, especially when communicating a particular system to other researchers, whether in the clinical or biomechanical field. It was illustrated in Chapter

3 that the interpretation of kinematic systems can also lead to confusion, once again causing misleading results.

The azimuth, elevation and roll system used within this thesis for specifying humeral positions is not new. Such descriptions are familiar to those in the field of robotics, and in essence, it is no more than a specific Euler angle rotation sequence in which one of the rotations occurs about a global axis rather than the local axis of the moving body. Its main advantage is in its ease of communication to those not familiar with the system, including investigators, clinicians and, importantly, subjects. Specifying a position on a globe is relatively easy for a normal subject to understand, and the analogy between specifying such a position on a globe and using the elbow to specify a similar position on an imaginary sphere centred on the shoulder is not a complex one.

In comparison with the Kapandji system (1982), the principal advantage is that elevation of the arm along planes of elevation can be easily represented. Due to the direction of the polar axis of the Kapandji system, activities involving constant latitude or longitude are unfamiliar motions. Hence, requesting such motions from subjects is difficult as the movements appear somewhat awkward and unnatural.

Considering presentation of humeral kinematics, a new method has been presented based on cartographic projections of the humeral globe onto a flat, two dimensional surface. These projections, referred to as workspace maps, are analogous with the definitions of humeral movements, that is azimuth and elevation, and also allow humeral rotation of the shoulder to be represented, as illustrated in Figure 7.5 and Figure 7.6.

Furthermore, they offer a number of advantages over previous representations of three dimensional humeral kinematics. Firstly, representations such as the joint sinus developed by Dempster (1965), and used by Engin and Tümer (1989), only illustrate the extremes of joint motion. Kapandji's cone of circumduction is also limited in this manner. Other representations such as the globographic system described by Engin and Chen (1986), and the spherical system described by An *et al.* (1991) do not lend themselves to two dimensional presentation particularly well, as it is often necessary to display two orthogonal views of the global representation to ensure complete description of the active workspace.

Workspace maps overcome these problems as they provide a precise method of specifying humeral azimuth, elevation and roll, and being a two dimensional projection, are easily presented.

8.1.2 Motion of the Scapula

Clinical definitions of human movement generally assume motion of a limb or extremity of the body, such as the head or a digit. Motions of these extremities are then expressed in terms of planar definitions (abduction/adduction, flexion/extension), together with a rotation, generally about one axis, as in the rotation of the humerus about its longitudinal axis. The inadequacies of these definitions for total shoulder motion have already been discussed. However, applying this terminology to describe the motions of the scapula in terms of clinical definitions is practically hopeless.

To specify the motions of the scapula, kinematic definitions are essential. Within this thesis, Euler angles have been employed as descriptions of kinematics of the scapula, in preference to the helical axis technique.

However, it must be pointed out that each individual rotation in an Euler angle sequence describes only a part of the three dimensional nature of scapular rotations. Furthermore, the rotation sequence adopted within this thesis (and previously used by Pronk 1991, and van der Helm and Pronk 1995) is only one of a number of definitions which could have been used, each providing differing results, and hence open to different interpretations.

The primary reason for adopting Euler angles in preference to the helical axis technique, and for choosing the specific Euler angle sequence employed was due to the analogy between the rotation angles chosen and clinical definitions of scapular motion. The rotation about the first axis, which is approaching vertical at rest corresponds well with the clinical definitions of protraction and retraction, while the second rotation about an axis normal to the plane of the scapula is well recognised as lateral rotation of the scapula. The final rotation, referred to as the tipping of the scapula about an axis made between the acromial angle and the root of the scapula spine is not clinically defined.

These angle definitions therefore enable the resulting motions to be communicated to others, including clinicians, with relative ease.

Whereas three dimensional rotations are generally difficult to perceive, displacements along three mutually perpendicular axes are relatively easy to visualise. However,

there appear to be no standard definitions to describe the translational components of scapula motion. It was hence necessary to define which co-ordinate system should be used to express these displacements. The local co-ordinate system has obvious advantages over a global system when describing rotations of the scapula, due to their sequence dependent nature, and the variations in resting posture of the scapula (Steindler 1962). However, in describing displacements, it was decided that the global system was preferred due to its universal nature, thereby enabling the results to be easily communicated to, and perceived by, others.

8.1.3 Issues Concerning Comparisons of Results

The motions of the shoulder girdle which allow the arm its expansive range of motion have never been fully investigated, nor has a suitable measurement technique been presented.

Despite the recent publication of a number of mathematical models of the shoulder girdle predicting muscle activity and/or joint reaction forces (Laursen 1995, Kedzior 1995, Meskers 1995, Makhsous 1996¹), there is a distinct lack of kinematic data relating to the motions of the hard tissues. Indeed, the Chalmers model (Makhsous 1996) allows muscles to be selected as active or passive during motions of the arm in order to investigate the effects of muscular disorders on joint reaction forces. For example, it should be possible to examine the motions and joint reaction forces of arm motions without any contributions from trapezius or serratus anterior. However, despite the significant effects on scapulohumeral rhythm caused through paralysis or wasting of these muscles (Barnett *et al.* 1995), the model always assumes a constant scapulohumeral rhythm (that presented by Hogfors *et al.*, 1991), regardless of muscular preferences. The need for kinematic data for both normal and pathological subjects is hence obvious.

Although the rotations of the scapula have been measured using a variety of techniques, as discussed in Chapter 4, there is scarcely any published data on the translational components of scapulohumeral kinematics. Laumann (1987) presented some results of a study measuring the distance between the vertebrae and the medial border of the scapula during arm abduction, but such measurements will be directly affected by the rotations of the scapula.

¹ This model is commercially available.

Considering the rotational components of scapulohumeral kinematics, comparisons of data between published studies are hindered due to a number of factors. Firstly, much of the early work is two dimensional. Although this does not directly inhibit comparisons of lateral rotation of the scapula, complications exist in comparing two dimensional projections of three dimensional movements with true three dimensional data. Many of the two dimensional studies measured the rotation of the scapula in the scapula plane, and the literature suggests that during the setting phase identified by Inman *et al.* (1944), the scapula tends to seek an optimum position of stability and then rotate laterally. It has been stated that throughout the setting phase, the scapula tends to rotate about a vertical axis to align more with the plane of arm elevation (Steindler 1962, Dvir and Berme 1978). As the data have been analysed using a rotation sequence which corresponds with this description, it is possible to compare the results of lateral rotation obtained here with the previously published work, although the out of plane rotations, particularly the forward/backward tip which is not clinically defined at all, will undoubtedly affect such comparisons.

Considering three dimensional comparisons of scapular motion, difficulties still exist. Many three dimensional studies appear to pay little attention to the kinematic definitions of three dimensional rotation, but instead simply present a number of orthogonal two dimensional projections of scapular motion (Wallace and Johnson 1982, Kondo *et al.* 1984).

Considering the studies in which Euler angles are presented, the sequence in which rotations are defined will obviously have an effect on the resulting three dimensional rotations. Equally important are the definitions of the co-ordinate systems which have been used. Considering all of these factors, the only studies which allow direct comparisons of data are those of Pronk (1991) and Johnson *et al.* (1993). Both of these use the rotation sequence adopted within this thesis. Comparison of these studies is presented in Chapter 4 (Figure 4.21), from which a good agreement may be observed. Compared to the study of Johnson *et al.* (1993), the work of Pronk (1991) used a method less similar to the one presented here, and the results are more complete. The results from this study are hence compared to those obtained by Pronk, and the differences discussed. Comparisons are also made with some of the two dimensional studies, and the findings presented in these papers discussed.

It is not possible however to compare the translational components of scapulohumeral kinematics presented within this thesis to other published work, quite simply because

no other results have been published. However, their relevance to the kinematics of the shoulder girdle mechanism are discussed.

8.2 RESULTS DURING VALIDATION

8.2.1 Evidence of a Learning Technique

The results of preliminary testing of the Locator were presented in Section 6.1. These results suggest evidence of a learning technique in the measurement of scapulohumeral kinematics using the system developed. However, from these results alone it is impossible to state whether the general reduction in the variance apparent in the data was due to the observer gaining familiarity with the apparatus or due to gaining familiarity with the anatomical landmarks of the single subject tested. Both of these would have led to a result similar to that shown in Section 6.1. However, if the reductions in variance in the data were due to the observer gaining familiarity with the anatomical landmarks of the single subject, then it is reasonable to assume that, if testing were to begin on a different subject, the degree of variance in the new data would be of a similar magnitude to that at the beginning of the preliminary studies. In this case, it may also be assumed that the variance in the data would reduce as the observer became more familiar with the surface anatomy of the new subject through repeated measurements.

To resolve this dilemma, a comparative analysis has been performed on the data from the validation studies.

In the preliminary data, a mean level of variance was calculated for each degree of freedom across five replicate measures on one subject. As thirty sets of data were collected on a single subject, this mean level of variance was calculated for each successive group of five replicate measures, and comparisons subsequently drawn.

In the validation studies, each observer collected only five sets of data from each subject. However, calculation of the variance in the data across the first set of data from each of the five subjects provides a comparable measure to that obtained in the first five sets of preliminary data. Similarly, by calculating the variance in the second, third, fourth and fifth sets of data across all subjects, the mean variance in the data can be compared to each other, and to the preliminary results.

Figure 8.1 illustrates the results of these comparisons for just one degree of freedom of scapular motion, lateral rotation. Figure 8.1(a) is a repeat of the result presented in

Section 6.1, showing the reduction of the mean variance in the data through thirty replicate measures on one subject. The results in this graph are normalised to the first mean variance component. All subsequent graphs in Figure 8.1 are normalised to the same value. Figure 8.1(b) and (c) show the results from observer 1 in the single and two channel validation studies respectively. Figure 8.1(d) and (e) show the same results for observer 2.

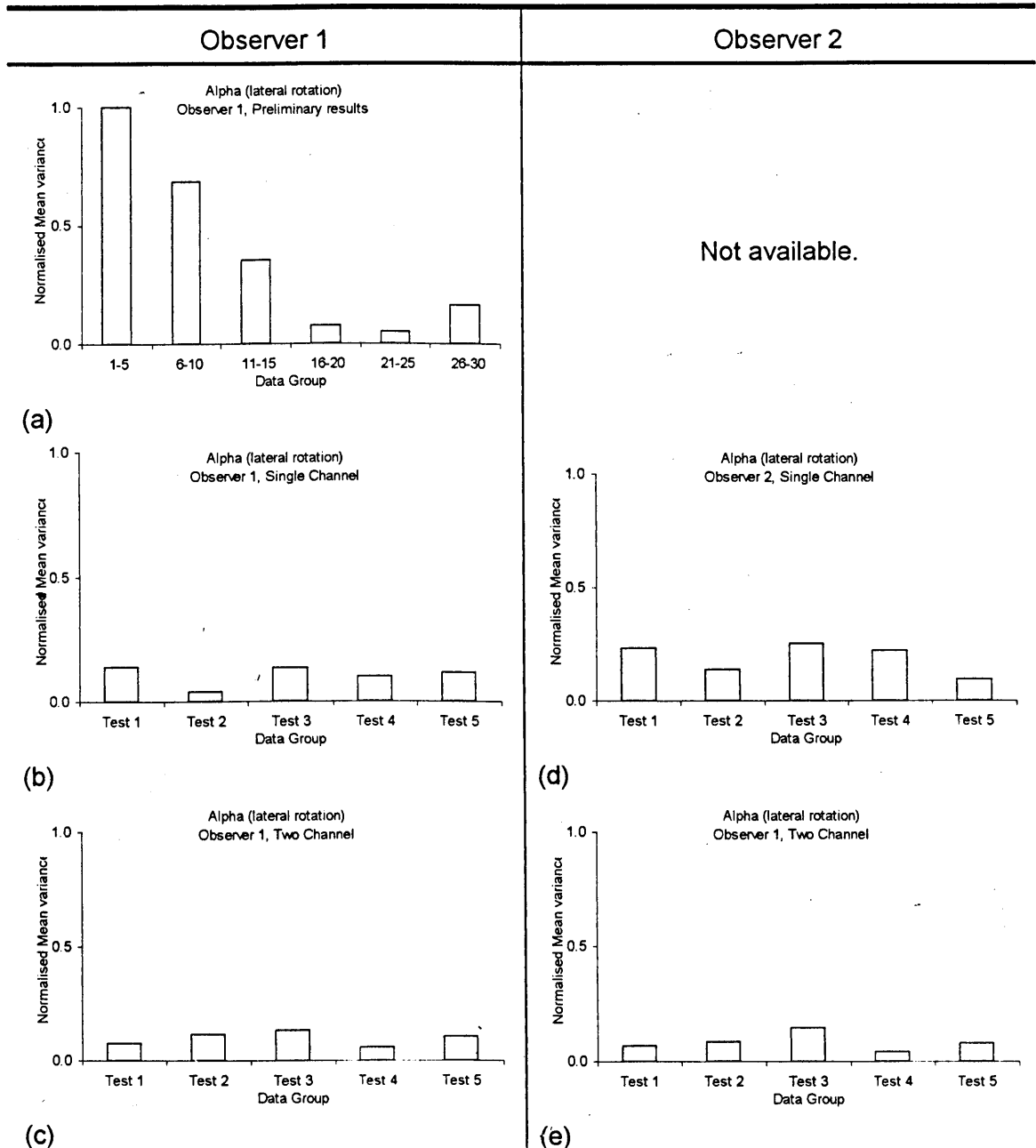


Figure 8.1: Comparisons of mean variance in the data between the preliminary results and the validation studies

The levels of variance in the data measured by observer 1 in the validation studies show no substantial difference over those obtained by the end of the preliminary

results. It can therefore be stated that the learning effects are not due to familiarity with the surface anatomy of any single subject. Nevertheless, it may still be argued that the reductions in the mean variance shown in Figure 8.1(a) are due to learning about surface anatomy rather than, or in addition to, learning how to use the apparatus. With this in mind, it is interesting to note the results of observer 2, especially in the single channel study (Figure 8.1(d)). Observer 2 had used the apparatus prior to collecting data for the single channel study, but only on a small number of occasions, and certainly did not have as much experience in using the system as observer 1. However, observer 2 was a trained orthopaedic surgeon, whereas observer 1 was an engineer. It is therefore reasonable to assume that observer 2 had, initially, a better knowledge of the surface anatomy of the shoulder than observer 1, and was hence more able to recognise anatomical landmarks, allowing more repeatable positioning of the Locator upon the scapula.

8.2.2 Validation Studies

The results from both the single and two channel system validation studies allow a thorough investigation into the inter-observer repeatability of the measurement system and the observed inter-subject variability, whilst also quantifying the measurement error inherent in the system. These parameters are best expressed in terms of the variance components for each factor together with their 95% confidence intervals, which may be compared to previous studies. Graphical comparisons are also made with work of Pronk (1991).

Degree of Freedom	Single channel	Two channel	Johnson <i>et al.</i> (1993)	Pronk (1991)
α (lateral rotation, °)	3.85	3.47	11.02	25
β (backward tip, °)	2.55	2.72	7.88	
γ (retraction, °)	3.63	3.57	6.04	
x (superior, mm)	7.01	7.45	-	-
y (lateral, mm)	4.64	6.20	-	-
z (posterior, mm)	10.08	9.08	-	-

Table 8.1: 95% confidence intervals in each measured parameter for the single and two channel studies, and comparisons with other published studies

Table 8.1 shows 95% confidence intervals for lateral rotation obtained in the validation studies to be in the region of 3-4°. For comparison, the data from Johnson *et al.*

(1993) gave a confidence interval of approximately 11° , while a similar measure from Pronk is 25° . Inman *et al.* (1944) obtained a confidence interval for lateral rotation of approximately 22° ¹. Additionally, the confidence intervals of Pronk and Inman *et al.* only account for inter-subject variation and measurement error, while the confidence intervals determined by Johnson *et al.* (1993) and in this study include both inter-subject and inter-observer variances, as well as measurement error.

It should be noted however that the confidence intervals determined here are based on five replicate measures. It is not stated in the cited texts whether or not this is the case. If only one test were considered, the confidence intervals presented would be a factor of $\sqrt{5}$ higher. Even taking this factor into account, the magnitude of the confidence intervals in this study would still only be approximately 30% of that obtained by Pronk (1991) or Inman *et al.* (1944), and significantly smaller than those of Johnson *et al.* (1993).

It is also interesting to note the similarity in the magnitude of the confidence intervals from the single and two channel studies. Considering that different subjects were measured in each of the studies, these results illustrate the repeatability of the system.

Degree of Freedom	Variance Components σ^2 or mm^2 (Proportion of Variance %)					
	Single Channel			Two Channel		
	Observer	Subject	Error	Observer	Subject	Error
α (lateral rotation)	0 (0%)	6 (6%)	3 (3%)	0 (0%)	0 (0%)	3 (3%)
β (backward tip)	0 (0%)	1 (9%)	2 (18%)	0 (0%)	1 (8%)	2 (10%)
γ (retraction)	1 (2%)	4 (16%)	2 (9%)	0 (0%)	4 (13%)	3 (8%)
x (superior)	0 (0%)	17 (7%)	9 (4%)	5 (3%)	18 (11%)	8 (5%)
y (lateral)	0 (0%)	10 (16%)	4 (6%)	0 (0%)	13 (6%)	7 (4%)
z (posterior)	4 (2%)	48 (25%)	14 (7%)	0 (0%)	29 (10%)	16 (6%)

Table 8.2: Components and proportions of variance table for the single and two channel studies

Examining the variance components for all degrees of freedom (Table 8.2), it can be seen that variations in the scapulohumeral rhythm between subjects has been observed, which is in agreement with the observations of previous authors (Doody *et*

¹ Quoted in Pronk (1991).

al. 1970b, Bagg and Forrest 1988, Hogfors *et al.* 1991). This is to be expected, as the data has not been normalised between subjects. The process of measuring the rotations and displacements relative to the initial position of the scapula normalises the initial position only, not motion subsequent to it, although it obviously has an effect in this too. Whether normalisation would eliminate these differences is difficult to say. Due to anatomical differences in both thorax shape and size, and scapula shape and size, and also in musculature of the shoulder girdle mechanism between subjects, differences in the motion of the scapula upon the thoracic cage between subjects are inevitable. However, if these anatomical differences could be scaled to a common measure, it is possible that all of the subject dependent characteristics of scapulohumeral kinematics may disappear. A suitable normalisation factor may be related to the shape and size of the thorax. For example, if the thorax were modelled as an ellipsoid, the depth to width aspect ratio of this ellipsoid will undoubtedly vary in a group of subjects, as do the retraction and protraction of the scapula during movements of the humerus. At this stage, it is not possible to state whether the variations in these properties are directly related, but there will obviously be an affect.

It is also interesting to note that the subject variances in the single channel study are larger than those in the two channel study. A simple explanation for this is that the subjects in the two channel study were all more alike than in the single channel study, but as all subjects were selected at random, this is unlikely. A more likely explanation is due to the control of the arm position allowed in the two channel study. Due to the visual feedback of arm position, all subjects elevated their arm in the same manner, with controlled degrees of azimuth and roll, creating a degree of uniformity between subjects. In the single channel study, such uniformity could not be enforced, and it is possible that each subject elevated their arm in a slightly different manner. The larger subject variation in scapulohumeral kinematics observed in the single channel study is therefore more likely to be due to larger differences in the elevation of the arm between subjects rather than larger differences in the resulting kinematics of the scapula.

In both the single and two channel studies, the inter-observer variation is low, peaking at a maximum of just over 3% of the total variation in the x displacements of the scapula, and accounting for less than 0.5% of the variance in all other degrees of freedom. This demonstrates a significant improvement over the results of Michiels and Grevenstein (1995), who found a 10% inter-observer variation in their measurements of lateral rotation of the scapula.

Considering the components of variance attributable to the measurement error, the two channel study does show an improvement over the data from the single channel study, with the error accounting for a maximum of 18% and 10% of the total variance for the one and two channel studies respectively. On average for the two channel study, the measurement error accounts for approximately 6% of the total variance in the data. As the subsequently determined confidence intervals show definite improvements over all other published data, an error component of this magnitude is acceptable.

Of all parameters measured, it is that of protraction of the scapula which demonstrates the largest confidence interval relative to the range of motion measured. However, this confidence interval is not unduly large compared with the other rotations, and the component of variance attributed to the observers of less than 1% of the total variance shows that the measures are valid.

The variations in the data between observers can be seen to be less than those arising from both subject variation and measurement error, confirming that the measurement technique is valid.

Overall, the results from the two channel study present few differences from those collected in the previous single channel study. It is acknowledged that using the fluid filled goniometer to measure arm abduction caused errors in this measurement of up to approximately 15°. These errors were mostly present at higher abduction angles (near 90°), as the subjects allowed their arms to "drop" a little while measuring the scapular position. It is expected that these errors would affect the repeatability of the experiment due to their effect on scapular position. However, the two channel study eliminates these errors, but the magnitude of the confidence intervals for all degrees of freedom are very similar.

Two possible explanations for this are as follows:

- 1 It may be assumed that at high levels of abduction, the effect of changes in arm position (of less than 20°) have very little effect on the position of the scapula.
- 2 The errors in measurement of arm abduction were almost entirely systematic errors, which each subject repeated to approximately the same extent on each test.

Observing the coefficients of the fitted data (Tables 6.1 and 6.3), it would appear unlikely that the first of these explanations is correct. It may be seen that a 20°

change in arm elevation can effect the position of the scapula by over 10° and over 15mm, both above the confidence intervals determined.

Considering the second argument, it may be expected that the extent of arm “drop” would be similar between tests, as the main factors associated with this are gravity and subject fatigue. As any one subject was tested on the same day of the week, and at a similar time of day for each test, it is unlikely that large differences in fatigue would exist. This presents the second explanation as the more likely.

This may be confirmed by graphical comparison of the data from the single and two channel studies (Figure 8.2).

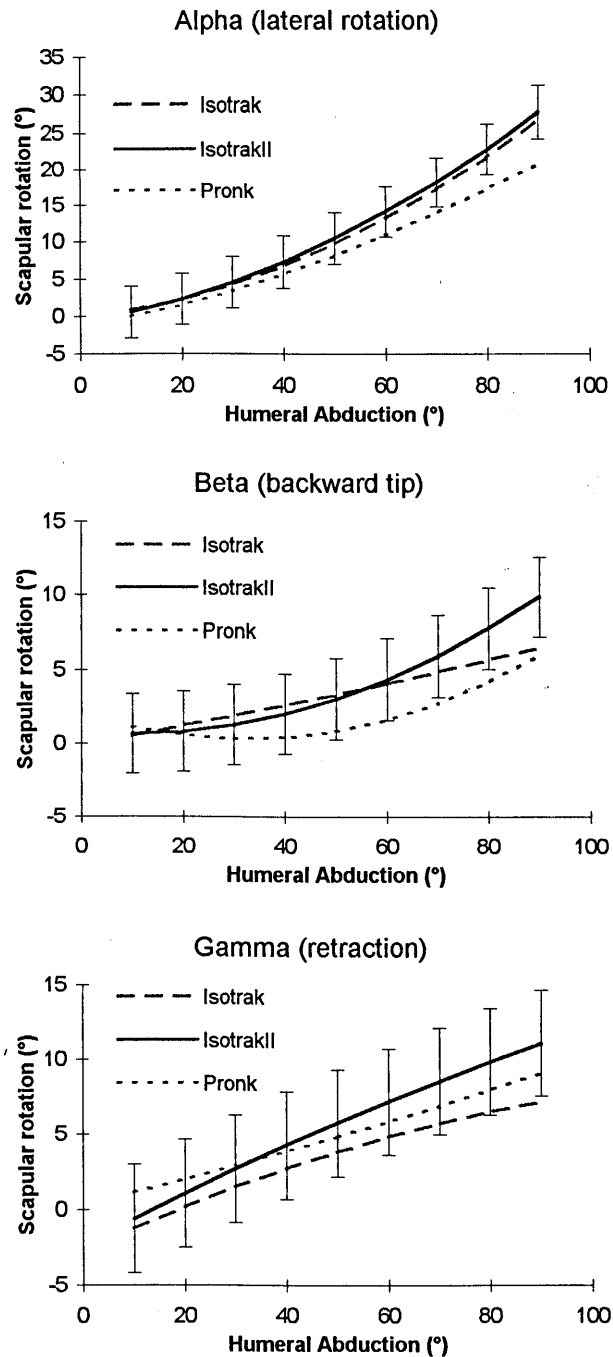


Figure 8.2: Comparisons of scapular rotations between the single channel and two channel studies, and also with the data from Pronk (1991)

If the second of the above arguments were true, then it would be expected that the rotations in the single channel would generally be lower than those of the two channel study. As can be seen from Figure 8.2, this is indeed the case.

It is also interesting to draw comparisons between the results of this work and that of Pronk (1991). Figure 8.2 shows that the rotations of the scapula measured by Pronk are also lower than those of the two channel study. A likely reason for this stems from

the different position of the origin of the recorded measurements between the studies. In Pronk's study, the motions of the scapula were measured relative to a point remote from the subject, hence upper body movements were not taken into account. In this study however, all motions were measured relative to the trunk, thereby eliminating the effects of any upper body movements.

It should also be stated that no previous study has considered or controlled the effect of humeral rotation on scapulohumeral rhythm. Although these effects are relatively small compared to the effect of humeral elevation, they can still account for up to 5° variation in the lateral rotation of the scapula, as discussed later in Section 8.3.2.

The degree of linearity present in all measured parameters is also surprising. The studies of Inman *et al.* (1944), and the subsequent work of Freedman and Munro (1966) and Poppen and Walker (1976) all found linear relationships between glenohumeral and scapulothoracic motions in abduction of the arm. However, these studies all described two or three phases of scapular motion, at which the ratio of scapula to glenohumeral rotations altered, or was not present at all. For example, Inman *et al.* (1944) identified the setting phase during the first 30° of abduction, during which little lateral rotation of the scapula occurred. A similar result was also noted by Poppen and Walker (1976). Meanwhile, Doody *et al.* (1970b) had illustrated non linear characteristics of scapulohumeral rhythm, a result strengthened by Bagg and Forrest (1988).

The results from this study illustrate a degree of non-linearity in the lateral rotation of the scapula during abduction of the arm. However, if the correlation coefficients of measured to predicted data for both linear and second order models are compared, it can be seen that the non-linear effects are indeed slight (Table 8.3).

Degree of Freedom	Regression Coefficients of Predicted to Measured Data	
	First Order Regression	Second Order Regression
α (lateral rotation, °)	0.974	0.997
β (backward tip, °)	0.918	0.987
γ (retraction, °)	0.952	0.955
x (superior, mm)	0.997	0.998
y (lateral, mm)	0.992	0.997
z (posterior, mm)	0.990	0.990

Table 8.3: Comparison of correlation coefficients (R^2) between first order and second order polynomial regression

Overall however, the second order polynomial regression lines show a marginally better correlation to the measured data. Furthermore, their use imposes less restrictions on the modelled kinematics, making them more suitable than linear regressions for modelling scapulohumeral kinematics more generally.

8.3 KINEMATIC MODEL OF THE SCAPULA

8.3.1 Introduction

The aim of this work was to produce a mathematical model capable of predicting the position and orientation of the scapula for a given arm position. Given the extreme range of motions available at the shoulder, a specific workspace had to be defined, within which the results of the model are valid. This workspace is illustrated in Figure 7.7. Previous studies concerning upper limb motions during activities of daily living were reviewed, and the workspace defined to encompass a large proportion of these activities. The scarcity of published kinematic data regarding such activities was surprising.

The data collected within this study, together with the results of the model provide, to the author's knowledge, the only database on the three dimensional kinematics of the scapula across a section of the complete humeral workspace, encompassing humeral azimuth, elevation and roll.

The model allows prediction of scapular kinematics at any humeral position within the defined workspace. Assuming the dynamic kinematics of the scapula are similar to

those in sequential static measurements, a sequence of finite humeral positions representing a specific motion or activity may be defined, and the kinematics of the scapula during this activity investigated.

Before discussing specific issues arising from the development of the model, the results presented in Section 7.6 are examined. For each degree of freedom, these results illustrate the motions of the scapula across the humeral workspace examined. Each degree of freedom of the scapula is discussed in turn.

8.3.2 α - Lateral Rotation of the Scapula

Equation 7.4 is the regression model for determining α from the humeral co-ordinates of azimuth, elevation and roll, while Figure 7.13 illustrates these results, showing the effects of azimuth and elevation on the rotation angle α of the scapula, at humeral rotations of (a) 60°, (b) 90° and (c) 180°.

It can be clearly seen that humeral azimuth has very little effect on α , showing that the rotation of the scapula about the local z axis is largely unaffected by the plane of elevation. The linearity in the relationship between humeral elevation and α , identified in the results of the validation studies can be seen to be present over the complete modelled workspace. Only Inman *et al.* (1944) and Pronk (1991) appear to have considered the motions of the scapula in any humeral motion other than elevation in the coronal plane, or in the plane of the scapula. Both of these studies measured the lateral rotation of the scapula during forward flexion (elevation in the sagittal plane, 0° azimuth), and abduction (elevation in the coronal plane, $\pm 90^\circ$ azimuth), and found little difference in the results. The only obvious difference in the rotations was in the size of the setting phase of the scapula, originally identified by Inman *et al.* (1944). This was the early period of arm elevation, during which the scapula rotated very little. During coronal plane elevation, the setting phase was evident for approximately the first 30° of elevation, compared to 45°-60° during sagittal plane elevation. Beyond the setting phase, the rotations of the scapula were very similar for both coronal and sagittal plane elevation. Indeed, Pronk (1991) stated that there were no significant differences in the lateral rotation of the scapula between the two motions.

Due to the strict control of humeral rotation adopted in this study, it was necessary to maintain the elbow flexed at 90° during all data collection. This meant that the lower levels of elevation in the coronal plane could not be tested as the trunk obstructed the forearm in such movements. It is hence not possible to state whether the setting phase identified by Inman *et al.* (1944) is present. However, the similarity in the lateral

rotation of the scapula between the two planes of elevation (that is, azimuth of 0° and -90°) is unquestionable.

Figures 7.13 (a), (b) and (c) also demonstrate the small effect of humeral rotation on α . Compared to the result with clinically neutral humeral rotation (90° roll, Figure 7.13(b)), it can be seen that internal rotation of the humerus (60° roll, Figure 7.13(a)) tends to increase the lateral rotation of the scapula throughout the range of azimuth and elevation, while external rotation has the opposite effect (180° roll, Figure 7.13(c)). This is probably caused by the twisting of the glenohumeral joint capsule and rotator cuff muscles. As the ligaments and muscles become taut, the head of the scapula is lifted or depressed, depending on the direction of the humeral rotation, introducing the offsets seen in the results.

The differences between the lateral rotation of the scapula as a result of humeral rotation amount to approximately 5° across the whole range of azimuth and elevation. This is the only study of scapulohumeral rhythm where humeral rotation has been controlled, and indeed many authors have paid little or even no attention to this parameter. However, these results suggest that many of the differences between other published studies, amounting in many cases to less than 5° , may have been a direct result of differences in the rotation of the humerus.

8.3.3 β - Backward Tip of the Scapula

Equation 7.5 is the regression model for determining β from the humeral co-ordinates of azimuth, elevation and roll, while Figure 7.14 illustrates these results, showing the effects of azimuth and elevation on the rotation angle β of the scapula, at humeral rotations of (a) 60° , (b) 90° and (c) 180° .

Unlike α , these results show that both azimuth and elevation have an obvious effect on β . It is evident that the backward tip of the scapula is greater during elevation in the sagittal plane (0° azimuth) than during elevation in the coronal plane ($\pm 90^\circ$ azimuth). The general backward tipping trend of the scapula throughout elevation is in agreement to the motions observed by Pronk (1991), and he too found that after the first 90° of elevation, the rotation of the scapula corresponding to backward tip was greater during forward flexion than during abduction.

Once again, the humeral rotation does not have a great effect on the results. However, it can be seen from Figure 7.14(a) that internal rotation of the humerus tends to tip the scapula forwards. Again, this result will be caused by the tightening of

the glenohumeral joint capsule and surrounding muscles imparting a moment on the scapula via the kinematic constraints imposed by the ligaments.

8.3.4 γ - Retraction of the Scapula

Equation 7.6 is the regression model for determining γ from the humeral co-ordinates of azimuth, elevation and roll, while Figure 7.15 illustrates these results, showing the effects of azimuth and elevation on the rotation angle γ of the scapula, at humeral rotations of (a) 60°, (b) 90° and (c) 180°.

As with β , these results show that both azimuth and elevation have an obvious effect on γ . This is the first rotation of the sequence, and previous studies have suggested that during the first 30° to 45° degrees of elevation (the setting phase), the scapula tends to seek an optimum position of stability and then rotate laterally (Inman *et al.*, 1944). It has been stated that throughout the setting phase, the scapula tends to rotate about a vertical axis to align more with the plane of arm elevation (Steindler 1962, Dvir and Berme, 1978).

This is confirmed here by examining the changes in the retraction of the scapula due to azimuth. For example, at a constant level of 40° humeral elevation and 90° humeral roll, the retraction angles of the scapula (γ) at a number of levels of azimuth are summarised in Table 8.4.

Azimuth (°)	0	30	60	90	120
γ (°)	-3.67	-0.76	2.98	7.56	12.97

Table 8.4: Retraction angles of the scapula with changing azimuth, relative to the initial scapula position

It is clearly seen that the plane of elevation does indeed have an effect on the retraction of the scapula, with greater amounts of azimuth, causing greater levels of scapula retraction.

The results of Pronk (1991) show that during abduction, the scapula retracts throughout the motion, in agreement with the findings presented here. However, his results also show that during forward flexion the scapula begins in a more retracted position, by up to 10°, and protracts up until approximately 80° of elevation, beyond which it retracts with increased elevation. This result seems contradictory to the ideas of previous authors and the results presented here. It is also surprising that the scapula would begin in a more retracted position when the arm is taken forwards.

The effect of humeral rotation on γ is again relatively small, and as with α and β , appears to be uniform over the range of azimuth and elevation. Overall, the effect of humeral rotation of 120°, from 60° roll to 180° roll increases γ by approximately 3° to 4°.

8.3.5 Displacements of the Scapula

The regression models for determining x , y , z displacements of the acromial angle of the scapula from the humeral co-ordinates of azimuth, elevation and roll are given in Equations 7.7, 7.8 and 7.9. Figures 7.16, 7.17 and 7.18 illustrate these results, showing the effects of azimuth and elevation on the x , y , z displacements of the acromial angle, at humeral rotations of (a) 60°, (b) 90° and (c) 180°.

Considering the superior x displacements, it can be seen from Figure 7.16 that the acromial angle is elevated throughout elevation of the arm, across all levels of humeral azimuth. This result suggests that the axis of rotation of the scapula is always medial of the acromial angle.

Out of all degrees of freedom of the scapula, it is the x displacements which exhibit the largest variation during humeral rotation. Internal rotation of the humerus, from 180° roll to 60° roll elevates the acromion by approximately 15mm across the range of azimuth and elevation. It is believed that this is due to the tightening of the ligaments within the glenohumeral joint capsule. As the ligaments become taut, relative motion between the humerus and scapula in the direction of humeral rotation can no longer occur. The humerus therefore attempts to rotate the scapula about an axis normal to the glenoid. However, such rotations cannot occur without elevation of the scapula due to the kinematic constraint imposed by the thoracic cage. By elevating, the scapula may rotate further, allowing further internal rotation of the humerus.

Considering the lateral y displacements, it can be seen from Figure 7.17 that the acromial angle travels medially throughout humeral elevation at all levels of azimuth. Again, relating this back to the lateral rotation of the scapula, this result is expected.

It can also be seen that increased azimuth causes the acromial angle to displace medially. This is due to the retraction of the scapula around the thoracic cage evident throughout humeral azimuth (discussed in Section 8.3.4 above).

Figure 7.18 illustrates the posterior z displacements of the acromial angle, showing the effects of azimuth and elevation at humeral rotations of (a) 60°, (b) 90° and (c) 180°. Comparing these to the retraction of the scapula across the humeral workspace,

the results are again in agreement. It can be seen that the acromial angle displaces backwards throughout humeral azimuth, due to the retraction of the scapula around the thorax. Similarly, in elevation of the humerus, retraction occurs and the acromial angle migrates posteriorly.

The effect of humeral rotation on both the y and z displacements is small. This is due to the kinematic constraints imposed on the scapula during the extremes of humeral rotation. It was discussed earlier how internal humeral rotation tends to elevate the scapula as the scapula is forced up on the wall of the thorax. However, the effect of this in terms of lateral displacements is small, as the scapula is still restrained in the y direction by the force through the glenohumeral joint in one direction, and the forces developed by muscles between the scapula and the thorax (predominately serratus anterior), together with the kinematic constraint of the clavicle in the other direction. Their combined effect is to maintain equilibrium in the y direction, hence the small changes in the lateral displacements.

Similarly, due to the shape of the thorax and the constraints of the scapula within the scapulothoracic gliding plane, elevation of the scapula by up to 30mm has little effect on the posterior displacements of the acromial angle.

It was stated in Chapter 2 that the scapula possesses five rather than six degrees of freedom, as the clavicle imposes a kinematic constraint. However, due to the unknown nature of this constraint, it was necessary to measure all six degrees of freedom of the kinematics of the scapula. Considering this kinematic constraint further, it may be stated that for all positions and orientations of the scapula, the distance between the acromioclavicular joint and the sternoclavicular joint will be constant, and equal to the length of the clavicle. The x , y , z displacements of the acromial angle relative to the Isotrak[®] receiver on the sternum were measured and modelled within this study. By assuming a fixed distance between the electrical centre of the Isotrak[®] receiver and the sternoclavicular joint, the x , y , z displacements of the acromial angle have been determined relative to the sternoclavicular joint across the modelled workspace. Figure 8.3 illustrates this, showing the x , y , z displacements of the acromial angle across the modelled workspace. It can be seen that the distances from the origin to each measured point are approximately equal.

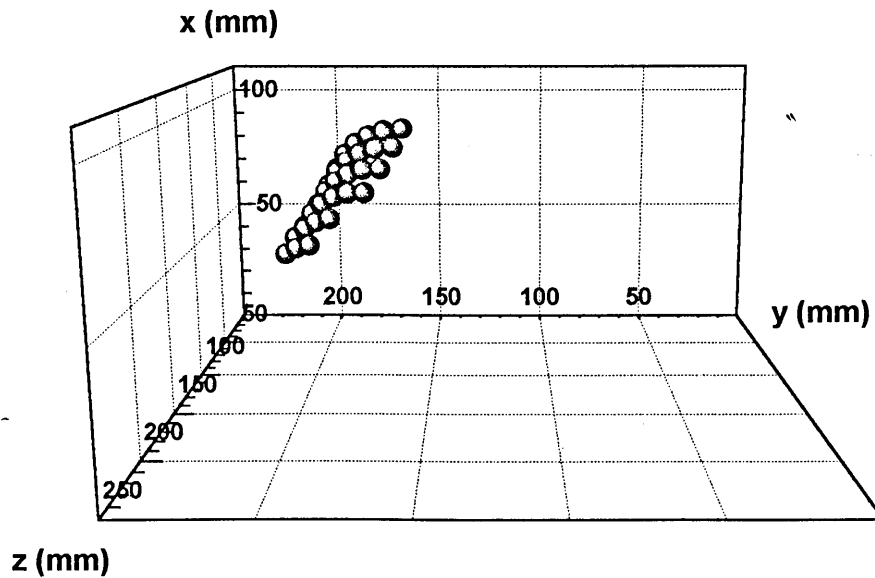


Figure 8.3: x , y , z co-ordinates of the acromial angle across the modelled workspace

Subsequently, the magnitudes of these vectors were calculated, and exhibited a standard deviation of just 3mm. Although the acromial angle is some distance from the acromioclavicular joint, the effect of the kinematic constraint of the clavicle is clearly demonstrated.

8.3.6 Prediction Intervals of the Model

In the development of the model, data was collected from ten subjects. To collect a representative set of data across the defined humeral workspace, twenty individual “tasks” were defined which each subject had to perform. Due to the time demands which this imposed on the subjects, no replicate measures were taken. As a consequence, the level of confidence in the model is much lower than in the validation studies. However, while bearing in mind that the two properties are different, it is interesting to compare the prediction intervals from the model with the confidence intervals obtained in the validation study (Table 8.5).

Degree of Freedom	Model	$\frac{\text{Model}}{\sqrt{5}}$	Two channel validation
α (lateral rotation, °)	6.05	2.71	3.47
β (backward tip, °)	5.60	2.50	2.72
γ (retraction, °)	10.25	4.58	3.57
x (superior, mm)	17.11	7.65	7.45
y (lateral, mm)	9.47	4.24	6.20
z (posterior, mm)	26.72	11.95	9.08

Table 8.5: Comparison of 95% prediction intervals of the model and 95% confidence intervals of the validation studies

It is obvious that the prediction intervals from the model will be larger than those from the validation studies, as replicate measures were not obtained. However, obtaining n replicate measures reduces the size of the confidence intervals by a factor of $1/\sqrt{n}$. If this factor is applied to the prediction intervals of the model, they become very similar in magnitude to those obtained in the validation studies (Table 8.5).

These results further demonstrate the repeatability of the measurement system, and suggests that if replicate measures had been obtained, the magnitude of the resulting confidence intervals would be much closer to those obtained in the validation study. They also suggest that the confidence intervals obtained in the validation studies are approximately valid over the complete humeral workspace, and not only over the single defined task of elevation in the coronal plane.

Furthermore, it may be argued that the primary factor contributing to the prediction intervals of the model is not subject variation, but measurement error, which was greatly reduced in the validation studies by obtaining replicate measures. Examination of the correlation coefficients of the regression models confirms this. For example, in the two channel validation study, the second order polynomial regression lines show a good correlation to the means of the measured data, with R^2 values of no less than 0.955, and generally greater than 0.99. The multivariate polynomial regressions determined in the development of the model show R^2 values between approximately 0.6 and 0.7, suggesting a poorer fit to the measured data. However, the error component in this data had not been reduced by determining the mean values from a number of replicate measures, as such measures were not available without further data collection. If higher order polynomials were fitted to the model data, then the

values of R^2 would undoubtedly be higher. However, as discussed in Chapter 5, the resulting polynomials would not necessarily provide a better estimation of the underlying relationships, as the polynomials may represent the „measured signal including the error component, rather than with the error component removed.

The suitability of using second order polynomials to model scapulohumeral rhythm was demonstrated in the validation studies. Also, as demonstrated in Chapter 7, the differences in predicted data resulting from second or third order regression models are insignificant.

However, it must still be stated that differences exist in scapulohumeral kinematics between subjects. Replicate measures would only serve to reduce the confidence intervals by reducing the error component in the data, allowing the inter-subject variations to be quantified, as demonstrated by the components of variance obtained from the validation studies.

8.3.7 Choice of Co-ordinate System

In Chapter 5, the co-ordinate systems used in the calculation and presentation of results throughout this thesis were defined. In general, these consisted of a global co-ordinate system for the trunk, and a local co-ordinate system for the scapula.

- However, it was also stated that the results were determined in the global frame. This co-ordinate system is shown in Figure 5.16, and the rotation sequence is α about z , β about y' then γ about x'' . All rotations obey the right hand rule.

It would be expected that, due to anthropometric differences between subjects, the prediction intervals from the global model would be larger than that from the local model. However, as shown in Table 8.6, this is not necessarily the case.

Degree of Freedom	Model Local Co-ordinate System	Model Global Co-ordinate System
α (lateral rotation, °)	6.05	9.23
β (backward tip, °)	5.60	7.26
γ (retraction, °)	10.25	5.03
x (superior, mm)	17.11	42.42
y (lateral, mm)	9.47	17.45
z (posterior, mm)	26.72	25.76

Table 8.6: Comparison of 95% prediction intervals between the model based on a local co-ordinate system and that based on a global co-ordinate system

Although the prediction intervals for α and β are larger in the global model, as expected, the prediction interval for γ is smaller, although this is probably due to the differences in the rotation sequences of the two analyses rather than the effect of considering the data in terms of a global co-ordinate system¹.

Of more interest are the prediction intervals for the displacements of the acromial angle. Considering x, representing vertical displacements, it can be seen that adopting the global model more than doubles the size of the resulting prediction interval (increase of 148%). Similarly, the prediction interval for y increases by over 80% of that determined in the local model, while the prediction interval of z remained almost unchanged.

However, these results are not too surprising, and indeed confirm the reasoning behind the use of the local co-ordinate system. Considering anthropometric differences between a group of subjects, the largest absolute difference between them is likely to be in height, hence the large variations in x. The second largest difference between the subjects is probably their breadth, hence the large y variations, while the depth of the thorax show smaller absolute differences relative to height and breadth, hence the smaller variations in z.

The choice of defining local a co-ordinate system for determining the rotations of the scapula, and zeroing the displacements to the initial position of the scapula may therefore be stated to be a wise one.

¹The results of the global model in terms of the regression coefficients for each subject and the model may be found in Appendix 4.

8.4 MEASURING MOTIONS OF THE SCAPULA

8.4.1 Introduction

In Chapter 5, a set of criteria for the development of a scapulohumeral measurement technique were defined. In summary, these stated that the system should be:

- non-invasive
- capable of measuring the complete three dimensional kinematics of the scapula
- capable of measuring the position of the scapula across a wide range of humeral positions, and not just elevation in the coronal or sagittal planes
- portable to allow its use in clinics and not just within the research laboratory
- relatively simple and quick to use, for the benefit of both subjects and observers

Additionally, any new measurement system must be validated to determine the inherent measurement error (intra-observer) and to investigate the inter-observer repeatability.

It was further discussed that none of the measurement systems presented in Chapter 4 fulfilled all of these criteria, and some were not covered by any of the published techniques.

It is important to consider the criteria listed above with reference to both this work and previously published techniques.

8.4.2 Inadequacies of Previous Measurement Techniques

The first of these criteria is that the measurement system should be non-invasive. This obviously rules out all radiographic techniques, whether of a two dimensional nature (Flecker 1929, Lockhart 1930, Inman *et al.* 1944, Fisk 1944, Jones 1956, Freedman and Munro 1966, Poppen and Walker 1976, Dvir and Berme 1978, Eto 1991, Michiels and Grevenstein 1995) or three dimensional (Wallace and Johnson 1987, Kondo *et al.* 1984, Hogfors *et al.* 1991). Similarly, studies involving the measurement of pins inserted directly into bones must be discounted (Inman *et al.* 1944, Sidles *et al.* 1991).

Considering the non-invasive techniques presented in Chapter 4, many of these measurement systems fail to meet the other criteria. The scapulohumeral goniometer developed by Doody *et al.* (1970a) only measures planar scapular rotation, as did the electrogoniometric method developed by Ito (1980) and the stereo-photogrammetric methods of Bagg and Forrest (1988).

Despite measuring the three dimensional rotations of the scapula, the work of Pronk (1991) unfortunately falls short of detailing the translational components of scapulohumeral kinematics. Also, due to the necessity of a frame in which subjects must be fixed, the system is not easily portable, and the data collection was time consuming, which would undoubtedly lead to subject fatigue. Further to this, as all motions were measured from a point remote from the subject, it is possible that upper body movements may have been ignored, undoubtedly affecting the data. This issue is discussed further discussed in Section 8.2.2.

Stereo-photogrammetry techniques were used by Laumann (1982, 1987), and Runciman (1993). Although no results are presented in the work by Runciman, the work of Laumann was one of the first to clearly illustrate the three dimensional nature of scapulohumeral rhythm. However, there appears to be no validation of the technique, which, due to the degree of scapular motion beneath the skin, may be subject to considerable measurement errors. As measurements were taken on 40 individual subjects, calculation of the mean values of the results will undoubtedly reduce any random error components, but it does not quantify the inter-subject variations or the expected measurement errors inherent in the system.

One of the advantages of employing stereo-photogrammetry techniques is that they could accurately measure both the position of the scapula and humerus in three dimensional space and indeed, this benefit appears to have been exploited by Runciman. It is unfortunate however that the work of Laumann considered only motions of the arm in the coronal and sagittal planes.

The only other non-invasive techniques for measurement of scapulohumeral motions presented in the literature are those of Moriwaka (1992), Johnson *et al.* (1993) and McQuade *et al.* (1995). The results from the "hand held" Isotrak[®] technique developed by Moriwaka suggest that the out of plane rotations of the scapula were not detected using this method. As the measurements relied on an observer grasping the scapula, which must have restrained scapula movement, this result is not too surprising.

The technique adopted by McQuade *et al.* (1995) shows remarkable similarities to that of Pronk (1991), although the authors appear ignorant of this and other techniques used for measuring three dimensional scapulohumeral rhythm, with the exception of the study by Hogfors *et al.* in 1991 (Johnson and Barnett, 1996). Considering the degree of similarity with other work, the results show surprising anomalies, with rotations of the scapula about a vertical axis of over 100°. As such rotations are surely anatomically impossible, this study highlights the necessity of not only developing a suitable measurement technique, but ensuring that all data analysis techniques are accurate also.

The study undertaken by Johnson *et al.* (1993), although not providing many results, is one of the only published studies on the measurement of scapulohumeral rhythm which addresses the issue of inter-observer repeatability. However, as with nearly all other published techniques, only the rotational components of scapulohumeral kinematics were observed, and the system was not able to measure the position of the humerus during data collection. Nevertheless, due to its potential for development, together with its portability and relative ease of use, it did serve as a basis for the technique developed here.

8.4.3 Validation of Measurement Systems

Referring back to the list of criteria for the development of a suitable measurement technique (detailed in Section 8.4.1), it is the last which is the most important, and which, interestingly has been investigated the least. Any system may be claimed to be capable of easily and effectively measuring scapular motion, but without suitable validation, such claims are unfounded. For example, if only one measurement of scapulohumeral rhythm is taken from each of a group of subjects using a technique not previously assessed, it is not possible to investigate the inter-subject variations. Any variations in the resulting data may be due to a number of sources; inter-subject variation, intra-subject variation, intra-observer variation or measurement error. A number of authors (Doody *et al.* 1970b, Bagg and Forrest 1988, Hogfors *et al.* 1991) claim to have shown large inter-subject variations in scapulohumeral rhythm, but none of these studies performed replicate measures on each subject. Similarly, Poppen and Walker's (1976) comparisons of normal and abnormal shoulder motion shows no regard for replicate measures from either group of subjects, yet claim differences exist in motion patterns between the group of 12 normal subjects and each of the 15 pathological cases.

The results within this thesis suggest that such claims are ambitious, as they assume great faith in the accuracy of the measurement system employed. Similarly, without knowledge of inter-observer effects, the system has little potential as a clinical tool for diagnostic purposes, as the results may differ depending on who performs the measurements. Furthermore, based on the confidence intervals determined in the scapulohumeral kinematics model, the variation in scapulohumeral rhythm between the normal and abnormal subjects identified by Poppen and Walker (1976) may simply be due to normal inter-subject variation and/or measurement error, and not due to pathological differences between subjects.

Even if replicate measures on a single subject are performed, separating all of the aforementioned sources of error is difficult. However, if it is assumed that intra-subject variations are insignificant, and intra-observer variations are an element of the measurement error, then replicate measures do allow inter-subject variations to be investigated, as in the validation studies presented in Chapter 6. Similarly, inter-observer variations have been assessed by analysing the results collected by different observers performing replicate measures on the same subjects.

Of all of the studies discussed in Chapter 4, only a few have undertaken any form of statistical investigation into the repeatability of their measurement systems, yet, as stated above, many have noted significant differences in scapulohumeral rhythm between subjects.

Only three previous studies have performed replicate measures on the same subjects. Doody *et al.* (1970a) performed four replicate measures on a group of 22 subjects. They found no significant differences on these replicate (intra-subject) measures at the $p=0.05$ level. However, they also claimed that significant inter-subject variances were observed, although the level of significance for this test was $p=0.01$. It is not stated whether the inter-subject differences were significant at the level $p=0.05$, the same level used investigating the intra-subject variation. However the findings of Youdas *et al.* (1994) question the validity of these results.

Ito (1980) performed upwards of ten replicate measures on a group of fifteen subjects, while Johnson *et al.* (1993) measured a group of fifteen subjects five times. Neither of these studies present results suggesting a subject dependent nature of scapulohumeral rhythm.

The work of Johnson *et al.* (1993) also investigated inter-observer variation, and concluded that the method was “highly repeatable in the hands of one observer”, but that differences between observers could be observed from the data.

The only other study in which observer variance was investigated was that performed by Michiels and Grevenstein (1995). The radiographic images of five abduction movements, chosen at random, were evaluated by five investigators. The results showed that up to 10% of the variance in the data could be attributed to investigators. An inter-observer variance of this size could account for the majority of differences in the data between the early two dimensional radiographic studies of Flecker 1928, Inman *et al.* 1944, Jones 1956, Freedman and Munro 1966 and Poppen and Walker 1976. The results obtained within this thesis show observer variation in lateral rotation to be considerably less than the results of Michiels and Grevenstein (1995), accounting for less than 0.5% of the total variation in the data.

It may be stated therefore that in the development of a new measurement system, whatever its application, the design of a suitable validation procedure is essential. In the measurement of scapulohumeral kinematics, there are no wholly accurate measurements with which the results can be compared, hence the accuracy or precision of the measurement system can only be judged by its repeatability, and hence the magnitude of the confidence intervals.

Furthermore, it is vital to perform validation procedures in realistic circumstances. For example to validate a technique for measuring scapulohumeral rhythm, the data for validation must be from measurements of scapulohumeral rhythm taken with the system in question. Measuring the accuracy of the measurement system on known, constructed objects, as in the case of Kondo *et al.* (1984) and McQuade *et al.* (1995) is not enough, as this does not reveal the error in measurements of scapulohumeral rhythm, only the error in the measurement of constructed objects.

8.4.4 Issues Concerning the Measurement Technique

It is important to note that the Locator provides a non-invasive method of identifying the position and orientation of the scapula and representing this position and orientation as a rigid structure external to the body. The fact that Isotrak[®] systems are used to measure the position of the Locator is of secondary importance, as this position may be measured by a variety of means, including photogrammetry. However, the Isotrak[®] system appears most suitable due to its ease of use and portability and accuracy. Also, as the technique requires an observer in close

proximity to the subject (to support the Locator during measurements), the use of cameras to record the kinematics of the Locator would be hindered due to obscured views incurring occlusion effects.

It must also be stated that the technique is a static (or quasi-static) rather than a dynamic technique. It is not possible to secure an external device to the scapula due to its relatively large movements under the skin. However, it was not initially assumed that the positions of the scapula measured at a number of static positions throughout a range of humeral motion automatically yield the same results as would be obtained during dynamic scapulohumeral kinematics. The inertia effect of the upper limb is not taken into account, nor any muscular dynamics effects, and it has been argued that, in static techniques, a possibility exists of the scapula "setting" into an "unnatural" posture (Michiels and Grevenstein, 1995). Precisely how the scapula could adopt an unnatural posture as a result of a natural humeral position is not stated. It is believed that the authors were referring to the possibility of an alternative scapular position in static rather than dynamic humeral motions.

Whether the kinematics of the scapula are the same in sequential static humeral positions as oppose to an equivalent dynamic humeral motion is, at this stage, impossible to say. A number of studies in the literature have investigated scapulohumeral rhythm in a dynamic situation including that mentioned above (Michiels and Grevenstein, 1995). As this study, using radiographic techniques, does not compare static to dynamic arm movements, it unfortunately falls short of answering the question. However, the authors did investigate the differences in lateral rotation of the scapula between abduction at a "high speed" and abduction at a "low speed". By fitting linear regression lines to their data, they found a statistically significant difference between the slope of the high speed and low speed series (slope of 0.654 and 0.670 respectively). However, the authors discounted these differences as of no physical significance.

By linear modelling of the data within this thesis, the regression coefficients may be compared to those above to investigate the differences in the rotation of the scapula during dynamic and sequential static arm movements (Table 8.7).

Linear regression coefficients for lateral rotation of the scapula				
Michiels and Grevenstein, 1995		This Study		
Low Speed	High Speed	Single Channel	Two Channel ¹	Model
0.670	0.654	0.676	0.661	0.682

Table 8.7: Gradients of linear regression lines fitted to the data¹; comparisons between this study and that of Michiels and Grevenstein, 1995

It can be seen that the differences between these results are negligible.

Other investigations of scapulohumeral rhythm during dynamic motions of the arm have shown similar results to that obtained in sequential static arm positions (Hogfors *et al.*, 1991).

8.5 AN APPLICATION OF THE MODEL

A model of three dimensional scapulohumeral kinematics has a number of applications, including the investigation of normal shoulder motion, the investigation of pathological shoulder motion and many uses as a diagnostic tool.

With regard to the first of these, the following graphs provide an illustration of the application of the model. These results show the three dimensional kinematics of the scapula during an upper limb feeding activity, using humeral co-ordinate data measured by Romilly *et al.* (1994). Figure 8.4 illustrates the three rotations of the scapula in comparison to the humeral co-ordinates, while Figure 8.5 presents the displacements of the acromial angle during the motion.

¹ These regression lines represent the scapulohumeral angle relative to humeral elevation rather than the absolute rotation of the scapula.

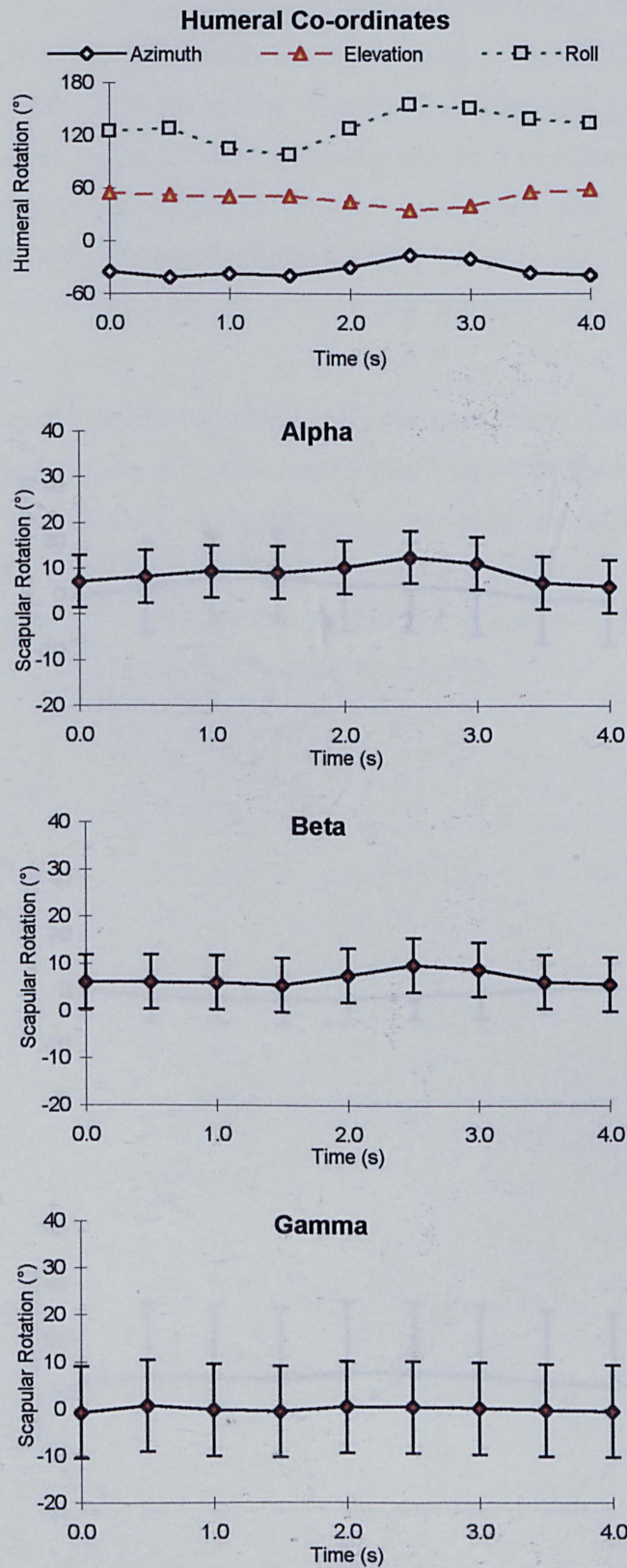


Figure 8.4: α , β , γ rotations of the scapula during an upper arm feeding activity measured by Romilly et al. (1994)

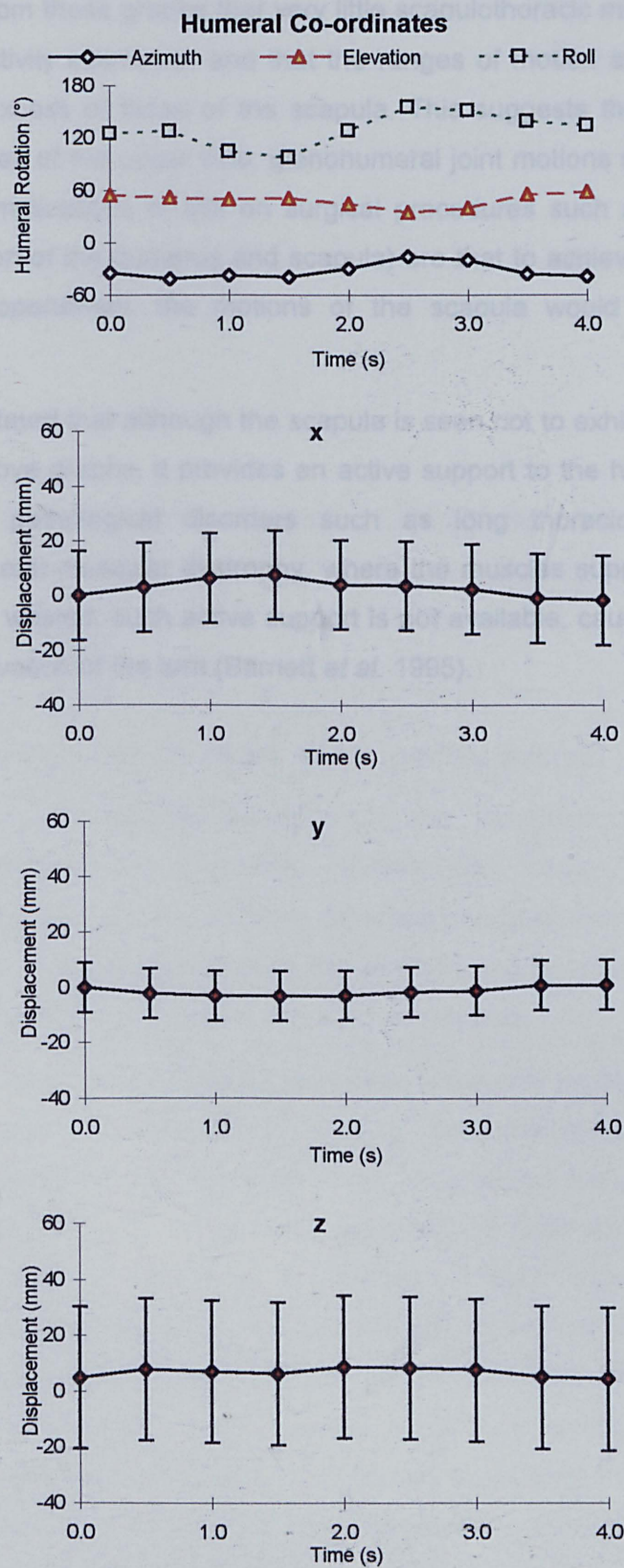


Figure 8.5: x, y, z displacements of the acromial angle during an upper arm feeding activity measured by Romilly et al. (1994)

It can be seen from these graphs that very little scapulothoracic motion occurs during the functional activity examined, and that the ranges of motion at the glenohumeral joint are far in excess of those of the scapula. This suggests therefore that during functional activities of the upper limb, glenohumeral joint motions are by far the most important. The implications of this on surgical procedures such as a glenohumeral arthrodesis (fusion of the humerus and scapula) are that to achieve a "normal" range of motion post-operatively, the motions of the scapula would have to increase dramatically.

It must also be stated that although the scapula is seen not to exhibit a large range of motion in the above graphs, it provides an active support to the humerus throughout the activity. In pathological disorders such as long thoracic nerve palsy, or facioscapulohumeral muscular dystrophy, where the muscles supporting the scapula are paralysed or wasted, such active support is not available, causing the scapula to "wing" during elevation of the arm (Barnett *et al.* 1995).

Chapter 9

Conclusions and Recommendations for Future Work

9.1 CONCLUSIONS

9.1.1 Design and Validation of the Measurement System

This thesis has presented the development and validation of a technique for measuring scapulohumeral kinematics. Furthermore, using this measurement technique, a mathematical model of three dimensional scapulohumeral kinematics has been determined, capable of predicting the position and orientation of the scapula from a given humeral position across a defined workspace.

The two channel measurement system presented is the only technique which fulfils all of the criteria stated in Chapter 5. It is a non-invasive method capable of simultaneously measuring the complete three dimensional kinematics of both the scapula and humerus in any arm position, providing the hand does not interfere with positioning the Locator (for example, in [unlikely] activities involving placing a hand over the shoulder being measured). It is also suitably portable to allow use in a clinical setting, and indeed, is currently being employed in two separate clinical studies within Newcastle upon Tyne and North Tyneside (UK); one investigating changes in scapulohumeral kinematics with age in a normal population, with a focus on the effects of rheumatoid arthritis, and the other observing the posture and function of the shoulder girdle mechanism following hemiplegia.

Furthermore, by the design of suitable experiments, the system has been shown to be observer independent, and capable of measuring the kinematics of the scapula with a greater precision than any other published technique. The 95% confidence intervals

for lateral rotation of the scapula during humeral elevation in the coronal plane is just 3.5° , based on five replicate measurements, with a modelled prediction interval of 6.1° based on just one measurement, compared with equivalent confidence intervals of 22° and 25° from Inman *et al.* (1944) and Pronk (1991) respectively.

Considering the quasi static nature of the measurement technique, it is concluded that the lateral rotations of the scapula during sequential static arm movements are not significantly different from those observed by other investigators during dynamic motions of the arm. It may be assumed that this relationship is also true for all other degrees of freedom of scapular kinematics.

It has also been demonstrated that a learning technique exists to develop the skills necessary to repeatably locate the relevant anatomical landmark of the scapula.

9.1.2 Results

A model of three dimensional scapulohumeral kinematics has been developed, and shown to be valid for a number of defined tasks, based on the data collected from a subject not used in the development of the model. Similarly, the predicted data from the model compares well with the results of the validation studies, and in general the rotations of the scapula also compare favourably with the results of Pronk (1991).

Hence, it may also be concluded that the statistical techniques and procedures adopted throughout the modelling process were suitable for such a problem.

Considering the general kinematics of the scapula, the following conclusions may be drawn:

- 1 At all levels of humeral azimuth, elevation of the arm causes the scapula to rotate laterally, retract and tip backwards. As a result of these motions, the posterior acromial angle is displaced superiorly, medially and posteriorly through humeral elevation.
- 2 Azimuth of the humerus has no noticeable effect on the lateral rotation of the scapula, although it causes the scapula to retract, and to tip backwards slightly. Hence, the acromial angle of the scapula displaces medially and posteriorly during humeral azimuth.
- 3 Rotation of the humerus has little effect on the kinematics of the scapula. However, when approaching maximal internal rotation, the effect of tightening of the ligaments around the glenohumeral joint

imposes a kinematic constraint on the scapula, which results in elevation of the scapula upon the thoracic cage.

- 4 The clavicle acts as a kinematic constraint to the scapula, limiting the motion of the acromioclavicular joint to the surface of a sphere with a radius equal to the length of the clavicle.

Considering the issue of inter-subject variations in scapulohumeral kinematics, these have been shown to exist. However, the methods used by previous authors to determine such differences have been shown to be wholly inappropriate as, in general, no replicate measurements were obtained from individual subjects.

9.1.3 General Issues

In the development of a new measurement system, whatever its application, the importance, and necessity of designing a suitable validation procedure is essential. Without such a process, the implications and relevance of any results are questionable.

A new method for presenting the position of the humerus has been presented. Workspace maps provide a precise method of specifying humeral azimuth, elevation and roll, and being a two dimensional projection, allow such definitions to be easily presented as a planar representation.

In the analysis of scapulohumeral kinematics, the choice of co-ordinate system has been demonstrated to be an important factor, especially when considering the translational components of scapular motion.

Data analysis software has been developed as an intuitive Windows™ application, WinMat, capable of analysing data from single channel Isotrak® systems, two channel Isotrak®II systems and three and four channel Fastrak® systems. The application allows a number of orientation formats to be specified at run time, providing a useful tool for analysis of any form of kinematic data.

9.2 RECOMMENDATIONS FOR FURTHER WORK

“The outcome of any serious research can only be to make two questions grow where before grew only one.” (Veblen, 1919).

Indeed, it is a common belief that good research generates more questions than answers. As such, the list of recommendations for future work could be as long as the

thesis before it. However, this section seeks to isolate a few key areas in which it is believed future efforts should be concentrated.

9.2.1 Replicate Data Collection

Within the validation studies, five replicate measures were obtained by each observer, from each subject. Due to the increased size of the workspace, and the associated demands on subjects, no replicate measures were obtained for the data collected in the development of the scapulohumeral kinematics model. As a direct consequence of this, the resulting confidence intervals were larger in the model than in the validation studies, and inter-subject variability across all of the defined humeral workspace could not be investigated.

In order to develop an understanding of pathological effects on scapulohumeral kinematics, it is vital to be aware of typical inter-subject variation. For example, it may be hypothesised that patients with a record of recurrent dislocation of the shoulder display an unusually large range of scapular retraction in the classic dislocation position (maximal external rotation at around 90° abduction). However, without fully investigating these motions in normal subjects, such hypothesis cannot be investigated.

It is suggested therefore that further data should be collected to investigate these issues, thereby providing further validation of the model presented here and developing a comprehensive database on normal scapulohumeral kinematics.

9.2.2 Increased Humeral Workspace

In the development of the scapulohumeral kinematics model, a specific humeral workspace was defined, based on the data from previous studies investigating functional activities of the upper limb. It is acknowledged that this only represents a subset of the complete humeral workspace, which should also be investigated.

Beyond this, the effects on scapulohumeral kinematics of removing the constraint from the elbow will allow more dextrous activities to be investigated

9.2.3 Humeral Kinematics and Model Development

Throughout this study, the kinematics of the humerus have been assumed to consist of three rotational degrees of freedom, namely azimuth, elevation and roll. However, in reality, the range of motion available at the glenohumeral joint also allow the humerus translational degrees of freedom, which have not been considered within this

work. At the periphery of the dextrous workspace, the importance of these translational degrees of freedom may become increasingly important, as the final extent of reach is facilitated almost entirely by translation of the glenohumeral joint, through movements of the shoulder girdle mechanism. It is suggested therefore that such motions should be investigated and accounted for within the model.

The effects of carrying or restraining external loads should also be investigated.

It is also foreseen that the model may be developed to include both passive and active soft tissues, examining the kinematic effects of each, together with prediction of internal joint forces in both static and dynamic activities.

9.2.4 Other Recommendations

It has been demonstrated that scapulohumeral kinematics are subject dependent. However, as every subject is anthropometrically different, this is unsurprising. It is not known whether the differences in scapulohumeral kinematics can be normalised. By initially investigating the effects of thoracic size and shape on scapulohumeral kinematics, it may be possible to assess whether such normalisation procedures would be possible.

The geometry of the thoracic cage will also be affected due to respiration. Although these effects are likely to be small, their contribution should be investigated.

9.2.5 Concluding Statement

A model for predicting the position and orientation of the scapula for a given arm position has been developed, and can be used to analyse the three dimensional kinematics of the scapula during functional activities of the upper limb. Analysis of scapular motion in this manner was hitherto impossible. As a result of the model developed within this thesis, such investigations are now relatively simple.

References

- Allander, E., Bjornsson, O.J., Olafsson, O., Sigfusson, N. and Thorsteinsson, J. (1974) Normal Range of Joint Movements in Shoulder, Hip, Wrist and Thumb with Special Reference to Side : A Comparison between Two Populations. *Int. Journ. of Epidem.* **3**(3), 253-261.
- An, K.N., Browne, A.O., Korinek, S., Tanaka, S. and Morrey, B.F. (1991) Three Dimensional Kinematics of Glenohumeral Elevation. *Journal of Orthopaedic Research* **1991**, 143-149.
- An, K.N., Jacobsen, M.C., Berglund, L.J. and Chao, E.Y.S. (1988) Technical Note - Application of a Magnetic Tracking Device to Kinesiologic Studies. *J. Biomechanics* **21**, 613-620.
- Bagg, S.D. and Forrest, W.J. (1988) A Biomechanical Analysis of Scapular Rotation during Arm Abduction in the Scapular Plane. *American Journal of Physical Medicine and Rehabilitation* **67**, 238-245.
- Barker, T.M., Nicol, A.C., Kelly, I.G. and Paul, J.P. (1996) Three-dimensional joint co-ordination strategies of the upper limb during functional activities. *Journal of Engineering in Medicine, Proc. IMechE, Part H* **210**, 17-26.
- Barnett, N.D., Mander, M., Peacock, J.C., Bushby, K., Gadner-Medwin, D. and Johnson, G.R. (1995) Winging of the Scapula: The Underlying Biomechanics and an Orthotic Solution. *Journal of Engineering in Medicine, Proc. IMechE, Part H* **209**, 215-223.
- Benati, M., Gaglio, S., Morasso, P., Tagliasco, V. and Zaccaria, R. (1980) Anthropomorphic Robots. 1. Representing Mechanical Complexity. *Biological Cybernetics* **38**, 125-140.
- Bisshopp, K.E. (1969) Rodrigues' Formula and the Screw Matrix. *Journal of Engineering for Industry. Transactions of the ASME*, 179-185.
- Boone, D.C. and Azen, S.P. (1979) Normal Range of Motion of Joints in Male Subjects. *J. Bone Jt. Surg.* **61-A**(5), 756-759.
- Braune, W. and Fischer, O. (1987) *The Human Gait*, Berlin: Springer.
- Browne, A.O., Hoffmeyer, P., Tanaka, S., An, K.N. and Morrey, B.F. (1990) Glenohumeral Elevation Studied in Three Dimensions. *J. Bone Jt. Surg.* **72-B**(5), 843-845.
- Buckley, M.A., Yardley, A., Johnson, G.R. and Carus, D.A. (1996) Dynamics of the Upper Limb During Performance of the Tasks of Everyday Living - A Review of the

- Current Knowledge Base. *Journal of Engineering in Medicine, Proc. IMechE, Part H* (In Press)
- Cappozzo, A. (1984) Gait Analysis Methodology. *Human Movement Science* **3**, 27-50.
- Cathcart, C.W. (1884) Movements of the Shoulder Girdle Involved in Those of the Arm on the Trunk. *Journal of Anatomy and Physiology* **18**, 210-218.
- Chao, E.Y.S. (1980) Justification of Triaxial Goniometer for the Measurement of Joint Rotation. *J. Biomechanics* **13**, 989-1006.
- Cleland, J. (1881) Shoulder Girdle and its Movements. *The Lancet* **7**, 283-284.
- Codman, E.A. (1934) *The Shoulder. Rupture of the Supraspinatus Tendon and other Lesions in or about the Subacromial Bursa*, Boston: Thomas Todd Company]
- Craig, J.J. (1989) *Introduction to Robotics: Mechanics and Control*, 2nd edn. Massachusetts: Addison Wesley Publishing Company.
- Culham, E. and Peat, M. (1993) Spinal and Shoulder Complex Posture. I: Measurement using the 3Space Isotrak. *Clin. Rehab.* **7**, 309-318.
- Culham, E. and Peat, M. (1994) Spinal and Shoulder Complex Posture. II: Thoracic Alignment and Shoulder Complex Position in Normal and Osteoporotic Women. *Clin. Rehab.* **8**, 27-35.
- Culham, E.G., Noce, R.R. and Bagg, S.D. (1995) Shoulder complex position and glenohumeral subluxation in hemiplegia. *Arch Phys Med Rehab* **76**, 857-864.
- De Lange, A., Huiskes, R. and Kauer, J.M.G. (1990) Effects of Data Smoothing on the Reconstruction of Helical Axis Parameters in Human Joint Kinematics. *J. Biomech. Engr.* **112**, 107-113.
- Dol'nikov, Y.I. (1965) Experimental Research on the Movements in the Large Joints of the Arm. NASA Report N72-33108, Russian Central Scientific Research Institute of Prosthetics and Orthopaedic Appliances.
- Dempster, W.T. and Arbor, A. (1965) Mechanisms of Shoulder Movement. *Arch Phys Med Rehab* **46**, 49-70
- Dimnet, J. and Guinguand, M. (1984) The Finite Displacements Vector's Method: An Application to the Scoliotic Spine. *J. Biomechanics* **17**(6), 397-408.
- Denavit, J. and Hartenberg, R.S. (1955) A Kinematic Notation for Lower-Pair Mechanisms Based on Matrices. *Journal of Applied Mechanics* **77**, 215-221.
- Doody, S.G., Waterland, J.C. and Freedman, L. (1970a) Prosthetics, Orthotics and Devices. Scapulo-Humeral Goniometer. *Arch Phys Med Rehab* **51** 711-713.
- Doody, S.G., Freedman, L. and Waterland, J.C. (1970b) Shoulder Movements during Abduction in the Scapular Plane. *Arch Phys Med Rehab* **51** 595-604.
- Duchenne, G.B. (1959) *Physiology of Motion. Demonstrated by Means of Electrical Stimulation and Clinical Study of Paralysis and Deformities*, Philadelphia, London: W. B. Saunders Company.
- Dvir, Z. and Berme, N. (1978) The Shoulder Complex in Elevation of the Arm : A Mechanism Approach. *J. Biomechanics* **11**, 219-225.
- Engin, A.E. and Chen, S.M. (1986) Statistical Data Base for the Biomechanical Properties of the Human Shoulder Complex - I: Kinematics of the Shoulder Complex. *J. Biomech. Engr.* **108**, 215-221.

- Engin, A.E. and Peindl, R.D. (1987) On the Biomechanics of Human Shoulder Complex - I. Kinematics for Determination of the Shoulder Complex Sinus. *J. Biomechanics* **20**(2), 103-117.
- Engin, A.E. and Tumer, S.T. (1989) Three Dimensional Kinematic Modelling of the Human Shoulder Complex - Part I: Physical Model and Determination of Joint Sinus Cones. *J. Biomech. Engr.* **111**, 107-112.
- Eto, M. (1991) Analysis of the Scapulohumeral Rhythm for Periarthritis Scapulohumeralis. *J. Jpn. Orthop. Assoc.* **65**, 693-707.
- Fick, R. (1911) *Handbuch der Anatomie und Mechanik der Gelenke, Teil 3*, Jena: Gustav Fischer.
- Fisk, G.H. (1944) Some observations of motion at the shoulder joint. *Canadian Med Assn J* **50**, 213-216.
- Flecker, H. (1929) Rontgenographic Study of the Movements of Abduction at the normal Shoulder Joint. *Med. J. Australia Supplement*, 122-123.
- Freedman, L. and Munro, R.R. (1966) Abduction of the Arm in the Scapular Plane : Scapular and Glenohumeral Movements. *J. Bone Jt. Surg.* **48-A**, 1503-1510.
- Fuss, F.K. (1994) A New Method of Clinical Assessment of Shoulder Kinematics by Means of the Parameters of Helical Axes. *European Journal of Physical Medicine and Rehabilitation* **4**, 125-130.
- Goldstein, H. (1980) *Classical Mechanics*, 2nd edn. Addison-Wesley.
- Grood, E.S. and Suntay, W.J. (1983) A Joint Co-ordinate System for the Clinical Description of Three Dimensional Motions: Application to the knee. *J. Biomech. Engr.* **105**, 136-144.
- Gupta, K.C. (1988) *Classical Mechanics of Particles and Rigid Bodies*, New York: John Wiley and Sons.
- Hoernle, A.F.R. (1907) *Studies in the Medicine of Ancient India. Part 1. Osteology or the Bones of the Human Body*. Oxford, England: Clarendon Press.
- Hogfors, C., Peterson, B., Sigholm, G. and Herberts, P. (1991) Biomechanical Model of the Human Shoulder Joint - II. The Shoulder Rhythm. *J. Biomechanics* **24**, 699-709.
- Hollinshead, W.H. (1991) *Functional Anatomy of the Limbs and Back*, 6th edn. Philadelphia: W.B.Saunders Company.
- Inman, V.T., Saunders, M. and Abbott, L.C. (1944) Observations on the Function of the Shoulder Joint. *J. Bone Jt. Surg.* **26**(1), pp1-30.
- Ito, N. (1980) Electromyographic Study of Shoulder Joint. *J. Jpn. Orthop. Assoc.* **54**, 1529-1540.
- Jobe, C.M. (1990) Gross Anatomy of the Shoulder. In: Rockwood C.A., Matsen III, M.A. (Eds) *The Shoulder*, 34-97. Philadelphia: W.B.Saunders Company]
- Johnson, G.R. and Anderson, J.M. (1990) Measurement of three-dimensional shoulder movement by an electromagnetic sensor. *Clin. Biomech.* **5**, 131-136.
- Johnson, G.R. and Barnett, N.D. (1996) Letters: The measurement of three-dimensional movements of the shoulder complex. *Clin. Biomech.* **11**, 240-242.
- Johnson, G.R. and Gill, J.M. (1987). Prediction of the Range of Hand Positions Available to a Patient with Movement Restrictions at the Joints of the Upper Limb. *International Journal Of Rehabilitation Research* (1985) **10**, Supplement 5 edn. 291.

- Johnson, G.R., Stuart, P.R. and Mitchell, S. (1993) A Method for the Measurement of Three Dimensional Scapular Movement. *Clin. Biomech.* **8**, 269-273.
- Johnston, T.B. (1934) The Movements of the Shoulder Joint. A Plea for the use of the 'Plane of the Scapula' as the Plane of Reference for Movements Occurring at the Humero-Scapular Joint. *British Journal of Surgery* **25**, 252-260.
- Jones, L. (1956) The Shoulder Joint. Observations on Comparative Anatomy, Physiology and Treatment. *California Medicine* **84**, 185-192.
- Jonsson, E., Lidgren, L. and Rydholm, U. (1987) Position of Shoulder Arthrodesis Measured with Moire Photography. *Clin Orthop Rel Res* **238**, 117-121.
- Kapandji, I.A. (1982) The Shoulder. 8th edn. W.B. Saunders Company Limited
- Kedzior, K., Wojtyra, M. and Zagrajek, T. 3D Dynamic Model of the Human Upper Extremity. In: Keskinien, K. L., Komi, P. V., Mero, A. (Eds.). *Proceedings of the 15th Congress of the International Society of Biomechanics*. Gummerus Kirjapaino, Jyvaskyla, Finland.
- Kinzel, G.L., Hall, A.S. and Hillberry, B.M. (1972) Measurement of the Total Motion Between Two Body Segments - I. Analytical Development. *J. Biomechanics* **5**, 93-105.
- Kinzel, G.L., Hillberry, B.M., Hall, A.S., Jr., Van Sickle, D.C. and Harvey, W.M. (1972) Measurement of the total motion between two body segments. II. Description of application. *J. Biomechanics*. **5**, 283-293.
- Kondo, M., Tazoe, S. and Yamada, M. (1984) Changes of the Tilting Angle of the Scapula following Elevation of the Arm. In: Bateman and Walsh, (Eds.) *Surgery of the Shoulder*,. 12-16.
- Lancaster, P. and Salkauskas, K. (1987) *Curve and Surface Fitting. An Introduction*. 2nd edn. London: Academic Press, Harcourt Brace Jovanovich.
- Langrana, N.A. (1981) Spatial Kinematic Analysis of the Upper Extremity Using a Biplanar Videotaping Method. *J. Biomech. Engr.* **103**, 11-17.
- Laumann, U. (1982) Kinesiology of the Shoulder - Electromyographic and Stereophotogrammetric Studies. In: Bateman and Walsh, (Eds.) *Surgery of the Shoulder*. 6-11.
- Laumann, U. (1987) Kinesiology of the Shoulder Joint. In: Kolbel/Helbig/Blauth, (Eds.). *Shoulder Replacement* 23-31. Berlin Heidelberg: Springer-Verlag
- Laursen, B., Jensen, B. R., Nemeth, G. and Sjøgaard, G. (1995) An EMG Driven Shoulder Model in Three Dimensions. In: Keskinien, K. L., Komi, P. V., Mero, A. (Eds.). *Proceedings of the 15th Congress of the International Society of Biomechanics*. Gummerus Kirjapaino, Jyvaskyla, Finland.
- Lenaric, J. and Umek, A. (1994) Simple Model of Human Reachable Workspace. *IEEE Transactions of Systems, Man and Cybernetics*. **24**, 1239-1245.
- Lockhart, R.D. (1930) Movements of the Normal Shoulder Joint and a case with Trapezius Paralysis Studied by Radiogram and Experiment in the Living. *J. Anat.* **64**, 288-302.
- Luttgens, K. and Wells, K.F. (1989) *Kinesiology. Scientific Basis of Human Motion*, 7th edn. Dubuque, Iowa: Wm. C. Brown.
- Makhsous, M. (1996) Shoulder Model Validation. Chalmers University of Technology, Sweden.
- Marey, E.J. (1885) *La Methode Graphique*, 2nd edn. Paris: G. Masson Editeur.

- Marr, D. (1982) *Vision: A Computational Investigation into the Human Representation and Processing of Visual Information*, San Francisco: W.H.Freedman.
- Meskers, C. G. M., Arwert, H. J., de Groot, J. H., Rozendaal, L. A. and Rozing, P. M. Shoulder Muscle Contraction Patterns at Varying External Loads. In: Keskinien, K. L., Komi, P. V., Mero, A. (Eds.). *Proceedings of the 15th Congress of the International Society of Biomechanics*. Gummerus Kirjapaino, Jyvaskyla, Finland.
- McQuade, K.J., Wei, S.H. and Smidt, G.L. (1995) Effects of local muscle fatigue on three-dimensional scapulohumeral rhythm. *Clin. Biomech.* **10**, 144-148.
- Michiels, I. and Grevenstein, J. (1995) Kinematics of shoulder abduction in the scapular plane. On the influence of abduction velocity and external load. *Clin. Biomech.* **10**, 137-143.
- Montgomery, D.C. and Runger, G.C. (1994) *Applied Statistics and Probability for Engineers*, New York: John Wiley & Sons.
- Moore, J.A., Small, C.F., Bryant, J.T., Ellis, R.E., Pichora, D.R. and Hollister, A.M. (1993) A Kinematic Technique for Describing Wrist Joint Motion: Analysis of Configuration Space Plots. *Journal of Engineering in Medicine, Proc. IMechE, Part H* **207**, 211-218
- Moriwaki, M. (1992) Analysis of Three Dimensional Motion of the Scapula and the Glenohumeral Joint. *J. Jpn. Orthop. Assoc.* **66**, 675-687.
- Muybridge, E. (1957) *Animals in Motion*, New York: Dover Publications.
- Neer II, C.S. (1990) *Shoulder Reconstruction*, Philadelphia: W.B.Saunders Company.
- Nicol, A.C. (1987) A new flexible electrogoniometer with widespread applications. In: *Biomechanics XB*, 1029-1033. Illinois: Human Kinetics
- Nicol, A.C. (1989) A triaxial flexible electrogoniometer. In: *Biomechanics XIB*, 964-967. Illinois: Human Kinetics
- Ozaki, J. (1989) Glenohumeral Movements of the Involuntary Inferior and Multidirectional Instability. *Clin Orthop Rel Res* **238**, 107-111.
- Palastanga, N., Field, D. and Soames, R. (1994) *Anatomy and Human Movement. Structure and Function*. 2nd edn. Oxford: Butterworth Heinemann.
- Panjabi, M.M., Krag, M.H. and Goel, V.K. (1981) A Technique for Measurement and Description of Three-Dimensional Six Degree of Freedom Motion of a Body Joint with an Application to the Human Spine. *J. Biomechanics* **14**, 447-460.
- Pearl, M.L., Harris, S.L., Lippitt, S.B., Sidles, J.A., Harryman, D.T. and Matsen, F.A. (1992) A system for describing positions of the humerus relative to the thorax and its use in the presentation of several functionally important arm positions. *Journal of Shoulder and Elbow Surgery* **1**, 113-118.
- Persaud, T.V.N. (1984) *Early History of Human Anatomy. From Antiquity to the Beginning of the Modern Era*. Illinois: Springfield.
- Poppen, N.K. and Walker, P.S. (1976) Normal and Abnormal Motion of the Shoulder. *Jour. Bone & Joint Surg.* **58-A(2)**, 195-201.
- Pronk, G. (1991) The Shoulder Girdle. Ph.D Thesis, University of Delft, Netherlands.
- Pronk, G.M. and van der Helm, F.C.T. (1991) The Palpator : An Instrument for Measuring the Positions of Bones in Three Dimensions. *J. of Med. Engng. Technol.* **15(1)**, 15-20.

- Raab, F.H., Blood, E.B., Steiner, T.O. and Jones, H.R. (1979) Magnetic Position and Orientation Tracking System. *IEEE Transactions on Aerospace and Electronic Systems* **AES-15**, 709-718.
- Rasch, P.J. and Burke, R.K. (1959) *Kinesiology and Applied Anatomy: The Science of Human Movement*. Philadelphia: Lea and Lebigier.
- Reuleaux F.(1963) *The Kinematics of Machinery: Outlines of a Theory of Machines*. New York: Dover Publications.
- Robinson, A.H., Morrison, J.L., Muehrcke, P.C., Kimerling, A.J. and Guptill, S.C. (1995) *Elements of Cartography*, 6th edn. New York: John Wiley and Son, Inc.
- Romilly, D.P., Anglin, C., Gosine, R.G., Hershler, C. and Raschke, S.U. (1994) A Functional Task Analysis and Motion Simulation for the Development of a Powered Upper Limb Orthosis. *IEEE Transactions on Rehabilitation Engineering* **2**, 119-128.
- Royal Yachting Association (1994) *Yachtmaster. Shore Based Course Notes*, 5th edn. Eastleigh, Hampshire: Royal Yachting Association.
- Runciman, R.J. (1993) Biomechanical Model of the Shoulder Joint. Ph.D. Thesis, University of Strathclyde, UK.
- Safaei-Rad, R., Shwedyk, E., Quanbury, A.O. and Cooper, J.E. (1990) Normal Functional Range of Motion of Upper Limb Joints During Performance of Three Feeding Activities. *Arch Phys Med Rehab* **71**, 505-509.
- Saha, A.K. (1950) Mechanism of Shoulder Movements and a Plea for the Recognition of the "Zero Position" of the Glenohumeral Joint. *Clin. Orthop.* **173**, 3-10.
- Salter, N. and Darcus, H.D. (1953) The Amplitude of Forearm and of Humeral Rotation. *Anatomy* **87**, 407-418.
- Selvik, G. (1974) A Roentgenstereophotogrammetric method for the study of the kinematics of the skeletal system. University of Lund, Sweden.
- Sennwald, G.R., Zdravkovic, V., Jacob, H.A.C. and Kern, H.P. (1993) Kinematic analysis of relative motion within the proximal carpal row. *Journal of Hand Surgery (GB)* **18 B**, 609-612.
- Shoup, T.E. (1976) Optical Measurement of the Centre of Rotation for Human Joints. *J. Biomechanics* **9**, 241-242.
- Sidles, J.A., Harryman, D.T., Harris, S.L. and Matsen, F.A. (1991) In-Vivo Measurements of Glenohumeral and Scapulothoracic Motion : Implications for Fusion Position in Glenohumeral Arthrodesis. *Proc. 37th Annual Meeting, Orthopaedic Research Society, March 4-7* 209
- Spiegelman, J.J. and Woo, S.L. (1987) A rigid-body method for finding centers of rotation and angular displacements of planar joint motion. *J. Biomechanics*. **20**, 715-721.
- Spoor, C.W. and Veldpaus, F.E. (1980) Technical Note - Rigid Body Motion Calculated from Spatial Co-ordinates of Markers. *J. Biomechanics* **13**, 391-393.
- Spring, K.W. (1986) Euler Parameters and the use of Quaternion Algebra in the Manipulation of Finite Rotations: A Review. *Mechanism and Machine Theory* **21**, 365-373.
- Steindler, A. (1962) *Kinesiology of the Human Body*, 2nd edn. Illinois: C.C.Thomas.
- Veblen, T. (1991). *The Place of Science in Modern Civilisation*.

- van der Helm, F.C.T. and Pronk, G.M. (1995) Three-dimensional recording and description of motions of the shoulder mechanism. *J. Biomech. Engr.* **117**, 27-40.
- Veldpaus, F.E., Woltring, H.J. and Dortmans, L.J.M.G. (1988) A Least-Squares Algorithm for the Equiform Transformation from Spatial Marker Co-ordinates. *J. Biomechanics* **21** 45-54.
- Wallace, W.A. (1982) The Dynamic Study of Shoulder Movement. In: Kessel and Bailey, (Eds.) *Shoulder Surgery*, 139-143.
- Wallace, W.A. and Johnson, F. (1982) A Biomechanical Appraisal of the Acromioclavicular Joint. In: Bailey and Kessel, (Eds.) *Shoulder Surgery*, 179-182.
- Winter, D.A. (1987) *The Biomechanics and Motor Control of Human Gait*, Waterloo: University of Waterloo Press.
- Woltring, H.J. (1994) 3-D Attitude Representation of Human Joints : A Standardisation Proposal. *J. Biomechanics* **27**, 1399-1414.
- Woltring, H.J., Huiskes, R. and De Lange, A. (1985) Finite Centroid and Helical Axis Estimation from Noisy Landmark Measurements in the study of Human Joint Kinematics. *J. Biomechanics* **18**(5), 379-389.
- Youdas, J.W., Carey, J.R., Garrett, T.R. and Suman, V.J. (1994) Reliability of Goniometric Measurements of Active Arm Elevation in the Scapula Plane Obtained in a Clinical Setting. *Arch Phys Med Rehabil* **75**, 1137-1144.

Appendix A1

Research Publication

This appendix contains a research publication written and published during the work undertaken within the thesis.

Entitled "Winging of the Scapula: The Underlying Biomechanics and an Orthotic Solution", concerns the motions of the scapula in a subject with facioscapulohumeral muscular dystrophy.

Reference:

Barnett, N.D., Mander, M., Peacock, J.C., Bushby, K., Gardner-Medwin, D. and Johnson, G.R. (1995) Winging of the Scapula: The Underlying Biomechanics and an Orthotic Solution. *Journal of Engineering in Medicine, Proc. IMechE, Part H* 209, 215-223.

Winging of the scapula: the underlying biomechanics and an orthotic solution

N D Barnett, BEng

Centre for Rehabilitation and Engineering Studies, University of Newcastle upon Tyne

M Mander, MSc, MCSP

Newcastle Community Physiotherapy Service, Newcastle upon Tyne

J C Peacock, MCSP

J C Peacock and Son Limited, Newcastle upon Tyne

K Bushby, MD, MRCP and D Gardner-Medwin, MD, FRCP

Newcastle General Hospital, Newcastle upon Tyne

G R Johnson, PhD, CEng, FIMechE

Centre for Rehabilitation and Engineering Studies, University of Newcastle upon Tyne

Winging of the scapula occurring in muscular disorders (muscular dystrophy and spinal muscular atrophy) or nerve injury has been investigated, resulting in a thorough understanding and presentation of the underlying biomechanics causing this occurrence. This includes a biomechanical explanation of the characteristic prominence of the medial border of the scapula upon attempted elevation, together with the biomechanical reasons for the rotation of the scapula in a direction contrary to the normal scapulohumeral rhythm. Based on these findings, a non-invasive alternative to the surgical technique for scapular stabilization has been devised, using an inflatable orthosis, placed between the scapula and an external restraint (such as a spinal jacket). The device has been tested on one subject using a 3SPACE™ Isotrak™ electromagnetic source and sensor system, and gave encouraging results. Elevation increased by up to 35° (37 per cent), and functional improvement in the use of the hand around the head and face has been achieved. The technique needs no aftercare or physiotherapy and is therefore both economical and functionally effective.

Key words: shoulder, biomechanics, winging scapula, fascioscapulohumeral muscular dystrophy

1 INTRODUCTION

The posture of the scapula depends almost entirely on muscular support between itself and the thorax. The clavicle forms the only bony, but indirect link, supporting the scapula at the acromion. Therefore, without the necessary forces from the scapulothoracic muscles, the scapula would be unable to react applied loads from the arm through the glenohumeral joint. Hence any physical or neurological impairment leading to muscular imbalance around the shoulder girdle mechanism can greatly affect functional mobility of the upper limb.

Winging of the scapula is defined as prominence of the medial or vertebral border of the scapula and has been classified into two distinct forms: static and dynamic (1). A fixed deformity in the shoulder girdle, spine or ribs may give rise to static winging, characteristically present at rest, with the arm by the side. Dynamic winging may occur as a result of insufficient strength and control in some of the scapulothoracic muscles. The reasons for the lack of strength in any (or most) of the scapulothoracic muscle group are numerous, from traumatic injury to the long thoracic nerve causing paralysis of serratus anterior, to spinal muscular atrophy or myopathies, particularly the scapulo-peroneal and fascioscapulohumeral types of

muscular dystrophy. The theories and ideas presented in this paper concern the dynamic condition.

The result of this muscle weakness is that the stable base for the humeral head (the glenoid) no longer exists since the scapula is unable to resist applied loads, causing the (characteristic) winging upon attempted movement. However, in many cases the muscles involved in the elevation of the glenohumeral joint which occurs during flexion and abduction of the arm (predominately deltoid, supraspinatus and the clavicular portion of pectoralis major) are generally unaffected. Hence, if the scapula could be artificially stabilized, these muscles would be capable of developing an effective moment between the trunk and the humerus, thereby increasing the range of useful motion available.

There is a requirement, therefore, for a means of restraining the scapula. There is no established therapeutic approach to the problem although many surgical techniques have been employed to perform this stabilization task. The majority of these involve fixing the scapula to ribs, thereby restoring its position on the posterior wall of the thorax. These have generally been limited to cases of muscular dystrophy. Ketenjian (2) used fascia, Mersilene or Dacron strips, tied through holes drilled in the medial border of the scapula and around the ribs. Copeland and Howard (3) cut bone grafts from the tibia and used them as struts across the medial border of the scapula, fixing these struts with

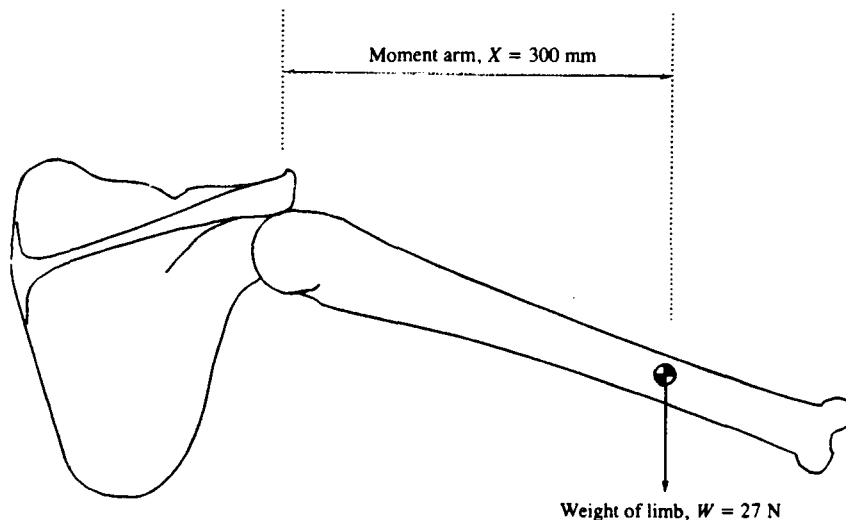


Fig. 1 Moment on the scapula due to the weight of the arm, causing lateral rotation

screws to the scapula and ribs. Bunch and Siegel (4) used a combination of the above procedures, fixing the scapula to the ribs with stainless steel wire while placing cortical and cancellous bone between and over the ribs anterior to the scapula. This formed a large bone graft incorporating the ribs and filling the cancellous bed between the ribs and the scapula. Spira (5) passed the sixth rib through a window cut in the scapula, while Letournel *et al.* (6) adopted a similar procedure which included wiring the scapula to the ribs.

Muscle transfer techniques have also been employed in efforts to restore normal scapular position. Tubby (7) and Marmor and Bechtol (8) transferred part of pectoralis major in separate cases of serratus anterior palsy. Rhomboid and trapezius (9) and pectoralis minor (10) transfers have also been performed.

After all of these procedures, the postoperative range of arm motion was greater than preoperatively, and almost all patients were happy with the result, claiming greater ability to sustain elevated arm positions. A few complications were reported, but none of a nature which could not be resolved or overcome. However, it should be noted that all of the surgical techniques involved a great amount of aftercare in the form of immobilization of the shoulder for up to three or four months, followed by long-term physiotherapy to strengthen the arm abductors.

Orthotic techniques of scapular stabilization have also been attempted, although it would appear that nothing has been published in this area within the last 50 years. Horwitz and Tocantins (11) designed an orthosis to support the weight of the arm via the elbow on a pelvic rest. Various sling supports have been designed (12, 13), also plaster spica casts to relax serratus anterior as a restorative treatment for paralysis of the muscle (14). However, as pointed out by Wolf (15), in the case of permanent paralysis or wasting of the muscles, an orthosis must allow for complete use of the arm, within the capabilities of the subject. Their orthosis was designed to this end and consisted of a chest brace with pads to press the scapula against the thorax. Although success was claimed, no scientific evidence or sound understanding of the cause of the winging was presented.

This paper discusses the biomechanical aspects of winging of the scapula, and presents a non-invasive orthotic technique for scapular stabilization based on the use of an inflated bag to compress the scapula on to the thoracic wall. Finally, a method for assessing the efficiency of the orthosis will be presented.

2 BIOMECHANICAL ANALYSIS

2.1 Biomechanical configuration

Normal motion of the scapula on the chest wall is achieved by the combined actions of the shoulder girdle muscles which both ensure equilibrium with externally applied forces and maintain kinematic control. The most commonly reported cause of winging is weakness primarily of serratus anterior (due to traumatic injury to the long thoracic nerve). In cases of fascioscapulohumeral muscular dystrophy, other muscles around the shoulder girdle are also affected. In this analysis the following assumptions will be made:

1. The rotator cuff muscles, pectoralis major and deltoid are generally active, while trapezius, rhomboids, levator scapulae and serratus anterior are inactive. This was found to be true in the case studied here. In subjects with long thoracic nerve palsy it is generally only serratus anterior which is affected, allowing the prominence of the medial border during motion of the arm (that is winging). The weaknesses in the other muscles allow for a more distinct 'contra-rotation' of the scapula, as discussed in Section 2.2.
2. The only kinematic constraint on the scapula results from the three degrees of freedom connection at the acromioclavicular joint. This means that the acromion is constrained to move on the surface of a sphere, with a radius equal to the length of the clavicle.

The system described above is under-constrained and, hence, is a mechanism whose configuration will be determined by the joint kinematics and muscular activity combined with the need for equilibrium.

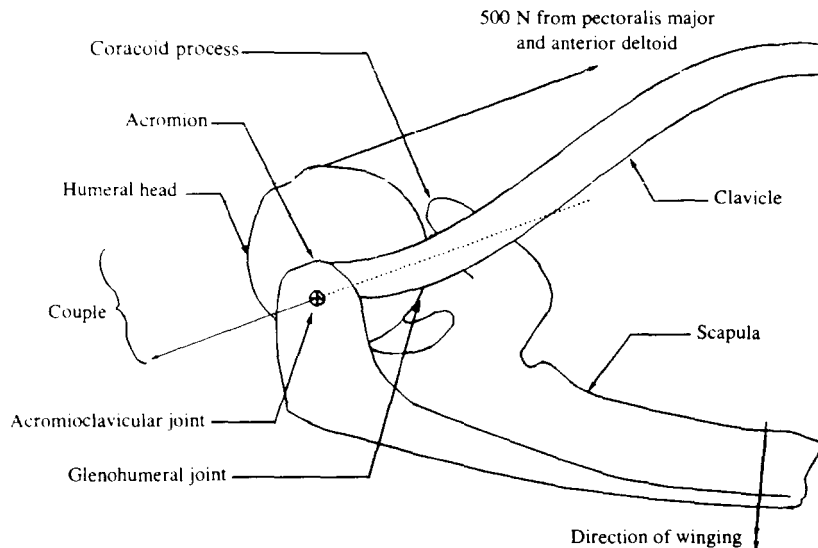


Fig. 2 Couple on the scapula due to the active muscles, causing winging

2.2 Consequences of applied loading

With the arm at the side, a moment will be applied to the scapula about an axis normal to the coronal plane, due to the weight of the arm W . This moment increases with elevation up to 90° , as the centre of gravity of the arm moves away from the body, increasing the distance X (see Fig. 1). In the normal shoulder, the scapulothoracic muscles oppose this moment (predominately serratus anterior, trapezius and the rhomboids), thereby maintaining the stability of the scapula. However, the absence of this necessary muscular support causes medial rotation of the scapula (approximately in the coronal plane) about the acromioclavicular joint. Whereas in the normal shoulder the scapula rotates in the same sense as the humerus [the

scapulohumeral rhythm, Codman (16)], in this situation it rotates in the opposite sense.

When elevation is attempted in the normal shoulder, the muscles involved in flexion and abduction of the humerus (primarily supraspinatus, deltoid and the clavicular portion of pectoralis major, with contributions from coracobrachialis and biceps) develop a moment on the scapula. As the scapula is held stable by the scapulothoracic muscles, elevation is possible. However, when the scapula is not restrained, these muscles act to produce a moment at the glenohumeral joint (Fig. 2). Because of their sites of attachment and hence the lines of action of any forces produced, a moment is produced about an approximately vertical axis through the acromioclavicular joint, resulting in the familiar winging

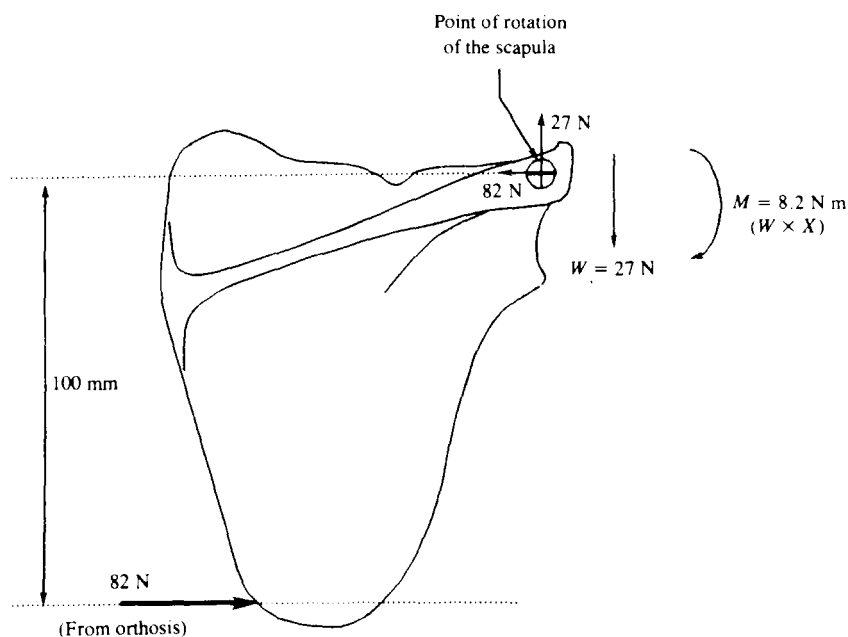


Fig. 3 Force diagram of the scapula (posterior aspect)

movement as well as the scapula rotation described above.

2.3 Biomechanical requirements of stabilization

Any system to prevent these movements must, therefore, counteract the moments by applying a force with components which are:

- (a) lateral to control the medial scapular rotation (in the coronal plane); and
- (b) anterior to oppose the couple producing winging.

These requirements are the same whether surgical or orthotic control is chosen. The magnitudes of these forces have been estimated as follows.

2.3.1 Lateral force component

Using data from Martin (17) and Snyder *et al.* (18) for anthropomorphic dimensions, and data from Dempster (19) for masses and centres of gravity of body segments, the required lateral component of the force was estimated to be 82 N, acting on the inferior angle, using the free body diagram in Fig. 3.

2.3.2 Anterior force component

In order to calculate the anterior force component it is necessary to estimate the forces developed by the active muscles. Data for the physiological cross-sectional areas (PCSA) of pectoralis major and anterior deltoid were obtained from Johnson (20). For the muscle strength a mean value of 0.46 N/mm^2 was used, based on the findings of several reports [Herzog (1985)*, Ikai and Fukunaga (1968)†, Ketchum *et al.* (1978)*, Morris (1948)†, Rechlinghausen (1920)†, Rutherford and Jones (1988)*]. Using these values, the required anterior component of

the force was determined to be approximately 100 N, acting on the medial border of the scapula, as shown in Fig. 4.

3 DESIGN OF THE ORTHOSIS

Any external device must be capable of supplying the forces required to stabilize the scapula, while at the same time being comfortable for the subject. This leads to two design requirements. It is necessary to apply the appropriate loads to the scapula through the skin and, whatever device is used, the required forces must be reacted on the trunk. The force applied to the scapula must have both a normal and a tangential component which can only be achieved by a structure which will conform to its bony contour. Problems arise with this requirement due to contact pressures between the skin and the force-supplying device, that is the force cannot be applied to a single point but must be spread over an area of the scapula. The orthosis must therefore be deformable to eliminate any point contact pressures, yet supportive enough to supply the forces. In the particular case examined here, the trunk reaction forces were transmitted by a moulded thermoplastic spinal jacket.

The subject examined in this study, a 14 year old girl, suffered from fascioscapulohumeral muscular dystrophy. This is a specific progressive muscle/genetically determined wasting disease affecting, initially at least, the muscles of the face and shoulder girdle. It was first described by Landouzy and Déjerine (23) and has been the subject of various reports since (1–5).

The subject was required to wear a spinal jacket in order to stabilize her trunk. Additional high-density foam padding within the spinal jacket was rejected as a means of restraining the scapula. It is unlikely that such support would suffice as the jacket would need to be applied more securely and the resulting constant compression would be both uncomfortable and potentially dangerous because of skin ischaemia. A pneumatic device was therefore chosen, which could be inflated intermittently as required after the jacket had been applied, thereby filling any cavities between the jacket and the scapula, and thereafter, with increasing pres-

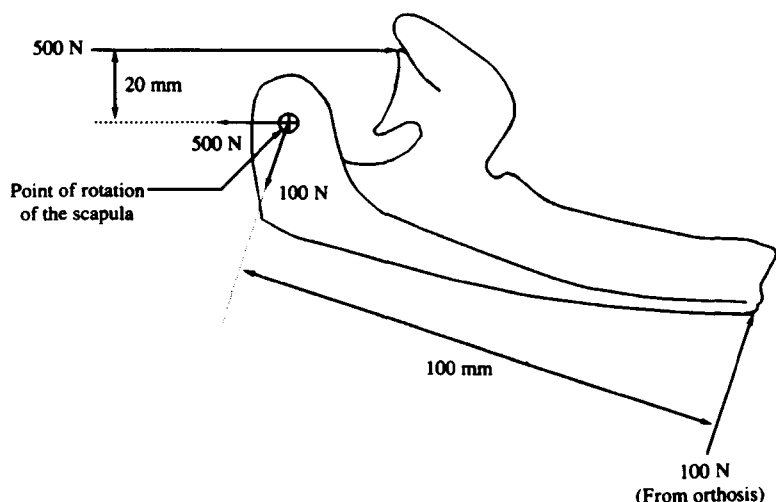


Fig. 4 Force diagram of the scapula (superior aspect)

* Quoted by Lee and Rim (21).

† Quoted by de Luca and Forrest (22).

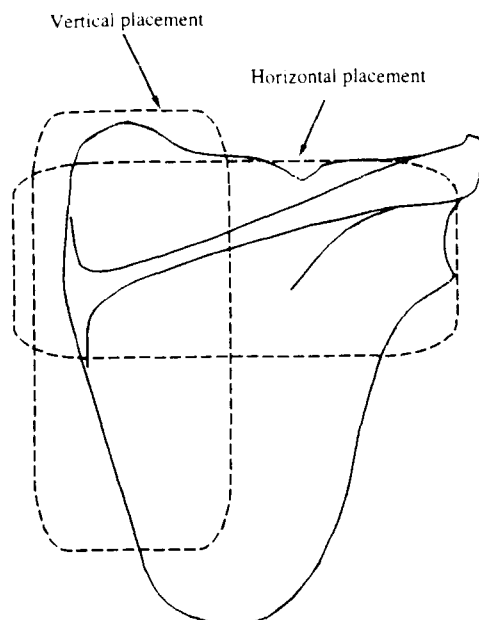


Fig. 5 Positioning of the device

sure, supplying the required forces. As such a device would be deformable, it would conform around the medial border of the scapula and therefore supply a force approximately equivalent to the resultant of the two required forces. It was also decided that the subject should be in complete control of the device, inflating the orthosis only when required. This would prevent the skin being subjected to a constant pressure and allow the user to eliminate any discomfort which may be caused by the device.

An attempt was made at this stage to estimate the pressure required to produce the required forces. While the normal force (that is the anterior component) can be produced by direct contact with a pressurized bag, the lateral component can only result from membrane stresses in the section of the bag conforming around the bony prominence at the medial border. If it is assumed that the maximum pressure to be used is 150 mmHg (0.2 bar approximately) then an area of 5000 mm² would be required to produce the required load. In fact, this area corresponded approximately to the area of the subject's scapula in this particular study, although it should be pointed out that an even pressure distribution would result in a force with a line of action displaced laterally from the medial border. On the basis of these (very) approximate calculations it was decided to

proceed with this design, using a rectangular bag of a size to cover the blade of the scapula. Initial tests with the system pressurized by a bulb, with a pressure gauge, showed the system to be effective. It was then necessary to determine the optimum inflation pressure and position of the bag, and to assess the overall efficiency of the orthosis.

4 METHODS OF ASSESSMENT

To the authors' knowledge, there have been no studies regarding the functional abilities of subjects with winging scapulae, hence it cannot be stated which motions should be assessed. Because of this, the problem has been studied in a variety of ways using equipment with which the authors have previous experience (24).

Evaluation was approached in two ways: a subjective assessment was made by the user and three-dimensional movement measurements were made in the clinic.

A four-week study was undertaken by the subject to investigate varying pressures within the cuff and the effects of its orientation (that is vertical or horizontal placement over the scapula, see Fig. 5). Pressures of 40 mmHg and 80 mmHg were recommended as an introduction to the device, to investigate the functional advantages gained from it. Throughout this study (and beyond), the subject had complete control of the orthosis and kept a written record of its use. She could monitor the pressure in the bag by means of the attached gauge and increase or decrease the pressure at will.

Subsequently, in the clinic, shoulder elevation angles and hand trajectories were recorded using a 3SPACE™ Isotrak™ system in conjunction with custom real-time software. The Isotrak™ consists of an electromagnetic source producing low-frequency waves received by a three-axis sensor; it provides data for all six degrees of freedom. This technique was chosen for its availability and the fact that the research group have considerable experience of its use for the measurement of upper limb movements.

For measuring shoulder movement, the source was attached to a rigid arm splint and the sensor to the manubrium sterni. Data were collected with the cuff deflated and inflated to pressures of 40, 80, 110 and 150 mmHg, this latter being the maximum the subject had found acceptable from the point of view of comfort during the four-week study.

The subject was then asked to repeatedly elevate her arm to the highest level she could achieve, while the

Table 1 Results of the four-week study undertaken by the subject

Orientation	Pressure	
	40 mmHg	80 mmHg
Vertical	Little functional use. Gave comfort. Increase in abduction by approximately 10° over and above that without the cuff	Functionally useful. Increased and sustained abduction over and above that achieved in 40 mmHg horizontal
Horizontal	Functional advantages. Comfortable. More sustained abduction achieved. Better than 40 mmHg vertical	Great functional advantages. Felt comfortable. Allowed controlled hand movements around face and head

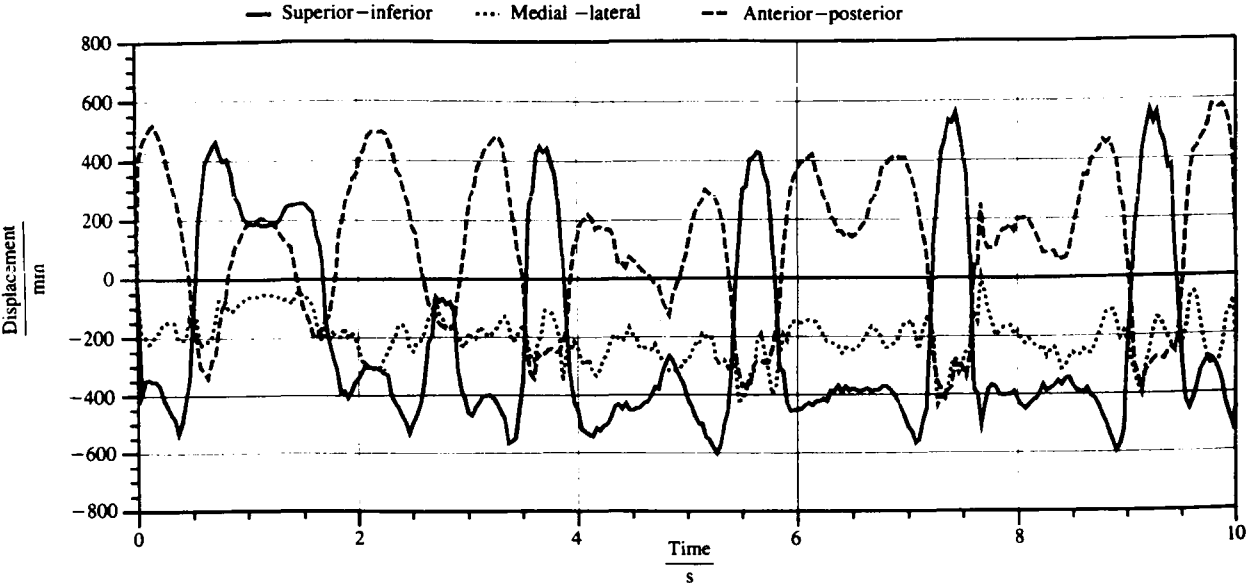


Fig. 6 Displacements of the hand coordinates with the device deflated

angles of flexion, abduction and rotation were recorded by the Isotrak™. Hand position was also monitored in a similar manner, with the sensor fixed to the back of the hand, and the source mounted on a wall adjacent to the subject. The subject was again asked to elevate her arm,

lifting her hand to her face and top of the head. Trajectory plots of hand motion were obtained from these data. Data were recorded for a period of ten seconds at each pressure, ten sets of data being collected in total (five for the arm measurements and five for the hand).

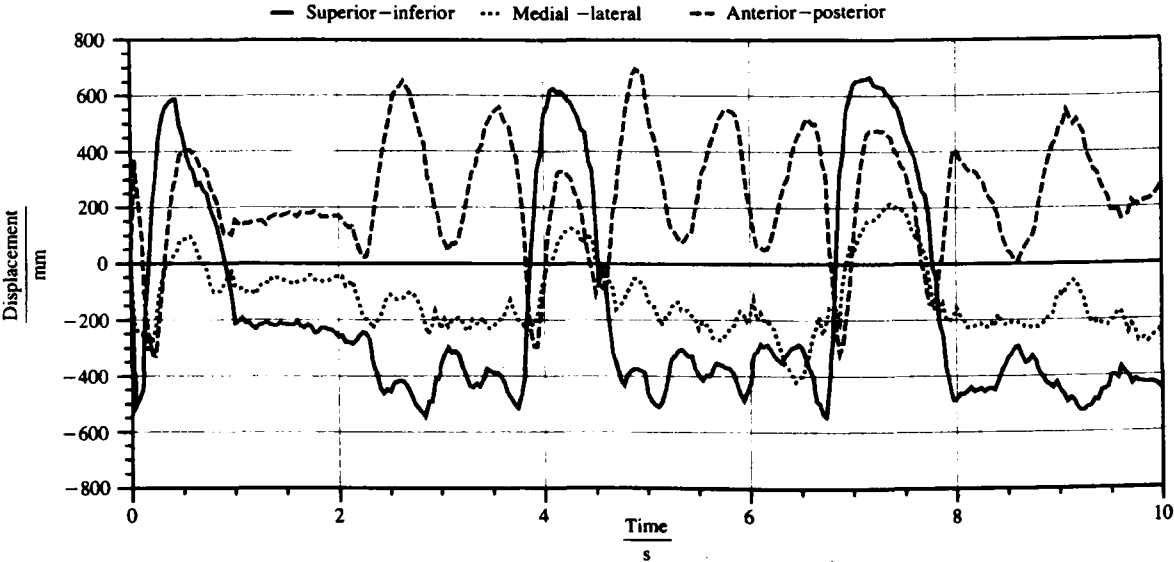


Fig. 7 Displacements of the hand coordinates with the device inflated to 150 mmHg

Table 2 Comparison of increases in arm elevation between this study and the quoted results of the surgical procedures

Study	Sample size <i>n</i>	Mean peak abduction (pre-operative)	Mean peak abduction (post-operative)	Mean increase
Ketenjian (2)	5	56°	87°	32°
Letourmel <i>et al.</i> (6)	16	77°	102°	25°
Bunch and Siegel (4)	12	68°	121°	53°
This study	1	95°*	130°†	35°

* Orthosis not inflated
† Orthosis inflated

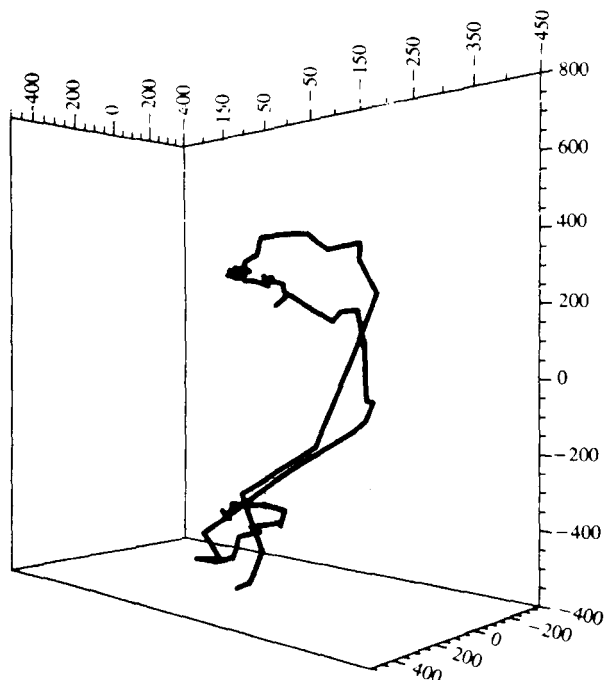


Fig. 8 Trajectory plot of the hand with the device inflated to 40 mmHg (all scales in mm)

5 RESULTS

The results of the four-week study by the subject are summarized in Table 1. It is also known that over one year from receiving the orthosis, the subject is still using it on a daily basis. The graphs in Figs 6 and 7 illustrate the x , y and z coordinates of the hand motion with the device deflated and at 150 mmHg.

Figures 8 to 11 are trajectory plots of the hand motion with the device at each pressure. Figure 12 illus-

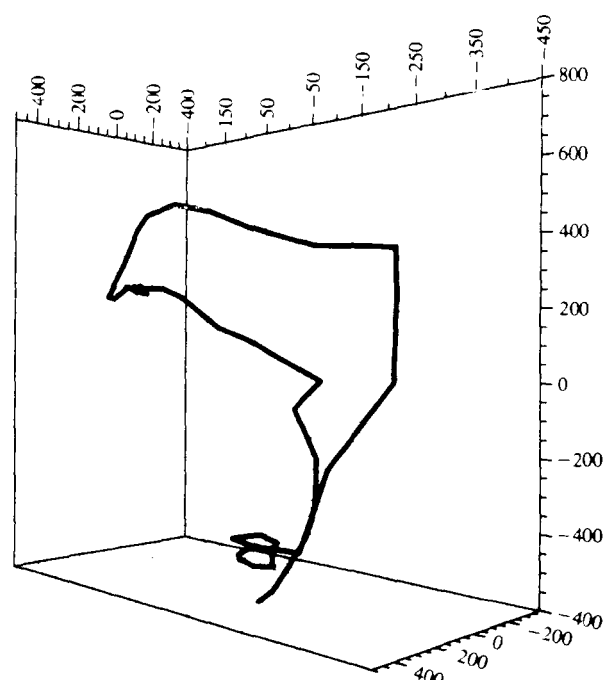


Fig. 10 Trajectory plot of the hand with the device inflated to 110 mmHg (all scales in mm)

trates the increase in arm elevation angles with increases in the cuff pressure, and Table 2 shows the results compared to other studies.

6 DISCUSSION

In order to assess the usefulness of any applied device, whether surgical or orthotic, it is essential to examine the functional abilities of the subject without such a device. In the opinion of the subject, the orthosis was a

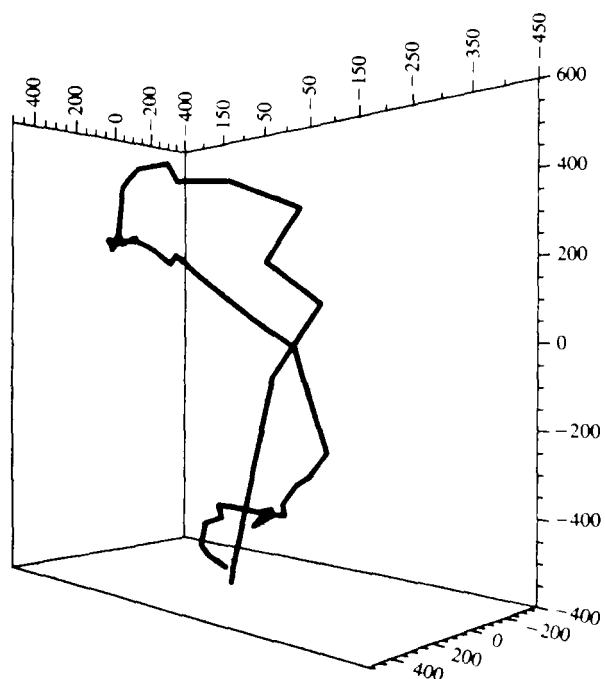


Fig. 9 Trajectory plot of the hand with the device inflated to 80 mmHg (all scales in mm)

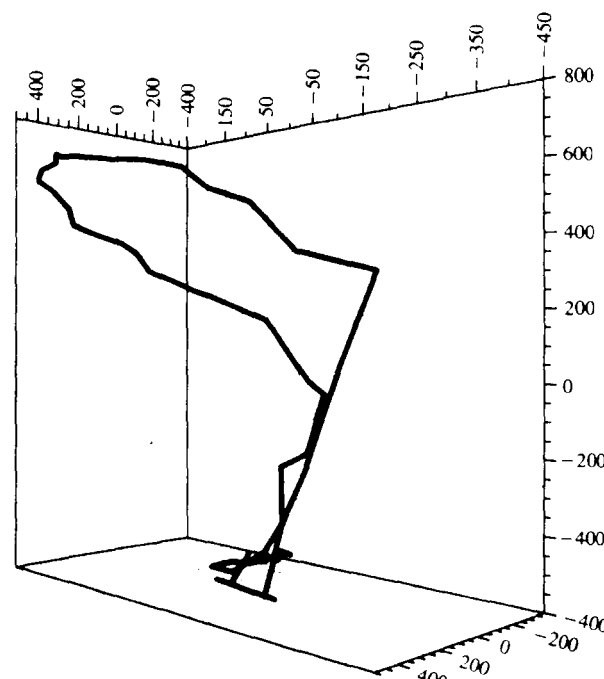


Fig. 11 Trajectory plot of the hand with the device inflated to 150 mmHg (all scales in mm)

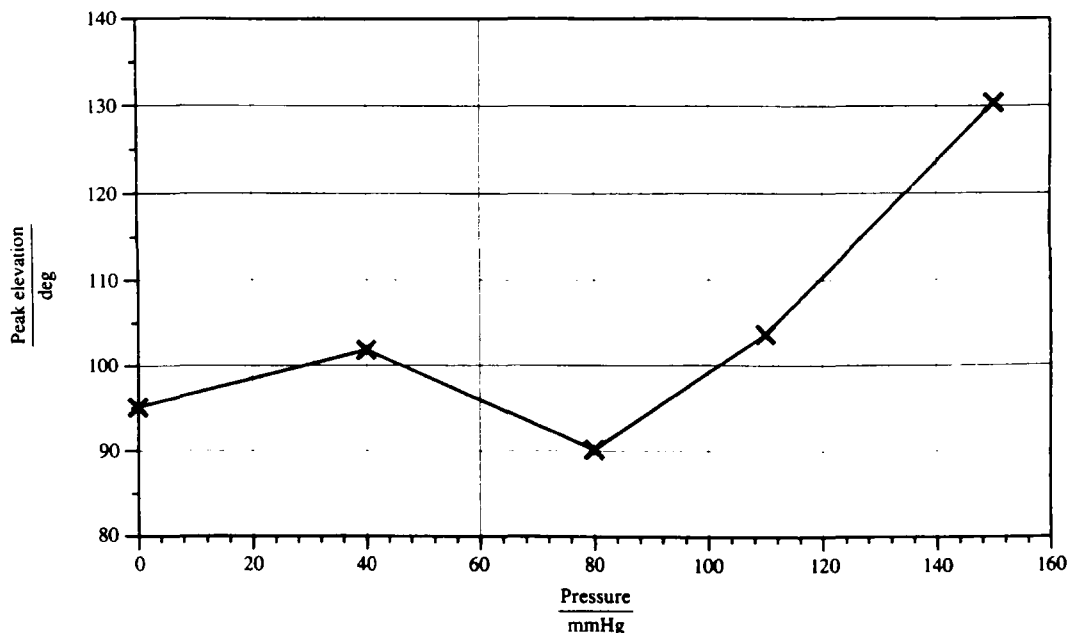


Fig. 12 Peak elevation angles plotted against cuff pressure

valuable aid and was found to be of more use when placed horizontally. The likely reason for this is that when placed in this position, the bony prominence of the scapula spine is in greater contact with the orthosis and hence the applied forces can be more directly transmitted to the scapula. Also, as the orthosis deforms around the scapula spine, greater membrane stresses will develop in the section of the bag conforming to the bony prominence, thereby increasing further the transmitted forces.

Prior to any assistance, the subject had developed a complex throwing action ('trick movement') to position the hand on the head. Such abilities were noticed by Ketenjian in some of his subjects. Such a motion can be seen to be characterized by an increase in the vertical coordinate of the hand, without any accompanying increase in the medial or anterior coordinates (see Fig. 6). The muscular impairment of the subject is such that it causes the inability to produce a moment on the scapula, consistent with the observed throwing motion. From these data, it can be seen that during elevation the subject keeps the hand as close to the body as possible, thereby minimizing the moment of the arm upon the scapula. Controlled motion (combined abduction and flexion) involves the production of moments on the scapula, and can be identified as an increase in all coordinates simultaneously, as illustrated in Fig. 7. Such motions are available to the subject only when the scapula is held stable by the device, thereby balancing the moment developed by the arm as it moves away from the body. The range of motion illustrated by the controlled motion trajectories (that is with the cuff inflated) can be seen to increase with pressure (see Figs 8, 9, 10 and 11), and yields great functional advantages for tasks such as combing of the hair. This was previously impossible for the subject without resting the elbows on a level surface and lowering the trunk and head, thereby effectively elevating the arms.

These trajectory plots clearly illustrate a growth in

the workspace available to the subject with increases in pressure within the orthosis. Consequently, the authors regard these plots as the assessment criterion for devices of this nature, with the proviso that comparisons are available from data collected before and after the application of such a device.

With regard to the arm elevation data, Fig. 12 clearly shows that increasing the pressure within the cuff greatly increases elevation angles achieved (an increase of over 35° overall). Once again, the effect of the trick movement can be seen, as elevation is greater with the cuff deflated than with the cuff inflated to 80 mmHg. However, the apparent lack of elevation with the cuff inflated to 80 mmHg compared to the elevation at other pressures is not explained by this alone, especially as the subject had previously commented on the usefulness of the device at this pressure. It must, however, be pointed out that fatigue was a factor throughout the latter part of the testing and may have reduced the available arm elevation. This could explain the apparent anomaly of a reduction in arm elevation at 80 mmHg.

The results show a considerable variation in arm elevation angles and hand position depending on the pressure within the cuff, as would be expected. It is difficult to estimate the precise force delivered to the scapula by the device at each, or any pressure. Effects due to changes in volume of the orthosis as the subject elevates her arm may considerably affect the pressure within the cuff and hence the stabilization force. The data in Fig. 12 would seem to suggest that the appropriate forces are being generated at pressures above 100 mmHg (0.13 bar) in that a large increase in peak elevation occurs. However, the approximate calculations presented earlier would suggest that this pressure is insufficient. It is probably reasonable to conclude, therefore, that the membrane and dynamic effects discussed earlier are responsible for the efficacy of the device. Pressures of this magnitude were regarded as acceptable from the safety point of view. In particular, it was noted that the

user had normal skin sensation. Furthermore, long-term skin damage was thought unlikely since the device is only used for a relatively short period of time.

7 CONCLUSIONS

In this paper, it has been demonstrated that knowledge of the anatomy and biomechanics of the shoulder girdle allows an improved understanding of the mechanisms of winging of the scapula. In particular, by the use of a simple biomechanical model, it has been demonstrated that relatively small forces are required to counteract the moments applied to the scapula during functional movements of the arm. However, there are problems in achieving the correct application of these forces, particularly the required shear loading. This would appear to be the first time that the underlying biomechanics relating to dynamically winging scapulae have been analysed in detail.

A single case study has demonstrated the viability of applying the necessary correcting forces using an inflated bag which can conform around the bony geometry of the scapula. However, this has relied upon the use of the spinal jacket which had been provided for other rehabilitation reasons. For those who already have a spinal jacket, this orthosis represents a single adaptation which can provide significant functional benefit. However, further work is required to achieve the same degree of control of the scapula in patients who do not require the use of a spinal jacket.

Attention has also been paid to the need to evaluate the orthosis in use. A frequent problem of the design of new rehabilitation techniques is the difficulty of realistic functional evaluation. While the user's subjective evaluation shows the practical benefits of the orthosis, improvement of the design can only be performed on the basis of physical measurement. In this study, it has been demonstrated that the Isotrak™ electromagnetic movement measurement system is a useful clinical tool for the study of upper limb movements in the rehabilitation setting. With regard to analysis and interpretation, it has been shown that hand trajectory plots serve as a useful representation of function, provided that they are compared before and after the orthosis is applied.

The design and evaluation of a new orthosis requires an understanding of the biomechanical requirements, the design of an appropriate structure and evaluation of function. This paper has addressed all of these issues in relation to orthotic control of the winging scapula. The authors acknowledge that this study has been limited by the application to a single patient. However, being designed according to the orthodox principles presented in this paper, they are confident that the device will be suitable for other patients with similar problems. Furthermore, it is acknowledged that this design may not be appropriate for the management of winging with other causes such as long thoracic nerve palsy. However, the application of basic mechanics and the experience gained here, put them in a strong position to investigate this group of patients.

ACKNOWLEDGEMENTS

The authors would like to acknowledge the help and patience of both the subject and her mother throughout

the duration of this study. They would also like to thank Engineering and Physical Science Research Council for the financial support of one of the authors (N.D.B.).

REFERENCES

- 1 Fiddian, N. J. and King, R. J. The winged scapula. *Clin. Orthop.*, 1985, **185**, 228–236.
- 2 Ketenjian, A. Y. Scapulocostal stabilization for scapular winging in facioscapulohumeral muscular dystrophy. *J. Bone Jt Surg.*, 1978, **60-A**, 476–480.
- 3 Copeland, S. A. and Howard, R. C. Thoracoscaphic fusion for facioscapulohumeral dystrophy. *J. Bone Jt Surg.*, 1978, **60-B(4)**, 547–551.
- 4 Bunch, W. H. and Sigel, I. M. Scapulothoracic arthrodesis in facioscapulohumeral muscular dystrophy. *J. Bone Jt Surg.*, 1993, **75-A(3)**, 372–376.
- 5 Spira, E. The treatment of a dropped shoulder. A new operative technique. *J. Bone Jt Surg.*, 1948, **30-A**, 229–233.
- 6 Letournel, E., Fardeau, M., Lytle, J. O., Serrault, M. and Gosselin, R. A. Scapulothoracic arthrodesis for patients who have facioscapulohumeral muscular dystrophy. *J. Bone Jt Surg.*, 1990, **72-A**, 78–84.
- 7 Tubby, A. H. A case illustrating the operative treatment of paralysis of the serratus magnus muscle by muscle grafting. *Br. Med. J.*, 1904, **2**, 1159–1160.
- 8 Marmor, L. and Bechtol, C. O. Paralysis of the serratus anterior muscle due to electric shock relieved by transplantation of the pectoralis muscle: a case report. *J. Bone Jt Surg.*, 1963, **45-A**, 156–160.
- 9 Hertzmark, M. H. Traumatic paralysis of the serratus anterior relieved by transplantation of the rhomboid. *J. Bone Jt Surg.*, 1951, **33-A**, 235.
- 10 Horwitz, M. T. Isolated paralysis of serratus anterior muscle. *Am. J. Orthop. Surg.*, 1959, **1**, 100.
- 11 Horwitz, M. T. and Tocantins, L. M. Isolated paralysis of the serratus anterior (magnus) muscle. *J. Bone Jt Surg.*, 1938, **20**, 720–725.
- 12 MacKenzie, C. *The action of muscles: including muscle rest and muscle re-education*, 2nd edition, 1930, (Paul B. Hoeber, New York).
- 13 Foucar, H. O. The 'Clover Leaf' sling in paralysis of the serratus magnus. *Br. Med. J.*, 1933, **2**, 856.
- 14 Berkheiser, E. J. and Shapiro, F. Alar scapula. Traumatic palsy of serratus magnus. *J. Am. Med. Assn.*, 1937, **108**, 1790–1793.
- 15 Wolf, J. The conservative treatment of serratus palsy. *J. Bone Jt Surg.*, 1941, **23-A**, 959–961.
- 16 Codman, E. A. *The shoulder*, 1934 (G. Miller, New York).
- 17 Martin, W. E. Children's body measurements for planning and equipping schools. Special publication number 4 (United States Department of Health, Education and Welfare, Maryland).
- 18 Snyder, R. G., Schneider, L. W., Owings, C. L., Reynolds, H. M., Golomb, D. H. and Schork, M. A. Anthropometry of infants, children and youths to age 18 for product safety design. Report number DB-270 277 (Consumer Product Safety Committee, United States Department of Commerce, Bethesda, Maryland).
- 19 Dempster, W. T. Space requirements of the seated operator: geometrical, kinematic and mechanical aspects of the body with reference to the limbs. *WADC Technical Note*, 55–159 (Wright Patterson Air Force Base, Ohio).
- 20 Johnson, G. R. A study of the shoulder complex with particular emphasis on the shoulder girdle. A study carried out during sabbatical leave at the Faculty of Medicine, University of Newcastle, New South Wales, 1990.
- 21 Lee, J. W. and Rim, K. Maximum finger force prediction using planar simulation of the middle finger. *Proc. Instn Mech. Engrs*, 1990, **204(H3)**, 169–178.
- 22 de Luca, C. J. and Forrest, W. J. Force analysis of individual muscles acting simultaneously on the shoulder during isometric abduction. *J. Biomechanics*, 1973, **23**, 405–414.
- 23 Landouzy, L. and Dejerine, J. De la Myopathie atrophique progressive. *Compte rendu Acad. Sci.*, 1884, **98**, 53–55.
- 24 Johnson, G. R. and Anderson, J. M. Measurement of three-dimensional shoulder movement by an electromagnetic sensor. *Clin. Biomechanics*, 1990, **5**, 131–136.

Appendix A2

Finite Helical Axis Parameters

This Appendix contains theory relevant to determining the parameters of the finite helical axis from rotation matrices and displacement vectors. The theory may also be used to determine the position of the finite centre of rotation of planar motions measured in three dimensions.

A2.1 INTRODUCTION

When a rigid body, in an initial position and orientation described by $\{A\}$, is subject to a finite motion, its new position and orientation are described by $\{B\}$ (Figure 2.1).

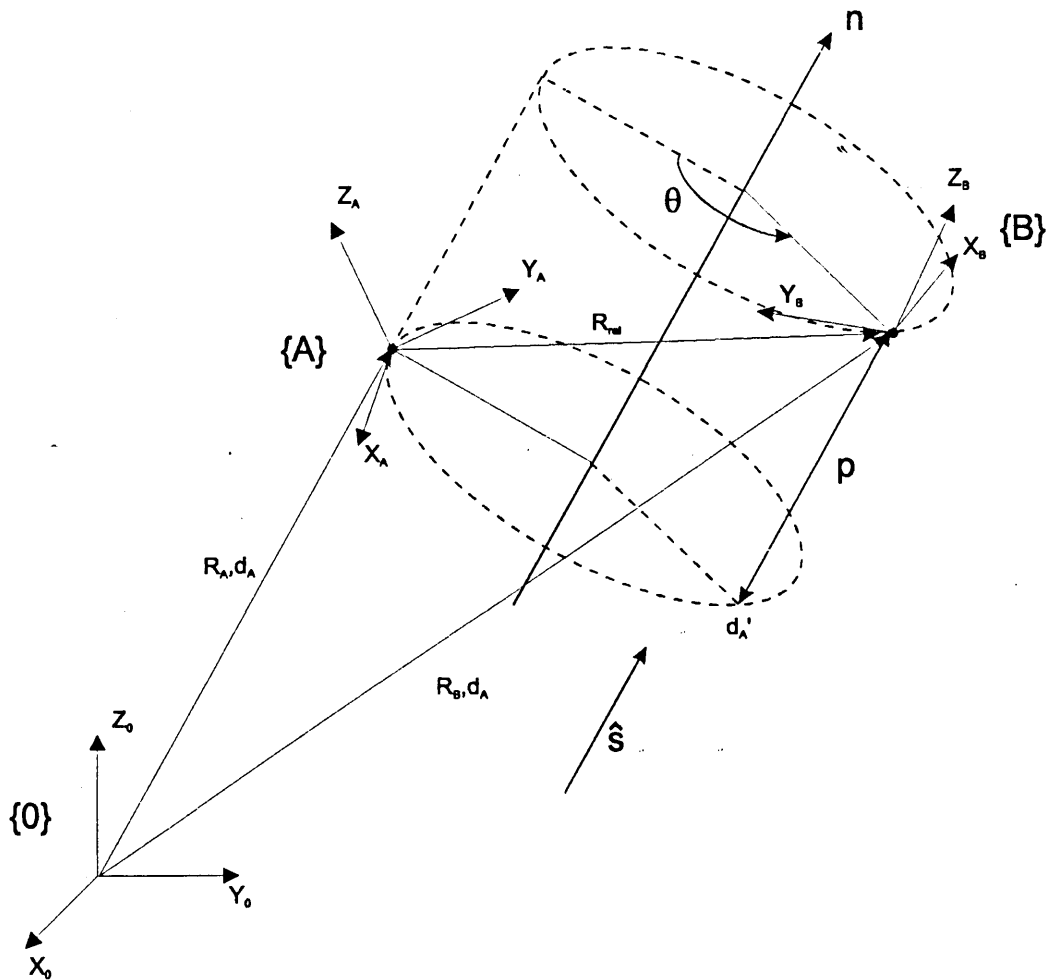
This motion may easily be described using the methods presented in Chapter 3 as a three component position vector, combined with three rotations to describe the change in orientation between $\{A\}$ and $\{B\}$. Alternatively, applying Chasles' Theorem, the motion may be represented as a single displacement p long the finite helical axis n , combined with a single rotation θ about this axis. Determination of the position and direction of the axis, together with the displacement p and the rotation θ completely describe all six degrees of freedom of the motion of the body between $\{A\}$ and $\{B\}$.



IMAGING SERVICES NORTH

Boston Spa, Wetherby
West Yorkshire, LS23 7BQ
www.bl.uk

**PAGE MISSING IN
ORIGINAL**



• Figure 2.1: Illustration of the finite helical axis

A2.2 THEORY

A2.2.1 Definitions

The origin for all measurements is $\{0\}$.

$\{R_A\}$ describes the orientation of $\{A\}$ relative to $\{0\}$.

$\{R_B\}$ describes the orientation of $\{B\}$ relative to $\{0\}$.

$\{d_A\}$ describes the position of $\{A\}$ relative to $\{0\}$.

$\{d_B\}$ describes the position of $\{B\}$ relative to $\{0\}$.

\hat{s} is a unit vector in the direction of the finite helical axis.

The rotation of the body between $\{A\}$ and $\{B\}$ about the finite helical axis is given by θ .

The displacement (or pitch component) of the body between $\{A\}$ and $\{B\}$ along the finite helical axis is given by p .

It is assumed that $\{R_A\}$, $\{R_B\}$, $\{d_A\}$ and $\{d_B\}$ are known quantities.

A2.2.2 Determination of the Direction of the Finite Helical Axis

\hat{s} is an unknown unit vector in the direction of the finite helical axis.

Let $\{R_{rel}\}$ be the relative rotation between $\{A\}$ and $\{B\}$. Hence,

$$R_{rel} = R_A^{-1} \cdot R_B \quad (2.1)$$

$\{R_{rel}\}$ is related to the direction of the finite helical axis by the following relationship:

$$R_{rel} - R_{rel}^{-1} = \begin{bmatrix} 0 & -S_z & S_y \\ S_z & 0 & -S_x \\ -S_y & S_x & 0 \end{bmatrix} \quad (2.2)$$

where the vector $S = (S_x, S_y, S_z)$ is a vector in the direction of the finite helical axis. Hence, from this, the unit vector \hat{s} can be determined.

A2.2.3 Determination of the Pitch Component, p

With \hat{s} known, the pitch component p can be easily determined using Equation 2.3.

$$p = (d_B - d_A) \cdot \hat{s} \quad (2.3)$$

A2.2.4 Determination of the Rotation, θ

The rotation θ about the finite helical axis is related to $\{R_{rel}\}$ by the following relationship:

$$2 \cdot \cos(\theta) = \text{tr}(R_{rel}) - 1 \quad (2.4)$$

Hence θ may be determined.

A2.2.5 Determination of the position of the Finite Helical Axis

The rotation about the finite helical axis, together with the translation along it are now known. The unit vector \hat{s} in the direction of the finite helical axis is also known. However, the position of the axis in space has not yet been specified.

A common method for specifying the position of the axis relies on determining a vector r_0 which is perpendicular to \hat{s} and passes through the origin $\{O\}$. The position of the finite helical axis is hence completely specified by this vector. However, this

does not reveal whereabouts on the axis the motion begins or ends, which may be of as much interest as knowledge of the axis itself.

An alternative method has therefore been developed, based on reducing the helical axis to a planar problem, and then calculating the finite centre of rotation.

The planar rotation between $\{A\}$ and $\{B\}$ about the finite helical axis may be represented as shown in Figure 2.2. The work plane is represented by the broken circle, and is normal to the finite helical axis. The finite centre of rotation between the start and end of the motion is represented by C .

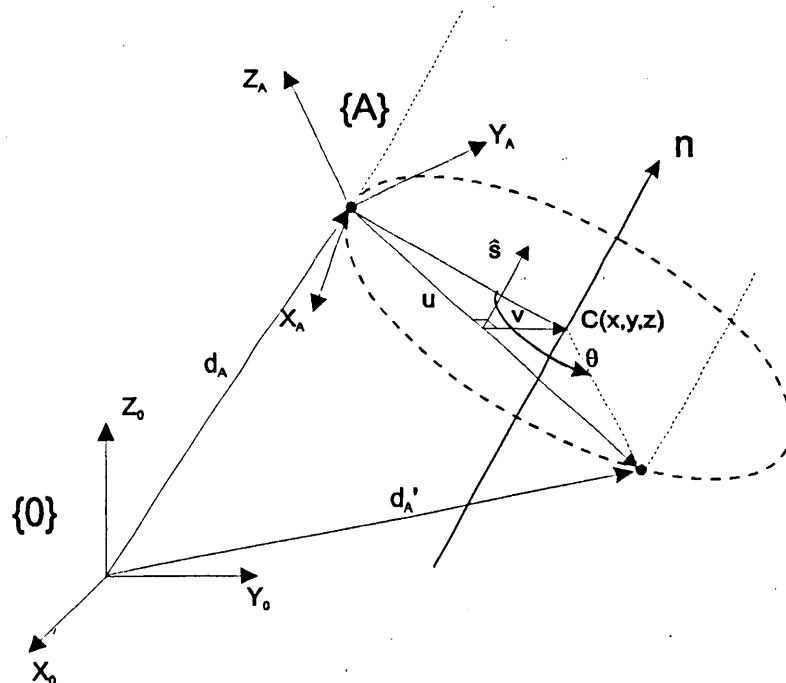


Figure 2.2: Reduction of the finite helical axis to a planar situation

The co-ordinates of C may be determined by knowledge of the vectors u and v . Using simple vector algebra:

$$C = d_A + \frac{u}{2} + v \quad (2.5)$$

The planar motion may be described as a vector u between the points d_A and d_A' , where d_A' may be determined from the relationship:

$$d_A' = d_B - p_n \cdot \hat{s} \quad (2.6)$$

Hence, the vector u may be determined from:

$$u = d_A' - d_A \quad (2.7)$$

The vector v may be calculated by knowledge of the direction of u and the unit vector \hat{s} which is normal to the work plane.

Let \hat{u} be a unit vector in the direction of u . \hat{s} is a unit vector perpendicular to \hat{u} , hence a unit vector \hat{v} may be calculated from :

$$\hat{v} = \hat{u} \times \hat{s} \quad (2.8)$$

Due to orthogonality, the vector \hat{v} will be in the direction of v , that is, towards the centre of rotation C .

It is now necessary to determine the magnitude of v in order to completely specify the position of C .

By simple trigonometry, v may be determined from:

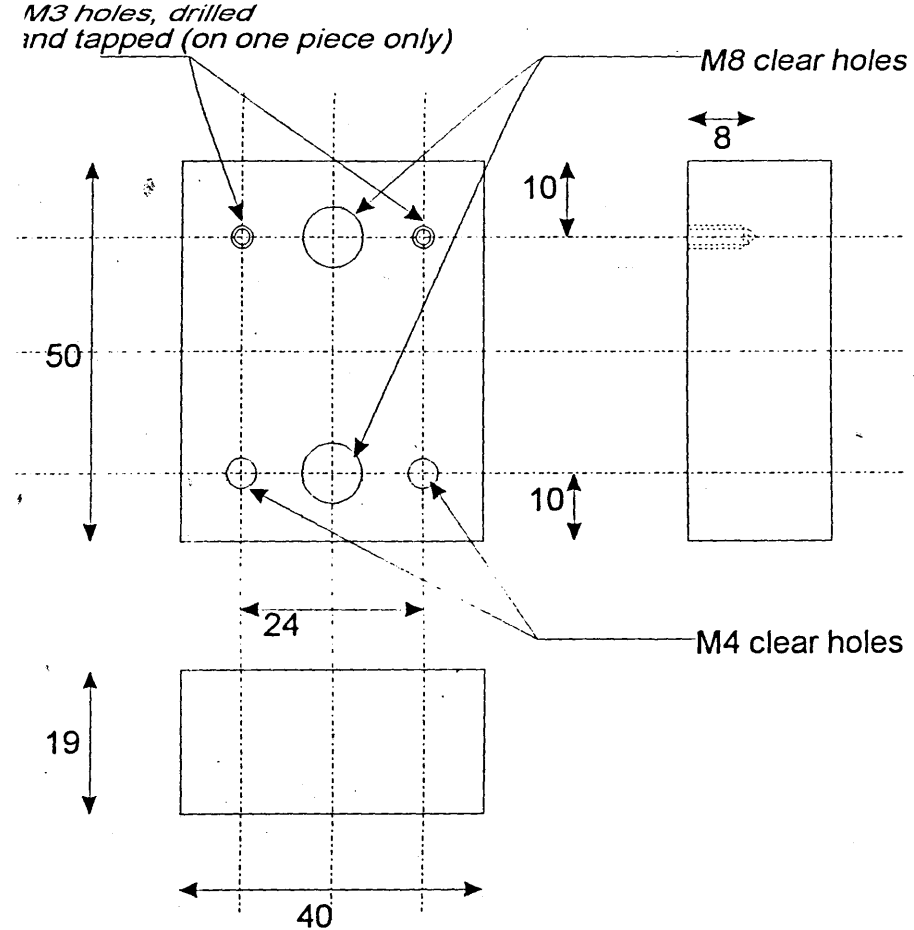
$$v = \hat{v} \cdot \frac{|u|}{2 \cdot \tan\left(\frac{\theta}{2}\right)} \quad (2.9)$$

Hence, using Equation 2.5, the co-ordinates of C may be determined. This represents the point of the helical axis at which the motion started. The point on the axis may be determined by simply adding the pitch component along the axis.

Appendix A3

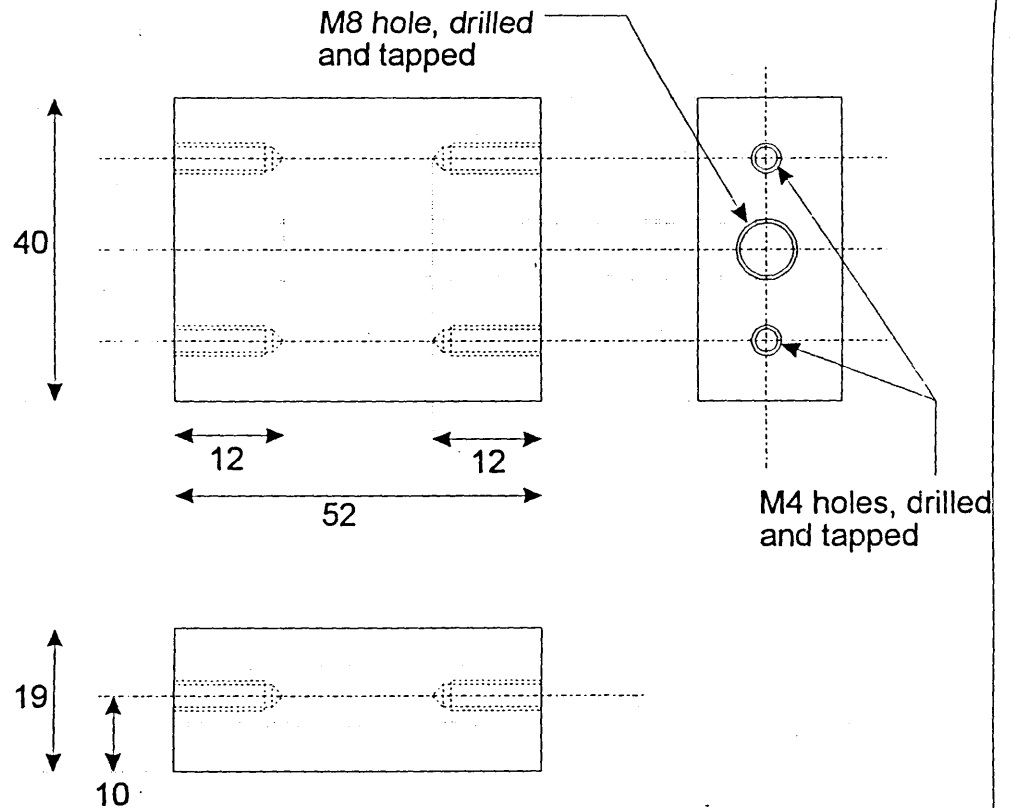
Design Drawings

This appendix contains design drawings for the Locator, the Sternal Receiver Mount and the Isotrak[®] calibration rig. These items are described in Chapter 5.



Part Number 1 (Carriage end).
2 No. of.

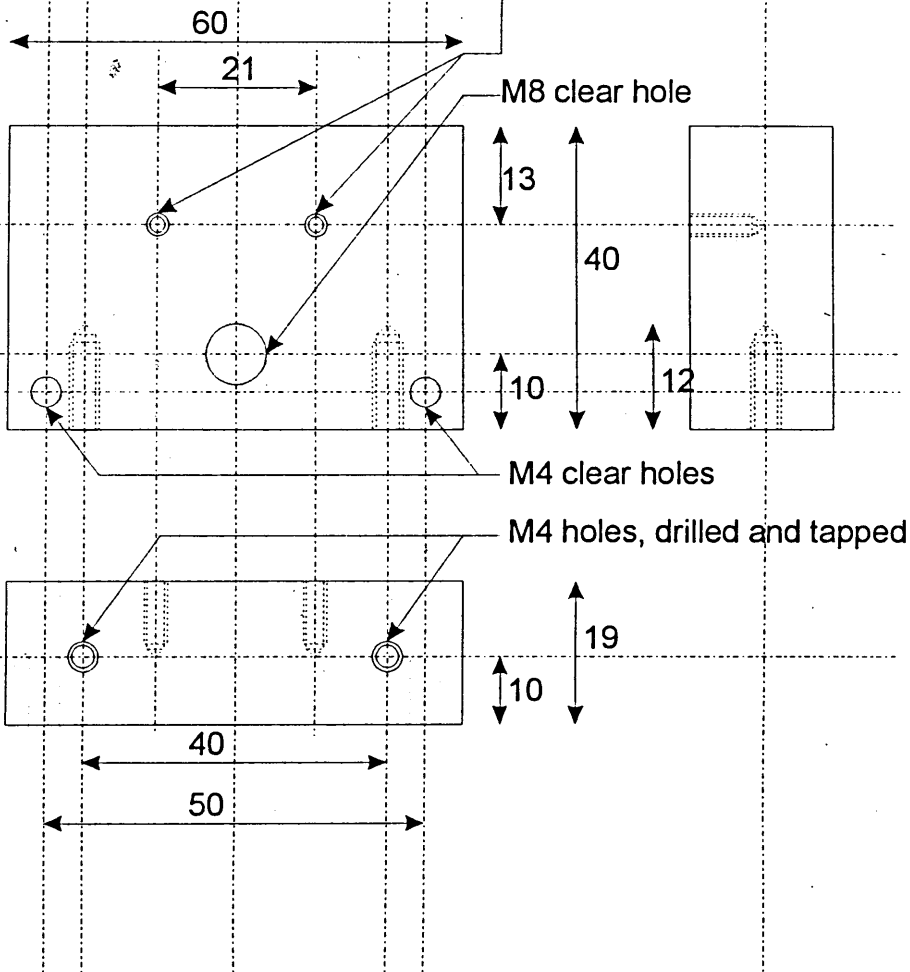
All dimensions in mm.
To be made in perspex.



Part Number 2 (Carriage base).
1 No. of.

Title	Helical Axis Rig.
Name	N. D. Barnett.
Dept	Mech.Eng.(Rm T4)
Sheet	1 of 3
Date	24.11.94.

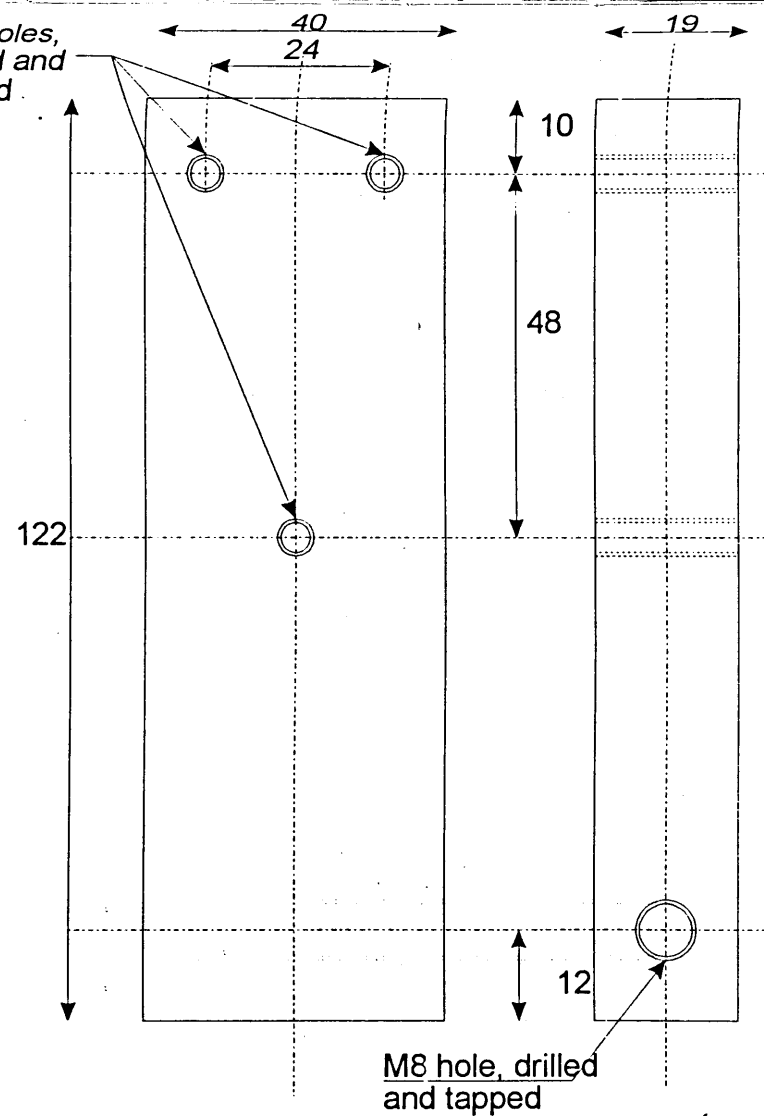
M3 holes, drilled and tapped
(one piece only)



Part Number 3 (Base end).
2 No. of.

All dimensions in mm.
To be made in perspex.

M5 holes,
drilled and
tapped



Part Number 4
(Helix arm).
1 No. of.

Title	<i>Helical Axis Rig.</i>
Name	<i>N. D. Barnett.</i>
Dept	<i>Mech.Eng.(Rm T4)</i>
Sheet	2 of 3
Date	24.11.94

Other parts.

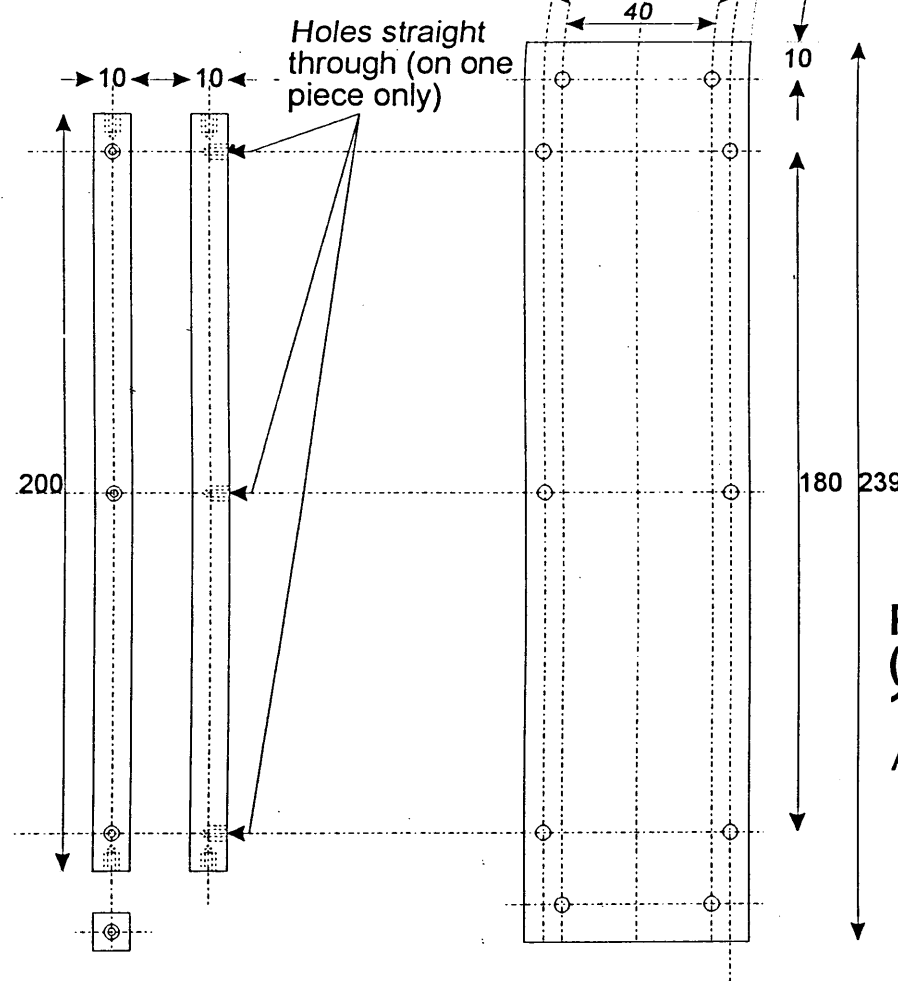
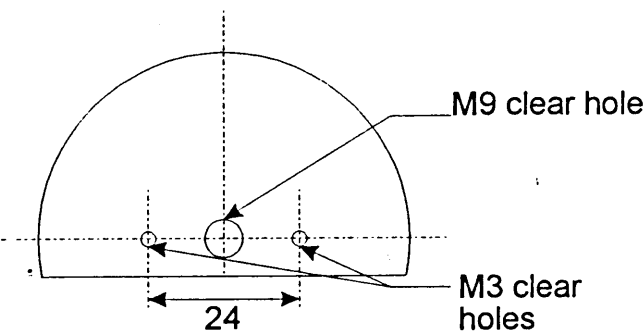
Nylon bolts:

- M3 x 25 2.No.
- M3 x 10 2.No.
- M4 x 25 18.No.
- M5 x 25 3.No.
- M8 nuts 6.No.
- M8 wing nuts 2.No.

M8 nylon studding (provided):

- 260mm 1.No.
- 100mm 1.No.

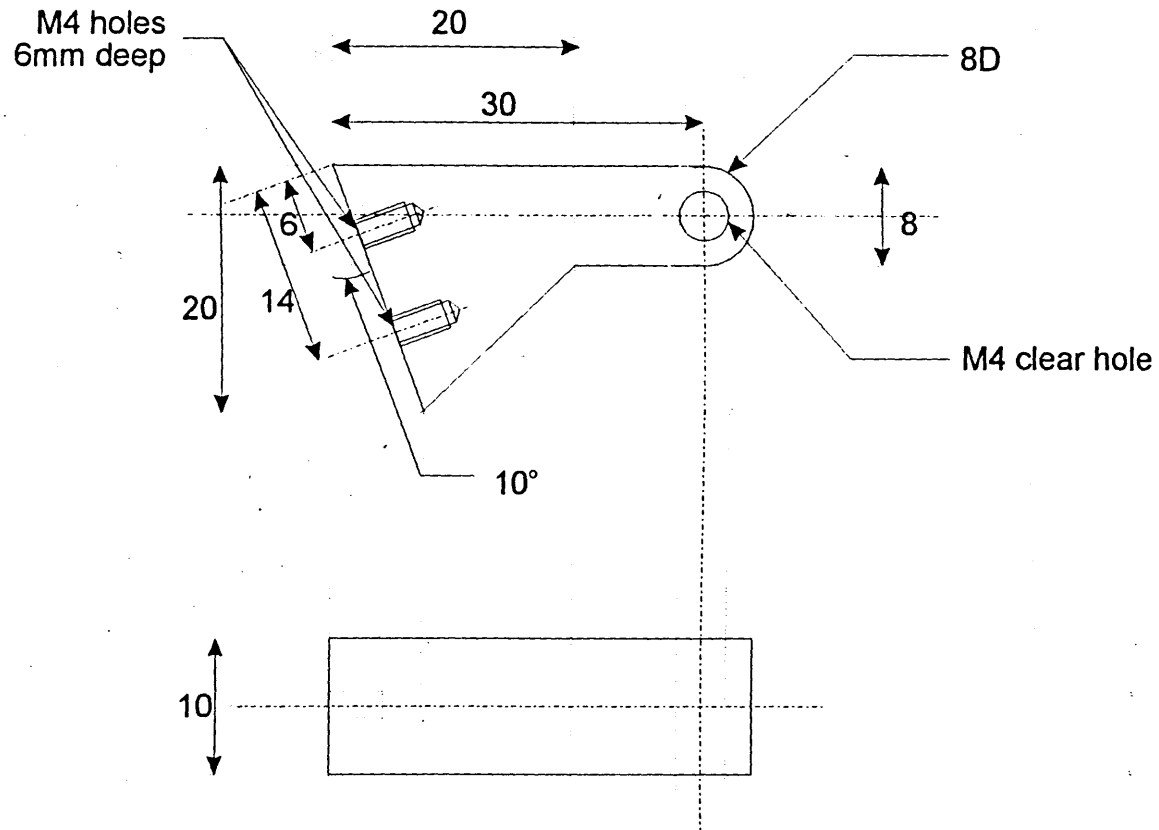
Protractor (provided),
drilled as shown below.



**Part Number 6
(Base plate).
1 No. of.**
All holes M4 clear.

**Part Number 5
(Base side).
2 No. of.**
All holes M4 drilled and
tapped, 6mm deep, unless
otherwise stated.
*All dimensions in mm.
To be made in perspex.*

Title	Helical Axis Rig.
Name	N. D. Barnett.
Dept	Mech.Eng.(Rm T4)
Sheet	3 of 3
Date	24.11.94.



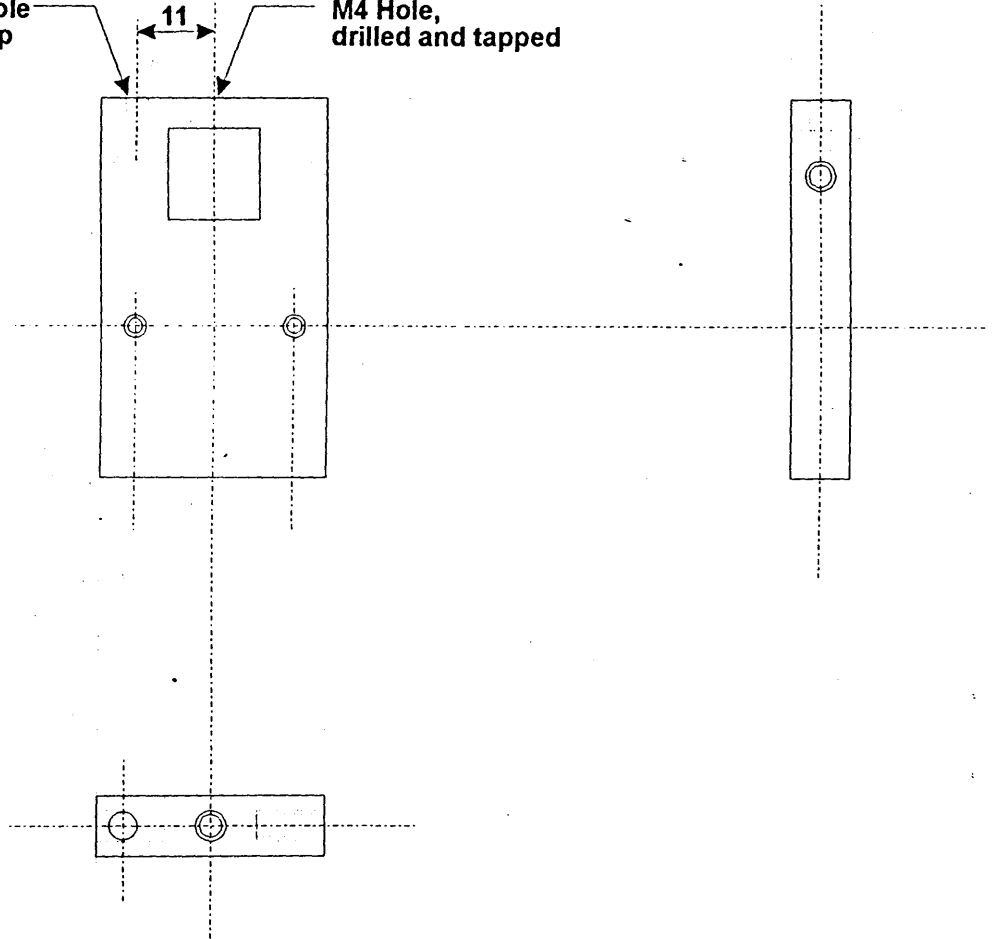
To be made in Perspex.
All dimensions in mm.

Title	Sternum support
Name	N. D. Barnett.
Dept	Mech.Eng.(Rm T4)
Sheet	2 of 3
Date	13.10.94

M4 Hole
6 deep

11

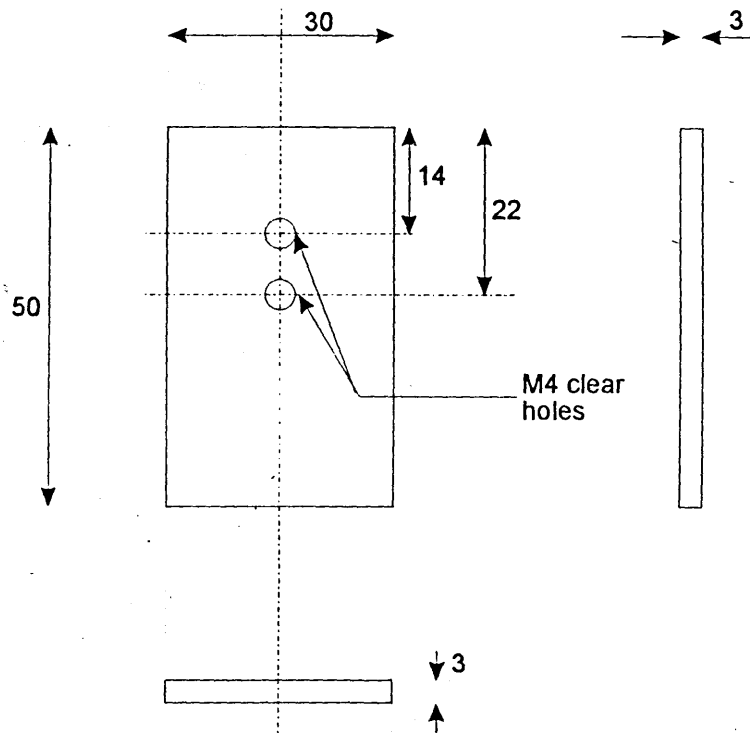
M4 Hole,
drilled and tapped



To be made in Perspex.

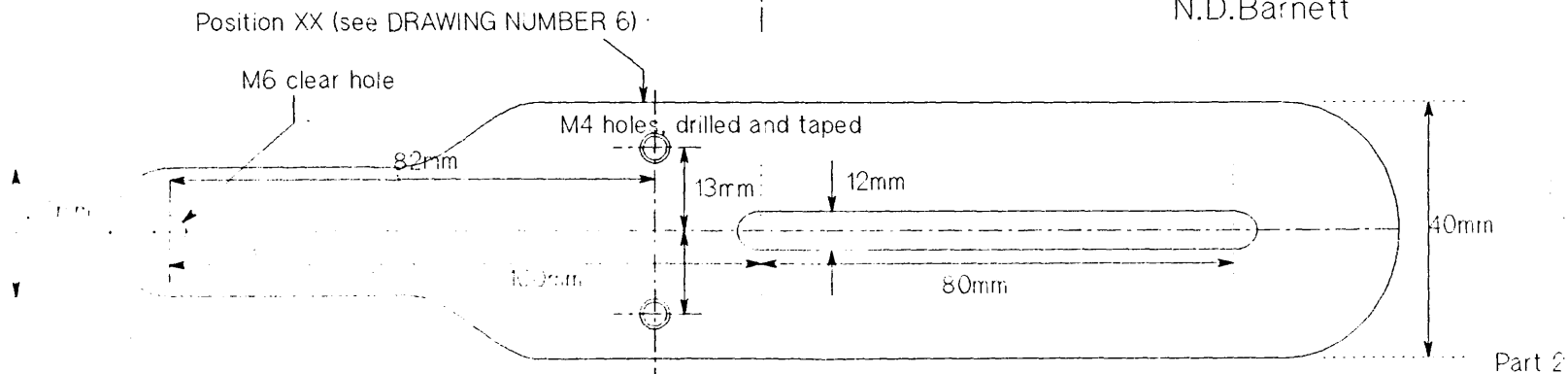
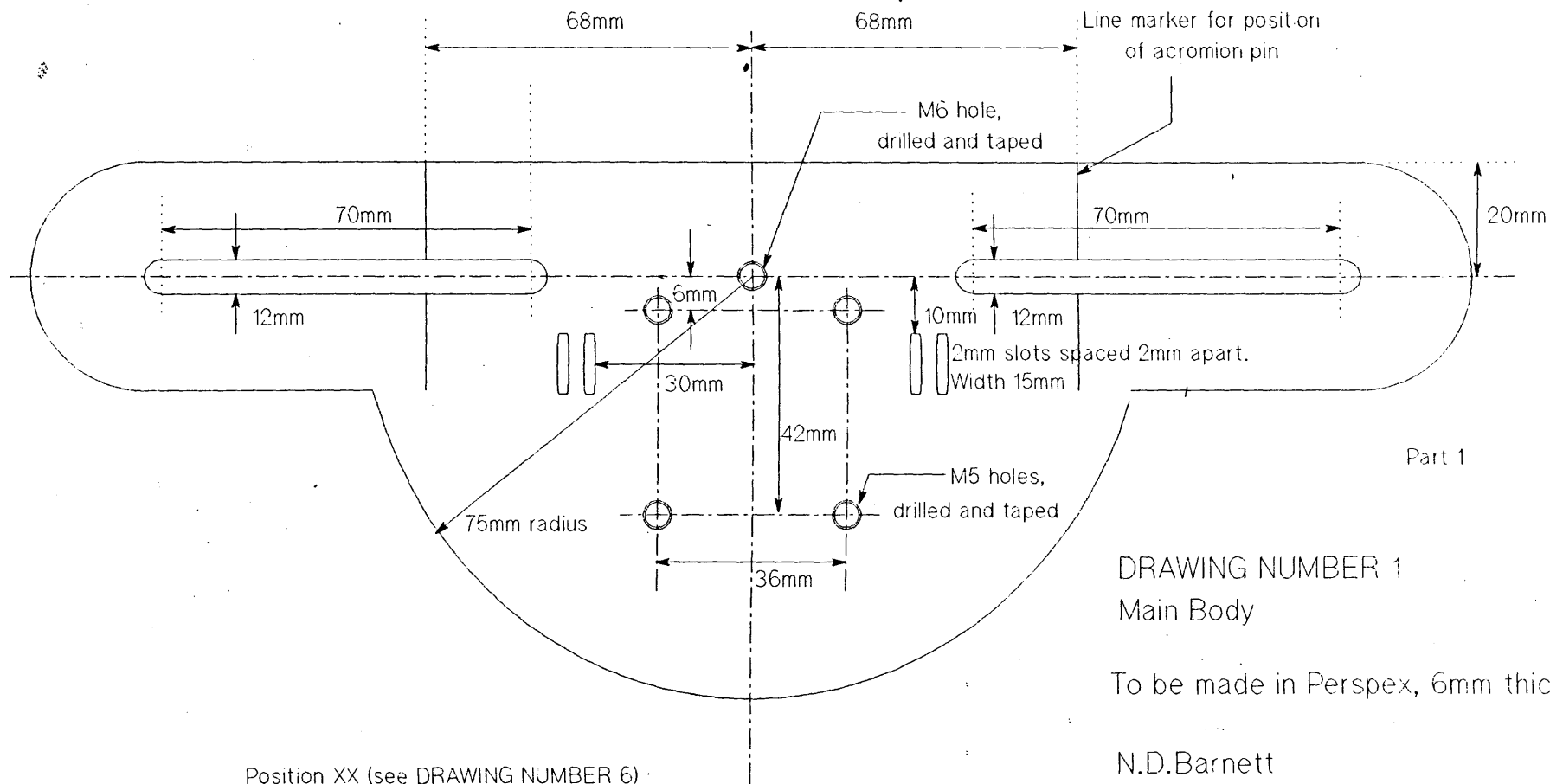
All dimensions in mm.

Title	<i>Sternum support</i>
Name	<i>N. D. Barnett.</i>
Dept	<i>Mech.Eng.(Rm M7)</i>
Sheet	<i>3 of 3</i>
Date	<i>10.4.96</i>

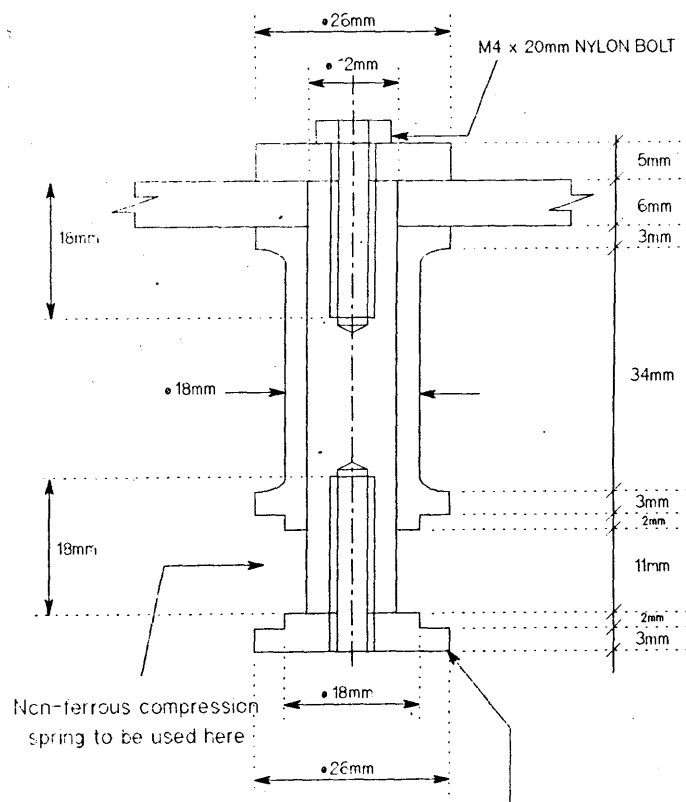


To be made in Perspex.
All dimensions in mm.

Title	<i>Sternum support</i>
Name	<i>N. D. Barnett.</i>
Dept	<i>Mech.Eng.(Rm T4)</i>
Sheet	<i>1 of 3</i>
Date	<i>13.10.94</i>



General Assembly for leg fixtures



Detail of ends specific
to individual pin.
See Drawing Numbers 4 and 5

DRAWING NUMBER 2

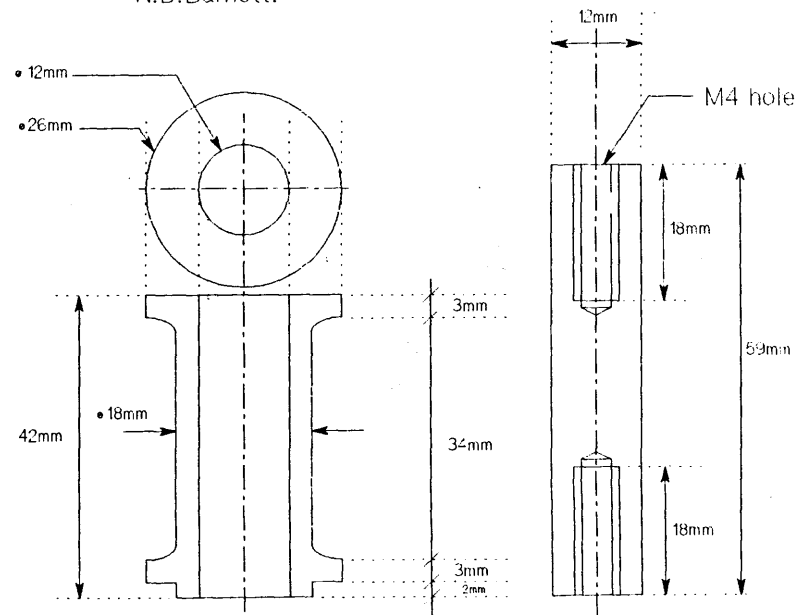
Pin detail for Acromion and

Root of scapular spine

Quantity of two number (2) required
for each part

All to be made in Perspex or nylon

N.D.Barnett.

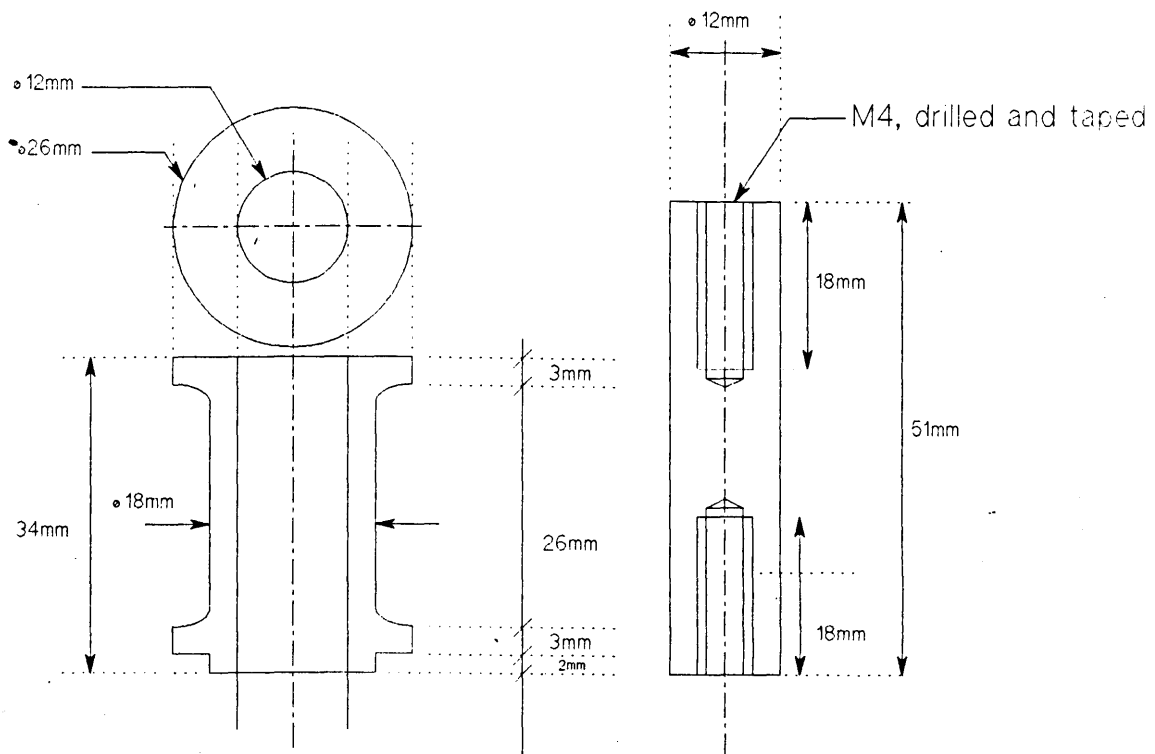
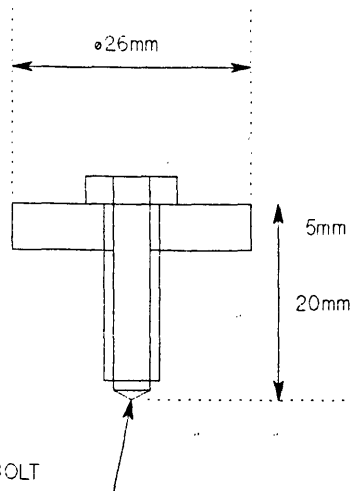


DRAWING NUMBER 3

Pin detail for inferior angle.

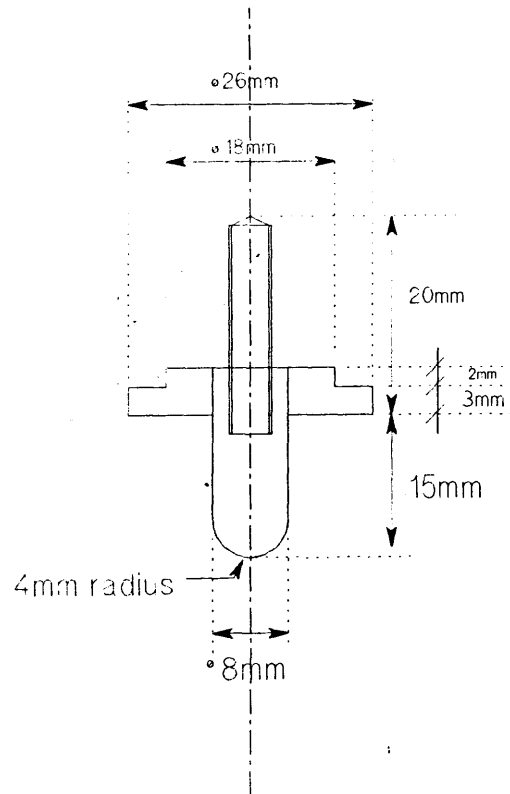
All to be made
in Perspex or Nylon

N.D.Barnett.

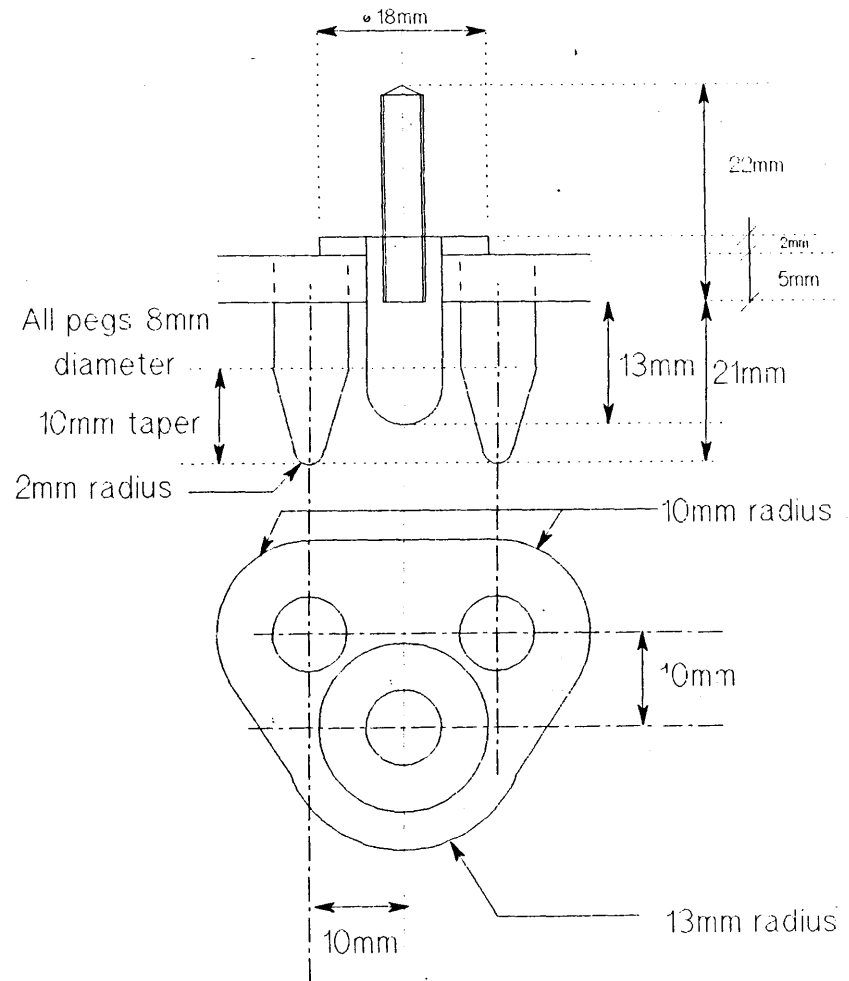


DRAWING NUMBER 4

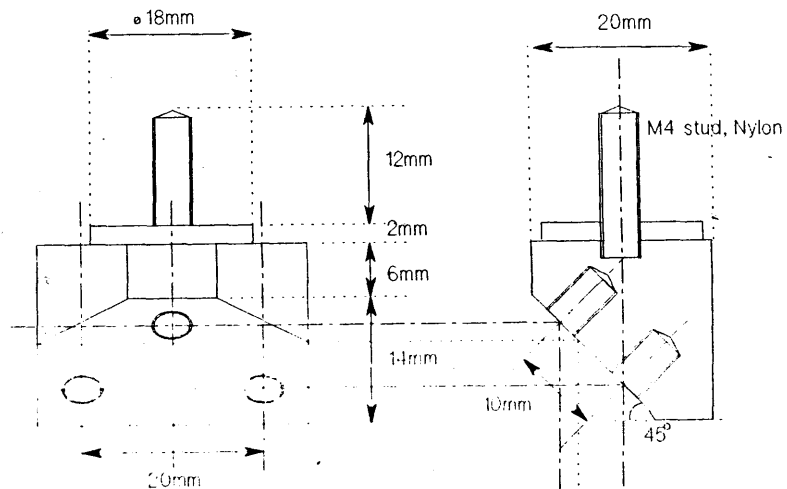
N.D.Barnett



End detail for
acromion pin



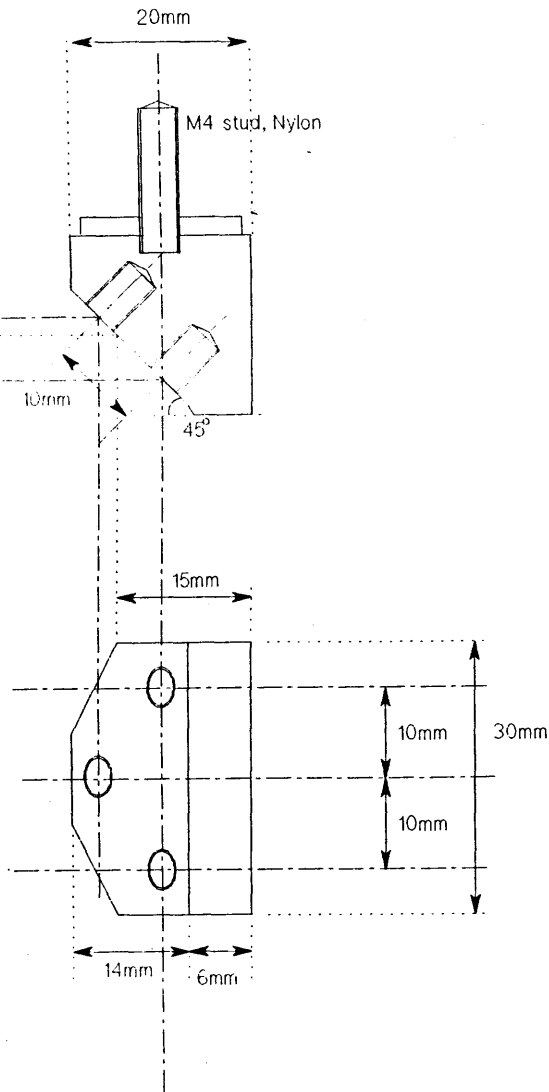
End detail for inferior
angle pin



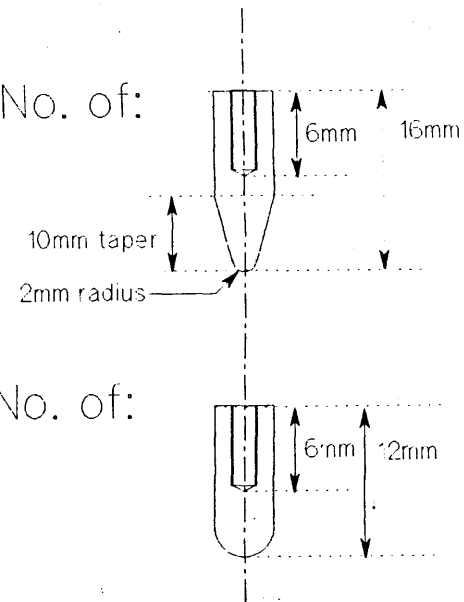
DRAWING NUMBER 5

End detail for root of the
scapula spine pin
N. D. Barnett.

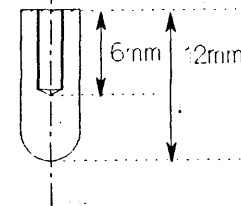
Made in perspex.
All hole drilled and taped, M4 x 6mm.



2 No. of:

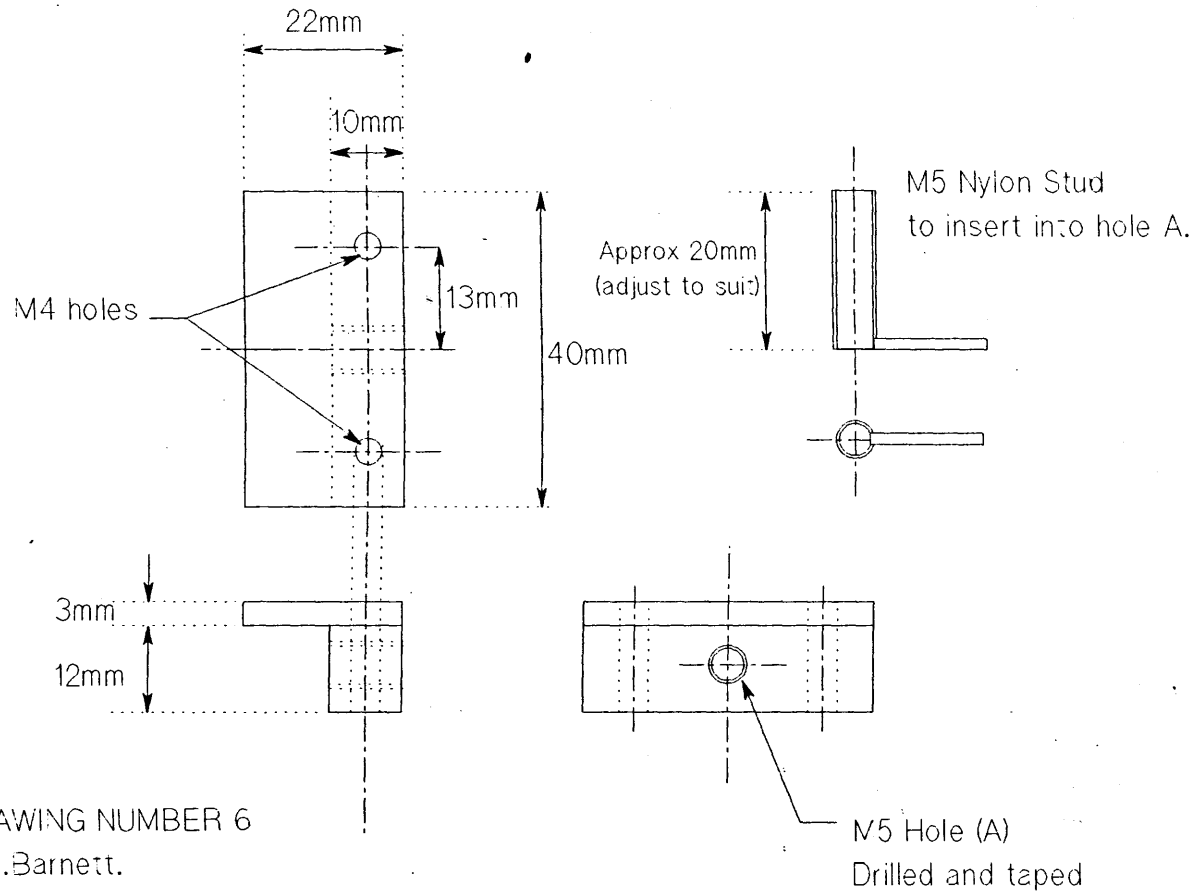


1 No. of:



All holes M4,
drilled and taped
All pegs 8mm
diameter

Made in perspex.



DRAWING NUMBER 6
N.D.Barnett.

To be made in perspex

This is to be fitted on the swing arm
of the main body (Part 2, Drawing 1)

See also Part 1, Drawing 1

The structure adds strength
to the whole unit, while the stud acts as a position
lock onto the radius of the main body (Part 1, Drawing 1)



IMAGING SERVICES NORTH

Boston Spa, Wetherby
West Yorkshire, LS23 7BQ
www.bl.uk

**PAGE MISSING IN
ORIGINAL**

Appendix A4

Results

This Appendix contains details of the numerical data obtained within the validation studies. The rotations of the scapula in the z_{α} , y_{β}' , x_{γ}'' rotation sequence are also included.

Beyond this, the regression coefficients obtained from modelling scapulohumeral kinematics on the eleven subjects used in Chapter 7 are presented, in both y_{β} , z_{α}' , x_{γ}'' and z_{α} , y_{β}' , x_{γ}'' rotation sequences. The regression coefficients for each subject and the final model using the global (thorax) co-ordinate system are also included.

A4.1 SINGLE CHANNEL VALIDATION STUDY

A4.1.1 Rotations of the Scapula

A4.1.1.1 Numerical Results (y_{β} , z_{α}' , x_{γ}'' sequence)

<i>Elevation</i>	<i>Abduction</i>	<i>alpha</i>	<i>SD</i>	<i>beta</i>	<i>SD</i>	<i>gamma</i>	<i>SD</i>
80	10	0.00	0.00	0.00	0.00	0.11	0.35
80	10	0.84	0.88	-0.29	0.36	-0.15	1.32
70	20	2.68	2.92	1.14	2.18	-0.77	2.29
60	30	3.90	2.80	1.84	1.42	-0.96	2.97
50	40	5.97	4.78	1.78	1.57	0.44	3.30
40	50	8.74	4.54	1.70	2.22	2.77	4.47
30	60	10.60	3.57	2.54	2.33	5.02	3.29
20	70	14.69	5.44	3.11	2.43	6.41	3.48
10	80	20.23	4.33	4.57	2.28	6.03	3.35
0	90	26.50	4.47	6.44	3.88	5.67	4.46

Table 4.1: Mean rotations and standard deviations for subject 1, y_{β} , z_{α}' , x_{γ}'' rotation sequence, single channel study

Elevation	Abduction	α	SD	β	SD	γ	SD
80	10	0.00	0.00	0.00	0.01	0.04	0.14
80	10	-0.07	0.96	0.47	1.01	-0.57	1.36
70	20	3.88	1.52	2.24	2.34	-0.99	2.13
60	30	4.94	2.61	2.13	1.75	0.33	3.80
50	40	5.81	1.99	2.68	1.65	1.20	2.78
40	50	6.35	2.53	2.03	2.05	2.56	3.37
30	60	9.02	4.27	1.42	3.46	3.92	4.49
20	70	11.45	4.87	0.97	2.98	4.89	3.99
10	80	14.81	6.03	2.07	3.18	6.51	4.30
0	90	19.58	6.29	3.58	3.56	5.52	5.07

Table 4.2: Mean rotations and standard deviations for subject 2, $y_\beta, z_\alpha', x_\gamma''$ rotation sequence, single channel study

Elevation	Abduction	α	SD	β	SD	γ	SD
80	10	0.00	0.00	0.00	0.00	-0.02	0.06
80	10	-0.06	0.66	-0.28	0.66	0.57	1.26
70	20	4.06	3.87	1.30	2.25	1.03	2.26
60	30	8.65	4.29	2.16	1.12	1.63	2.55
50	40	10.74	3.43	3.50	2.20	1.84	3.46
40	50	15.14	4.50	4.75	2.42	1.81	4.08
30	60	18.21	6.20	5.09	3.01	1.68	4.56
20	70	24.83	5.36	6.08	3.12	0.54	4.86
10	80	29.72	4.47	6.35	3.20	-1.36	4.59
0	90	34.32	5.88	7.91	5.10	-2.58	4.27

Table 4.3: Mean rotations and standard deviations for subject 3, $y_\beta, z_\alpha', x_\gamma''$ rotation sequence, single channel study

Elevation	Abduction	α	SD	β	SD	γ	SD
80	10	0.00	0.00	0.01	0.01	-0.12	0.36
80	10	0.30	1.52	0.16	0.92	-0.18	0.80
70	20	2.66	2.22	1.98	2.14	-2.13	2.50
60	30	4.19	2.67	2.64	2.02	-1.16	3.17
50	40	6.14	3.63	3.60	1.65	0.95	3.69
40	50	12.06	6.00	5.77	3.13	3.98	4.41
30	60	15.92	5.21	5.49	2.18	7.12	4.04
20	70	20.47	4.99	5.76	3.59	10.00	5.62
10	80	24.19	4.81	7.03	4.37	12.56	5.23
0	90	27.58	4.82	8.75	4.82	9.38	5.20

Table 4.4: Mean rotations and standard deviations for subject 4, $y_\beta, z_\alpha', x_\gamma''$ rotation sequence, single channel study

Elevation	Abduction	α	SD	β	SD	γ	SD
80	10	0.00	0.00	0.01	0.01	0.05	0.15
80	10	0.72	1.58	-0.39	1.78	0.32	1.45
70	20	0.71	2.50	1.28	1.49	1.04	1.84
60	30	1.93	2.28	2.67	3.12	2.17	3.97
50	40	3.56	2.91	3.57	2.76	4.40	5.20
40	50	5.69	3.17	3.38	2.54	8.40	3.30
30	60	8.69	3.66	4.06	2.68	11.27	3.78
20	70	15.17	2.52	5.61	4.68	13.53	4.14
10	80	21.41	2.66	7.40	4.75	14.23	4.12
0	90	25.36	4.84	9.23	5.50	13.13	6.77

Table 4.5: Mean rotations and standard deviations for subject 5, $y_\beta, z_\alpha, x_\gamma$ rotation sequence, single channel study

A4.1.1.2 Graphical Results ($z_\alpha, y_\beta, x_\gamma$ sequence)

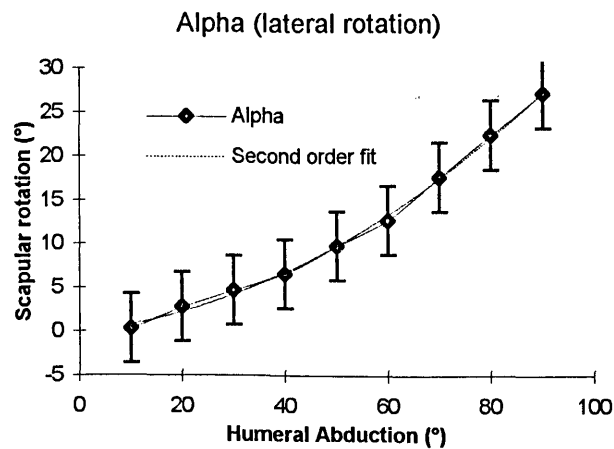


Figure 4.1: Rotation angle α during humeral abduction, $z_\alpha, y_\beta, x_\gamma$ one channel study

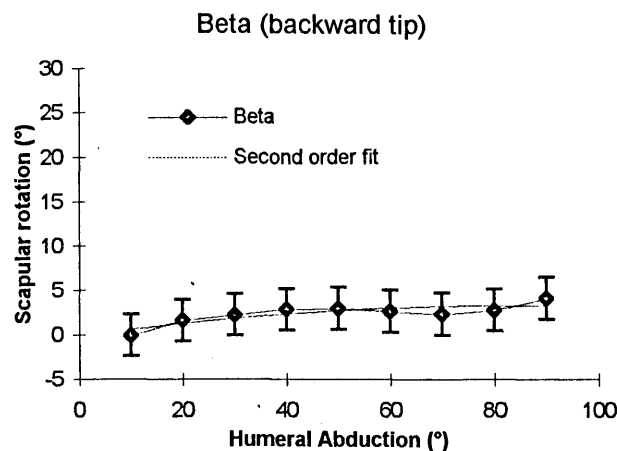


Figure 4.2: Rotation angle β during humeral abduction, $z_\alpha, y_\beta, x_\gamma$ one channel study

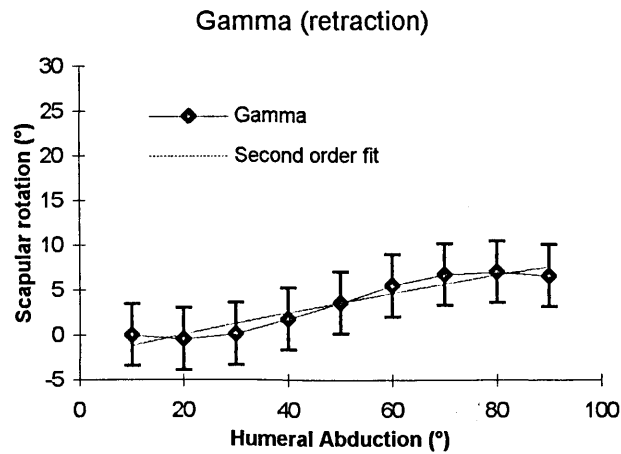


Figure 4.3: Rotation angle γ during humeral abduction, $z_\alpha, y_\beta', x_\gamma''$ one channel study

A4.1.1.3 Numerical Results ($z_\alpha, y_\beta', x_\gamma''$ sequence)

Elevation	Abduction	alpha	SD	beta	SD	gamma	SD
80	10	0.00	0.00	0.00	0.00	0.00	0.00
80	10	0.84	0.88	-0.28	0.38	-0.23	1.20
70	20	2.66	2.91	1.15	2.22	-0.73	2.34
60	30	3.83	2.84	1.89	1.47	-1.16	2.67
50	40	5.98	4.76	1.75	1.60	0.30	3.10
40	50	8.75	4.60	1.34	2.44	2.48	4.18
30	60	10.74	3.64	1.62	2.39	4.72	2.95
20	70	14.93	5.54	1.58	2.19	6.03	3.18
10	80	20.51	4.38	2.42	2.80	5.80	3.32
0	90	26.90	4.58	3.54	4.55	5.98	3.75

Table 4.6: Mean rotations and standard deviations for subject 1, $z_\alpha, y_\beta', x_\gamma''$ rotation sequence, one channel study

Elevation	Abduction	alpha	SD	beta	SD	gamma	SD
80	10	0.00	0.00	0.00	0.01	0.00	0.01
80	10	-0.09	0.94	0.47	1.02	-0.58	1.35
70	20	3.80	1.48	2.32	2.42	-1.20	1.82
60	30	4.90	2.54	2.15	1.90	-0.15	3.00
50	40	5.86	2.02	2.52	1.70	1.41	3.18
40	50	6.42	2.56	1.74	2.09	2.10	2.47
30	60	8.97	4.42	0.74	3.64	3.70	4.17
20	70	11.46	5.03	-0.03	2.86	4.79	3.94
10	80	14.75	6.16	0.34	3.92	6.40	4.35
0	90	19.61	6.42	1.34	4.71	6.12	4.61

Table 4.7: Mean rotations and standard deviations for subject 2, $z_\alpha, y_\beta', x_\gamma''$ rotation sequence, one channel study

Elevation	Abduction	α	SD	β	SD	γ	SD
80	10	0.00	0.00	0.00	0.00	0.00	0.00
80	10	-0.07	0.68	-0.28	0.65	0.30	1.09
70	20	4.12	3.89	1.23	2.17	0.93	2.15
60	30	8.70	4.28	1.97	1.21	1.27	1.90
50	40	10.80	3.37	3.23	2.42	1.88	3.50
40	50	15.24	4.43	4.34	2.71	1.96	4.13
30	60	18.29	6.09	4.82	3.15	1.74	4.41
20	70	24.88	5.21	5.94	3.26	0.86	4.49
10	80	29.53	4.23	7.25	3.69	-1.25	3.89
0	90	34.03	5.55	9.42	5.53	-1.85	3.65

Table 4.8: Mean rotations and standard deviations for subject 3, $z_\alpha, y_\beta', x_\gamma''$ rotation sequence, one channel study

Elevation	Abduction	α	SD	β	SD	γ	SD
80	10	0.00	0.00	-0.01	0.01	0.00	0.01
80	10	0.30	1.52	0.16	0.92	-0.10	0.62
70	20	2.66	2.24	2.07	2.02	-2.06	2.49
60	30	4.18	2.69	2.68	1.96	-1.23	3.18
50	40	6.22	3.81	3.40	1.47	1.02	3.59
40	50	12.46	6.35	4.82	2.39	3.67	4.51
30	60	16.40	5.54	3.48	1.63	6.10	4.40
20	70	21.12	5.47	2.10	2.76	9.11	5.16
10	80	25.09	5.50	1.66	3.08	11.01	4.65
0	90	28.60	5.52	3.59	4.00	9.20	3.41

Table 4.9: Mean rotations and standard deviations for subject 4, $z_\alpha, y_\beta', x_\gamma''$ rotation sequence, one channel study

Elevation	Abduction	α	SD	β	SD	γ	SD
80	10	0.00	0.00	-0.01	0.01	0.00	0.00
80	10	0.71	1.58	-0.39	1.79	0.54	1.26
70	20	0.72	2.50	1.25	1.52	0.79	2.03
60	30	1.89	2.32	2.57	3.19	1.82	3.92
50	40	3.73	3.04	3.26	2.91	4.32	5.20
40	50	6.09	3.25	2.55	2.47	7.70	3.22
30	60	9.34	3.88	2.21	2.31	11.12	3.71
20	70	16.11	2.97	1.98	4.05	12.82	3.99
10	80	22.63	3.02	2.07	3.76	13.05	3.70
0	90	26.75	5.75	2.48	4.26	13.20	4.16

Table 4.10: Mean rotations and standard deviations for subject 5, $z_\alpha, y_\beta', x_\gamma''$ rotation sequence, one channel study

A4.1.2 Displacements of the Scapula, Numerical Results

Elevation	Abduction	x	SD	y	SD	z	SD
80	10	0.00	0.00	0.00	0.00	0.00	0.00
80	10	1.69	2.45	0.04	0.60	-0.10	2.18
70	20	1.81	4.53	0.65	3.10	-4.26	4.84
60	30	5.17	4.64	-0.20	3.92	-5.14	5.90
50	40	10.22	6.55	-1.71	4.13	-1.91	7.66
40	50	16.51	6.00	-4.09	6.07	2.34	9.21
30	60	22.82	5.99	-5.86	4.27	6.99	7.05
20	70	28.15	7.08	-6.24	4.77	10.19	9.50
10	80	34.69	6.03	-6.69	3.95	9.38	10.88
0	90	38.53	5.64	-7.58	4.60	10.79	11.27

Table 4.11: Mean displacements and standard deviations for subject 1, one channel study

Elevation	Abduction	x	SD	y	SD	z	SD
80	10	0.00	0.00	0.00	0.00	0.00	0.00
80	10	-0.43	2.64	0.45	1.38	-0.70	1.49
70	20	0.87	3.54	-1.04	2.39	0.07	3.53
60	30	5.12	5.13	-4.18	3.07	4.42	5.98
50	40	5.53	5.17	-5.43	2.44	7.64	7.79
40	50	9.59	7.15	-9.58	2.54	10.27	6.50
30	60	12.65	9.28	-12.67	4.58	14.53	9.18
20	70	17.38	9.12	-18.38	4.75	18.63	11.45
10	80	20.79	10.88	-19.43	4.72	22.64	15.20
0	90	28.25	9.03	-20.80	3.78	21.09	13.65

Table 4.12: Mean displacements and standard deviations for subject 2, one channel study

Elevation	Abduction	x	SD	y	SD	z	SD
80	10	0.00	0.00	0.00	0.00	0.00	0.00
80	10	-1.18	2.06	-0.37	1.30	2.07	3.00
70	20	5.18	6.08	-4.38	2.37	4.36	6.90
60	30	12.05	8.72	-6.20	3.02	5.37	6.54
50	40	17.03	10.83	-6.63	4.69	5.69	9.09
40	50	23.44	9.43	-6.97	3.10	5.30	11.57
30	60	29.53	11.11	-8.50	5.64	4.03	13.28
20	70	35.76	11.66	-6.63	5.03	1.00	13.84
10	80	43.59	9.02	-3.34	5.62	-5.90	11.89
0	90	45.56	9.13	-1.98	6.40	-8.13	10.67

Table 4.13: Mean displacements and standard deviations for subject 3, one channel study

Elevation	Abduction	x	SD	y	SD	z	SD
80	10	0.00	0.00	0.00	0.00	0.00	0.00
80	10	-0.23	2.48	-0.45	1.59	-0.01	2.21
70	20	0.02	4.39	-2.23	3.84	1.10	6.46
60	30	1.93	5.28	-3.99	4.58	1.14	6.01
50	40	3.02	5.22	-5.16	4.93	8.59	7.32
40	50	9.19	4.46	-10.85	7.02	16.59	9.68
30	60	16.85	5.07	-16.40	5.63	23.05	9.74
20	70	24.48	7.06	-24.24	7.88	31.30	10.95
10	80	28.71	5.51	-28.11	7.40	34.94	10.13
0	90	33.58	6.92	-24.83	7.74	31.45	8.99

Table 4.14: Mean displacements and standard deviations for subject 4, one channel study

Elevation	Abduction	x	SD	y	SD	z	SD
80	10	0.00	0.00	0.00	0.00	0.00	0.00
80	10	-0.07	2.51	0.01	0.58	2.25	3.81
70	20	0.25	5.68	-2.95	1.81	4.62	5.81
60	30	1.53	4.53	-3.55	2.03	7.40	8.35
50	40	4.36	5.03	-6.80	5.08	15.94	12.53
40	50	7.55	6.33	-10.55	3.12	24.73	8.67
30	60	11.69	7.47	-12.36	4.07	31.08	10.51
20	70	20.36	11.64	-14.80	3.30	36.47	10.30
10	80	27.73	9.61	-11.40	5.05	37.02	9.12
0	90	32.66	10.27	-9.86	4.18	36.44	11.73

Table 4.15: Mean displacements and standard deviations for subject 5, one channel study

A4.2 TWO CHANNEL VALIDATION STUDY

A4.2.1 Rotations of the scapula

A4.2.1.1 Numerical Results (y_β , z_α' , x_γ'' sequence)

Elevation	Abduction	alpha	SD	beta	SD	gamma	SD
80	10	0.00	0.00	0.00	0.00	0.02	0.04
80	10	-0.15	0.24	-0.12	0.64	0.89	2.16
70	20	-4.45	2.75	-0.31	1.62	6.00	3.41
60	30	-7.78	3.37	-1.11	2.14	7.83	5.05
50	40	-11.23	2.22	-1.33	1.99	9.45	4.18
40	50	-12.33	1.70	-1.49	3.10	11.01	4.54
30	60	-12.95	3.46	-2.12	3.89	10.43	4.52
20	70	-16.93	2.56	-3.47	3.75	10.65	5.38
10	80	-19.69	4.08	-5.00	4.18	11.35	5.52
0	90	-27.59	2.53	-8.64	4.11	9.18	5.37

Table 4.16: Mean rotations and standard deviations for subject 1, y_β , z_α' , x_γ'' rotation sequence, two channel study

Elevation	Abduction	α	SD	β	SD	γ	SD
80	10	0.00	0.00	0.00	0.01	-0.02	0.06
80	10	-0.08	0.33	-0.35	0.74	-0.60	1.49
70	20	-1.04	2.55	-1.46	2.37	-1.16	1.97
60	30	-2.17	3.40	-1.33	2.51	-0.11	1.99
50	40	-5.18	3.68	-1.76	2.91	2.07	1.84
40	50	-8.03	4.61	-1.49	2.19	4.96	2.30
30	60	-12.84	5.91	-3.28	2.91	7.47	2.59
20	70	-19.57	5.36	-5.40	1.87	9.37	4.04
10	80	-23.36	3.37	-6.66	2.39	12.26	3.47
0	90	-31.11	5.74	-8.80	3.56	10.49	5.16

Table 4.17: Mean rotations and standard deviations for subject 2, $y_\beta, z_\alpha', x_\gamma''$ rotation sequence, two channel study

Elevation	Abduction	α	SD	β	SD	γ	SD
80	10	0.00	0.00	0.00	0.00	0.01	0.03
80	10	-0.11	1.16	-0.61	1.25	-0.45	1.28
70	20	-4.22	2.23	-0.83	3.03	0.12	2.36
60	30	-6.87	3.63	-3.15	2.46	-0.80	2.30
50	40	-7.41	4.62	-1.55	3.33	0.75	2.79
40	50	-11.68	5.23	-3.81	4.03	1.14	2.97
30	60	-14.53	5.90	-4.13	3.39	2.40	3.12
20	70	-19.00	7.63	-5.27	4.13	2.91	3.45
10	80	-22.59	7.99	-6.86	5.15	4.63	4.55
0	90	-29.88	8.12	-10.90	4.99	4.49	4.02

Table 4.18: Mean rotations and standard deviations for subject 3, $y_\beta, z_\alpha', x_\gamma''$ rotation sequence, two channel study

Elevation	Abduction	α	SD	β	SD	γ	SD
80	10	0.00	0.00	0.00	0.00	0.02	0.06
80	10	0.17	0.62	-0.01	0.51	0.42	1.38
70	20	-1.97	2.18	-1.60	1.89	2.19	2.05
60	30	-3.46	2.66	-1.87	0.86	1.93	2.69
50	40	-7.10	2.23	-2.11	2.72	3.62	3.01
40	50	-10.59	4.16	-2.87	3.04	6.74	2.88
30	60	-12.83	3.52	-5.06	2.78	9.15	2.78
20	70	-17.46	5.03	-6.44	3.66	9.86	2.81
10	80	-19.79	3.79	-7.70	4.02	10.07	3.70
0	90	-23.86	5.21	-9.19	4.78	9.57	4.53

Table 4.19: Mean rotations and standard deviations for subject 4, $y_\beta, z_\alpha', x_\gamma''$ rotation sequence, two channel study

Elevation	Abduction	α	SD	β	SD	γ	SD
80	10	0.00	0.00	0.00	0.00	0.00	0.00
80	10	-0.06	0.48	-0.12	0.48	-0.05	0.58
70	20	-2.00	2.11	-1.14	2.08	-0.92	3.80
60	30	-4.96	2.02	-3.19	2.76	-0.83	3.82
50	40	-6.29	2.04	-3.15	1.95	0.58	5.21
40	50	-9.91	4.26	-4.60	2.25	4.15	6.27
30	60	-12.38	3.48	-7.10	1.65	9.33	5.66
20	70	-19.97	4.49	-10.06	1.96	12.57	6.40
10	80	-24.84	5.13	-12.55	2.52	15.05	7.13
0	90	-27.71	5.75	-15.30	4.93	14.44	8.60

Table 4.20: Mean rotations and standard deviations for subject 5, y_β , z_α , x_γ rotation sequence, two channel study

A4.2.1.2 Graphical Results (z_α , y_β , x_γ sequence)

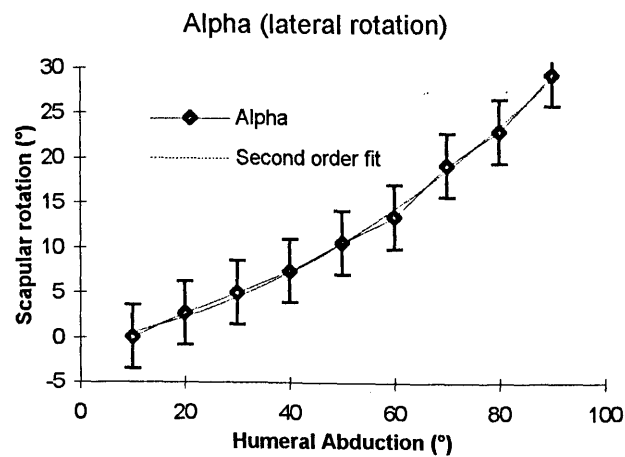


Figure 4.4: Rotation angle α during humeral abduction, z_α , y_β , x_γ two channel study

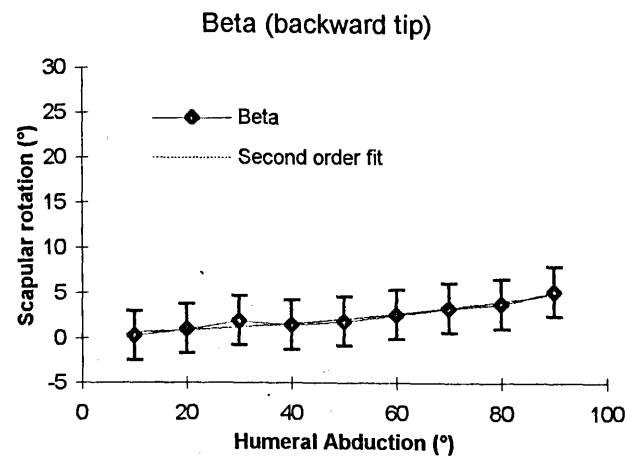


Figure 4.5: Rotation angle β during humeral abduction, z_α , y_β , x_γ two channel study

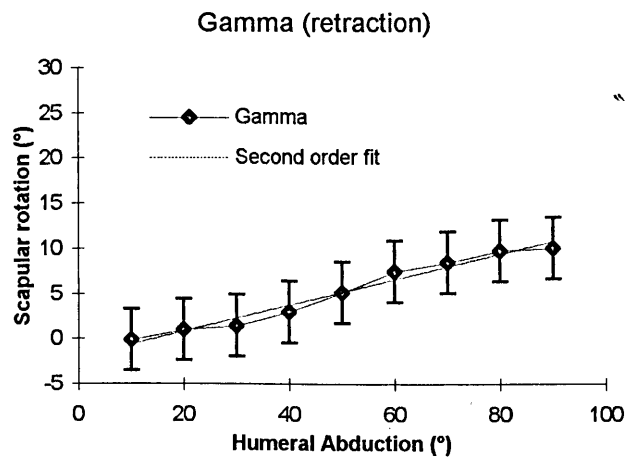


Figure 4.6: Rotation angle γ during humeral abduction, $z_\alpha, y_\beta', x_\gamma''$ two channel study

A4.2.1.3 Numerical Results ($z_\alpha, y_\beta', x_\gamma''$ sequence)

Elevation	Abduction	alpha	SD	beta	SD	gamma	SD
80	10	0.00	0.00	0.00	0.00	0.00	0.00
80	10	0.15	0.25	0.11	0.64	0.22	0.48
70	20	4.46	2.67	-0.14	1.76	5.55	2.91
60	30	7.76	3.36	-0.03	2.47	7.24	4.25
50	40	11.25	2.18	-0.54	2.28	9.19	3.95
40	50	12.35	1.76	-0.83	3.27	10.51	3.97
30	60	13.00	3.60	-0.38	4.18	10.31	4.67
20	70	17.15	2.26	0.36	4.50	9.85	4.41
10	80	20.14	3.99	0.94	4.99	10.54	4.84
0	90	28.49	2.47	3.15	5.46	10.01	4.82

Table 4.21: Mean rotations and standard deviations for subject 1, $z_\alpha, y_\beta', x_\gamma''$ rotation sequence, two channel study

Elevation	Abduction	alpha	SD	beta	SD	gamma	SD
80	10	0.00	0.00	0.00	0.01	0.00	0.00
80	10	0.08	0.33	0.35	0.73	-0.14	0.21
70	20	0.98	2.56	1.55	2.33	-1.46	2.28
60	30	2.15	3.38	1.39	2.51	-0.09	1.96
50	40	5.26	3.63	1.63	2.89	1.46	2.10
40	50	8.10	4.61	0.91	2.26	4.43	1.84
30	60	13.10	5.84	1.79	3.22	7.12	2.40
20	70	20.11	5.12	2.59	2.56	8.66	3.73
10	80	24.23	3.07	1.95	2.13	10.95	3.10
0	90	32.08	5.91	2.57	3.50	10.46	3.77

Table 4.22: Mean rotations and standard deviations for subject 2, $z_\alpha, y_\beta', x_\gamma''$ rotation sequence, two channel study

<i>Elevation</i>	<i>Abduction</i>	<i>alpha</i>	<i>SD</i>	<i>beta</i>	<i>SD</i>	<i>gamma</i>	<i>SD</i>
80	10	0.00	0.00	0.00	0.00	0.00	0.00
80	10	0.10	1.15	0.66	1.21	-0.58	1.13
70	20	4.20	2.23	0.82	3.07	0.46	2.25
60	30	6.76	3.53	3.32	2.68	-1.08	2.22
50	40	7.33	4.58	1.45	3.53	0.74	2.75
40	50	11.68	5.34	3.63	4.06	0.60	2.36
30	60	14.63	6.04	3.35	3.56	2.37	3.03
20	70	19.17	7.83	4.34	4.04	2.58	3.15
10	80	23.01	8.15	5.27	4.77	4.23	4.29
0	90	30.56	8.16	8.39	5.16	4.57	3.40

Table 4.23: Mean rotations and standard deviations for subject 3, $z_\alpha, y_\beta', x_\gamma''$ rotation sequence, two channel study

<i>Elevation</i>	<i>Abduction</i>	<i>alpha</i>	<i>SD</i>	<i>beta</i>	<i>SD</i>	<i>gamma</i>	<i>SD</i>
80	10	0.00	0.00	0.00	0.00	0.00	0.00
80	10	-0.17	0.63	0.01	0.51	0.03	0.47
70	20	2.03	2.19	1.55	1.89	1.86	1.25
60	30	3.50	2.63	1.74	0.89	2.04	2.89
50	40	7.20	2.40	1.67	2.63	3.37	2.66
40	50	10.84	4.40	1.61	2.73	6.42	2.63
30	60	13.48	3.86	2.99	2.06	8.65	2.39
20	70	18.26	5.46	3.34	3.03	9.30	2.46
10	80	20.80	4.21	4.20	3.34	9.44	3.42
0	90	25.10	5.77	4.56	3.58	10.05	2.93

Table 4.24: Mean rotations and standard deviations for subject 4, $z_\alpha, y_\beta', x_\gamma''$ rotation sequence, two channel study

<i>Elevation</i>	<i>Abduction</i>	<i>alpha</i>	<i>SD</i>	<i>beta</i>	<i>SD</i>	<i>gamma</i>	<i>SD</i>
80	10	0.00	0.00	0.00	0.00	0.00	0.00
80	10	0.06	0.48	0.11	0.48	-0.17	0.39
70	20	1.97	2.08	1.20	2.08	-1.37	3.14
60	30	4.92	1.94	3.25	2.75	-0.83	3.82
50	40	6.33	2.00	3.16	1.83	0.05	4.20
40	50	10.18	4.23	3.99	2.20	3.67	5.43
30	60	13.33	3.42	5.11	1.62	8.76	4.92
20	70	21.60	4.11	5.77	2.13	11.81	6.00
10	80	27.00	5.04	6.29	2.20	13.32	6.13
0	90	30.66	6.64	6.96	2.63	14.93	6.62

Table 4.25: Mean rotations and standard deviations for subject 5, $z_\alpha, y_\beta', x_\gamma''$ rotation sequence, two channel study

A4.2.2 Displacements of the Scapula, Numerical Results

Elevation	Abduction	x	SD	y	SD	z	SD
80	10	0.00	0.00	0.00	0.00	0.00	0.00
80	10	0.22	1.06	0.44	0.44	-0.92	1.32
70	20	-10.27	8.83	8.77	6.31	-16.63	7.58
60	30	-20.05	10.27	16.21	6.94	-23.67	9.81
50	40	-25.78	9.97	22.77	4.88	-28.91	10.32
40	50	-26.94	11.04	27.57	5.06	-32.40	11.68
30	60	-27.82	9.51	29.41	6.96	-32.88	12.47
20	70	-29.96	8.48	34.23	9.50	-33.73	11.71
10	80	-27.92	10.51	37.55	11.03	-35.65	13.87
0	90	-27.59	10.38	41.19	11.48	-37.69	13.30

Table 4.26: Mean displacements and standard deviations for subject 1, two channel study

Elevation	Abduction	x	SD	y	SD	z	SD
80	10	0.00	0.00	0.00	0.00	0.00	0.00
80	10	0.35	1.21	-0.01	0.33	-0.21	1.65
70	20	1.56	6.78	3.23	3.49	-0.96	4.63
60	30	-1.19	5.12	7.30	2.73	-5.09	5.98
50	40	-5.00	6.23	11.72	4.01	-10.94	7.80
40	50	-10.14	4.98	17.51	4.94	-17.87	4.15
30	60	-15.12	5.03	24.09	4.99	-27.70	5.49
20	70	-23.63	6.06	29.72	5.95	-32.66	8.08
10	80	-31.46	6.69	33.91	7.89	-36.82	8.26
0	90	-40.44	5.38	39.66	5.31	-37.80	8.10

Table 4.27: Mean displacements and standard deviations for subject 2, two channel study

Elevation	Abduction	x	SD	y	SD	z	SD
80	10	0.00	0.00	0.00	0.00	0.00	0.00
80	10	-0.22	2.80	-0.46	2.30	0.69	1.74
70	20	-4.91	5.55	5.64	6.12	-3.20	5.64
60	30	-5.04	4.40	5.90	6.33	-4.22	4.35
50	40	-8.96	7.65	10.43	7.08	-6.88	6.81
40	50	-11.03	6.31	14.01	8.16	-9.87	8.51
30	60	-13.46	5.63	17.81	10.12	-13.68	9.23
20	70	-17.74	7.51	24.99	9.59	-14.97	9.60
10	80	-21.50	7.09	28.64	8.52	-16.65	11.23
0	90	-27.50	7.51	36.40	13.04	-19.76	9.93

Table 4.28: Mean displacements and standard deviations for subject 3, two channel study

Elevation	Abduction	x	SD	y	SD	z	SD
80	10	0.00	0.00	0.00	0.00	0.00	0.00
80	10	0.19	1.31	-0.54	1.30	-0.15	0.61
70	20	-0.55	4.66	1.76	2.08	-4.31	4.07
60	30	-4.90	5.97	3.84	2.93	-5.38	7.21
50	40	-12.68	7.05	9.31	3.84	-9.20	7.19
40	50	-18.58	6.11	15.50	4.85	-16.47	6.58
30	60	-20.57	6.70	20.01	4.80	-23.46	7.02
20	70	-25.14	6.32	26.92	6.64	-25.74	7.01
10	80	-26.97	7.38	29.14	4.56	-26.80	9.88
0	90	-30.71	7.87	32.29	5.16	-27.93	8.27

Table 4.29: Mean displacements and standard deviations for subject 4, two channel study

Elevation	Abduction	x	SD	y	SD	z	SD
80	10	0.00	0.00	0.00	0.00	0.00	0.00
80	10	-0.05	0.90	-0.05	0.58	0.30	0.83
70	20	1.51	4.37	-0.15	3.38	0.37	6.33
60	30	1.01	5.72	1.28	4.43	-1.85	8.41
50	40	-0.65	8.01	2.24	5.66	-6.21	9.89
40	50	-4.68	7.69	6.42	4.86	-14.81	12.30
30	60	-8.79	7.46	11.27	5.38	-29.82	12.41
20	70	-15.73	8.35	23.64	6.35	-43.34	15.05
10	80	-19.92	5.87	30.75	7.98	-51.91	15.28
0	90	-22.14	5.55	32.95	11.92	-58.09	15.86

Table 4.30: Mean displacements and standard deviations for subject 5, two channel study

A4.3 SCAPULOHUMERAL KINEMATICS MODEL

A4.3.1 Subject Regression Coefficients ($y_\beta, z_\alpha', x_\gamma''$ sequence)

Term	Gamma	Alpha	Beta	x	y	z
Intercept	5.13	32.43	15.16	55.56	-21.47	26.84
azimuth	-0.06	-0.09	0.00	-0.30	0.06	-0.09
elevation	-0.30	-0.33	-0.23	-0.33	0.27	-0.48
roll	-0.10	-0.31	-0.08	-0.81	-0.01	-0.11
azimuth ²	1.4E-04	-1.6E-04	-3.7E-04	-1.5E-04	-4.8E-04	-1.6E-04
elevation ²	2.5E-03	1.0E-03	1.9E-03	-7.5E-04	8.5E-04	2.1E-03
roll ²	3.9E-04	1.3E-03	3.2E-04	3.2E-03	4.6E-04	-7.6E-06

Table 4.31: Regression coefficients for subject 1, $y_\beta, z_\alpha', x_\gamma''$ rotation sequence

Term	Gamma	Alpha	Beta	x	y	z
Intercept	-23.27	25.57	4.98	60.95	4.04	-38.66
azimuth	-0.30	-0.06	0.07	-0.30	0.40	-0.64
elevation	-0.17	-0.27	-0.10	-0.15	0.34	-0.49
roll	0.22	-0.04	0.11	-0.52	-0.14	0.50
azimuth ²	-2.3E-04	-3.7E-04	3.2E-04	-1.9E-03	1.5E-04	-2.2E-04
elevation ²	-2.0E-04	-5.6E-04	2.0E-04	-5.1E-03	1.9E-03	-1.1E-03
roll ²	-5.4E-04	1.6E-04	-3.7E-04	1.8E-03	2.3E-04	-1.2E-03

Table 4.32: Regression coefficients for subject 2, $y_\beta, z_\alpha', x_\gamma''$ rotation sequence

Term	Gamma	Alpha	Beta	x	y	z
Intercept	-36.72	26.25	-8.91	92.01	17.34	-88.10
azimuth	0.23	0.15	0.31	-0.72	-0.26	0.79
elevation	0.01	-0.15	-0.09	-0.19	0.05	0.18
roll	0.76	0.06	0.49	-1.56	-0.66	2.14
azimuth ²	2.6E-03	1.0E-03	1.9E-03	-3.5E-03	-3.9E-03	7.8E-03
elevation ²	-5.8E-04	-1.8E-03	2.8E-04	-5.0E-03	2.9E-03	-3.7E-03
roll ²	-3.5E-03	-4.2E-04	-2.1E-03	6.6E-03	3.3E-03	-1.0E-02

Table 4.33: Regression coefficients for subject 3, $y_\beta, z_\alpha', x_\gamma''$ rotation sequence

Term	Gamma	Alpha	Beta	x	y	z
Intercept	-8.07	13.47	9.15	37.77	-7.43	-16.51
azimuth	-0.01	0.01	0.01	-0.09	0.05	0.00
elevation	-0.03	-0.30	-0.11	-0.51	0.16	-0.05
roll	0.10	0.20	0.06	-0.30	-0.07	0.36
azimuth ²	6.4E-04	7.3E-05	-5.8E-05	-9.6E-05	-5.5E-04	1.5E-03
elevation ²	-7.6E-04	3.6E-04	-4.7E-04	2.4E-03	1.3E-03	-2.3E-03
roll ²	-2.4E-04	-8.8E-04	-1.6E-04	8.7E-04	4.9E-04	-1.4E-03

Table 4.34: Regression coefficients for subject 4, $y_\beta, z_\alpha', x_\gamma''$ rotation sequence

Term	Gamma	Alpha	Beta	x	y	z
Intercept	-14.58	43.54	2.77	105.46	-27.70	-28.51
azimuth	-0.01	-0.03	0.02	-0.13	0.09	-0.03
elevation	-0.03	-0.28	-0.24	-0.06	0.14	-0.17
roll	0.24	-0.22	0.12	-0.94	0.05	0.66
azimuth ²	1.1E-03	-5.1E-04	1.7E-05	-1.3E-03	-1.2E-03	2.4E-03
elevation ²	-1.2E-03	-9.5E-04	1.6E-03	-6.4E-03	4.6E-03	-3.2E-03
roll ²	-7.1E-04	5.4E-04	-3.9E-04	2.6E-03	2.4E-04	-2.3E-03

Table 4.35: Regression coefficients for subject 5, $y_\beta, z_\alpha', x_\gamma''$ rotation sequence

Term	Gamma	Alpha	Beta	x	y	z
Intercept	-0.90	14.32	9.64	22.28	16.44	-0.24
azimuth	-0.23	0.05	0.00	-0.04	0.15	-0.46
elevation	-0.13	-0.30	-0.23	-0.15	0.09	-0.34
roll	0.06	0.14	0.08	-0.05	-0.42	0.36
azimuth ²	-4.3E-04	8.6E-04	2.1E-04	4.4E-04	-9.4E-04	-1.5E-04
elevation ²	-1.5E-03	-6.3E-04	2.4E-04	-2.3E-03	3.3E-03	-5.1E-03
roll ²	-3.5E-05	-7.1E-04	-1.7E-04	-7.7E-04	1.9E-03	-1.0E-03

Table 4.36: Regression coefficients for subject 6, $y_\beta, z_\alpha', x_\gamma''$ rotation sequence

Term	Gamma	Alpha	Beta	x	y	z
Intercept	-21.94	21.44	2.29	61.71	13.50	-47.36
azimuth	-0.12	0.00	0.07	-0.41	0.21	-0.19
elevation	-0.12	-0.26	-0.14	-0.30	0.27	-0.35
roll	0.34	0.15	0.12	-0.41	-0.42	1.06
azimuth ²	5.3E-04	5.7E-04	5.2E-04	-2.0E-03	-1.1E-03	2.1E-03
elevation ²	-3.4E-04	-1.8E-03	5.0E-04	-4.7E-03	2.0E-03	-2.0E-03
roll ²	-1.0E-03	-8.3E-04	-2.9E-04	8.2E-04	1.8E-03	-3.8E-03

Table 4.37: Regression coefficients for subject 7, $y_\beta, z_\alpha', x_\gamma''$ rotation sequence

Term	Gamma	Alpha	Beta	x	y	z
Intercept	-12.42	12.96	3.83	16.41	10.43	-16.15
azimuth	0.01	0.07	0.14	-0.07	0.10	0.09
elevation	-0.04	-0.35	-0.03	-0.48	0.23	-0.15
roll	0.26	0.14	0.11	0.22	-0.37	0.52
azimuth ²	7.0E-04	6.7E-04	8.1E-04	5.7E-04	-5.4E-04	1.8E-03
elevation ²	-3.9E-04	1.4E-03	-3.2E-04	2.6E-04	3.5E-04	-3.1E-04
roll ²	-1.1E-03	-5.5E-04	-4.1E-04	-1.3E-03	1.7E-03	-2.4E-03

Table 4.38: Regression coefficients for subject 8, $y_\beta, z_\alpha', x_\gamma''$ rotation sequence

Term	Gamma	Alpha	Beta	x	y	z
Intercept	10.55	7.29	15.11	-13.98	3.18	42.63
azimuth	-0.12	-0.08	0.10	-0.53	0.16	-0.12
elevation	-0.09	-0.19	-0.14	-0.12	0.00	-0.03
roll	0.03	0.18	0.05	0.24	-0.21	0.01
azimuth ²	-3.1E-04	-1.1E-04	3.8E-04	-1.4E-03	3.2E-04	-7.2E-04
elevation ²	-1.8E-03	-1.4E-03	-2.0E-04	-3.8E-03	3.0E-03	-6.0E-03
roll ²	-1.5E-04	-7.7E-04	-1.4E-04	-1.4E-03	9.3E-04	-3.2E-04

Table 4.39: Regression coefficients for subject 9, $y_\beta, z_\alpha', x_\gamma''$ rotation sequence

Term	Gamma	Alpha	Beta	x	y	z
Intercept	-16.20	35.61	11.47	54.61	6.62	-8.54
azimuth	-0.04	-0.07	0.13	-0.45	0.11	-0.01
elevation	-0.08	-0.28	-0.07	-0.51	0.29	-0.16
roll	0.23	-0.19	0.08	-0.59	-0.34	0.39
azimuth ²	6.1E-04	-6.8E-04	5.3E-04	-2.0E-03	-9.2E-04	1.4E-03
elevation ²	-2.0E-04	-2.6E-04	-4.6E-04	-1.6E-05	9.8E-04	-2.4E-03
roll ²	-7.9E-04	7.6E-04	-1.5E-04	1.8E-03	1.5E-03	-1.4E-03

Table 4.40: Regression coefficients for subject 10, $y_\beta, z_\alpha', x_\gamma''$ rotation sequence

Term	Gamma	Alpha	Beta	x	y	z
Intercept	-17.47	35.48	2.84	78.73	-6.77	-37.00
azimuth	-0.25	-0.05	0.07	-0.42	0.28	-0.49
elevation	0.00	-0.22	-0.12	-0.20	0.06	0.07
roll	0.28	-0.10	0.24	-0.72	-0.12	0.66
azimuth ²	-2.5E-04	-2.8E-04	7.2E-04	-2.7E-03	7.8E-04	1.6E-04
elevation ²	-2.9E-03	-2.5E-03	-9.1E-04	-5.1E-03	3.9E-03	-7.8E-03
roll ²	-1.0E-03	2.4E-04	-9.4E-04	2.3E-03	7.2E-04	-2.5E-03

Table 4.41: Regression coefficients for subject 11, $y_\beta, z_\alpha', x_\gamma''$ rotation sequence

Term	Alpha	Beta	Gamma	x	y	z
Intercept	24.72	6.21	-12.35	51.95	0.74	-19.24
azimuth	-0.01	0.08	-0.08	-0.31	0.12	-0.11
elevation	-0.27	-0.13	-0.09	-0.27	0.17	-0.18
roll	0.00	0.13	0.22	-0.49	-0.25	0.60
azimuth ²	9.7E-05	4.5E-04	4.6E-04	-1.3E-03	-7.6E-04	1.4E-03
elevation ²	-6.5E-04	2.2E-04	-6.8E-04	-2.8E-03	2.3E-03	-2.9E-03
roll ²	-1.1E-04	-4.4E-04	-7.9E-04	1.5E-03	1.2E-03	-2.4E-03

Table 4.42: Regression coefficients for final model, y_{β} , z_{α} , x_{γ} rotation sequence

A4.3.2 Subject Regression Coefficients (z_{α} , y_{β} , x_{γ} sequence)

Term	Alpha	Beta	Gamma	x	y	z
Intercept	39.80	10.95	4.90	55.56	-21.47	26.84
azimuth	-0.12	0.03	-0.07	-0.30	0.06	-0.09
elevation	-0.38	-0.09	-0.26	-0.33	0.27	-0.48
roll	-0.41	-0.01	-0.09	-0.81	-0.01	-0.11
azimuth ²	-2.3E-04	-3.2E-04	1.3E-04	-1.5E-04	-4.8E-04	-1.6E-04
elevation ²	9.8E-04	3.2E-04	2.2E-03	-7.5E-04	8.5E-04	2.1E-03
roll ²	1.6E-03	8.0E-05	3.4E-04	3.2E-03	4.6E-04	-7.6E-06

Table 4.43: Regression coefficients for subject 1, z_{α} , y_{β} , x_{γ} rotation sequence

Term	Alpha	Beta	Gamma	x	y	z
Intercept	23.95	11.92	-22.29	60.95	4.04	-38.66
azimuth	-0.10	0.21	-0.28	-0.30	0.40	-0.64
elevation	-0.29	0.02	-0.13	-0.15	0.34	-0.49
roll	-0.04	0.06	0.21	-0.52	-0.14	0.50
azimuth ²	-5.9E-04	6.6E-04	-1.5E-04	-1.9E-03	1.5E-04	-2.2E-04
elevation ²	-2.9E-04	-3.5E-04	-4.5E-04	-5.1E-03	1.9E-03	-1.1E-03
roll ²	1.9E-04	-2.6E-04	-5.2E-04	1.8E-03	2.3E-04	-1.2E-03

Table 4.44: Regression coefficients for subject 2, z_{α} , y_{β} , x_{γ} rotation sequence

Term	Alpha	Beta	Gamma	x	y	z
Intercept	25.47	8.18	-34.13	92.01	17.34	-88.10
azimuth	0.15	0.24	0.22	-0.72	-0.26	0.79
elevation	-0.15	-0.10	0.01	-0.19	0.05	0.18
roll	0.10	0.15	0.72	-1.56	-0.66	2.14
azimuth ²	1.0E-03	9.6E-04	2.5E-03	-3.5E-03	-3.9E-03	7.8E-03
elevation ²	-2.0E-03	7.8E-04	-5.3E-04	-5.0E-03	2.9E-03	-3.7E-03
roll ²	-6.2E-04	-5.5E-04	-3.3E-03	6.6E-03	3.3E-03	-1.0E-02

Table 4.45: Regression coefficients for subject 3, z_{α} , y_{β} , x_{γ} rotation sequence

Term	Alpha	Beta	Gamma	x	y	z
Intercept	12.37	11.66	-7.76	37.77	-7.43	-16.51
azimuth	0.00	0.02	-0.01	-0.09	0.05	0.00
elevation	-0.31	-0.09	-0.02	-0.51	0.16	-0.05
roll	0.21	0.04	0.09	-0.30	-0.07	0.36
azimuth ²	1.4E-04	-2.1E-04	6.2E-04	-9.6E-05	-5.5E-04	1.5E-03
elevation ²	3.0E-04	-3.6E-04	-7.7E-04	2.4E-03	1.3E-03	-2.3E-03
roll ²	-8.9E-04	-1.1E-04	-2.4E-04	8.7E-04	4.9E-04	-1.4E-03

Table 4.46: Regression coefficients for subject 4, z_{α} , y_{β} , x_{γ} rotation sequence

Term	Alpha	Beta	Gamma	x	y	z
Intercept	43.96	6.03	-13.76	105.46	-27.70	-28.51
azimuth	-0.03	0.03	-0.01	-0.13	0.09	-0.03
elevation	-0.32	-0.18	-0.01	-0.06	0.14	-0.17
roll	-0.23	0.06	0.22	-0.94	0.05	0.66
azimuth ²	-5.0E-04	-2.6E-04	1.0E-03	-1.3E-03	-1.2E-03	2.4E-03
elevation ²	-6.3E-04	1.5E-03	-1.4E-03	-6.4E-03	4.6E-03	-3.2E-03
roll ²	5.9E-04	-1.8E-04	-6.4E-04	2.6E-03	2.4E-04	-2.3E-03

Table 4.47: Regression coefficients for subject 5, z_{α} , y_{β}' , x_{γ}'' rotation sequence

Term	Alpha	Beta	Gamma	x	y	z
Intercept	13.93	12.04	-0.22	22.28	16.44	-0.24
azimuth	0.00	0.09	-0.22	22.28	0.15	-0.46
elevation	-0.36	-0.12	-0.12	22.28	0.09	-0.34
roll	0.15	0.01	0.04	22.28	-0.42	0.36
azimuth ²	6.8E-04	3.0E-04	-4.6E-04	2.2E+01	-9.4E-04	-1.5E-04
elevation ²	-4.0E-04	4.2E-04	-1.4E-03	2.2E+01	3.3E-03	-5.1E-03
roll ²	-6.7E-04	7.1E-05	8.3E-05	2.2E+01	1.9E-03	-1.0E-03

Table 4.48: Regression coefficients for subject 6, z_{α} , y_{β}' , x_{γ}'' rotation sequence

Term	Alpha	Beta	Gamma	x	y	z
Intercept	20.95	12.19	-19.59	61.71	13.50	-47.36
azimuth	-0.02	0.13	-0.10	-0.41	0.21	-0.19
elevation	-0.28	-0.05	-0.09	-0.30	0.27	-0.35
roll	0.14	-0.05	0.29	-0.41	-0.42	1.06
azimuth ²	4.5E-04	2.9E-04	4.6E-04	-2.0E-03	-1.1E-03	2.1E-03
elevation ²	-1.6E-03	4.8E-04	-3.8E-04	-4.7E-03	2.0E-03	-2.0E-03
roll ²	-7.7E-04	2.6E-04	-8.8E-04	8.2E-04	1.8E-03	-3.8E-03

Table 4.49: Regression coefficients for subject 7, z_{α} , y_{β}' , x_{γ}'' rotation sequence

Term	Alpha	Beta	Gamma	x	y	z
Intercept	12.06	8.82	-11.35	16.41	10.43	-16.15
azimuth	0.08	0.14	0.01	-0.07	0.10	0.09
elevation	-0.36	0.01	-0.03	-0.48	0.23	-0.15
roll	0.16	0.01	0.24	0.22	-0.37	0.52
azimuth ²	7.7E-04	6.1E-04	6.8E-04	5.7E-04	-5.4E-04	1.8E-03
elevation ²	1.4E-03	-3.9E-04	-4.2E-04	2.6E-04	3.5E-04	-3.1E-04
roll ²	-6.6E-04	-1.4E-05	-1.0E-03	-1.3E-03	1.7E-03	-2.4E-03

Table 4.50: Regression coefficients for subject 8, z_{α} , y_{β}' , x_{γ}'' rotation sequence

Term	Alpha	Beta	Gamma	x	y	z
Intercept	11.04	13.33	10.76	-13.98	3.18	42.63
azimuth	-0.09	0.19	-0.10	-13.98	3.18	42.63
elevation	-0.23	-0.06	-0.07	-13.98	3.18	42.63
roll	0.16	0.00	0.01	-13.98	3.18	42.63
azimuth ²	-1.9E-04	6.7E-04	-2.3E-04	-1.4E+01	3.2E+00	4.3E+01
elevation ²	-1.4E-03	3.0E-04	-1.7E-03	-1.4E+01	3.2E+00	4.3E+01
roll ²	-6.9E-04	9.7E-05	-5.5E-05	-1.4E+01	3.2E+00	4.3E+01

Table 4.51: Regression coefficients for subject 9, z_{α} , y_{β}' , x_{γ}'' rotation sequence

Term	Alpha	Beta	Gamma	x	y	z
Intercept	33.52	17.51	-15.12	54.61	6.62	-8.54
azimuth	-0.08	0.17	-0.03	-0.45	0.11	-0.01
elevation	-0.31	-0.02	-0.07	-0.51	0.29	-0.16
roll	-0.16	0.00	0.22	-0.59	-0.34	0.39
azimuth ²	-6.4E-04	4.7E-04	6.1E-04	-2.0E-03	-9.2E-04	1.4E-03
elevation ²	-1.3E-04	-5.7E-04	-2.5E-04	-1.6E-05	9.8E-04	-2.4E-03
roll ²	6.7E-04	1.3E-04	-7.3E-04	1.8E-03	1.5E-03	-1.4E-03

Table 4.52: Regression coefficients for subject 10, $z_\alpha, y_\beta', x_\gamma''$ rotation sequence

Term	Alpha	Beta	Gamma	x	y	z
Intercept	34.91	12.20	-15.50	78.73	-6.77	-37.00
azimuth	-0.08	0.21	-0.21	-0.42	0.28	-0.49
elevation	-0.24	-0.07	0.03	-0.20	0.06	0.07
roll	-0.03	0.07	0.24	-0.72	-0.12	0.66
azimuth ²	-3.0E-04	1.0E-03	-1.4E-04	-2.7E-03	7.8E-04	1.6E-04
elevation ²	-2.7E-03	1.0E-04	-2.8E-03	-5.1E-03	3.9E-03	-7.8E-03
roll ²	-2.6E-05	-2.9E-04	-8.3E-04	2.3E-03	7.2E-04	-2.5E-03

Table 4.53: Regression coefficients for subject 11, $z_\alpha, y_\beta', x_\gamma''$ rotation sequence

Term	Alpha	Beta	Gamma	x	y	z
Intercept	24.72	11.35	-11.28	51.95	0.74	-19.24
azimuth	-0.03	0.13	-0.07	-0.31	0.12	-0.11
elevation	-0.29	-0.07	-0.07	-0.27	0.17	-0.18
roll	0.01	0.03	0.20	-0.49	-0.25	0.60
azimuth ²	5.7E-05	3.8E-04	4.6E-04	-1.3E-03	-7.6E-04	1.4E-03
elevation ²	-5.9E-04	2.0E-04	-7.2E-04	-2.8E-03	2.3E-03	-2.9E-03
roll ²	-1.1E-04	-7.0E-05	-7.1E-04	1.5E-03	1.2E-03	-2.4E-03

Table 4.54: Regression coefficients for final model, $z_\alpha, y_\beta', x_\gamma''$ rotation sequence

A4.4 MODEL IN GLOBAL ROTATIONS AND DISPLACEMENTS

The following tables give the regression coefficients for the scapulohumeral kinematics model in terms of rotations and displacements in the co-ordinate system of the Isotrak[®] receiver on the sternum. The co-ordinate system is shown in Figure 5.16, and the rotation sequence is α about z , β about y' then γ about x'' . All rotations obey the right hand rule.

Term	Alpha	Beta	Gamma	x	y	z
Intercept	-23.64	-12.60	146.19	86.36	186.49	167.60
azimuth	0.09	0.00	-0.04	-0.35	0.04	-0.04
elevation	0.26	0.26	-0.22	-0.23	0.33	-0.53
roll	0.22	0.09	0.06	-0.97	-0.27	0.31
azimuth ²	1.2E-04	6.1E-04	9.3E-04	1.1E-04	-2.2E-03	2.2E-03
elevation ²	-7.6E-04	-1.3E-03	1.8E-03	-2.1E-03	9.3E-04	1.9E-03
roll ²	-7.9E-04	-3.2E-04	-3.2E-04	3.9E-03	1.6E-03	-1.8E-03

Table 4.55: Global regression coefficients for subject 1, $z_\alpha, y_\beta', x_\gamma''$ rotation sequence

Term	Alpha	Beta	Gamma	x	y	z
Intercept	-20.17	-17.78	126.83	141.77	193.46	103.41
azimuth	0.18	-0.09	-0.28	-0.27	0.34	-0.55
elevation	0.30	0.20	-0.12	-0.25	0.40	-0.44
roll	0.04	0.04	0.18	-0.44	-0.24	0.52
azimuth ²	5.3E-04	-1.3E-04	-3.2E-04	-1.6E-03	2.7E-04	3.6E-07
elevation ²	-2.0E-04	4.4E-04	-3.9E-04	-3.7E-03	2.2E-04	-1.6E-03
roll ²	-2.3E-04	-3.0E-04	-4.6E-04	1.3E-03	9.7E-04	-1.4E-03

Table 4.56: Global regression coefficients for subject 2, z_{α} , y_{β}' , x_{γ}'' rotation sequence

Term	Alpha	Beta	Gamma	x	y	z
Intercept	-29.17	-4.09	115.16	170.66	213.14	72.35
azimuth	0.01	-0.31	0.24	-0.93	-0.35	0.88
elevation	0.13	0.05	0.08	-0.58	-0.02	0.45
roll	0.05	-0.38	0.78	-2.06	-0.99	2.48
azimuth ²	-8.2E-05	-1.6E-03	2.7E-03	-5.8E-03	-4.2E-03	8.4E-03
elevation ²	1.8E-03	1.2E-03	-1.5E-03	-5.7E-04	3.3E-03	-6.8E-03
roll ²	-2.7E-05	1.8E-03	-3.6E-03	9.2E-03	4.9E-03	-1.2E-02

Table 4.57: Global regression coefficients for subject 3, z_{α} , y_{β}' , x_{γ}'' rotation sequence

Term	Alpha	Beta	Gamma	x	y	z
Intercept	-3.86	-5.88	139.89	76.95	185.20	151.91
azimuth	-0.01	-0.04	-0.01	-0.05	0.01	0.01
elevation	0.23	0.22	-0.06	-0.51	0.22	-0.15
roll	-0.25	-0.17	0.10	-0.06	-0.25	0.44
azimuth ²	-5.9E-04	1.9E-04	7.4E-04	6.7E-04	-1.1E-03	2.1E-03
elevation ²	-4.0E-04	1.0E-04	-7.0E-05	2.2E-03	6.1E-04	-1.6E-03
roll ²	1.1E-03	6.8E-04	-3.0E-04	-1.7E-04	1.3E-03	-1.8E-03

Table 4.58: Global regression coefficients for subject 4, z_{α} , y_{β}' , x_{γ}'' rotation sequence

Term	Alpha	Beta	Gamma	x	y	z
Intercept	-35.33	-20.43	135.25	164.00	184.60	147.44
azimuth	0.04	-0.02	-0.03	-0.06	0.10	-0.11
elevation	0.19	0.26	-0.04	-0.05	0.25	-0.18
roll	0.16	0.07	0.16	-0.57	0.09	0.28
azimuth ²	1.1E-04	7.1E-04	1.2E-03	-1.1E-03	-1.5E-03	2.7E-03
elevation ²	9.3E-04	-7.2E-04	-1.6E-03	-4.6E-03	4.6E-03	-5.8E-03
roll ²	-3.3E-04	-1.4E-04	-3.3E-04	9.5E-04	4.7E-05	-4.7E-04

Table 4.59: Global regression coefficients for subject 5, z_{α} , y_{β}' , x_{γ}'' rotation sequence

Term	Alpha	Beta	Gamma	x	y	z
Intercept	-10.58	-7.18	140.70	91.03	214.33	134.83
azimuth	0.07	-0.09	-0.24	0.02	0.18	-0.50
elevation	0.21	0.26	-0.13	-0.09	0.07	-0.37
roll	-0.10	-0.10	0.04	0.06	-0.36	0.26
azimuth ²	-1.5E-04	-6.8E-04	-5.5E-04	6.8E-04	-6.7E-04	-4.8E-04
elevation ²	2.3E-04	1.7E-04	-1.2E-03	-2.0E-03	3.5E-03	-5.3E-03
roll ²	5.7E-04	3.2E-04	2.1E-05	-1.4E-03	1.7E-03	-5.4E-04

Table 4.60: Global regression coefficients for subject 6, z_{α} , y_{β}' , x_{γ}'' rotation sequence

Term	Alpha	Beta	Gamma	x	y	z
Intercept	-2.90	-17.07	126.06	80.62	234.40	91.11
azimuth	0.08	-0.05	-0.14	-0.21	0.19	-0.19
elevation	0.20	0.16	-0.10	-0.33	0.23	-0.29
roll	-0.24	0.00	0.26	0.45	-0.64	1.00
azimuth ²	-2.9E-04	4.9E-05	1.7E-04	4.7E-04	-1.1E-03	1.8E-03
elevation ²	1.2E-03	9.4E-04	-3.8E-04	-2.7E-03	1.6E-03	-2.6E-03
roll ²	1.2E-03	2.4E-05	-7.3E-04	-2.9E-03	2.8E-03	-3.5E-03

Table 4.61: Global regression coefficients for subject 7, z_{α} , y_{β} , x_{γ} rotation sequence

Term	Alpha	Beta	Gamma	x	y	z
Intercept	-12.37	-4.54	138.62	81.76	204.51	127.25
azimuth	0.06	-0.10	-0.09	-0.17	0.16	-0.19
elevation	0.25	0.18	-0.02	-0.39	0.17	-0.08
roll	-0.08	-0.07	0.11	0.14	-0.30	0.27
azimuth ²	1.7E-04	-3.2E-04	-8.2E-05	-4.0E-04	-1.3E-05	-3.3E-04
elevation ²	-7.6E-04	1.1E-04	-4.0E-04	-1.1E-03	1.0E-03	-2.0E-03
roll ²	2.9E-04	1.7E-04	-4.4E-04	-8.8E-04	1.4E-03	-1.1E-03

Table 4.62: Global regression coefficients for subject 8, z_{α} , y_{β} , x_{γ} rotation sequence

Term	Alpha	Beta	Gamma	x	y	z
Intercept	1.29	-3.27	149.64	25.21	204.48	179.73
azimuth	0.19	-0.12	-0.12	-0.61	0.22	-0.17
elevation	0.25	0.19	-0.04	-0.34	0.07	-0.02
roll	-0.13	-0.12	0.02	0.12	-0.10	0.10
azimuth ²	7.9E-04	-4.0E-04	-2.6E-04	-1.9E-03	4.3E-04	-7.6E-04
elevation ²	-7.7E-05	3.1E-04	-1.5E-03	-1.8E-03	2.9E-03	-5.9E-03
roll ²	6.1E-04	5.1E-04	-1.4E-04	-6.8E-04	3.5E-04	-7.0E-04

Table 4.63: Global regression coefficients for subject 9, z_{α} , y_{β} , x_{γ} rotation sequence

Term	Alpha	Beta	Gamma	x	y	z
Intercept	-22.19	-26.94	135.31	104.20	217.16	152.78
azimuth	0.14	-0.10	-0.04	-0.40	0.12	0.01
elevation	0.25	0.14	-0.07	-0.45	0.32	-0.22
roll	0.04	0.14	0.30	-0.32	-0.53	0.65
azimuth ²	7.6E-04	1.8E-06	7.5E-04	-1.3E-03	-9.6E-04	1.8E-03
elevation ²	-2.4E-04	9.0E-04	2.4E-04	2.8E-04	-1.4E-04	-6.6E-04
roll ²	-3.9E-05	-7.0E-04	-1.1E-03	6.2E-04	2.4E-03	-2.6E-03

Table 4.64: Global regression coefficients for subject 10, z_{α} , y_{β} , x_{γ} rotation sequence

Term	Alpha	Beta	Gamma	x	y	z
Intercept	-21.88	-15.31	122.02	138.28	196.43	93.04
azimuth	0.13	-0.12	-0.18	-0.33	0.20	-0.43
elevation	0.21	0.13	-0.04	-0.40	0.19	-0.12
roll	-0.05	-0.05	0.36	-0.53	-0.37	0.80
azimuth ²	4.1E-04	-5.6E-04	-1.8E-04	-1.7E-03	4.4E-04	4.1E-05
elevation ²	1.2E-03	2.2E-03	-1.3E-03	-3.1E-03	2.0E-03	-5.5E-03
roll ²	4.2E-04	3.0E-04	-1.4E-03	1.6E-03	1.8E-03	-3.1E-03

Table 4.65: Global regression coefficients for subject 11, z_{α} , y_{β} , x_{γ} rotation sequence

Term	Alpha	Beta	Gamma	x	y	z
Intercept	-15.89	-11.98	135.37	102.26	203.78	132.84
a	0.09	-0.09	-0.08	-0.30	0.10	-0.09
b	0.23	0.19	-0.07	-0.32	0.20	-0.18
c	-0.03	-0.05	0.20	-0.37	-0.36	0.63
a^2	1.4E-04	-1.6E-04	5.3E-04	-1.0E-03	-1.1E-03	1.7E-03
b^2	1.7E-04	2.2E-04	-5.0E-04	-1.6E-03	1.9E-03	-3.0E-03
c^2	2.4E-04	2.0E-04	-7.4E-04	9.8E-04	1.7E-03	-2.6E-03

Table 4.66: Global regression coefficients for final model, z_{α} , y_{β}' , x_{γ}'' rotation sequence

Appendix A5

WinMat User Guide

A5.1 INTRODUCTION

WinMat is a data analysis system for use with Polhemus® Isotrak®, Isotrak®II and Fastrak® systems. It uses Isotrak data files (*.dat, CREST format, 3 or 35 line header) as its input, and outputs a text file containing headed lists of rotations and displacements (*.out).


It's primary purpose is to perform various co-ordinate transformations on the input data, and calculate the rotation angles and displacements of the system being measured.

It's use is best described by example. As such, the following sections will detail the analysis of a four channel Fastrak® file. All other types of file (Isotrak®, Isotrak®II etc.) follow exactly the same operations, but have less options available (as illustrated later).

A5.2 ANALYSING A DATA FILE USING WINMAT

This example relates to analysing a four channel file. The procedures for one, two and three channel files are identical, but less options are available, as discussed later.

A5.2.1 Opening a file

Upon starting the application by double clicking on the WinMat icon , you are presented with a standard Windows style menu. To open the data file which you want to analyse, select **File**, **O**pen..., and choose your file (<yourfile>.dat) from the list. WinMat then reads the data file into memory and displays the following view.

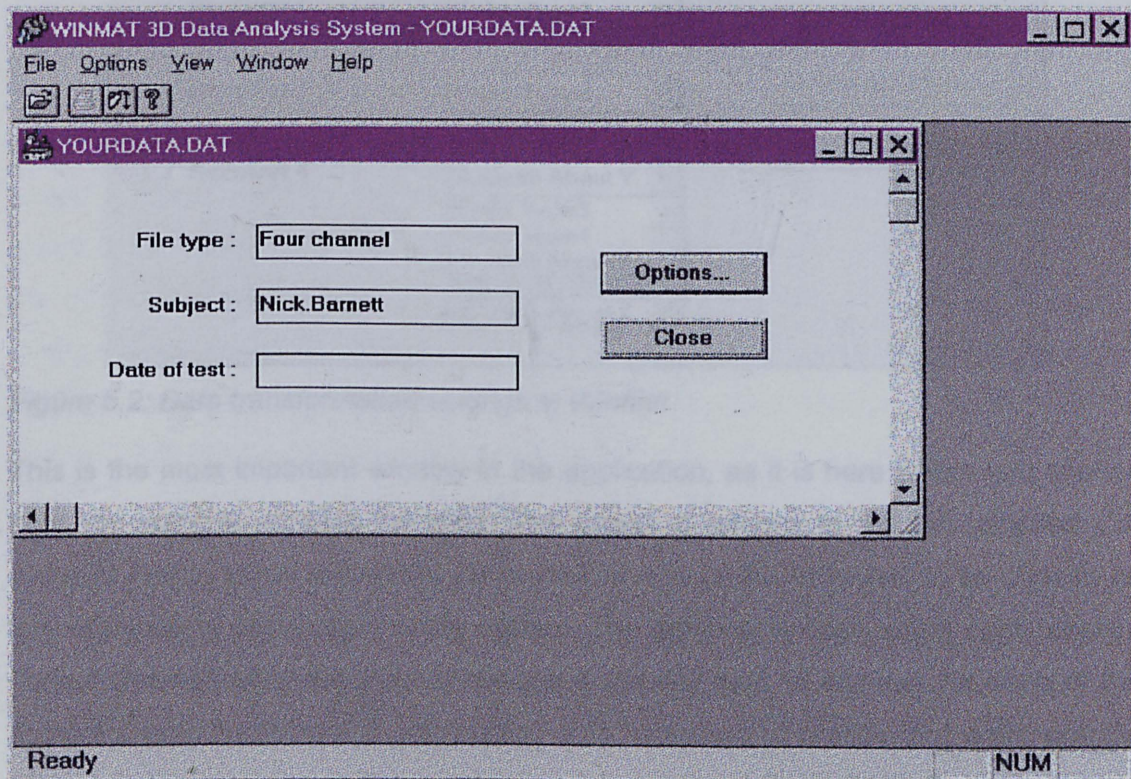


Figure 5.1: An open data file in WinMat

Within this view, the name of the subject, and the date of the test (not yet implemented, Feb. '96) can be checked to ensure that you have the correct file.

If the file is not the correct one, click on the button **Close** to close the file, and then repeat the steps above to open a different one.

To continue, click on the button **Options....** , and the window below will be displayed.

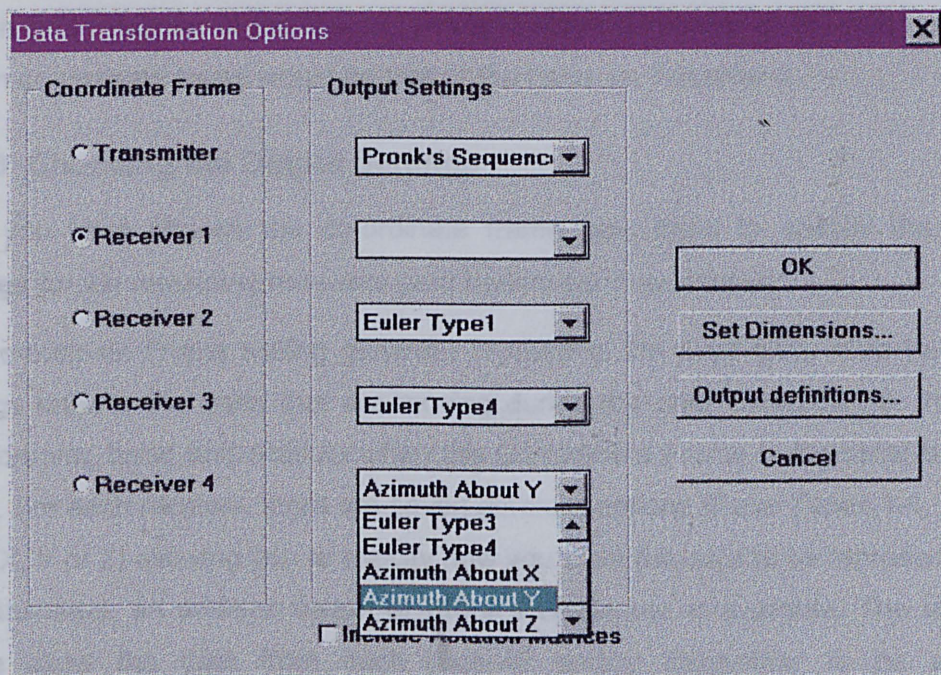


Figure 5.2: Data transformation settings in WinMat

This is the most important window in the application, as it is here where you choose how you want to analyse the data. The group of options to the left, labelled *Co-ordinate Frame* allows either the transmitter or one of the receivers to be chosen as the reference or global co-ordinate system. The group of options to the right, labelled *Output Settings* allow the user to choose a specific type of analysis for each of the receivers (and transmitter if applicable). It is important to realise that each specific Output Setting applies to the receiver or transmitter in line with it. For example, in Figure 5.2, the chosen Output Setting for the *Transmitter* is *Pronk's Sequence*, while for *Receiver 3*, the chosen output is *Euler Type 4*. These settings are discussed further below.

A5.2.2 Choosing the Co-ordinate Frame

The box labelled **Co-ordinate Frame** allows you to specify the co-ordinate system required as the base for all rotations and displacements. This co-ordinate system will usually be the receiver (or transmitter) that was not moving during the data collection. For example, if collecting data on the upper limb, you may have a receiver on the thorax (receiver 1), one on the upper arm (receiver 2), one on the forearm (receiver 3), and one on the hand (receiver 4), and perhaps the transmitter on a Locator to measure scapula position. In such a situation, it is most likely that you would want to know the position of the upper arm, forearm, hand and scapula all relative to the thorax, hence chosen the co-ordinate frame would be Receiver 1. If you wanted the

position and rotations of the thorax, arm and scapula relative to the hand, then the chosen co-ordinate frame would be that of the hand, ie. Receiver 4.

A5.2.3 Choosing the Output Settings

Once you have chosen the co-ordinate frame, you need to specify the **Output Settings** for the remaining receivers (and transmitter if applicable).

The Co-ordinate Frame setting generally represents the fixed part, while the Output Settings refer to the parts that are moving during the data collection (ie. the upper arm, forearm, hand and scapula when the Co-ordinate Frame is the receiver on the chest). For each receiver, there are seven different options (Euler Types 1-4, Azimuth about X, Y or Z) allowing you to specify how you want the data to be represented. For the transmitter, an addition option of Pronk's Sequence is available. The variety of setting allow the data from each receiver and/or transmitter to be analysed independently. However, before describing each of these settings, it is important to define the global co-ordinate system (Figure 5.3).

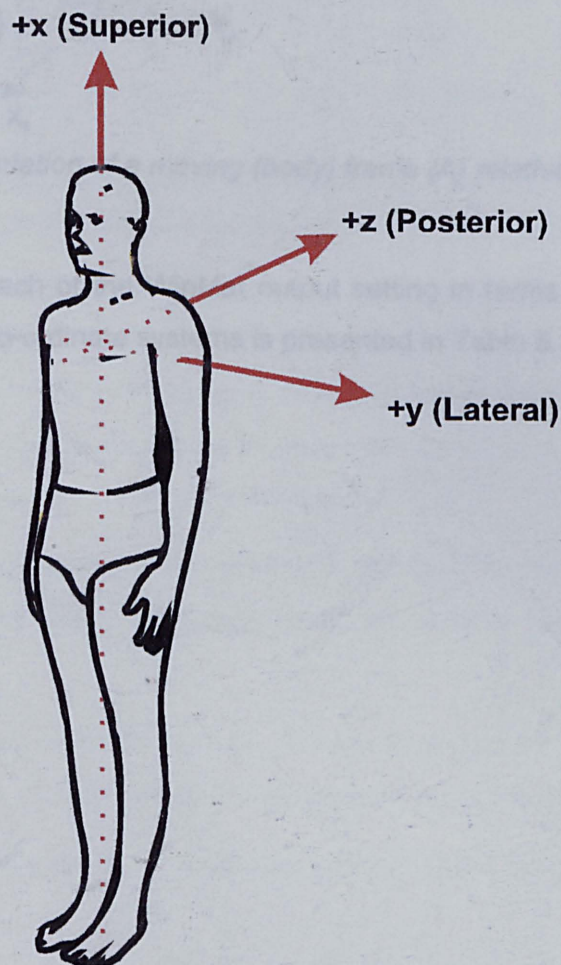


Figure 5.3: Definition of global co-ordinate system

Figure 5.4 is a schematic illustration to represent the position and orientation of an object $\{A\}$ relative to a global co-ordinate system $\{0\}$ at two finite positions during its motion. The position and orientation of $\{A\}$ may be measured globally, relative to co-ordinate system $\{0\}$, or locally relative to the co-ordinate system $\{A_0\}$.

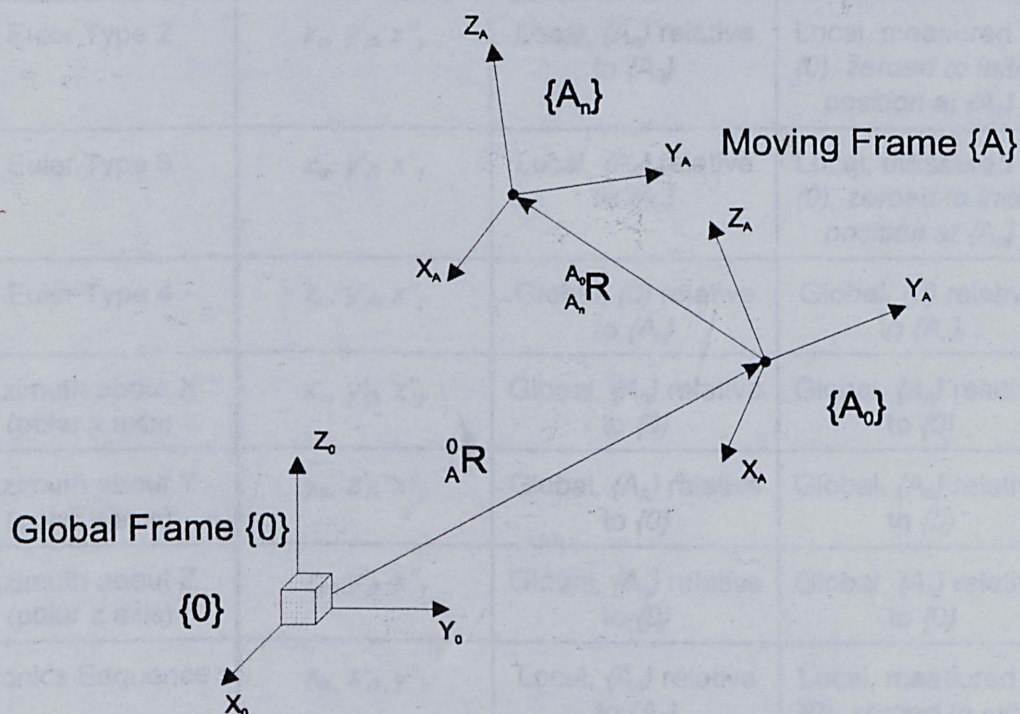


Figure 5.4: Representation of a moving (body) frame $\{A\}$ relative to the global frame $\{0\}$

An explanation of each of the WinMat output setting in terms of rotation sequences and local or global co-ordinate systems is presented in Table 5.1.

Output Setting	Rotation Sequence	Rotations Co-ordinate system	Displacements co-ordinate system
Euler Type 1	$z_{\alpha} y'_{\beta} x''_{\gamma}$	Global, $\{A_n\}$ relative to $\{0\}$	Global, $\{A_n\}$ relative to $\{0\}$
Euler Type 2	$z_{\alpha} y'_{\beta} x''_{\gamma}$	Local, $\{A_n\}$ relative to $\{A_0\}$	Local, measured in $\{0\}$, zeroed to initial position at $\{A_0\}$
Euler Type 3	$z_{\alpha} y'_{\beta} x''_{\gamma}$	Local, $\{A_0\}$ relative to $\{A_n\}$	Local, measured in $\{0\}$, zeroed to initial position at $\{A_n\}$
Euler Type 4	$z_{\alpha} y'_{\beta} x''_{\gamma}$	Global, $\{0\}$ relative to $\{A_n\}$	Global, $\{0\}$ relative to $\{A_n\}$
Azimuth about X (polar x axis)	$x_{\alpha} y'_{\beta} z''_{\gamma}$	Global, $\{A_n\}$ relative to $\{0\}$	Global, $\{A_n\}$ relative to $\{0\}$
Azimuth about Y (polar y axis)	$y_{\alpha} z'_{\beta} x''_{\gamma}$	Global, $\{A_n\}$ relative to $\{0\}$	Global, $\{A_n\}$ relative to $\{0\}$
Azimuth about Z (polar z axis)	$z_{\alpha} y'_{\beta} x''_{\gamma}$	Global, $\{A_n\}$ relative to $\{0\}$	Global, $\{A_n\}$ relative to $\{0\}$
Pronk's Sequence	$x_{\alpha} z'_{\beta} y''_{\gamma}$	Local, $\{A_n\}$ relative to $\{A_0\}$	Local, measured in $\{0\}$, zeroed to initial position at $\{A_0\}$

Table 5.1: Definition of WinMat Output Settings

Hence, Euler Type rotations are general local and global rotation definitions. Azimuth types are specific rotation definitions suitable for spherical representation of humeral motion. Pronk's Sequence is identical to the definition of Euler Type 2, except that a different rotation sequence is used to describe the rotations of the scapula in angles approximately analogous with medical definitions.

To summarise, the Co-ordinate system will generally be the fixed part during the data collection, and Output Settings must be chosen for each of the moving parts.

An "on-line" summary of these settings can be displayed by clicking on the **Output Definitions...** button, or selecting **Help, Rotations...** from the menu..

All displacements are calculated relative to the specified co-ordinate frame regardless of output setting.

When the Co-ordinate Frame is not set as the Transmitter, it is assumed that measurements of scapulohumeral kinematics are being measured and that a Locator

is attached to the Transmitter. Hence, the co-ordinates of the three feet on a Locator in the calculated specified co-ordinate frame. To enter the dimensions of the scapula as measured on the Locator, click on the button **Set Dimensions...** button, or selecting **Options, Set Dimensions...** from the menu. This will allow you to enter the distance from the acromion leg to the leg over the root of the scapula spine (along the top of the Locator), the distance from the Locator centre to the inferior angle leg (down the swing arm on the Locator, and the angle of the swing arm on the Locator (measured on the outer scale).

A5.3 THE OUTPUT FILE

The output file (<yourfile>.out) contains the headed lists of rotations and displacements. The first three lines are header information (filename, subject name and the date of the test). Beyond this, the rotations of the first receiver (or transmitter) are listed in the output format as chosen. The displacements of this receiver will follow (or, if the transmitter, the co-ordinated of the feet of the Locator). After this will come the rotations and displacements of the other receivers, each labelled with the receiver number, the output format and the reference frame, as shown below.

```
C:\DATA\YOURFILE.DAT
```

```
Nick.Barnett
```

```
Euler Type 1 rotations of the Transmitter
```

```
in the frame of Receiver 1
```

```
-0.34 +3.05 -2.77
```

```
-0.41 +3.07 -2.74
```

```
+65.95 +1.48 -1.07
```

```
...
```

```
X, Y, Z Coordinates of the Locator Feet (in mm)
```

```
in the frame of Receiver 1
```

```
Coordinates of the Acromion foot
```

+258.50 +7.33 -2.16

+258.49 +7.13 -2.29

+281.44 +312.02 -0.26

...

Coordinates of the Root of the Scapula Spine foot

+258.83 +107.15 -6.98

+258.95 +106.95 -7.06

+190.17 +352.70 -2.12

...

Coordinates of the Inferior Angle foot

+165.06 +109.90 -2.09

+165.19 +109.83 -2.13

+149.89 +267.85 +0.26

...

Euler Type 3 rotations of Receiver 2

in the frame of Receiver 1

-0.00 +0.01 +0.00

-0.01 -0.18 +0.06

-31.84 +2.45 +7.17

...

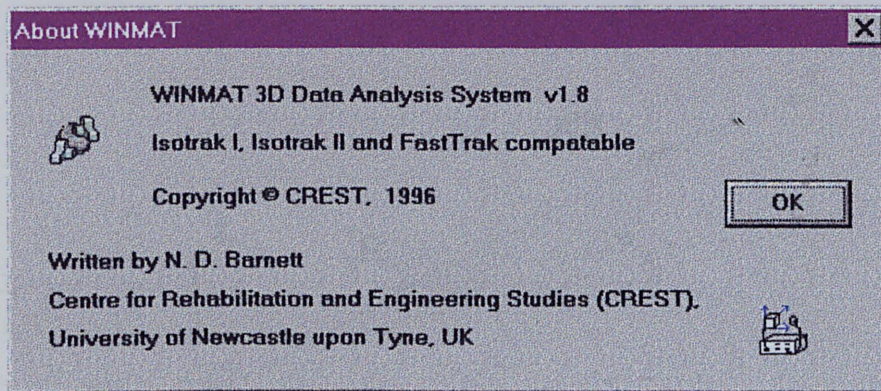
X, Y, Z Displacements of Receiver 2 (in mm)

in the frame of Receiver 1

+537.59 +812.78 +292.41

...

etc. for receivers 3 and 4.



A5.4 APPENDIX - FRAME TRANSFORMATIONS

The mathematical definitions for all rotation and displacement transformations used in WinMat are listed here. To satisfy all of the output settings, we must identify all possible cases of transformation. These fall into three general categories, which may be further divided for each individual output format setting

1. When the specified output is in the frame of the transmitter, and the moving part is any receiver.
2. When the specified output is in the frame of any receiver, and the moving part is the transmitter.
3. When the specified output is in the frame of a receiver, and the moving part is any one of the other receivers.

These three cases shall be dealt with in turn, starting with the easiest of them!

A5.4.1 Frame in Transmitter {T}, motion in any Receiver {C}

Euler Type 1

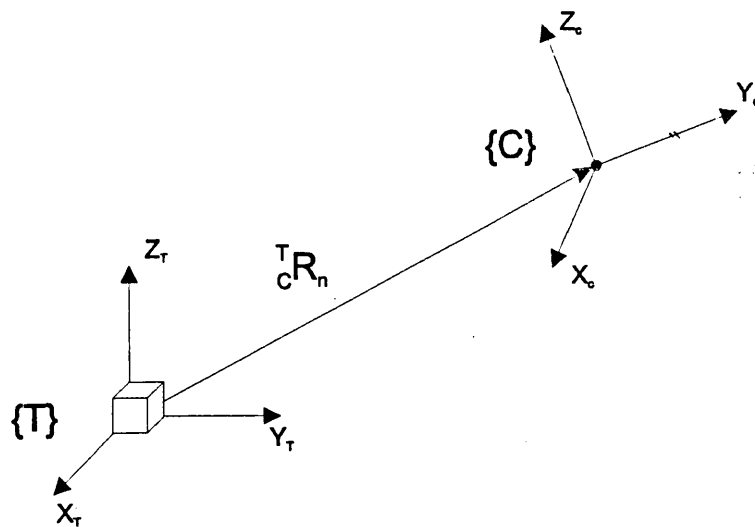


Figure 5.5: Euler type 1 rotations of receiver $\{C\}$ relative to the frame of the transmitter $\{T\}$

$$[{}^T_C R_n] = [{}^T_C R_n]$$

Euler Type 2

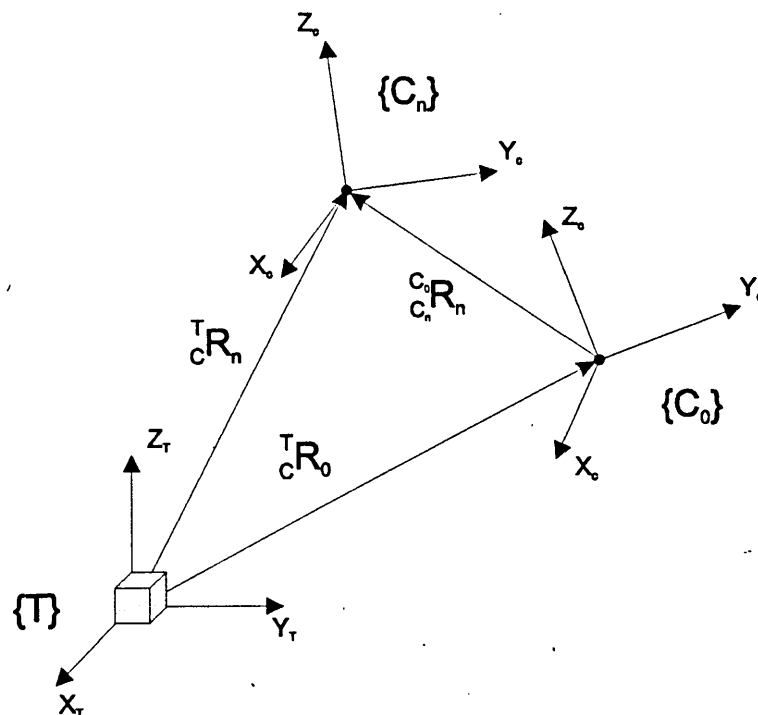


Figure 5.6: Euler type 2 rotations of receiver $\{C\}$ relative to the frame of the transmitter $\{T\}$

$$[{}^{C_0}_C R_n] = [{}^T_C R_0]^T \cdot [{}^T_C R_n]$$

Euler Type 3

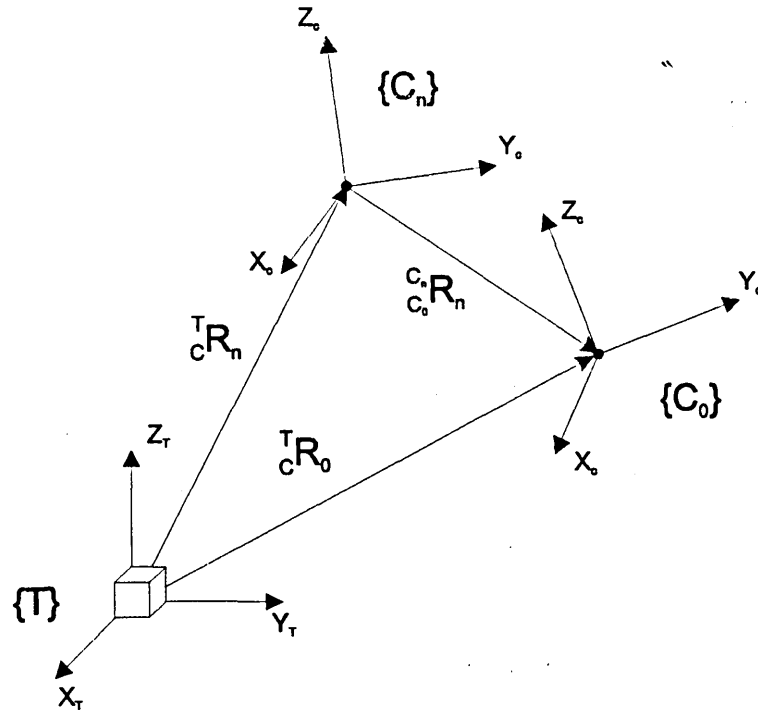


Figure 9: Euler type 3 rotations of receiver {C} relative to the frame of the transmitter {T}

$$\begin{bmatrix} C_0^n R_n \end{bmatrix} = \begin{bmatrix} T_C R_n \end{bmatrix}^T \cdot \begin{bmatrix} T_C R_0 \end{bmatrix}$$

Euler Type 4

$$\begin{bmatrix} C_0^n R_n \end{bmatrix} = \begin{bmatrix} T_C R_n \end{bmatrix}^T$$

Azimuth about X, Y, Z

$$\begin{bmatrix} T_C R_n \end{bmatrix} = \begin{bmatrix} R_{X,Y,Z} \end{bmatrix} \cdot \begin{bmatrix} T_C R_n \end{bmatrix}$$

where $R_{X,Y,Z}$ represents a rotation of 90° about the X or Y axis of the frame so that the Azimuth rotation will occur about the Y, X axis respectively. By default, azimuth occurs about Z, in which case the pre-multiplier $R_{X,Y,Z}$ is not necessary.

For Azimuth about X,

$$R_{X,Y,Z} = \begin{bmatrix} 0 & 0 & 1 \\ 0 & 1 & 0 \\ -1 & 0 & 0 \end{bmatrix}$$

For Azimuth about Y,

$$R_{X,Y,Z} = \begin{bmatrix} 1 & 0 & 0 \\ 0 & 0 & -1 \\ 0 & 1 & 0 \end{bmatrix}$$

Displacements

$$\begin{bmatrix} {}^T_c d_n \end{bmatrix} = \begin{bmatrix} {}^T_c d_n \end{bmatrix}$$

Displacements are zeroed to the initial position when using Euler Types 2 and 3.

A5.4.2 Frame in any Receiver {C}, motion in Transmitter {T}

Euler Type 1

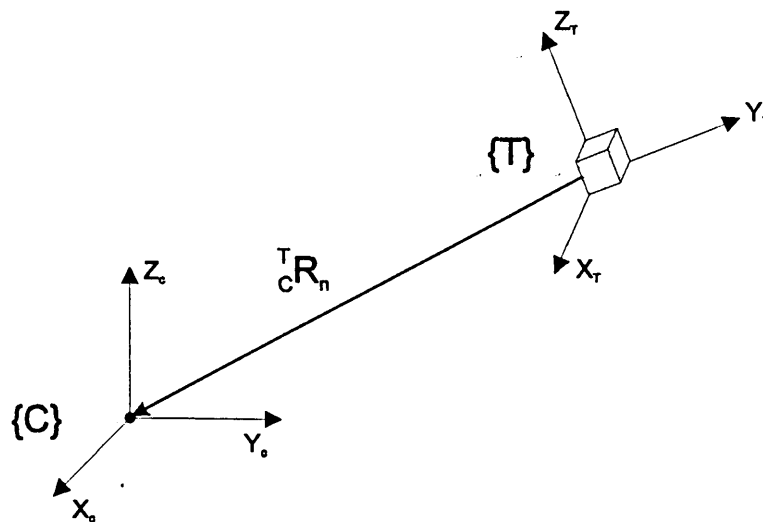


Figure 5.7: Euler type 1 rotations of the transmitter {T} relative to the frame of receiver {C}

$$\begin{bmatrix} {}^c_T R_n \end{bmatrix} = \begin{bmatrix} {}^T_c R_n \end{bmatrix}^T$$

Euler Type 2

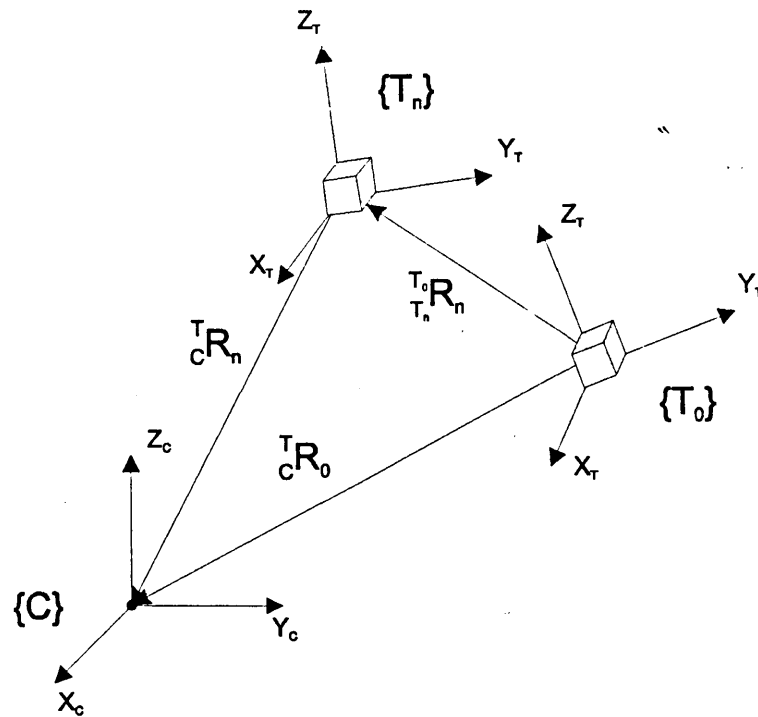


Figure 5.8: Euler type 2 rotations of the transmitter $\{T\}$ relative to the frame of receiver $\{C\}$

$$\begin{bmatrix} T_n R_n \end{bmatrix} = \begin{bmatrix} T_C R_0 \end{bmatrix} \cdot \begin{bmatrix} T_C R_n \end{bmatrix}^T$$

When using Pronk's Sequence:

$$\begin{bmatrix} T_n R_n \end{bmatrix} = \begin{bmatrix} R_Y \cdot R_Z \end{bmatrix} \cdot \left[\begin{bmatrix} T_C R_0 \end{bmatrix} \cdot \begin{bmatrix} T_C R_n \end{bmatrix}^T \right]$$

where R_Y is a rotation of 90° about the local Y axis and R_Z is a rotation of 90° about the local Z axis.

Euler Type 3

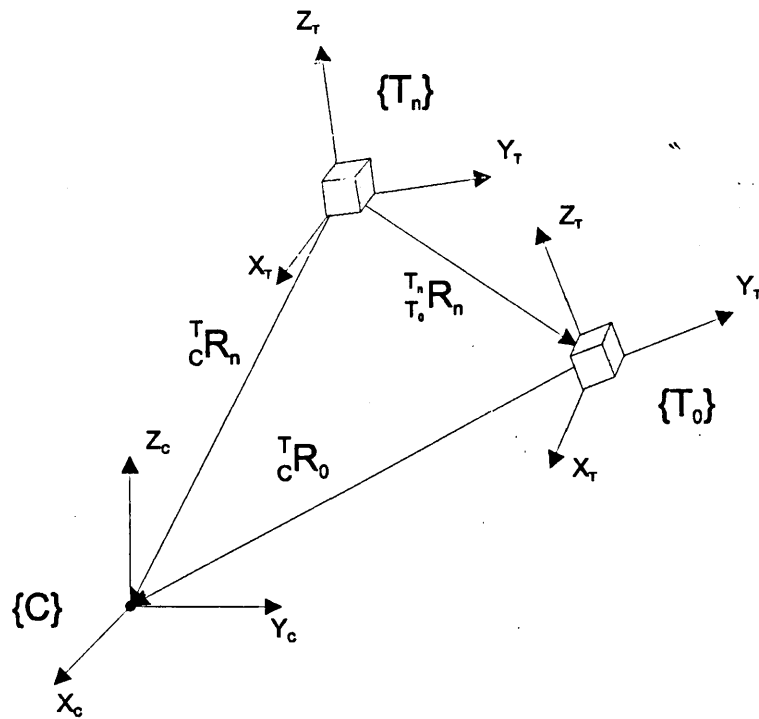


Figure 5.9: Euler type 3 rotations of the transmitter $\{T\}$ relative to the frame of receiver $\{C\}$

$$\begin{bmatrix} T_n R_n \end{bmatrix} = \begin{bmatrix} T_n R_n \end{bmatrix} \cdot \begin{bmatrix} T_c R_0 \end{bmatrix}^T$$

Euler Type 4

$$\begin{bmatrix} T_n R_n \end{bmatrix} = \begin{bmatrix} T_n R_n \end{bmatrix}$$

Azimuth about X, Y, Z

$$\begin{bmatrix} C R_n \end{bmatrix} = \begin{bmatrix} R_{X,Y,Z} \end{bmatrix} \cdot \begin{bmatrix} T_n R_n \end{bmatrix}^T$$

Displacements

$$\begin{bmatrix} C d_n \end{bmatrix} = \begin{bmatrix} T_n R_n \end{bmatrix}^T \cdot \begin{bmatrix} -T_c d_n \end{bmatrix}$$

Displacements are zeroed to the initial position when using Euler Types 2 and 3, and Pronk's sequence.

A5.4.3 Frame in any Receiver $\{C1\}$, motion in any other Receiver $\{C2\}$

Euler Type 1

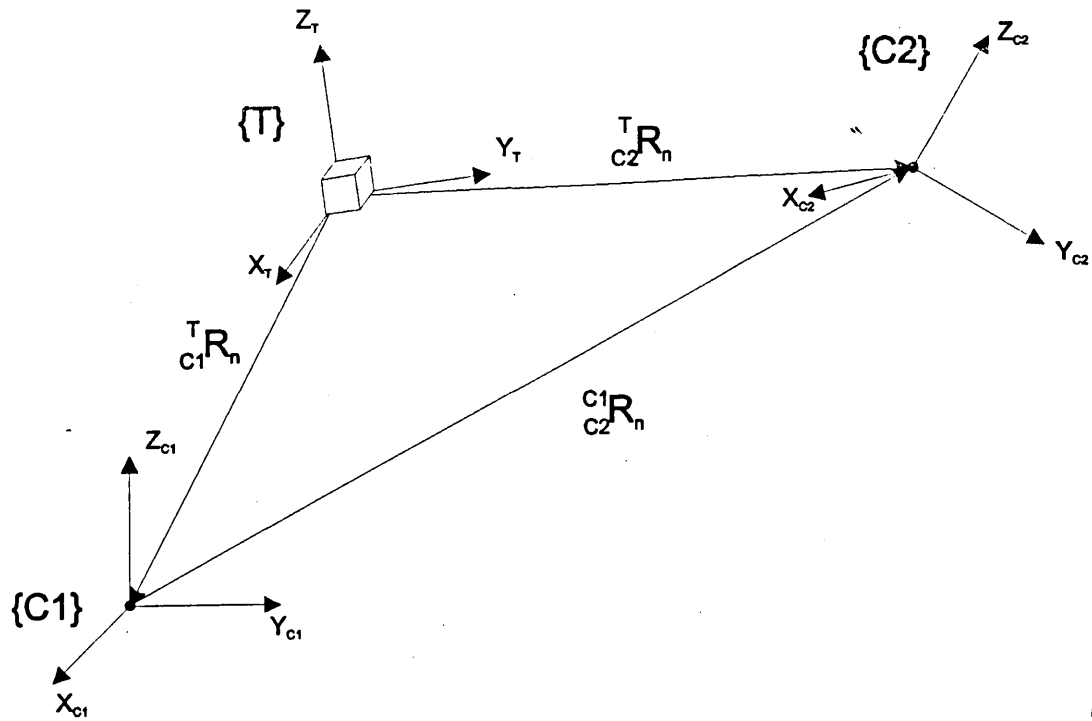


Figure 5.10: Euler type 1 rotations of receiver {C2} relative to the frame of receiver {C1}

$$\begin{bmatrix} C1_{C2}^T R_n \end{bmatrix} = \begin{bmatrix} T_{C1}^T R_n \end{bmatrix}^T \cdot \begin{bmatrix} T_{C2}^T R_n \end{bmatrix}$$

Euler Type 2

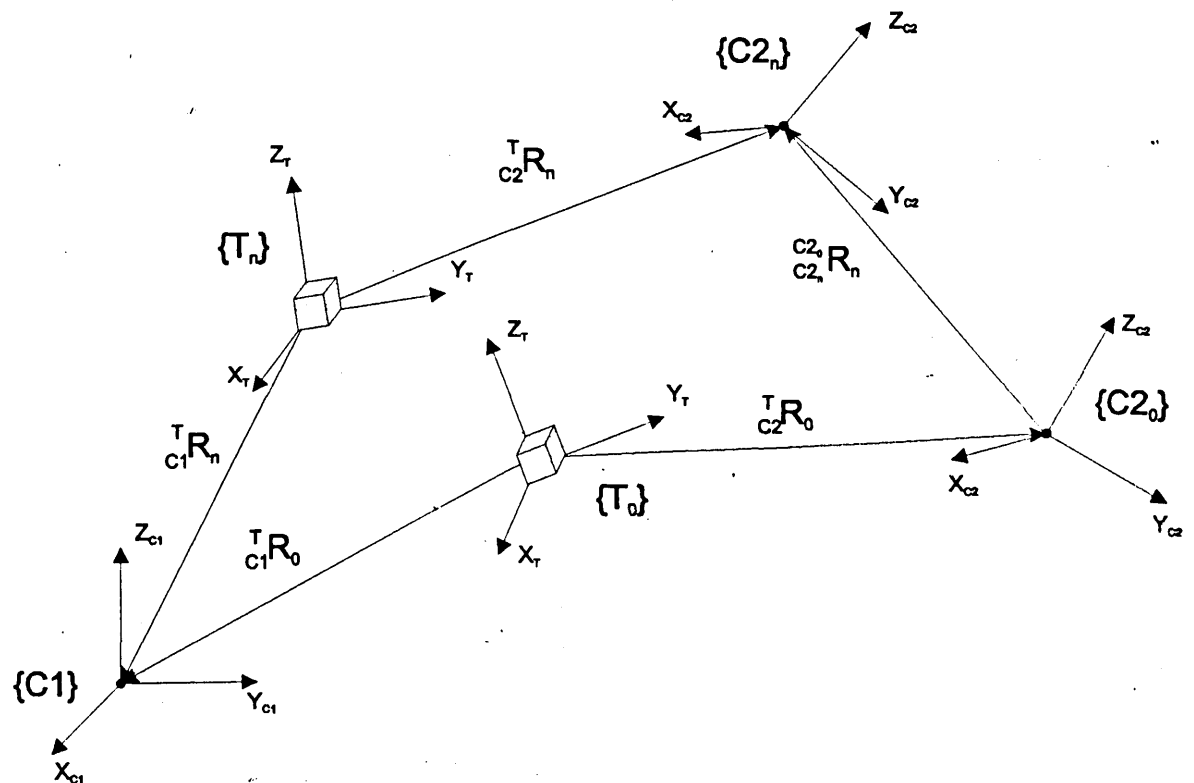


Figure 5.11: Euler type 2 rotations of receiver {C2} relative to the frame of receiver {C1}

$$\begin{bmatrix} c_{2_0}^2 R_n \\ c_{2_n}^2 R_n \end{bmatrix} = \left[\begin{bmatrix} c_{1_0}^T R_0 \\ c_{2_0}^T R_0 \end{bmatrix}^T \cdot \begin{bmatrix} c_{2_0}^T R_0 \end{bmatrix} \right]^T \cdot \left[\begin{bmatrix} c_{1_n}^T R_n \\ c_{2_n}^T R_n \end{bmatrix}^T \cdot \begin{bmatrix} c_{2_n}^T R_n \end{bmatrix} \right]$$

Euler Type 3

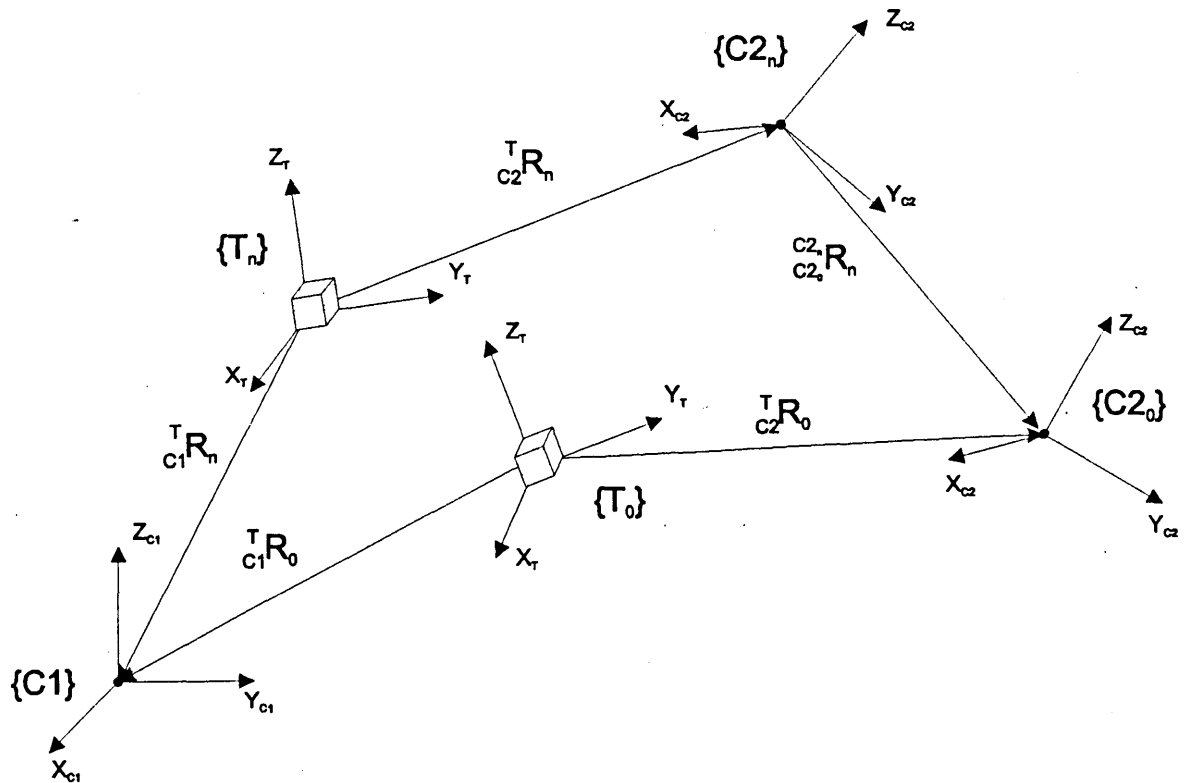


Figure 5.12: Euler type 3 rotations of receiver {C2} relative to the frame of receiver {C1}

$$\begin{bmatrix} c_{2_0}^2 R_n \\ c_{2_n}^2 R_n \end{bmatrix} = \left[\begin{bmatrix} c_{1_0}^T R_n \\ c_{2_0}^T R_n \end{bmatrix}^T \cdot \begin{bmatrix} c_{2_0}^T R_n \end{bmatrix} \right]^T \cdot \left[\begin{bmatrix} c_{1_n}^T R_n \\ c_{2_n}^T R_n \end{bmatrix}^T \cdot \begin{bmatrix} c_{2_n}^T R_n \end{bmatrix} \right]$$

Euler Type 4

$$\begin{bmatrix} c_{2_0}^2 R_n \\ c_{2_n}^2 R_n \end{bmatrix} = \begin{bmatrix} c_{2_0}^T R_n \\ c_{2_n}^T R_n \end{bmatrix}^T \cdot \begin{bmatrix} c_{1_0}^T R_n \\ c_{1_n}^T R_n \end{bmatrix}$$

Azimuth about X, Y, Z

$$\begin{bmatrix} c_{2_0}^2 R_n \\ c_{2_n}^2 R_n \end{bmatrix} = [R_{X,Y,Z}] \cdot \begin{bmatrix} c_{1_0}^T R_n \\ c_{1_n}^T R_n \end{bmatrix}^T \cdot \begin{bmatrix} c_{2_0}^T R_n \\ c_{2_n}^T R_n \end{bmatrix}$$

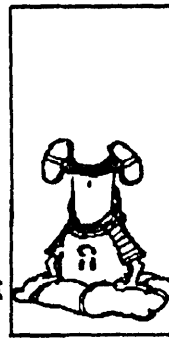
Displacements

$$\begin{bmatrix} c_{2_0}^1 d_n \\ c_{2_n}^1 d_n \end{bmatrix} = \begin{bmatrix} c_{1_0}^T R_n \\ c_{1_n}^T R_n \end{bmatrix}^T \cdot \begin{bmatrix} -c_{1_0}^T d_n \\ -c_{1_n}^T d_n \end{bmatrix} + \begin{bmatrix} c_{1_0}^T R_n \\ c_{1_n}^T R_n \end{bmatrix}^T \cdot \begin{bmatrix} c_{2_0}^T d_n \\ c_{2_n}^T d_n \end{bmatrix}$$

Displacements are zeroed to the initial position when using Euler Types 2 and 3.



I DID IT!
I DID IT!



SOMEHOW I
IMAGINED THIS
EXPERIENCE WOULD
BE MORE REWARDING.

